Department of Civil Engineering
Nottingham Transportation Engineering Centre

ASSESSMENT OF BOND BETWEEN ASPHALT LAYERS

by

Muslich Hartadi Sutanto, ST, MT

Thesis submitted to the University of Nottingham
for the degree of Doctor of Philosophy

November 2009

To
Allah
Rasulullah
Gina
My Parents
My Family

ABSTRACT

Asphalt pavements are usually constructed in several layers and most of pavement design and evaluation techniques assume that adjacent asphalt layers are fully bonded together and no displacement is developed between them. However, full bonding is not always achieved and a number of pavement failures have been linked to poor bond condition

Theoretical research showed that the distribution of stresses, strains and deflections within the pavement structure is highly influenced by the bond condition between the adjacent layers. Slippage at the interface between the binder course and the base could significantly reduce the life of the overall pavement structure. If slippage occurs within the interface between the surfacing and the binder course, the maximum horizontal tensile strain at the bottom of the surfacing becomes excessive and causing the rapid surfacing failure. This condition becomes worse when a significant horizontal load exists.

This thesis is concerned with the assessment of bond between asphalt layers. The main objective of this thesis is to provide guidance for assessing bond between asphalt layers, in order to facilitate the construction of roads with more assurance of achieving the design requirements. Further modification to the modified Leutner test has been performed. An investigation regarding the torque bond test and the effect of trafficking on bond have also been undertaken. A bond database on the modified Leutner test has been developed. An analysis has been performed to estimate the achievable values of bond strengths on typical UK road constructions obtained from the bond database. The values were then compared to the results from an analytical analysis to predict the required bond strength at the interface and other standards in Germany and Switzerland to recommend specification limits of bond strength for UK roads.

ACKNOWLEDGEMENTS

All praise and thanks are due to Allah the Almighty who sustained me throughout and enable me to pursue this study.

I am indebted to my supervisors Professor A.C. Collop and Professor G.D. Airey for their invaluable guidance, support, encouragement and constructive criticism throughout the course of this study. I would also to thank Dr. Y.K. Choi (former Research Associate), Dr. S.E. Zoorob (former Research Officer), R.C. Elliott (Scott Willson Ltd.), Dr. I. Widyatmoko (Scott Willson Ltd.), Dr. N.H. Thom (Senior Lecturer) and Dr. J.R. Grenfell (Research Officer) for their help, advice and discussions. I would like also to say special thanks to the other NTEC academic staff, namely, Prof. S.F. Brown, Assoc. Prof Tony Parry, Dr. Lloyd Bennett and Assoc. Prof A.R. Dawson.

I would like to express my appreciation and sincere gratitude to the Indonesian government and the Muhammadiyah University of Surakarta for supporting the study at the University of Nottingham. The work carried out in this thesis was funded under a contract placed with Scott Wilson Ltd by the UK Highways Agency (HA) and the Road Emulsion Association (REAL) Ltd. The views expressed in this work are not necessarily those of the HA, the Department for Transport or REAL. The Finite Element model presented in the modification to the Leutner test was developed by Dr. S. Wang (former Research Associate at NTEC). The specimens used in the automatic torque test investigation were part of the RILEM (Réunion Internationale des Laboratoires d'Essais et de Recherches sur les Matériaux et les Constructions) TC 206 ATB/TG4 - Interlaboratory Test on Interlayer Bonding of Asphalt Pavements and obtained from a trial section constructed in Macerata, Italy by the Universita Politechnica delle Marche.

Special thanks go to Barry Brodrick, Chris Fox and Andy Leyko for their invaluable help and hard work during the developments of the equipment and the instrumentation installations. Thanks to Carole Yates, Angela Gilbert and Sheila Provost for their help in processing the order forms and other office administration works. I would also very happy to thank Jon Watson, Mick Winfield, Rich Blakemore, Lawrence Pont and all the NTEC technical staffs for their invaluable help regarding laboratory experimental works.

I would also like to thank my friends Dr. S. Sunarjono, Dr. H. Thamrin, P.S. Pudyastuti, T. Widjanarko, Dr. D. Harmanto, Dr. J. Olivera, Dr. H. Taherkhani, Dr. Y. Lee, Dr. C. Joe-Kwan, Dr. M. Yusof, Dr. R. Isola, Dr. M.C. Liao, Dr. P. Jitareekul, Md. Izzi, L. Brito and all my colleagues at NTEC for their invaluable help and discussions.

Finally, my deep appreciation and thanks go to my wife Gina, my parents H. S. Sutanto and Hj. Fathonah Sutanto, my father and mother in law H. Sugiro and Hj. Tina Sugiro, my brothers Fajar and Dony, and my sisters in law Nana and Hanum for their continuous support throughout the study.

DECLARATION

The research reported in this thesis was conducted at the University of Nottingham, Department of Civil Engineering, Nottingham Transportation Engineering Centre (NTEC), between March 2004 and September 2007. This thesis is the result of my own work, except where specific reference has been made to the work of others. No part of the work has been submitted for any degree.

Muslich Hartadi Sutanto
Nottingham
November 2009

TABLE OF CONTENTS

LIST OF FIGURES

LIST OF TABLES

Chapter 1

INTRODUCTION

1.1 Background

Asphalt pavements are usually composed of several layers and most of pavement design and evaluation procedures assume that those layers are fully bonded together. A typical practice to achieve the full bond condition is to apply a thin film of bituminous bond coat (or tack coat) at the interface between adjacent layers. However, full bonding is not always achieved since many cases of bond failures have been reported in several countries [TRRL, 1976; Kennedy, 1978; TRRL, 1979; Kennedy and Lister, 1980; Peattie, 1980; SETRA/DTC, 1986; Shaat, 1992; Lepert *et al.*, 1992; Hachiya and Sato, 1997; Raab and Partl, 1999; Hakim, 2002; Sutanto, 2004; Charmot *et al.*, 2005; Tashman *et al.*, 2007; Bognacki *et al.*, 2007].

In the UK, a significant number of bond failures have been reported by Peattie [1980], where fifty six cases of premature bond failures between the surfacing and binder course of (mainly) newly constructed roads across the UK were found in the early-70s. Those incidents were assessed by a working party led by the Transport Research Laboratory (TRL). They performed an extensive investigation and found that compaction of a surfacing at high temperature over a cold binder course laid on a poor quality foundation is likely to cause a poor interface bond condition [TRRL, 1976; Kennedy, 1978; TRRL, 1979; Kennedy and Lister, 1980]. The Department of the Environment for Northern Ireland also found that some sections of newly constructed roads in Northern Ireland, UK experienced bond failures soon after they were opened to traffic [Shaat, 1992]. A more recent case of bond failure in the UK was reported by Hakim [2002], where a debonding problem between bases was found in a three year old pavement structure. Although the stiffnesses of the foundation and the individual layers were reasonably good, results from a Falling

Weight Deflectometer (FWD) test on this debonded pavement structure demonstrated that the effective stiffness and residual life of the pavement were low.

A literature review revealed that the incidents of bond failures in several countries mainly occurred at the interface between the surfacing and binder course, particularly at some locations of roads that suffer from a high horizontal loading (e.g. curve, intersection, upward or downward gradients). The condition could become more critical when the high horizontal loadings occur during the summer due to lower interface bond strength and stiffness associated with higher pavement temperature. Furthermore, Collop and Thom [2002] highlighted that the introduction of thin surfacing course system into the UK results in a higher shear stress at the interface beneath the surfacing, which may cause a more critical bond condition at this interface.

Several theoretical research projects have been performed by researchers to investigate the effect of bond on pavement performance. The research showed that the bond affects the distribution of stresses, strains and deflections within a pavement structure. Furthermore, a full slippage at the interface between the binder course and the base could significantly reduce the life of the overall pavement structure [Romain, 1968; Uzan et al., 1978; Brown and Brunton, 1984; Shahin et al., 1987; Al Hakim, 1997; Hachiya and Sato, 1997; Kruntcheva et al., 2000b]. Shahin *et al.* [1987] demonstrated that if slippage occurs within the interface between the surfacing and the layer underneath, the maximum horizontal tensile strain at the bottom of the surfacing could become excessive, causing a rapid surfacing failure. This condition becomes worse when a significant horizontal load exists.

1.2 Need for the Research

Due the importance of bond and to ensure a good pavement performance, the availability of a standard test method for a routine testing of bond in the UK is necessary. Choi et al. [2005] reviewed several candidate test methods and demonstrated the suitability of the Leutner test as a laboratory-based test for routine testing of bond in the UK. They modified the Leutner test by introducing a 5mm gap

into the shear plane, developed a testing protocol for the modified Leutner test (with the 5mm gap) and utilised the testing protocol to perform bond tests on a limited number of field cores as well as laboratory manufactured samples. However, they recommended in the modified Leutner testing protocol that the minimum upper layer thickness to be tested should be at least 30mm; therefore, the test might not be suitable to determine the bond strength underneath a thin surfacing layer less than 30mm in thickness. Raab and Partl [2004b, 2005] using the LPDS (Layer Parallel Direct Shear) test, which is quite similar to the Leutner test, have successfully performed bond tests on cores containing thin surfacings by gluing steel platens on top of the surfacings. However, the effects of surfacing thicknesses and extensions on the measured bond strengths have not been investigated comprehensively.

Another bond test method known as the “manual” torque bond test has been widely used in the UK and is included as a mandatory test in the guidelines document SG3/05/234 [British Board of Agreement, 2004] to determine the interface bond strengths beneath thin surfacing course systems. The test is performed by manually twisting a handheld torque wrench, attached to a metal platen glued on top of a core specimen, at a constant rate to induce a twisting shear failure at the interface. Although a laboratory testing procedure is also available, the test is typically performed in-situ and generally limited to the uppermost interface. The guidelines document SG3/05/234 requires the test is performed in such way that the torque wrench is twisted at a constant rotation rate of 180°/min. Because the rotation angle at the interface may be different from that of the torque wrench (Section 4.2 of Chapter 4), performing the test at a constant rotation of the torque wrench may affect the variability of results. To investigate the effect of the rotation rate used in the manual torque bond test on the variability of results, it is necessary to perform a torque test investigation in a well controlled environment and loading condition.

To achieve a good interface bond condition, it is important to understand a number of factors that may affect the state of bond at the interface and a literature review revealed that many of them have been identified by researchers. Among these factors, Choi *et al*. [2005] indicated that bond between layers improved with trafficking at elevated temperature where the initial bond strength is low or

intermediate. However, only a limited number of cores were successfully tested and an un-realistic interface treatment (excessive amount of water/talcum powder mixture) was used to achieve the low initial bond condition. Therefore, additional investigation is necessary to confirm this.

It has been mentioned in the first paragraph of this section that Choi *et al*. [2005] identified the suitability of the Leutner test for laboratory measurement of bond properties between asphalt layers and a modified Leutner testing protocol has been developed. However, only a limited number of samples have been tested in the modified Leutner apparatus. Therefore, a more comprehensive investigation covering a wider range of mixture types in the UK needs to be undertaken for the modified Leutner test to be accepted as a robust method for determining the bond between asphalt layers.

In addition to the availability of a standardised bond test method, the availability of specification limits of bond strength in the UK is also of significant importance. The absence of specification limits for bond strengths in the UK would cause dilemmas during construction because neither the contractors nor the engineers will have a clear idea regarding the interface bond strength to be achieved. Furthermore, because thin surfacing course systems (which are associated with higher shear stress at the interface beneath the surfacing) have been widely used in the UK, the availability of specification limits is crucial to ensure a good state of bond at the interface between the thin surfacing and the layer underneath.

1.3 Research Objectives

The main objective of this research is to provide guidance for assessing bond between asphalt layers, in order to facilitate the construction of roads (particularly in the UK) with more assurance of achieving the design requirements. To achieve the main objective, several sub-objectives have been defined:

1. To undertake further modifications to the modified Leutner apparatus to enable the bond strength beneath thin surfacings less than 30mm in thickness to be determined.
2. To conduct a torque test investigation using an apparatus that is able to control the loading rate accurately and to be performed in a well controlled environment, particularly to investigate the effect of loading rate used in the manual torque bond test on the variability of results.
3. To investigate the development of bond with trafficking at elevated temperature for a wider range of material combinations, particularly for situations where the initial bond condition is low or intermediate.
4. To develop a database of bond strengths and stiffnesses measured using the modified Leutner test for a wide range of UK material combinations (including thin surfacing course systems) and bond conditions (obtained from field cores and laboratory manufactured specimens).
5. To recommend specification limits of shear bond strength for UK roads.

1.4 Scope

The scope of this thesis consists of a literature review (Chapter 2) followed by five chapters regarding the works undertaken and a final chapter presenting the main conclusions and recommendations for future research. The literature review covers the reported pavement failures associated with poor bond condition, the effect of bond on pavement performance, the available bond test methods and the factors affecting bond between asphalt layers.

Chapter 3 presents the modification to the modified Leutner test to enable the measurement of bond strength beneath thin asphalt surfacing. The effects of surfacing thicknesses on the measured bond strengths were investigated. Similar to the modification to the LPDS test by means of steel extension performed by Raab and Partl [2004b, 2005], the main modification to the modified Leutner test is an extension of the thickness of the thin asphalt layer to provide sufficient area to apply the load. Two different extension materials were assessed and the effects on the measured bond strengths were investigated. After it had been modified to cover thin

asphalt surfacings, the test was then used to measure the bond strengths of two thin surfacing materials over a range of temperatures and loading rates. Results from the experimental investigation were also compared with results from a Finite Element analysis performed by Dr. S. Wang (a research associate at The University of Nottingham). A new modified Leutner testing protocol was written after the modified Leutner test had been further modified in this research study. Since August 2008, the new modified Leutner testing protocol has been included as a standard testing protocol in the Specification for Highway Works [The Highways Agency, 2008].

Chapter 4 is particularly intended to investigate the effect of loading rates used in the manual torque bond test on the variability of results. Basic formulae for calculating the shear stress and the shear reaction modulus of the interface using the torque test principle are briefly explained in this chapter. A mechanically controlled (automatic) torque bond test apparatus, similar to an apparatus developed by Diakhaté *et al*. [2006, 2007], was specially developed and used to perform the investigation in more controlled environment and loading condition. A series of manual as well as automatic torque bond tests was performed and the results were compared and discussed. The automatic torque bond test was then used to perform a series of investigations at two different loading rates and three different temperatures to investigate the effect of loading rates used in the manual torque bond test on the variability of results. A series of modified Leutner tests was also performed for comparison with results from the manual as well as automatic torque bond tests. Although quite similar to the apparatus developed by Diakhaté *et al*. [2006, 2007], the automatic torque bond test apparatus is more rigid and capable of performing a cyclic zero-mean torsional load. Therefore, the automatic torque bond test was also used to investigate the behaviour of the interface under repeated loading.

Chapter 5 presents an investigation into the effect of trafficking at elevated temperature on bond, especially when the initial bond condition at the interface is low or intermediate. An investigation to achieve the low or intermediate initial bond condition using a more realistic interface treatment was performed. The trafficking investigation was performed in two different laboratory trafficking procedures covering a wider range of UK material combinations (including thin surfacings). The

first laboratory trafficking procedure was performed by confining a core specimen in a steel mould and trafficking was simulated by applying a repeated vertical stress until a set number of cycles. In the second procedure, the trafficking was performed on material combinations that showed improvement in the first trafficking procedure and a French Wheel Tracker machine [British Standards Institution, 2003b] was used to apply a rolling wheel load on a double layered prismatic specimen confined in a steel mould until a set number of wheel passes. The modified Leutner test that had been further modified to cover thin surfacings was used to determine the interface shear strength after the trafficking at each number of cycles or wheel passes had been performed.

Chapter 6 presents the development of a bond database for UK materials and constructions measured using the modified Leutner test. Modified Leutner tests on a wide range of UK material combinations (including thin surfacings) and bond conditions were performed on cores taken from laboratory prepared slabs as well as field coring. Laboratory investigations on the effect of ageing and moisture on bond strengths were also performed on laboratory prepared samples.

Chapter 7 presents a recommendation on the specification limits of bond strength for UK road constructions. Results obtained from the bond database were analysed to estimate the achievable values of bond strength on UK roads. A simple analysis to predict the required bond strengths on typical UK road constructions was also carried out. The achievable values of bond strength obtained from the bond database were then compared to the predicted required bond strengths obtained from the analytical analysis and other standards in Germany and Switzerland to recommend specification limits of bond strength for UK roads.

Chapter
2

LITERATURE REVIEW

2.1 Asphalt Pavement Structure

Asphalt pavements are designed to withstand traffic loading safely, economically and conveniently throughout their design life. An asphalt pavement structure consists of several layers of different materials laid over a subgrade. Figure 2.1 shows a typical asphalt pavement structure in the UK.

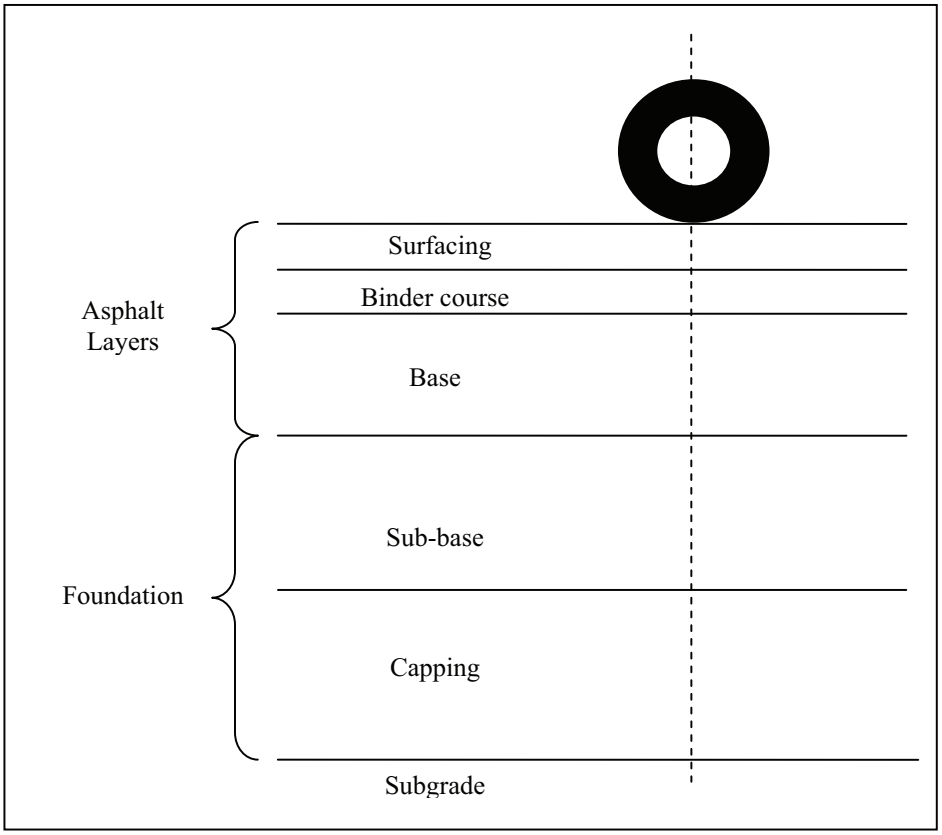

Figure 2.1 – A typical UK asphalt pavement structure (Adapted from Read and Whiteoak, 2003)

The surfacing is designed to provide a safe and smooth riding quality for the traffic and to protect the underlying layers from the ingress of water. The binder course and base are the main structural layers that have the role of distributing the traffic load to the layers underneath and protecting them from excessive stresses. The sub-base and capping (if used) form a foundation to distribute the load to the subgrade and to provide a platform for construction of asphalt layers. The surfacing, binder course and base layers are usually made of bituminous materials, whilst the foundation layers are usually made of granular materials.

2.2 Analytical Pavement Design

2.2.1 Basic Philosophy

Analytical pavement design is based on the philosophy that the structure should be treated in the same way as any other civil engineering structure, for which the basic procedure may be summarised as follows:

a) Specify the loading;
b) Consider available and permitted materials;
c) Estimate the dimensions and properties of each individual layer of pavement material;
d) Carry out structural analysis;
e) Compare critical stresses/strains and/or deflections with allowable values;
f) Make adjustment until the requirement is achieved;
g) Consider the economic feasibility of the result.

In analytical pavement design, knowledge of structural analysis and relevant material properties is very important. Linear elastic theory is known to be the simplest approach and it has been demonstrated to be valid as long as proper care is taken. The linear elastic theory can be used in pavement analysis to predict the state of stress, strain and deflection under vertical load induced by wheel load. The analysis can be extended to consider a horizontal load arising at the contact area

between the tyre and the pavement in a steep gradient or in a section of road where the vehicle usually accelerates, brakes or turns. The influence of bond between pavement layers on the distribution of stresses, strains and deflections can also be analysed.

2.2.2 Failure Mechanism

Traditionally, analytical pavement design assumed two classical modes of failure: fatigue cracking at the base of the asphalt layer and permanent deformation at the top of the subgrade. In the classical design approach, horizontal tensile strain at the base of the asphalt layer and vertical compressive strain at the top of the subgrade (Figure 2.2) are used to determine the critical life due to fatigue and permanent deformation respectively and should not exceed the allowable values within the design life.

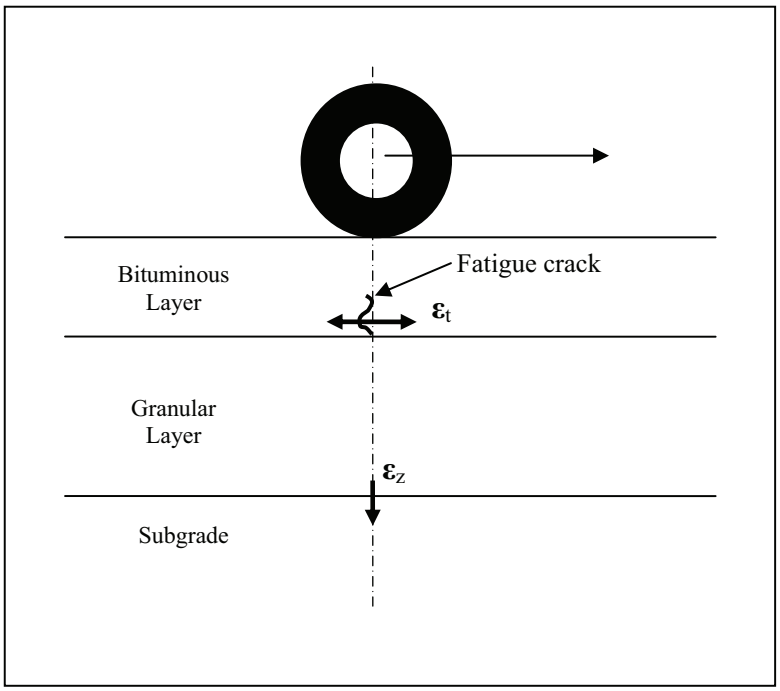

Figure 2.2 – Critical strains in the classical approach of asphalt pavement design (Adapted from Read and Whiteoak, 2003)

It should be noted that the aforementioned classical mode of failure was not supported by fact in thick asphalt pavement structures. Nunn *et al.* [1997] found that a properly maintained long life asphalt pavement having more than 180mm thick asphalt layer(s) showed no evidence of structural deterioration due to fatigue at the bottom of the asphalt layers or deformation at the top of the subgrade. In a thick asphalt pavement structure, fatigue cracking may initiate from the surfacing and permanent deformation may take place within the bituminous materials.

Nunn *et al.* [1997] revealed that surface initiated cracking is common on UK trunk roads and motorways. Similarly, Myers and Roque [2001] reported that surface initiated longitudinal wheelpath cracking is the predominant mode of failure on interstate highways in Florida, USA. Although the failure mechanism of surface initiated cracking typically observed in a thick asphalt pavement has not been fully understood, high surface tensile stress close to the edge of the tyre, low stiffness upper layer caused by high surface temperature and age hardening of the binder in the surface course are recognised as the main mechanisms that may cause surface initiated cracking [Washington State Department of Transportation, 2009].

Matsuno and Nishizawa [1992] found that high tensile strains occur at the edges of the tyre at or near the top of the surfacing layer. Specifically, these high strains occur when the surfacing is at low stiffness due to high surfacing temperature. Myers and Roque [2001] and Read and Whiteoak [2003] also reported a similar condition as shown in Figure 2.3. The tensile stress near the edge of the tyre, shown in red, extends only approximately 10mm into the surfacing layer explaining that it may initiate longitudinal cracking in the wheelpath, but another mechanism is required for the crack to propagate downwards. Read and Whiteoak [2003] noted an increasing conviction that the crack is further propagated by thermally induced stress caused by the contraction of the asphalt layers associated with temperature variations. The crack propagates downwards due to temperature gradient that causes greater contraction at the surface. The risk of cracking increases as the binder hardens and becomes too stiff to withstand the tensile stress.

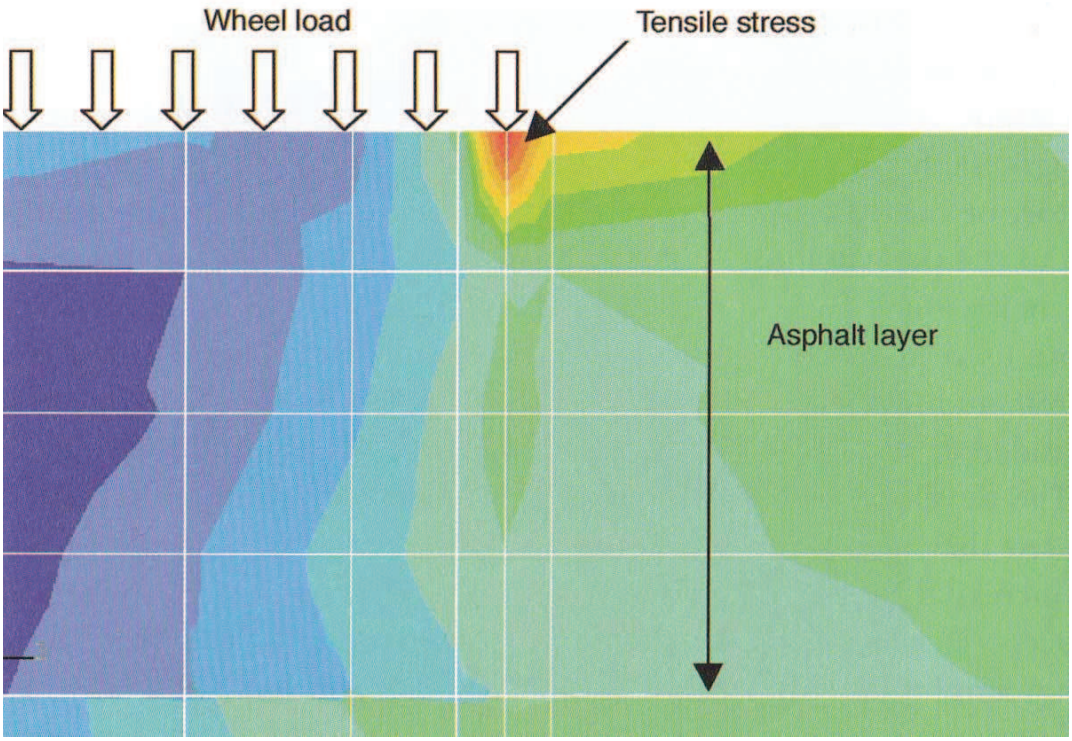

Figure 2.3 – Near surface pavement stresses induced by tyre loading (Read and Whiteoak, 2003)

Permanent deformation in asphalt pavements is usually observed in the form of rutting that takes place in the wheelpath of the vehicle. Rutting can be classified into two categories:

- Structural rutting, caused by cumulative permanent deformation of the pavement. In the classical design approach, this form of rutting, could be considered to represent structural pavement failure and empirically associated with vertical compressive strain in the subgrade.
- Non structural rutting, caused by permanent deformation localised at the wheel track, within the bituminous layers. This form of rutting can be reinstated by the replacement of the top layers only.

The consideration of the failure mechanism should be taken carefully because most of pavement rutting observed in thick asphalt pavements in the UK is mainly caused by permanent deformation within the bituminous layers as result of repeated

heavy vehicle loadings. The greatest permanet deformation occurs at high service temperature. Aggregate interlock, void content, bitumen type and bitumen content are known as the primary factors influencing permanent deformation. Under such conditions, the behaviour is governed by bitumen viscosity [Read and Whiteoak, 2003]

2.2.3 Bond between Asphalt Layers

Most of pavement design and evaluation techniques assume that adjacent pavement layers are fully bonded together and no displacement is developed between them. The bond between layers is very important to ensure that those layers work together as a composite structure to withstand traffic and environmental (e.g. temperature induced) loadings. To achieve that condition, a thin film of bituminous bond coat (or tack coat) is usually applied at the interfaces. However, full bonding is not always achieved and a number of pavement failures linked to poor bond condition have been reported [TRRL, 1976; Kennedy, 1978; TRRL, 1979; Kennedy and Lister, 1980; Peattie, 1980; SETRA/DTC, 1986; Shaat, 1992; Lepert *et al.*, 1992; Hachiya and Sato, 1997; Raab and Partl, 1999; Hakim, 2002; Sutanto, 2004; Charmot *et al.*, 2005; Tashman *et al.*, 2007; Bognacki *et al.*, 2007]. Details regarding the failures associated with poor bond condition are presented in Section 2.3 of this Chapter.

Because full bonding is not always achieved, a theoretical evaluation to investigate the effect of interlayer bond condition on pavement performance is necessary. Theoretical research showed that poor interlayer bond condition affects stress/strain distributions within a pavement structure and reduces the capability of the pavement to support traffic and environmental loadings [Romain, 1968; Uzan et al., 1978; Brown and Brunton, 1984; Shahin et al., 1987; Al Hakim, 1997; Al Hakim *et al.*, 1997; Hachiya and Sato, 1997; Al Hakim *et al.*, 1998; Kruntcheva *et al.*, 2000b; Romanoschi and Metcalf, 2001a, 2002, 2003; Khweir and Fordyce, 2003; Kulkarni 2004]. When horizontal loadings exist, poor bond condition at the interface beneath the surfacing could cause slippage cracking or horizontal permanent deformation at the surfacing layer. Poor load transfer from the surfacing to the layer

underneath, caused by the poor bond condition, leads to a high stress concentration within the surfacing material. Slippage cracking or horizontal permanent deformation will initiate at the top of the surfacing when the surfacing material is unable to withstand the induced horizontal stresses. Further details regarding the effect of bond on pavement performance are presented in Section 2.4 of this Chapter.

2.3 Pavement Failures Associated with Poor Bond Condition

In the early-70s, a significant number (56) of premature bond failures between the surfacing and binder course, occurring shortly after the completion of (mainly) newly constructed roads, were reported to the Asphalt and Coated Macadam Association [Peattie, 1980]. The surfacing had slipped and tearing had resulted. In order to investigate the factors that might contribute to those bond failures and to find methods of preventing them, a working party led by the Transport Research Laboratory (TRL) performed an extensive investigation by testing existing pavements and conducting pilot-scale experiments in the laboratory [TRRL, 1976; Kennedy, 1978; TRRL, 1979; Kennedy and Lister, 1980; Peattie, 1980].

The Department of the Environment for Northern Ireland found bond failures on some sections of pavements, soon after newly overlaid roads were opened to traffic in 1980 [Shaat, 1992]. As cited by Lepert *et al.* [1992], a study by SETRA/DTC [1986] in 1986 showed that severe pavement failures caused by interface bond problems affected 5% of the French highway network. In Switzerland, Raab and Partl [1999] reported several cases of slippage cracking and horizontal permanent deformation related to poor bond condition at the interface beneath the surfacing on some locations of roads where the shearing forces induced by horizontal loadings were high (e.g. curve, intersection, upward and downward gradients) or where an asphalt surfacing was laid over a concrete layer (e.g. bridge deck). Sutanto [2004] reported that in August 2001, a severe horizontal permanent deformation and delamination of an HRA surfacing were found in some locations where the vehicles brake and turn (curve, intersection) on a newly overlaid road section in Sragen, Indonesia. Charmot *et al.* [2005] reported that slippage, as shown in Figure 2.4,

occurred on 44% of an overlay project in Nevada, USA in June 2002, soon after completion of the project.

Figure 2.4 – Premature slippage failure on an overlay project in Nevada, USA (Charmot *et al.*, 2005)

In Japan, surfacing failures caused by bond problems have been frequently reported at some locations on airport runways where a high-speed aircraft usually brakes and turns sharply [Hachiya and Sato, 1997]. In 2005, an area of a landing runway close to the high-speed taxiway at Newark International Airport, USA, experienced slippage failure at the interface between the first and second asphalt layers and a horizontal permanent deformation was observed on the surfacing [Bognacki *et al.*, 2007].

Another form of deterioration that may be associated with poor bond condition is blistering on the surfacing layer [Brown and Darnell, 1987; Hironaka and Holland, 1987; Raab and Partl, 1999]. Blistering may occur when the bond underneath the surfacing is poor and unable to withstand vertical tensile stresses associated with the expansion of gasses caused by trapped moisture or microbial activity at the interface.

Raab and Partl [2004a] reported that bond problems not only occur between the surfacing and binder course, but also between deeper layers. Bond problems can also occur at the interface between bases or between base and bituminous or cementious sub-base (Figure 2.5). There was no information whether any structural failures (i.e. rutting or cracking) were observed on the corresponding pavement. Hakim [2002] showed bond failures between bases in a three year old pavement structure and reported that the effective stiffness and residual life of the pavement calculated from the results of a Falling Weight Deflectometer (FWD) test were low. Because the stiffnesses of the foundation and the individual layers were reasonably good, the researcher was convinced that the low effective stiffness and residual pavement life were due to the poor bond condition.

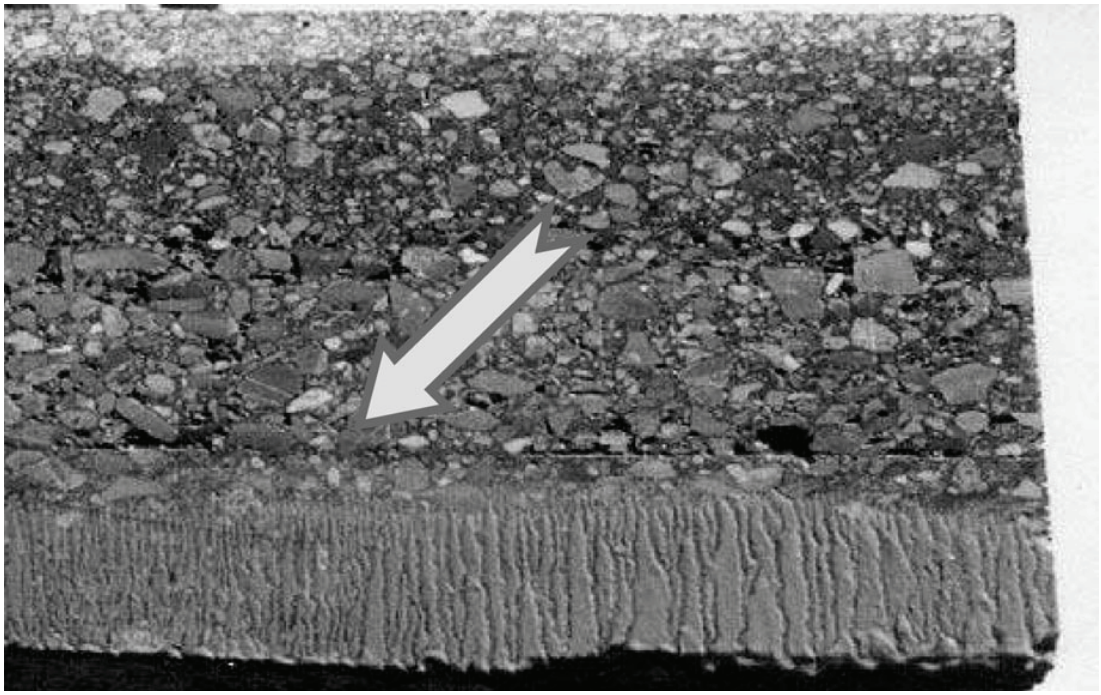

Figure 2.5 – Bond failure between base and sub-base in a slab taken from a newly built Swiss motorway (Raab and Partl, 2004a)

Slippage cracking or horizontal deformation on the surface of a pavement structure seems to be the most common visual evidence of pavement failures associated with poor interface bond condition. The failures clearly indicate that full

bond is not always achieved and an investigation into the effect of interface bond condition on pavement performance is necessary.

2.4 Effect of Bond on Pavement Performance

Recognising that full bond is not always achieved, theoretical investigations have been performed by several researchers to provide better insight on the implications of interface bond condition on pavement performance.

2.4.1 Mode of Separation

Bond failures at the interface could be categorised by the following separation modes (Figure 2.6): shear (mode-A), tensile (mode-B) and mixed shear-tensile (mode-C). Note that these definitions are for the purposes of this study and do not correspond exactly with conventional fracture mechanics terminology.

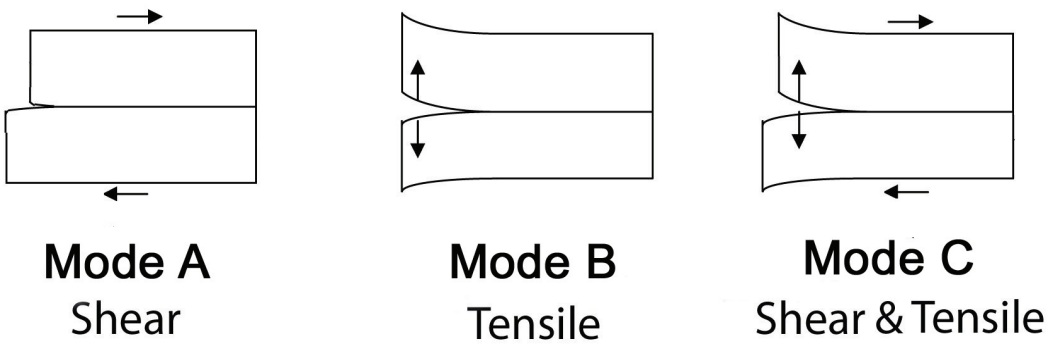

Figure 2.6 – Separation modes

In a pavement structure, shear separation (mode A) could occur in the transverse or longitudinal direction and is typically generated by traffic and/or temperature induced shear stresses at the interface. The temperature induced shear stress is caused by contractions of the asphalt layers due to temperature variations. In terms of traffic induced shear stress, De Beer *et al.* [1999] investigated tyre-

pavement contact stresses of a free rolling, slow moving tyre using a Vehicle-Road-Surface-Pressure-Transducer-Array (VRSPTA) and demonstrated that transverse and longitudinal contact stresses could be as high as 12% and 20% of the vertical contact stress, respectively. Additionally, horizontal loadings induced by the vehicle on some locations of the road where the vehicle accelerates, decelerates, brakes, turns, ascends or descends generate further shear stresses at the interface. The reported cases of bond failure clearly show that shear separation (mode A) was frequently observed in the field.

Tensile separation (mode B) may occur as a result of blistering as discussed in Section 2.3 of this Chapter. However, Raab and Partl [1999] considered that the incidence of bond failure associated with blistering in a real pavement structure is quite rare. Tensile separation could also be caused by vertical tensile stress due to suction of the tyre. Similar to the phenomenon in a suction cup, adhesion is generated at the contact area between pavement and tread block of the tyre. When the tread block leaves the contact area, an adhesive force holds the pavement surface and generates a tensile stress within the surfacing (Figure 2.7). It should be noted that information regarding the significance of tensile stress generated by the suction of the tyre has neither been reported nor confirmed by the incidence of bond failure in a real pavement structure.

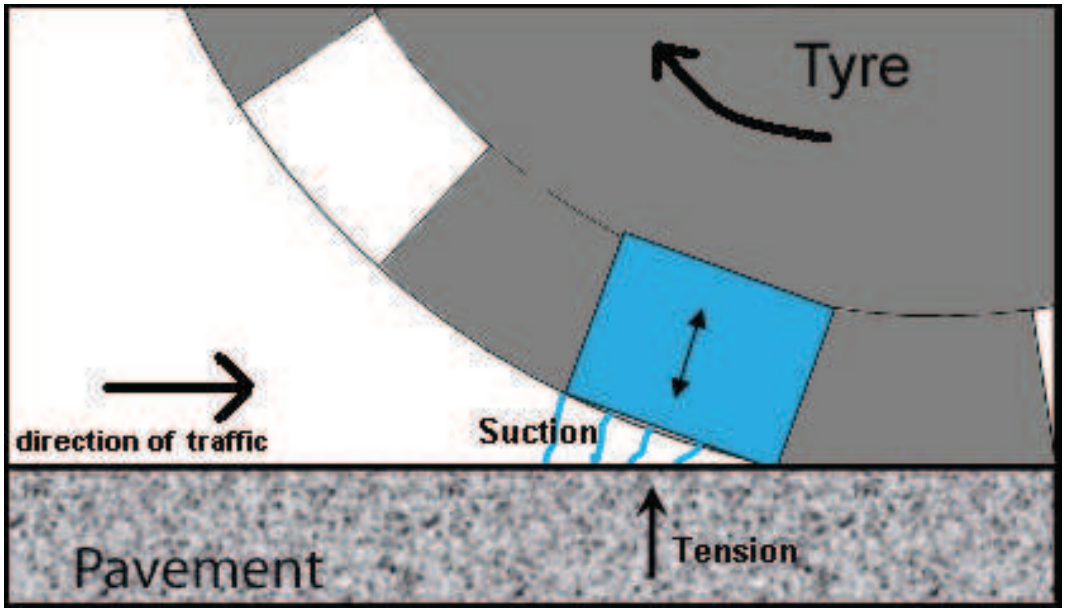

Figure 2.7 – Tyre suction phenomenon (Adapted from Bernhard, 2005).

A mixed shear-tensile separation (mode C) could occur at the interface beneath a thin surfacing layer. When the interface shear strength beneath the thin surfacing is relatively low, leading to low ability to transfer horizontal loadings to the layer underneath, the horizontal loadings are concentrated in the surfacing layer and may cause buckling of the thin surfacing layer at the front of the tyre. If the interface has not been separated and an interface tensile adhesion still exists, the buckling would generate a vertical tensile stress (while a shear stress induced by the horizontal loading also takes place) at the interface beneath the thin surfacing located at the front of the tyre (Figure 2.8). Information regarding bond failure in a real pavement structure associated with the mixed shear-tensile separation mode was not found during the literature search and it is considered that this phenomenon would be rarely found in a real pavement structure because it would only occur due to combined effect of the following conditions:

- The appearance of excessive horizontal loading;
- Poor horizontal load transfer to the layer underneath due to relatively low interface shear strength;
- The appearance of buckling within the thin surfacing layer; and
- The interface not having been separated in shear mode such that interface tensile adhesion still exists.

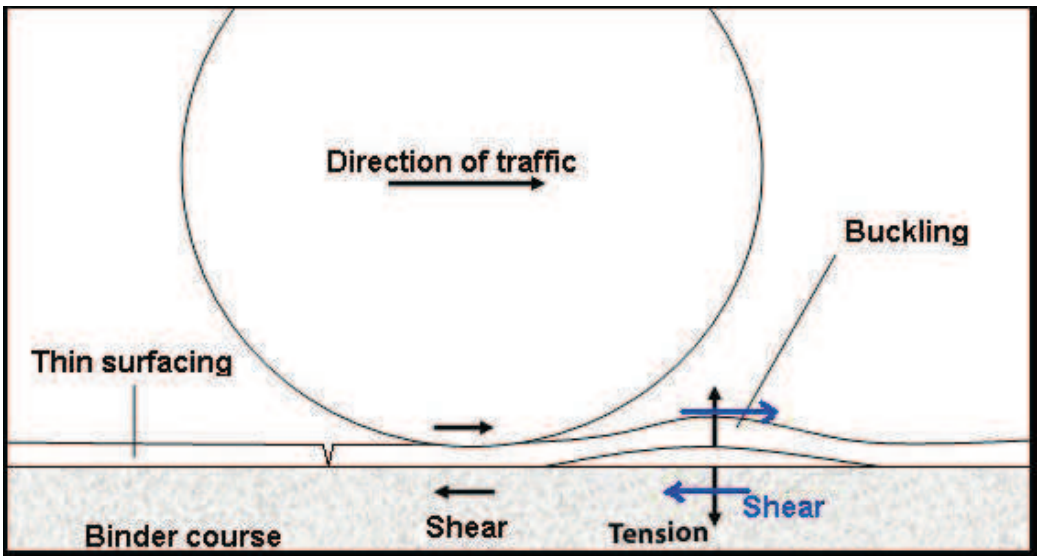

Figure 2.8 – Shear-tensile separation associated with buckling (Adapted from Raab and Partl, 2004a).

2.4.2 Modelling of Bond Condition at the Interface

The determination of a representative interface model to characterise bond condition at the interface between layers is essential. In theoretical research of bond, several researchers have focussed on the capability of the interface to withstand traffic and environmentally induced shear stresses and transferring them to the layer underneath. In elastic layered theory, Burmister [1945] provided solutions for two different interface conditions: full friction (i.e. full bond) and frictionless (i.e. full slip). The solutions of Burmister only take account two extreme interface conditions: full bond, which is highly desirable or full slip, which is very unlikely because interlayer friction may still exist [Brown and Brunton, 1984]. Based on the statement of Whiffin and Lister [1962], which mentioned the admission of some researchers that the interface is not fully bonded nor fully slipped, Uzan *et al.* [1978] introduced a method for the solution of elastic layered systems in between those two extreme conditions. They adopted Goodman's constitutive law [Goodman *et al.*, 1968] to represent the interface condition:

$$\tau = K_s(\Delta U) \tag{2.1}$$

where τ denotes the shear stress at the interface (in MPa), ΔU is the relative horizontal displacement at the interface (in mm), and K_s is the shear reaction modulus of the interface (in MPa/mm).

The well-known elastic layered computer program BISAR [Shell, 1998] employs the concept of shear spring compliance to account for the relative displacements (slip) between pavement layers. The shear spring compliance is the inverse of the shear reaction modulus at the interface between adjacent layers. The definition of the shear spring compliance, AK, is given by:

$$AK = \frac{\text{relative horizontal displacement between layers}}{\text{shear stress acting at the interface}} \left[m^3 / N \right] \tag{2.2}$$

The relation is treated mathematically through the parameter α, defined as:

$$\alpha = \frac{AK}{AK + \frac{1+\upsilon}{E}.a} \tag{2.3}$$

where a denotes the radius of the load (m), E is the modulus of the layer above the interface (Pa), v is the Poisson's ratio of that layer and α is the friction parameter of the interface (with $0 \leq \alpha \leq 1$, $\alpha = 0$ means full bond, $\alpha = 1$ means full slip).

Kruntcheva *et al.* [2000b] used a thin, soft elastic interlayer material inserted between the surfacing and binder course to simulate the interface bond condition in a Finite Element (FE) analysis using the ANSYS software [Ansys Inc, 1999]. The model was tested for different pavement layer thicknesses and interlayer stiffnesses. The results were compared to the results obtained from another analysis using BISAR software [Shell, 1998].

Romanoschi and Metcalf [2002] divided the typical shear stress-displacement curve of the interface between adjacent pavement layers into three stages (Figure 2.9 (a)):

- Linear shear stage (0-1). At this stage, linear behaviour characterises the shear stress-displacement relationship. Failure occurs when the shear strength of the interface, Smax, is reached.
- Post failure stage (1-2). This stage is representing the condition when the interface has failed but the adjacent layers have not been completely separated and still exhibit some shear resistance.
- Friction stage (2-3). After the adjacent layers have been completely separated, a friction model characterises the contact between adjacent layers.

Due to the cyclic nature of the load at pavement interfaces and since the post failure stage may appear only once, they considered that only the linear shear and friction stages were useful to characterise the interface condition. A two-stage interface constitutive model presented in Figure 2.9(b) was proposed and incorporated into an FE analysis using ABAQUS software [Hibbitt, Karlsson and

Sorensen, Inc., 2004]. In the first stage, the interface shear displacement is proportional to the interface shear stress until the interface shear strength is reached. Once the interface has failed, the behavior is characterized by the friction coefficient, μ.

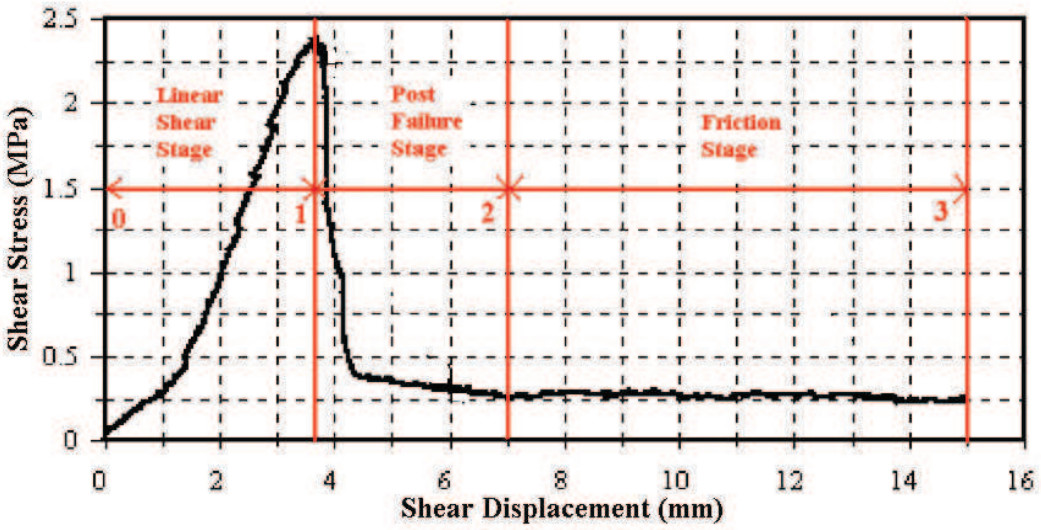

(a) Typical shear stress-displacement curve

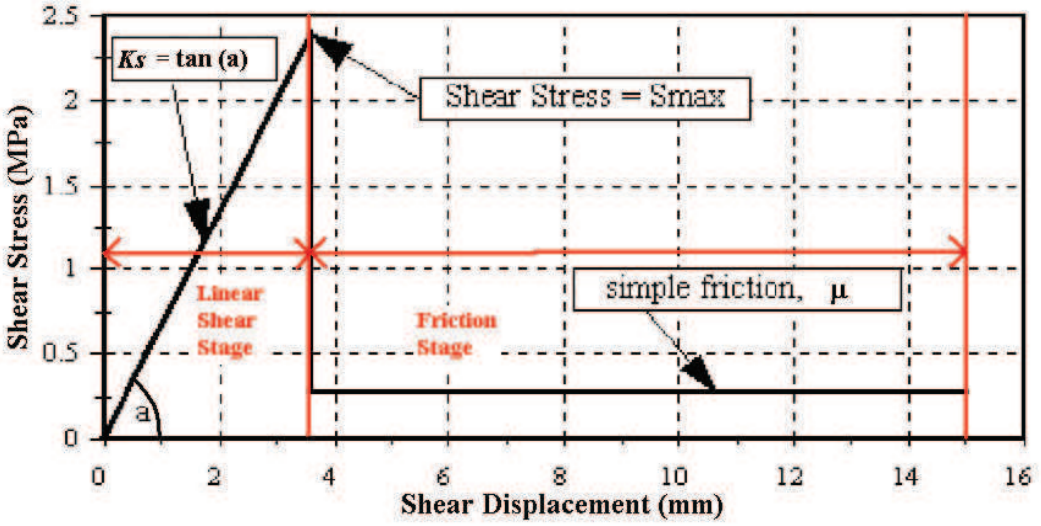

(b) Two-stage interface constitutive model

Figure 2.9 – Typical shear stress-displacement curve and two-stage interface constitutive model proposed by Romanoschi and Metcalf (Adapted from Romanoschi and Metcalf, 2002)

Ozer *et al.* [2008] introduced a fracture based friction model to characterise pavement layer interfaces. A fracture based elasto-plastic constitutive relationship was implemented in the frictional interface model. Various modes of strength degradation at the interface (pure tensile, pure shear, shear with tensile and shear with compression) were formulated by a nonlinear softening model and integrated into the elasto-plastic constitutive model. Interface elements were developed and incorporated as user elements (UEL) in an FE analysis using ABAQUS software [Hibbitt, Karlsson and Sorensen, Inc., 2004]. The model was validated with an experimental investigation performed by Canestrari and Santagata [2005].

Among those aforementioned models to characterise the interface bond condition; the shear reaction modulus, K_s, seems to be the most widely used by researchers. Although the models incorporated into the FE analysis might be more accurate in representing the bond conditions, the parameter *Ks* is less complicated and can easily be incorporated into the well known BISAR software to analyze the effect of bond on the state of stress, strain and deflection within the pavement structure.

2.4.3 Theoretical Studies on the Effect of Bond on Pavement Performance

Romain [1968] investigated the influence of bond in a four layer structure as shown in Figure 2.10, where layer thicknesses and stiffnesses are shown relative to the contact radius and subgrade stiffness, respectively. Using the solutions provided by Burmister [1945], fully bonded and fully slipped interfaces were used to show the effect of bond on the variation of stresses, strains and deflections. As cited by Uzan *et al.* [1978], the results shown in Table 2.1 demonstrate the typical increment of stresses, strains and deflections when bond conditions at the interfaces change from full bond to full slip. The higher maximum tensile strains in the first layer compared to those in the second layer, when the interface between the first and the second layers is fully slipped, may cause the first layer to fail more rapidly than the second layer.

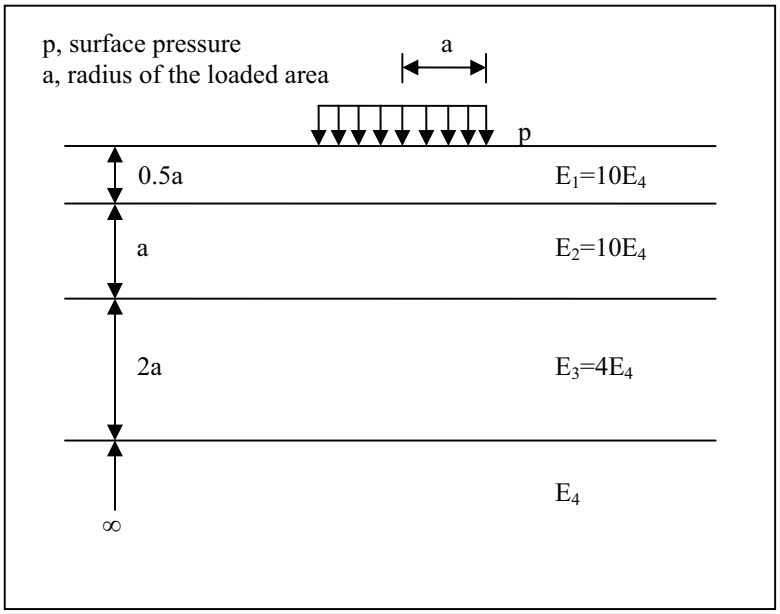

Figure 2.10 – Schematic drawing of the four layer pavement studied by Romain (Adapted from Romain, 1968 and Uzan *et al.*, 1978)

Table 2.1 Relative results of four-layer pavement considering different bond conditions (Adapted from Romain, 1968 and Uzan *et al.*, 1978)

	Bond conditions			
	First layer – second layer	**Full slip**	**Full bond**	**Full slip**
	Second layer – third layer	**Full bond**	**Full slip**	**Full slip**
	Third layer – fourth layer	**Full bond**	**Full bond**	**Full bond**
First layer	Max. compressive stress	0.79	1.07	0.89
	Max. tensile stress	2.19	1.92	2.69
	Max. compressive strain	2.83	1.07	3.07
	Max. tensile strain	1.93	1.10	2.07
	Deflection	1.20	1.19	1.43
Second layer	Max. compressive stress	1.74	0.98	1.81
	Max. tensile stress	1.08	2.26	2.73
	Max. compressive strain	1.27	1.72	2.25
	Max. tensile strain	1.30	1.44	1.89
Third layer	Max. compressive stress	1.55	1.48	2.29
	Max. tensile stress	1.38	1.23	1.77
	Max. compressive strain	1.28	0.92	1.18
	Max. tensile strain	1.22	0.92	1.29
Fourth layer	Max. compressive stress	1.40	1.74	2.40
	Max. compressive strain	1.37	1.37	1.97
	Deflection	1.19	1.39	1.58

Uzan *et al.* [1978] analysed the influence of bond between the surfacing and the binder course in a four layer structure (Figure 2.11) using the BISAR computer program [Shell, 1998]. As clearly seen in Figure 2.12, they found significant change in the radial tensile stress when the shear reaction modulus K_s varied between 1 and 100 MPa/mm. Furthermore, they investigated the influence of interface conditions on the distribution of radial (horizontal) strain through the whole depth of the pavement structure. As shown in Figure 2.13, they found an increase of the radial tensile strain at the bottom of the surfacing and the asphaltic concrete layer when K_s varied from full adhesion (full bond) to perfectly smooth (full slip). It can also be seen that the radial (horizontal) tensile strain at the bottom of the surfacing exceeds the strain at the bottom of the asphaltic layer and the radial (horizontal) strain at the top of the asphaltic concrete layer shifts to compressive when the interface condition is changed to full slip. This condition could cause the surfacing to fail more rapidly than the asphaltic concrete layer.

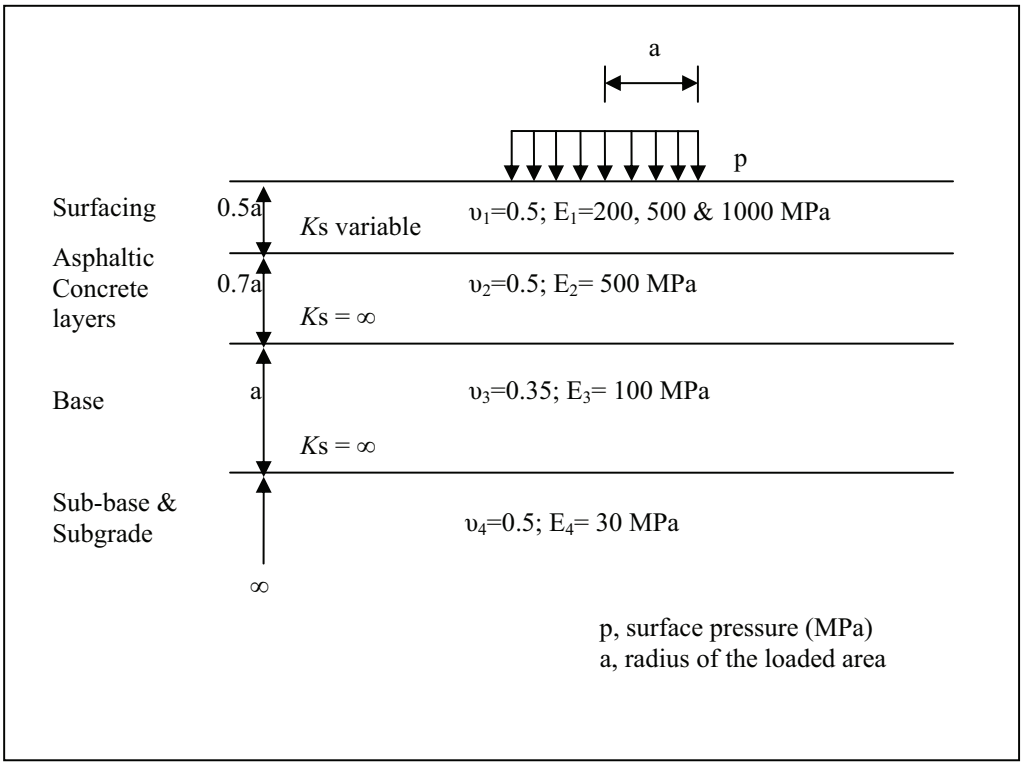

Figure 2.11 – Schematic drawing of the four layer structure analysed by Uzan *et al.* (Adapted from Uzan *et al.*, 1978)

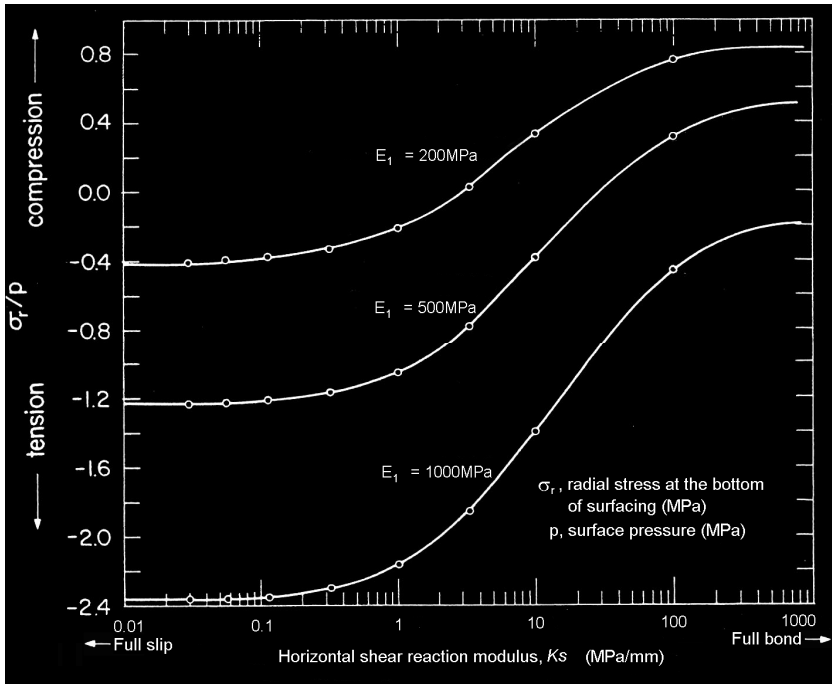

Figure 2.12 – Influence of interface condition on radial stress at the bottom of surfacing (Adapted from Uzan *et al.*, 1978)

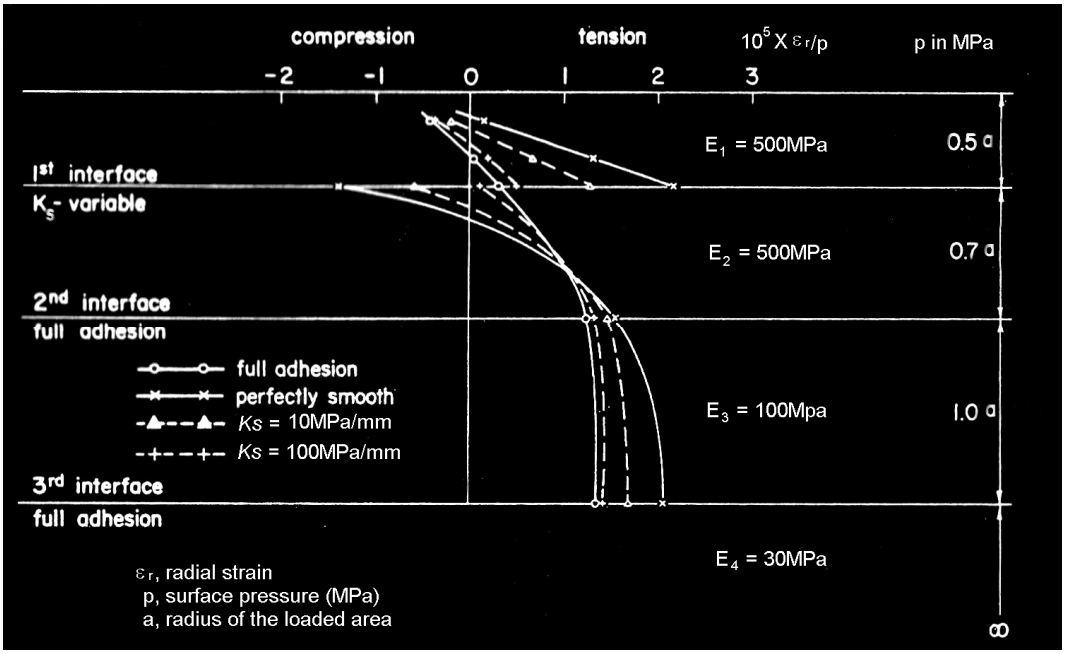

Figure 2.13 - Distribution of horizontal strain with depth (Adapted from uzan *et al.*, 1978).

Brown and Brunton [1984], using the BISAR program, studied the influence of bond at either the first or the second interface on the lives of several pavement structures. The results of their calculations as shown in Figure 2.14 demonstrate the reduction of pavement lives up to 75% if the interface condition changes from full bond to full slip. It can also be seen that the changes of bond condition at the second interface typically have more significant effect than the changes at the first interface. Like Uzan *et al.* [1978], they considered the two extreme interface conditions (i.e. full bond and full slip) as unrealistic. Subsequently, they used a value of 0.7 as friction parameter of the interface α (K_s= 6.6 ~ 9.9 MPa/mm, depending on the material used) to represent the intermediate bond condition. They concluded that an intermediate bond condition at the interface could potentially reduce the life of the pavement by up to 30%.

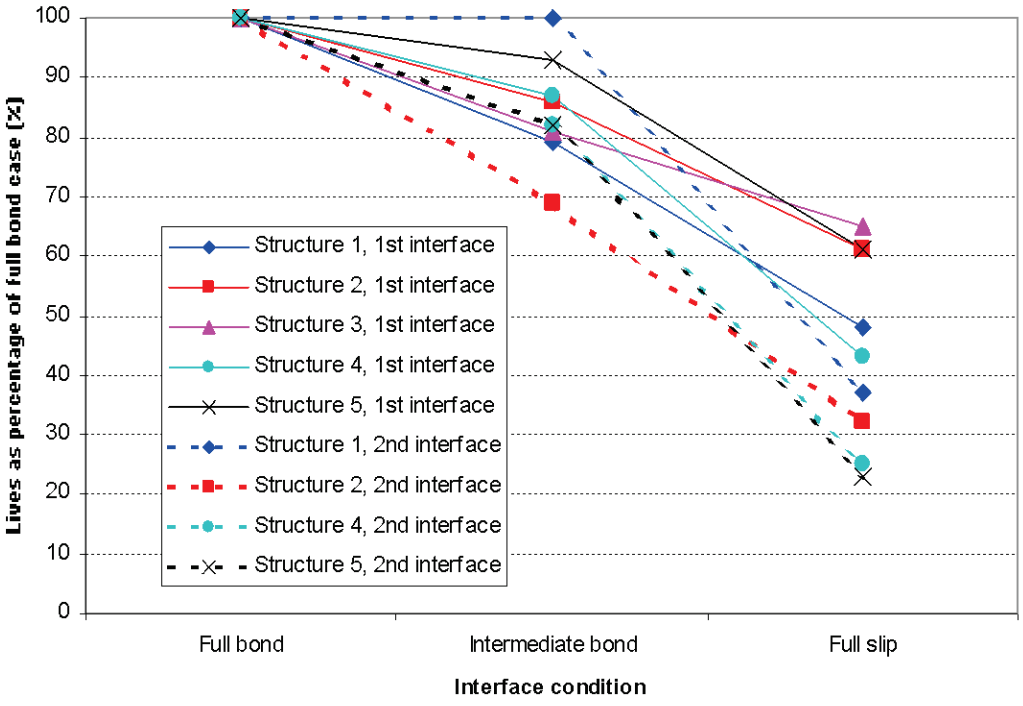

Figure 2.14 - Influence of bond conditions on pavement lives (Adapted from Brown and Brunton, 1984)

Shahin *et al.* [1987] used the BISAR program to investigate the effect of bond between an asphalt overlay and the underlying old surfacing in an airport pavement under a 106kN DC-9 aircraft load. It should be noted the tyre contact pressure of the DC-9 aircraft of 900kPa [Douglas Aircraft Company, 1984] is 50% higher than that of the standard wheel load normally used in the design of road pavements. Figure 2.15 shows the effect of slippage on the distribution of the horizontal strain. If slippage occurs, the horizontal tensile strain exists at the bottom of the asphalt overlay and the magnitude exceeds the horizontal tensile strain at the bottom of the old asphalt surfacing. They presented the effect of bond on the number of DC-9 load repetitions (Figure 2.16). They concluded that in the case of slippage, the asphalt overlay could fail more rapidly rather than the old surfacing.

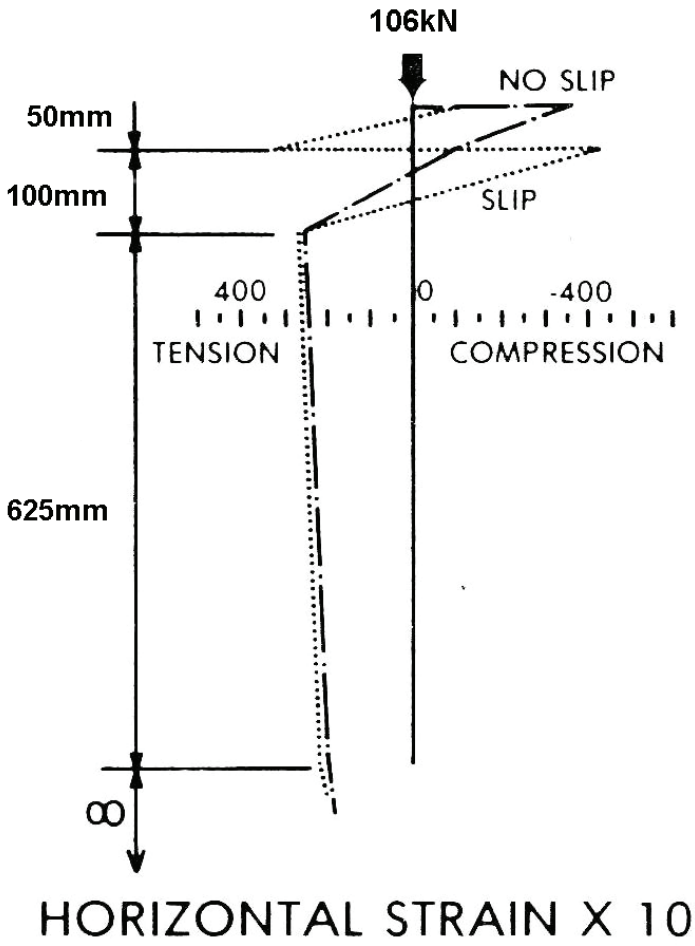

Figure 2.15 - Distribution of horizontal strain (Adapted from Shahin *et al.*,1987)

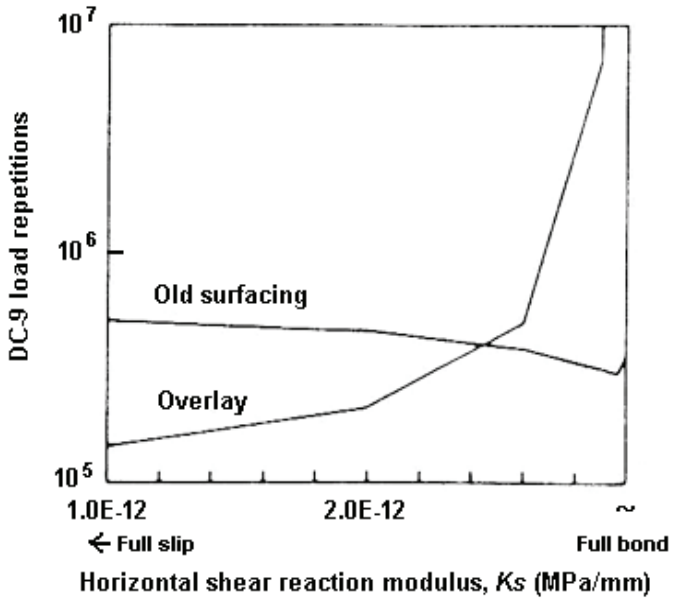

Figure 2.16 - Effect of bond on pavement life (Adapted from Shahin *et al.*,1987)

Shahin *et al.* [1987] also investigated the effect of horizontal loads on the top pavement surface. Horizontal loads are applied to the pavement surface when the aircraft accelerates, decelerates, brakes or turns. The magnitude of the horizontal load is driven by the friction coefficient between the tyre and the pavement surface, which will vary with pavement and tyre conditions up to a limiting value of 0.8 [Barber, 1962]. Assuming the horizontal load is half of the vertical load, Shahin *et al.* [1987] compared the horizontal strain at the surface of the overlay, with and without the presence of interlayer slippage as shown in Figure 2.17. As clearly seen in Figure 2.17, there was almost a 50% increase in the maximum horizontal tensile strain at the top of the surfacing when K_s changed from full adhesion (full bond) to perfectly smooth (full slip). Furthermore, they investigated the distribution of the maximum tensile strains on the pavement surface and their directions. Figure 2.18 shows that the largest tensile strain is located just outside the contact area and the direction is 180 degrees from the direction of the applied horizontal load. They stated that the high magnitude of tensile strains along the edge of the contact area (Figure 2.18) can lead to progressive failure around the back edge of the contact

area and concluded that this behaviour agrees with the crescent shaped slippage crack shown in Figure 2.19.

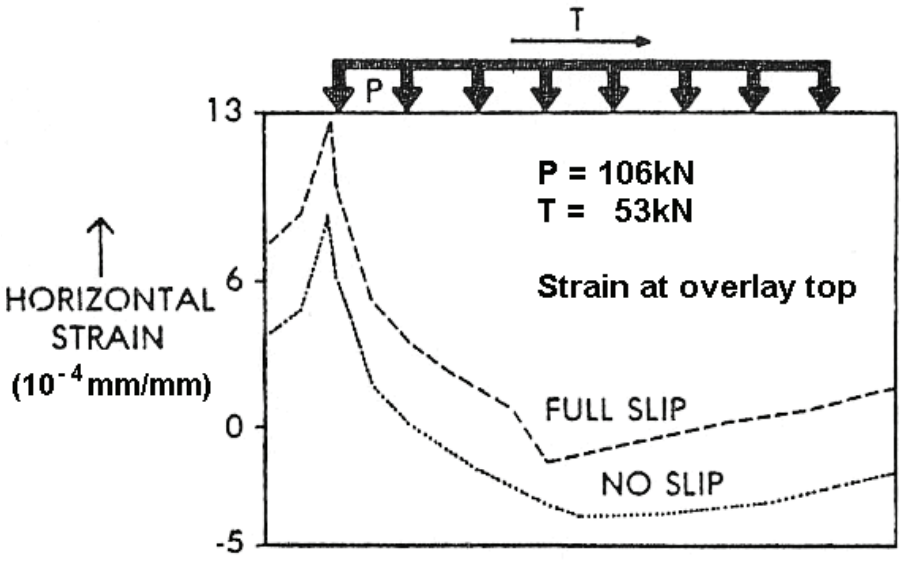

Figure 2.17 - Effect of bond and horizontal load on horizontal strain on the pavement surface (Adapted from Shahin *et al.*, 1987)

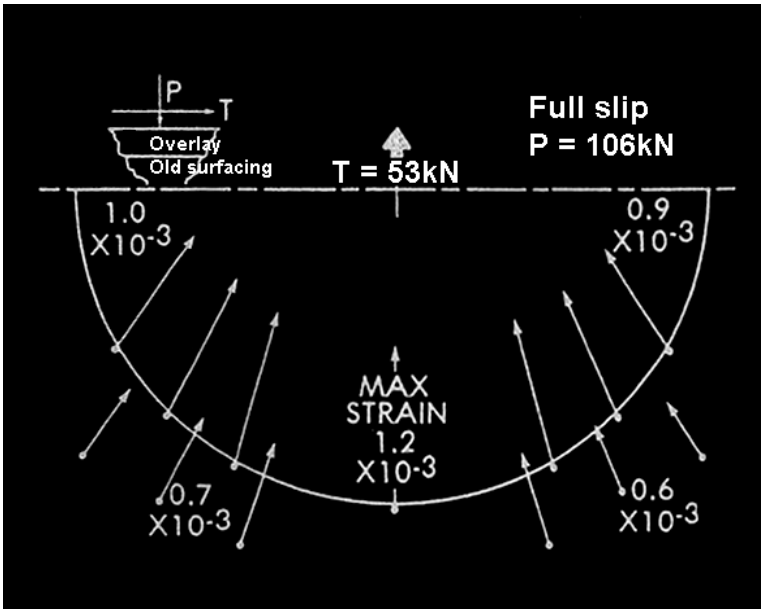

Figure 2.18 – Distribution of tensile strains on the pavement surface along the edge of the contact area (Adapted from Shahin *et al.*,1987)

Figure 2.19 – Crescent shaped slippage crack (From West *et al.*,1987)

After performing numerical analysis to identify the range of bond condition, Al Hakim [1997] concluded that shear reaction modulus varies from 0.01 MPa/mm to 100 MPa/mm and there is no significant difference in pavement response beyond these two limits. Subsequently, the researcher divided the bond condition into three ranges of shear reaction modulus, K_s, as follow:

- $K_s \leq$ 0.01 MPa/mm full slip;
- 0.01 MPa/mm$< K_s <$100 MPa/mm intermediate case;
- $K_s \geq$ 100 MPa/mm approximately full bonding

Al Hakim [1997] investigated the effect of bond at the interface between the surfacing and the binder course on the lives of four typical pavement structures classified as weak, medium, strong and very strong. The shear reaction modulus K_s was taken to vary between 0.01 MPa/mm (full slip) and 100 MPa/mm (approximately full bond). Figure 2.20 shows the reduction of pavement life by up to 40%, when the shear reaction modulus decreases from 100MPa/mm to 10MPa/mm. When full slippage occurs, the pavement life could decrease by over 50%.

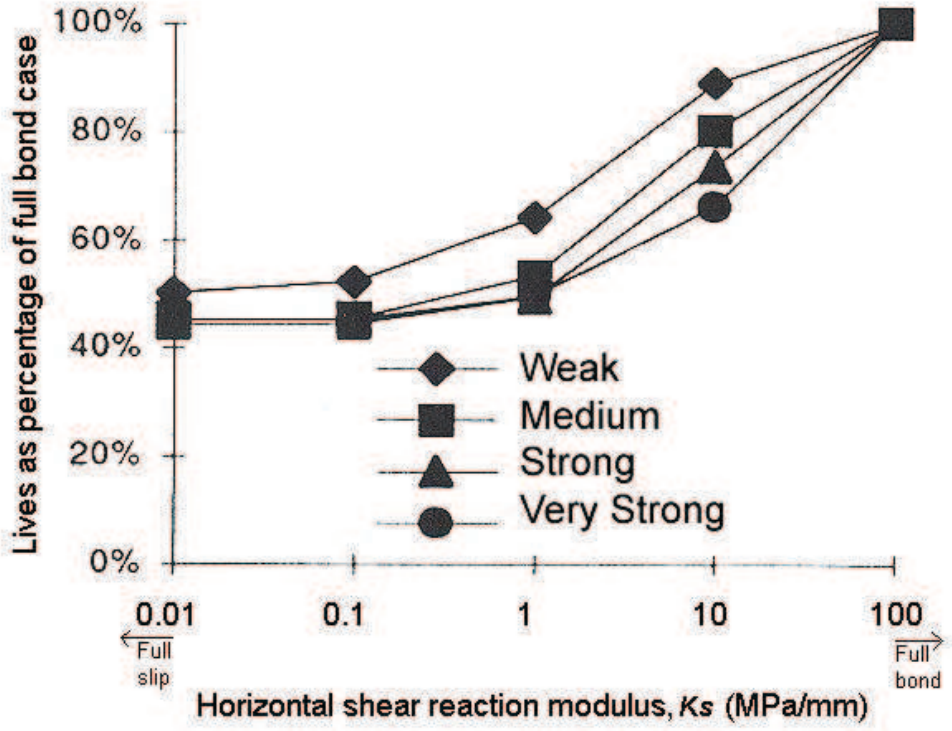

Figure 2.20 - Influence of bond on pavement life (Adapted from Al Hakim, 1997)

Hachiya and Sato [1997] utilised the BISAR program to investigate the influence of bond between the surfacing and the binder course in an airport pavement structure. They found that the reduction of surfacing thickness typically increases the shear stress at the interface underneath the surfacing, which may cause a more critical bond condition at this interface. Furthermore, the shear stress becomes larger when a horizontal loading exists. In terms of the effect of bond, Figure 2.21 shows that the horizontal tensile stresses at the bottom of the surfacing of the smooth (fully slipped) interfaces are typically five times higher than with the rough (fully bonded) interfaces.

Kruntcheva *et al.* [2000b] employed the computer program BISAR to investigate the influence of bond condition on pavement life to failure. They considered three configurations of loading and bond condition in the analysis: 1) standard vertical dual load, single partially bonded interface; 2) standard vertical dual load, multiple partially bonded interfaces; 3) standard vertical dual load +

horizontal friction force, single partially bonded interface. They followed Al Hakim *et al.* [1998] in classifying the value of the shear reaction modulus less than 0.01MPa/mm as a fully slipped interface and higher than 100MPa as a fully bonded interface. Some of their findings are shown in Figure 2.22. According to the analysis, they concluded that:

- Full slip between the binder course and the base could reduce the pavement life up to 80%, whereas full slip at the other interfaces could reduce the pavement life approximately 40%.
- The inclusion of horizontal friction force could significantly reduce the pavement life with respect to the bond condition between the surfacing and the binder course.

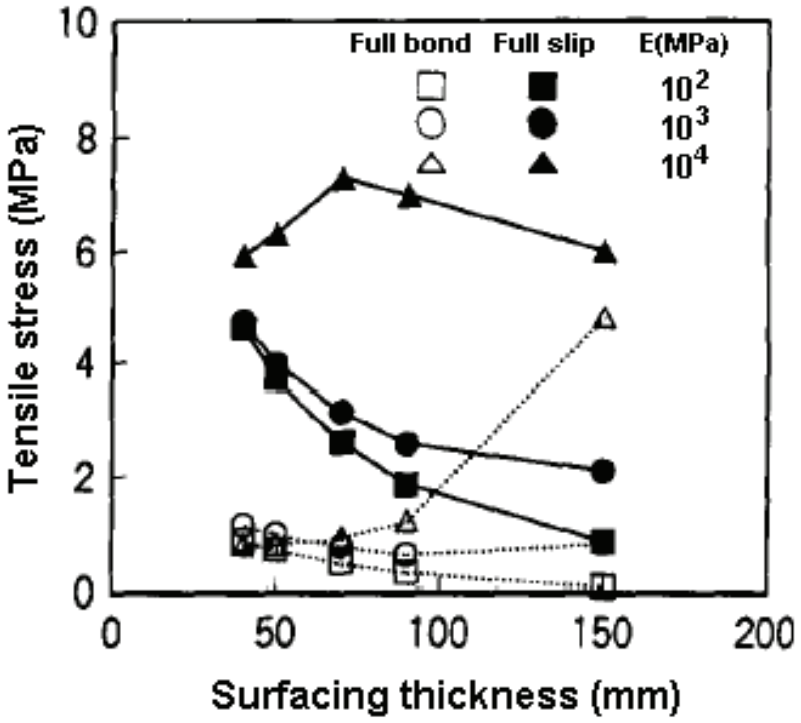

Figure 2.21 - Effect of bond condition and the thickness of the surfacing (i.e. wearing course) on horizontal tensile stress at the bottom of the surfacing (From Hachiya and Sato, 1997)

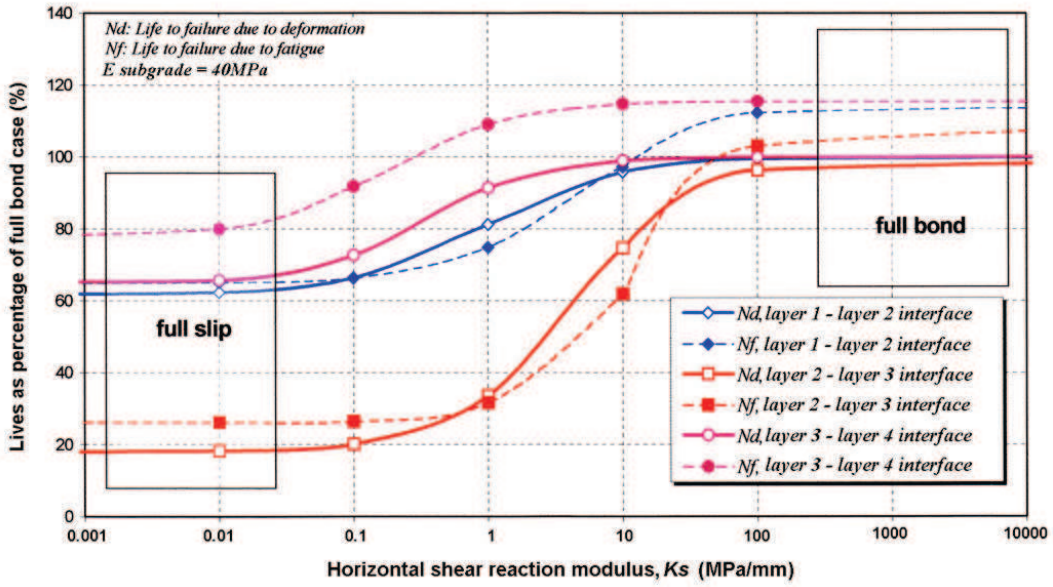

Figure 2.22 - Influence of bond on pavement life (From Kruntcheva *et al.*, 2000)

The review of theoretical investigations on the effect of bond on pavement performance showed that bond between layers is an important component of the whole pavement structure and proper bonding is essential to ensure good pavement performance. Because of that, the determination of mechanical properties of bond at the interface between layers is of significant importance and several test methods have been developed in different countries.

2.5 Testing of Bond between Pavement Layers

To quantify the mechanical properties of the interface between pavement layers, two approaches are broadly used:

- Destructive testing carried out in-situ or in the laboratory and,
- Non-destructive tests carried out on existing pavements.

Although the following summary does not include all the test methods currently used in the world to assess bond condition at the interface between pavement layers, it can be considered as reasonably comprehensive.

2.5.1 Destructive Tests

According to where the test is performed, destructive testing can be categorised into in-situ destructive testing and laboratory destructive testing. The in-situ destructive testing is usually performed by partially coring or cutting the pavement structure, followed by in-situ testing. Whereas the laboratory destructive testing is usually performed by taking the samples from the pavement structure or laboratory manufactured specimens, followed by laboratory testing.

2.5.1.1 Tensile bond test

The tensile bond test is a commonly used method to determine the tensile bond strength [Tschegg *et al.*, 1995] and it is a standard method in Austria [Roffe and Chaignon, 2002]. In the UK, the tensile bond test is used as a standard test method for determining the bond between concrete pavement layers in BS EN 13863-2 [British Standards Institution, 2003e].

The tensile bond test can be performed either in laboratory or in-situ. The laboratory tensile bond test is typically performed by taking cores or slabs from the pavement structure or laboratory manufactured specimens. Metal plates are glued to the top and bottom surfaces of the specimens. A tension machine is then used in the axial direction to pull the specimen off. This laboratory test can be used to determine the tensile bond properties at each interface between bound layers within the pavement structure by cutting the specimen at the positions above and below the interface of interest. Testing at different temperatures can be performed by conditioning the specimens in a temperature controlled cabinet prior to testing.

In Germany, the tensile bond test is used to determine the tensile bond strength beneath a thin layer [DIN, 2003]. In this test, partial coring of 100mm diameter is performed (until approximately 10mm below the interface) on a 150mm core specimen and a 100mm diameter plunger is glued to the surface of the core. A steel ring is then placed around the plunger and fixed to the base support. The tension testing machine is then used to pull the plunger in the axial direction. A schematic diagram of this pull-off test is shown in Figure 2.23.

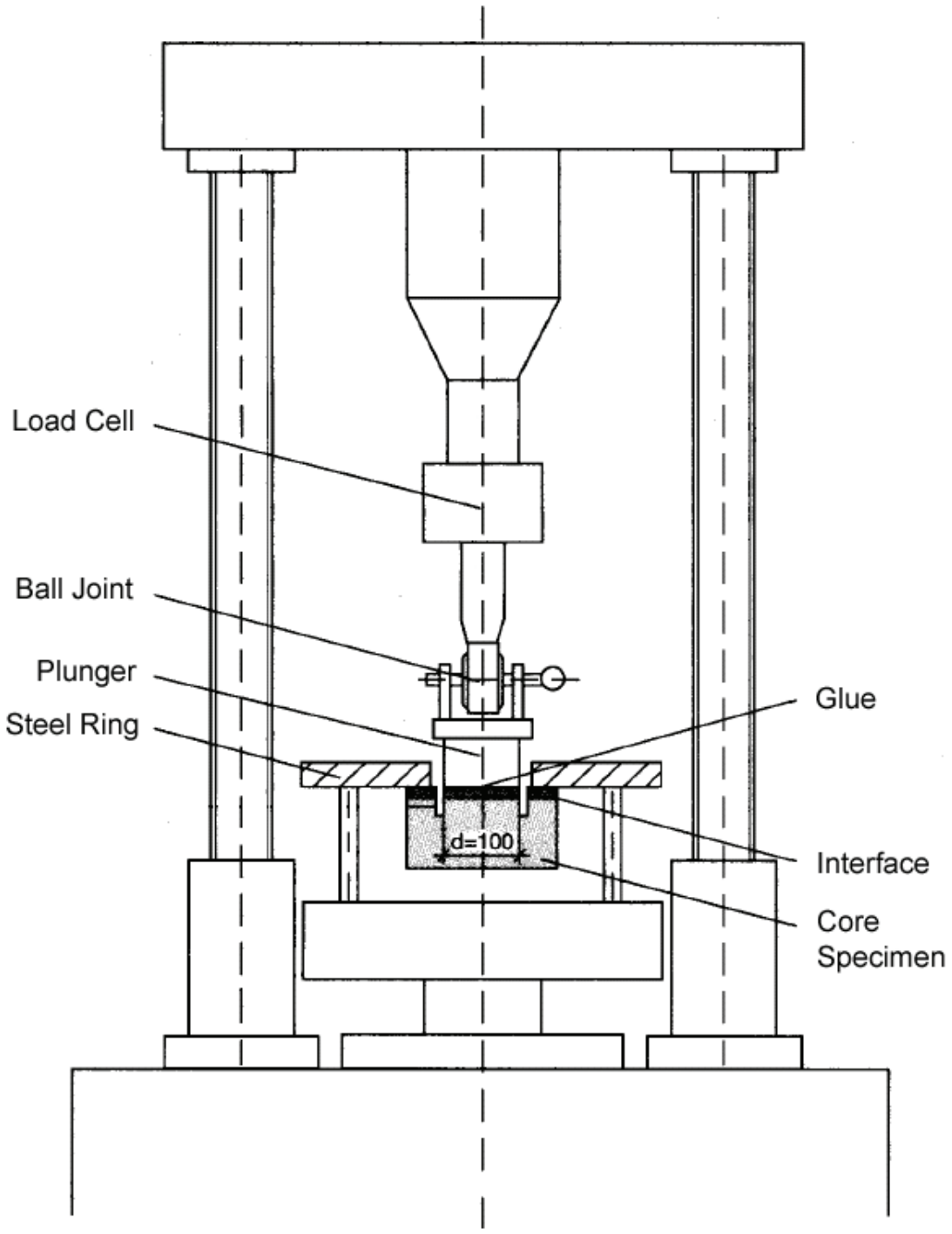

Figure 2.23 – Schematic diagram of the tensile bond test used in Germany (From DIN, 2003)

In the in-situ tensile bond test, a partial core or cut is carried out until a certain depth below the interface of interest. A metal plate, glued on top of the surfacing, is attached to an in-situ tension machine and the top layer is pulled-off in the axial direction. This in-situ test is typically limited to the interface between the surfacing and the layer below. Figure 2.24 shows the in-situ tensile bond test used by the Swiss Federal Laboratories for Materials Testing and Research (EMPA) to measure the tensile bond properties at the interface of an asphalt surfacing laid over a concrete lower layer [Raab and Partl, 1999].

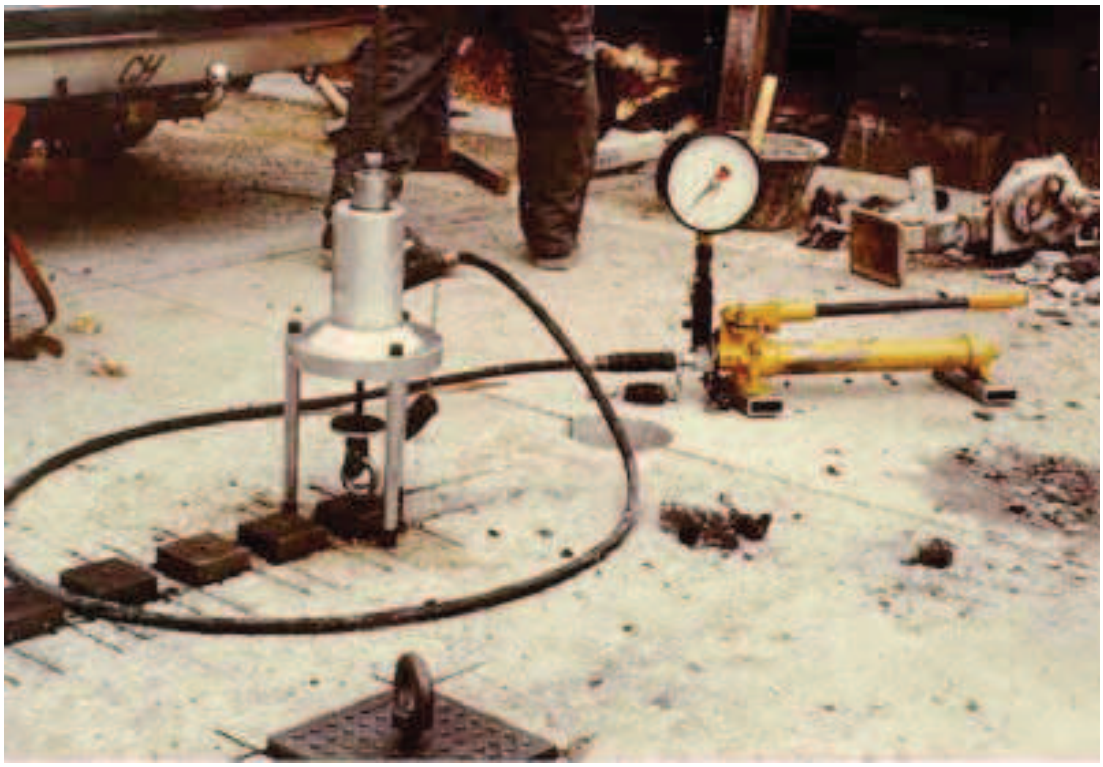

Figure 2.24 – In-situ tensile bond test (From Raab and Partl, 1999)

Tschegg *et al.* [1995] and Partl and Raab [1999] noted that tensile bond tests show extensive scattering of results. This could be caused by many factors, the most significant of which include eccentric loading, small core diameters and/or large aggregate size and strain concentrations resulting from constrained radial strains. The test is also not suitable for determining the interface bond properties when the tensile strength of the asphalt layer is lower than the tensile strength of the

interface. Furthermore, the test measures only the tensile bond strength and can not be used to assess the effect of aggregate interlock at the interface.

2.5.1.2 Torque bond test

The torque bond test is typically performed by twisting the top of a core specimen at a constant torque or rotation rate to induce a twisting shear failure at the interface. The value of torque at failure is recorded and the shear strength of the interface can then be calculated using equation (4.4) or equation (4.5), explained later in Chapter 4. The torque bond test is available in both manual and mechanically controlled variants.

According to Walsh and Williams [2001], the manual torque bond test was originally developed in Sweden for in-situ assessment of bond condition. In this test, a partial core is taken (encompassing the interface of interest) and a torque is applied manually at the top of the core. The testing procedure of the manual torque bond test in the guidelines document SG3/98/173 [British British Board of Agreement, 2000] requires the torque is applied manually at a constant torque rate so that failure occurs in (60±30) seconds. This procedure results in difficulty in controlling the torque rate, because the torque strength is unknown and the value of the torque strength is also affected by the torque rate. To avoid the aforementioned difficulty, Choi *et al.* [2005] used a constant torque rate of 600Nm/minute, which was achieved by synchronising the movement of the torque dial gauge with the second hand of an analogue clock. Babtie [2000] also found it difficult to keep the application of torque parallel to the interface resulting in axial bending on the specimen. Additionally, they reported that considerably high force is needed to twist off the surfacing and that sudden failure could lead to the risk of strains and falls to the operator.

For practical reasons, the manual torque bond test is generally limited to the interface between thin surfacing and the lower layer material and is typically undertaken in-situ. Choi *et al.* [2005] developed a laboratory-based manual torque bond test that allows the test to be undertaken in a more controlled environment (Figure 2.25). This laboratory-based manual torque bond test is able to test the

shear strength of an interface other than the interface below the surfacing by taking a full depth core and cutting the core specimen at the positions above and below the interface of interest. The core is then clamped below the interface using a clamping unit which is rigidly fixed to the floor. The core must be clamped properly to give a firm grip, so that it does not rotate during testing. However, care is necessary to avoid over tightening and consequent damage to the specimen. Testing at various temperatures is also possible by conditioning the core specimen in a temperature controlled cabinet.

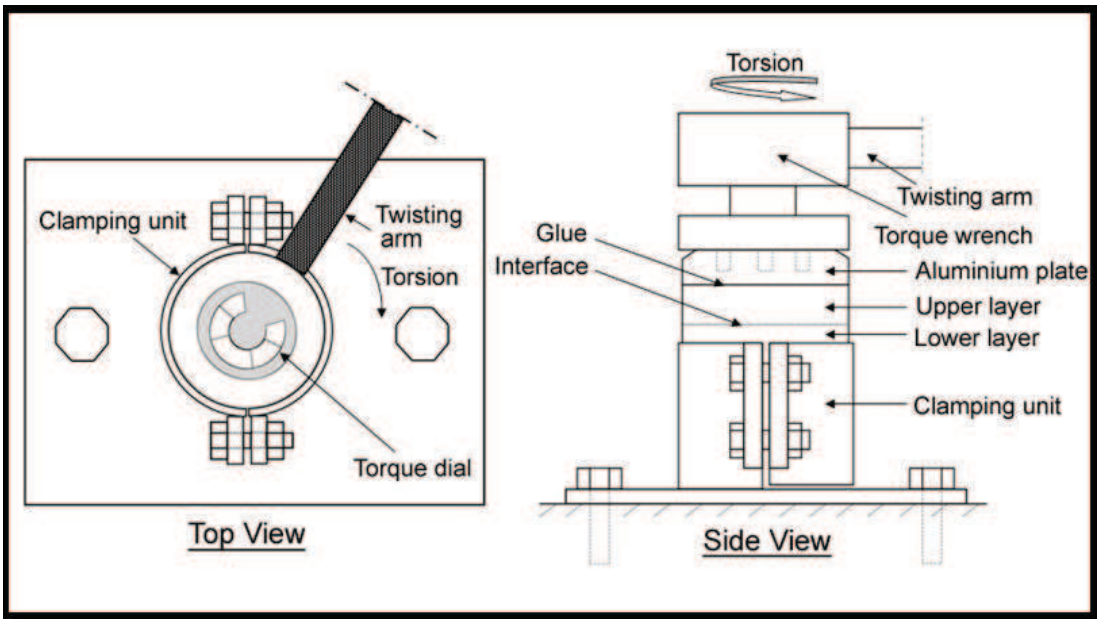

Figure 2.25 – Schematic diagram of the laboratory based manual torque bond test developed by Choi *et al*. [2005]

In 2004, the guidelines document SG3/05/234 [British Board of Agreement, 2004] superseded the guidelines document SG3/98/173 [British British Board of Agreement, 2000]. The guidelines document SG3/05/234 requires the test to be performed at a constant rotation rate so that the torque wrench sweeps an angle of 90° within (30±15) seconds. It should be noted that due to the effect of adjacent layers stiffnesses and thicknesses, the rotation at the interface may be different to that of the torque wrench (see section 4.2 in Chapter 4). Therefore, the variability of the actual rotation rate at the interface would be affected by the variability of stiffnesses and thicknesses of the adjacent layers, which may lead to more variable

results. It is also interesting to note that in both the guidelines document SG3/98/173 and the guidelines document SG3/05/234, the manual torque bond test is applied without lateral support at the top part of the specimen (see also Figure 2.25). This condition may cause the appearance of lateral shear stress acting at the interface in addition to the interface shear stress induced by the torque.

A mechanically controlled in-situ torque test known as the CISST (Carleton In-situ Shear Strength Test) has been developed in Carleton University, Canada [El Halim *et.al.*, 1997]. The test was designed to determine the in-situ shear strength of the surfacing material, but it can also be used to measure the interface torque bond strength between the surfacing and the layer underneath. Similar equipment named the TVIST (Torsional vibration and in-situ testing) was developed by EMPA to measure the interface torque bond strength [Raab and Partl, 1999]. The TVIST is able to apply both torsion and vertical loadings and it is available in both in-situ (Figure 2.26(a)) and laboratory (Figure 2.26(b)) variants.

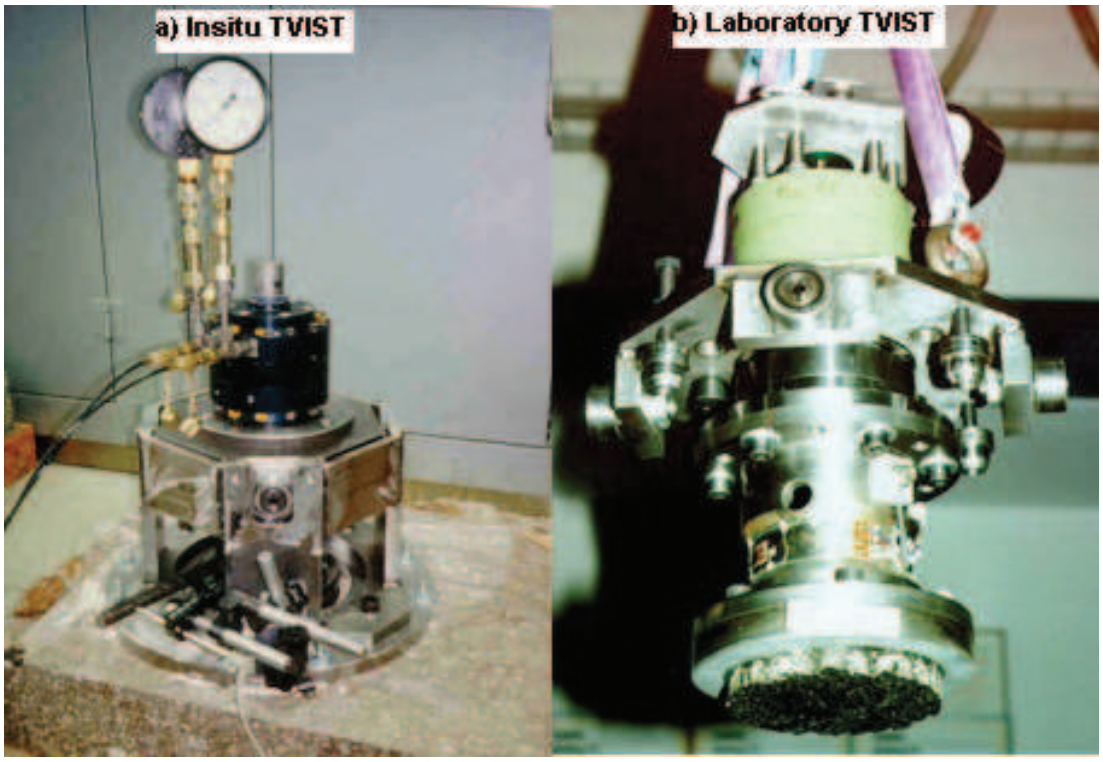

Figure 2.26 – TVIST equipments (From Raab and Partl, 1999)

Diakhaté *et al*. [2006, 2007] also developed a mechanically controlled torque bond apparatus (Figure 2.27). The apparatus has a chain-sprocket mechanism to transfer a tensile force generated by a tension testing machine and convert it into a torque. Using this apparatus, the loading rate can be controlled accurately. However, both the manual and mechanically controlled torque bond tests share a limitation related to the inability to determine interface bond properties when the torque strength of the asphalt layer is lower than that of the interface.

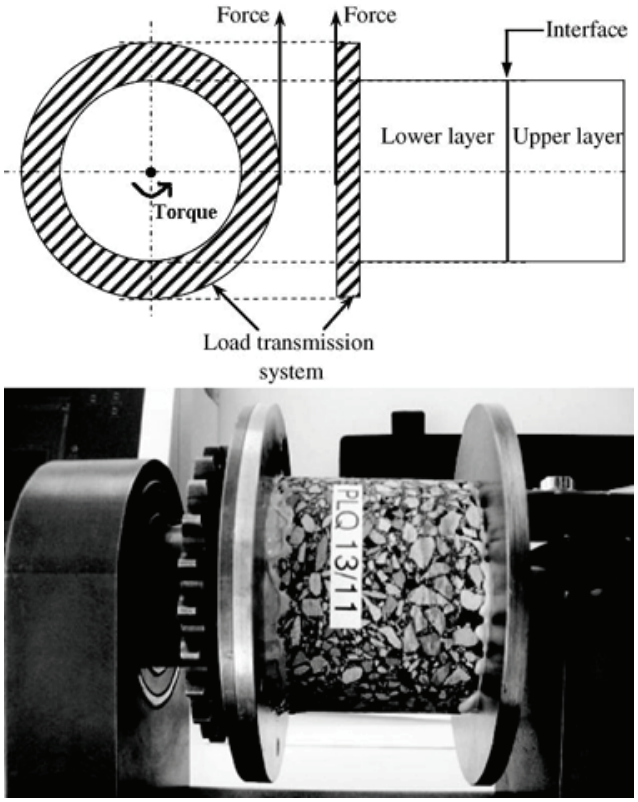

Figure 2.27 – Photograph and schematic diagram of the torque bond apparatus developed by Diakhaté *et al*. [2006, 2007].

2.5.1.3 Direct shear test

The direct shear test is a well-known laboratory test and is a relatively rapid test to investigate the mechanical properties of the interface. This test is able to investigate interface shear strengths and stiffnesses. Figure 2.28 shows a schematic diagram of the direct shear test principle.

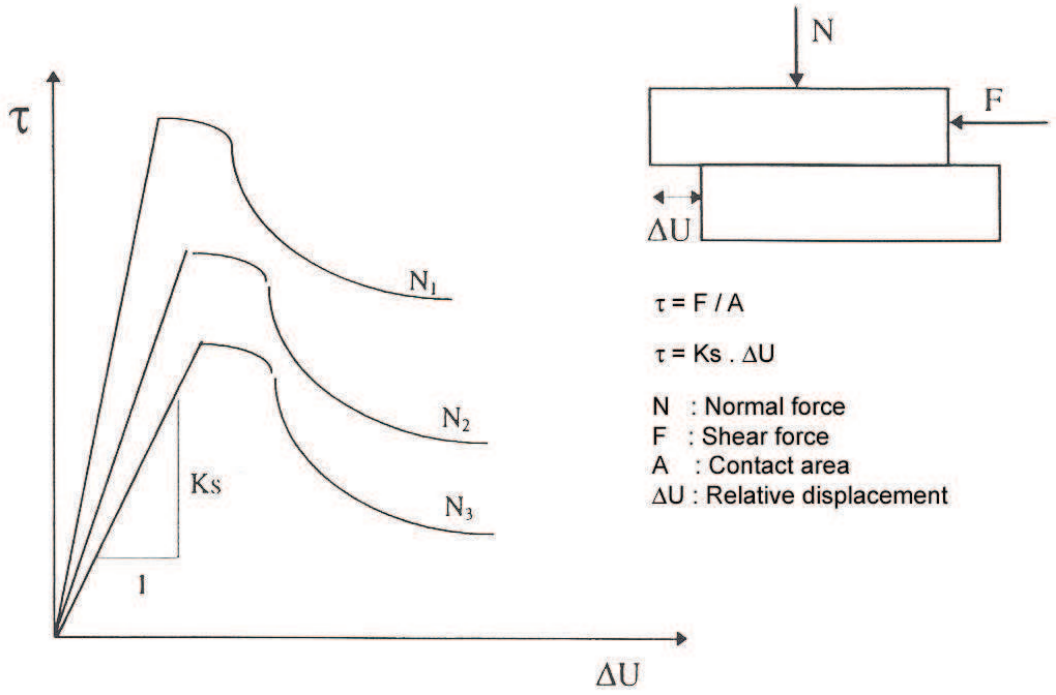

Figure 2.28 - Schematic diagram of the direct shear test principle (From Al Hakim, 1997)

The direct shear test allows the application of shear force parallel to the plane of an interface between layers, which approximates the direction of shear stress in a pavement structure. Many variants of the direct shear test have been developed in different countries. In general, the test can be divided into two categories: direct shear test with normal load and direct shear test without normal load. The main difference between the two categories is that the direct shear test with normal load considers the shear-normal load combination and dilatancy effect, which are not considered in the test without normal load.

Direct shear test with normal load

Uzan *et al*. [1978], using a double layered rectangular specimen of plan dimension 150mm by 100mm, performed the direct shear tests at a constant displacement rate of 2.5 mm/minute to investigate the interface properties between asphalt layers on laboratory prepared samples. They performed an extensive testing programme to investigate the effect of the amount of tack coat, temperatures and normal load.

Conceptually similar equipments named the Dynamic Shear Box developed at The University of Nottingham, UK and the ASTRA (Ancona Shear Testing Research and Analysis) apparatus designed at Università Politecnica delle Marche, Italy have been used by Carr [2001] and Ferrotti [2007], respectively.

The Dynamic Shear Box (Figure 2.29) uses a double layered slab of plan dimension 320mm by 200mm and is subjected to repeated shear loads combined with the application of a normal load. The ASTRA apparatus is capable of testing either prismatic (plan dimension of 100mm by 100mm) or cylindrical (94-100mm diameter) double layered specimens. The ASTRA test is typically carried out at a constant displacement rate of 2.5 mm/minute and a constant vertical load, perpendicular to the plane of the interface, is applied during the test. A schematic diagram of the ASTRA apparatus is presented in Figure 2.30.

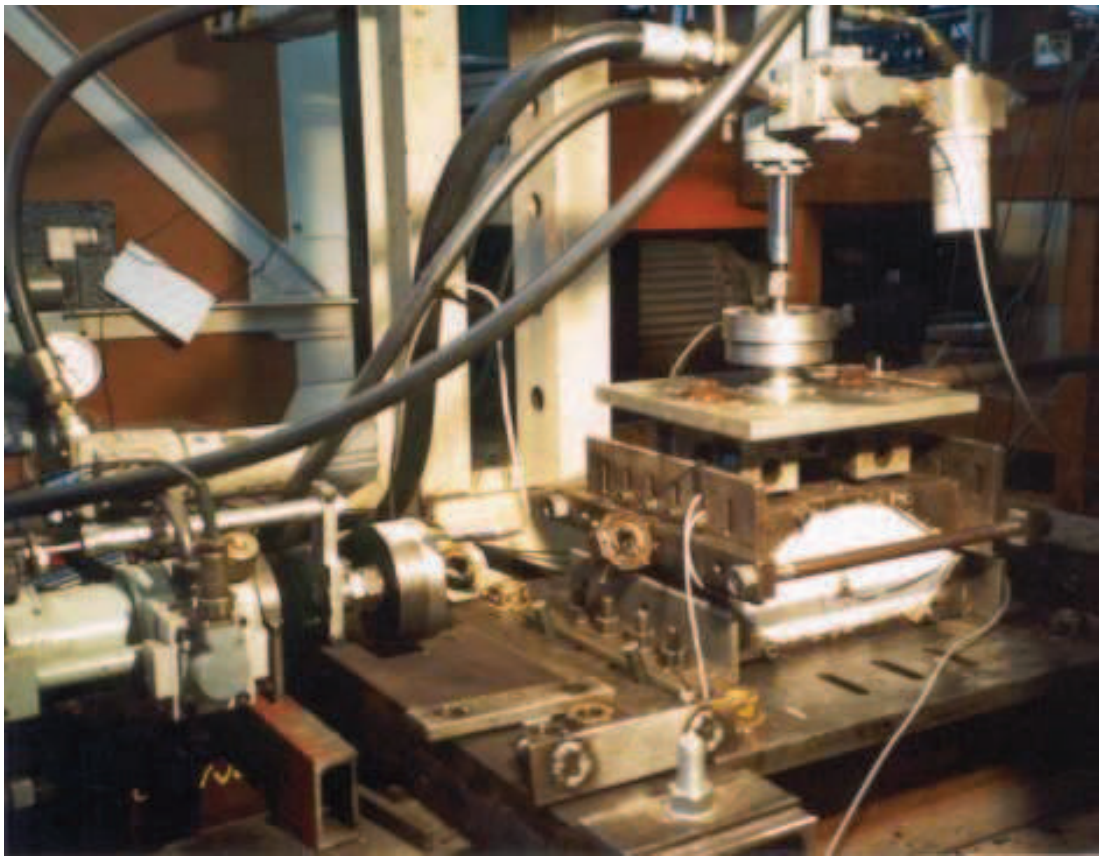

Figure 2.29 – The Nottingham dynamic shear box (From Carr, 2001)

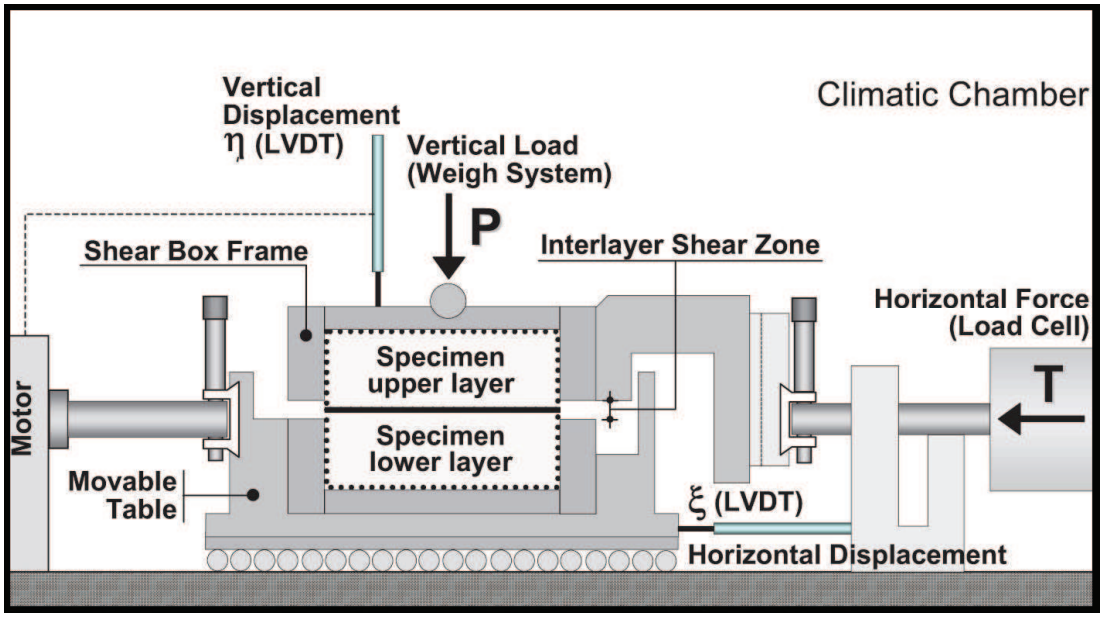

Figure 2.30 - Schematic diagram of the ASTRA apparatus (From Ferrotti, 2007)

Crispino et al. [1997] developed a dynamic shear test to determine the dynamic shear reaction modulus of the interface between asphalt layers. They performed the test at different frequencies and temperatures. They concluded that the dynamic shear reaction modulus of the interface is three times higher than the static shear reaction modulus. The schematic diagram of the dynamic shear tester developed by Crispino et al. [1997] is shown in Figure 2.31.

Mohammad *et al*. [2002] investigated the bond between asphalt layers on several tack coats to determine the optimum application rates. They performed the test by placing a simple shearing apparatus inside the Superpave Shear Tester (SST). The shearing apparatus as shown in Figure 2.32 is specifically designed to ensure that failure occurs at the interface of a cylindrical specimen 150 mm in diameter. The specimen is subjected to shearing load at a constant rate of 222.5N/min until failure. The applied shear loads and their corresponding shear displacements are recorded, so that a shear stress-displacement curve as well as shear strength of the interface can be obtained.

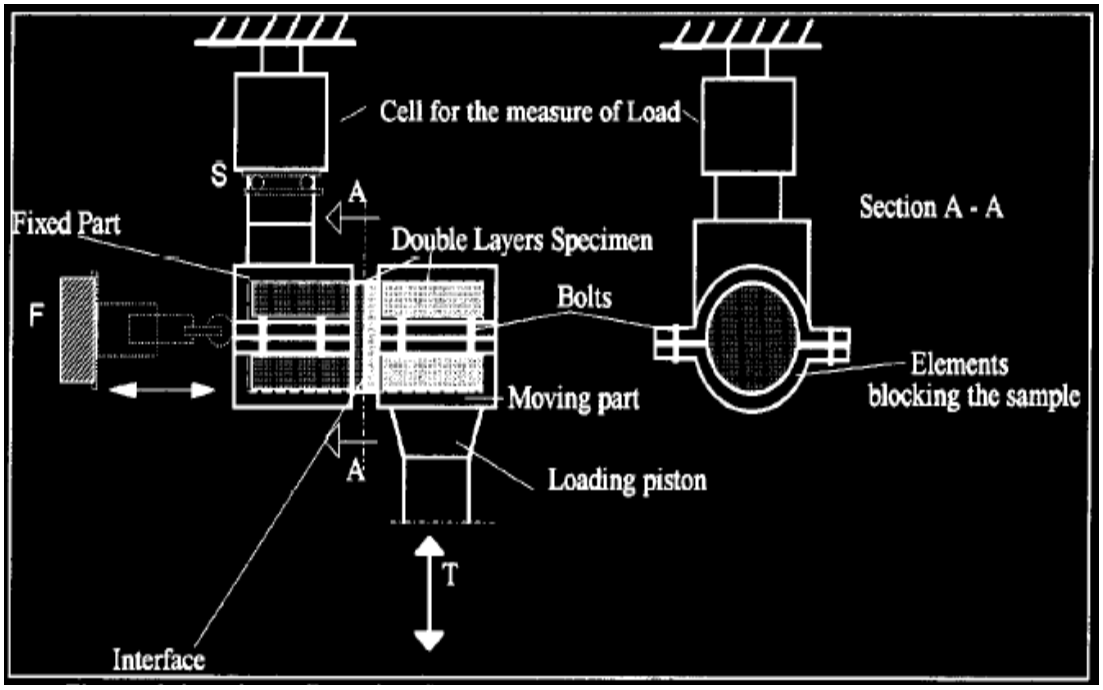

Figure 2.31 - Schematic diagram of the dynamic shear tester developed by Crispino *et al.* [1997]

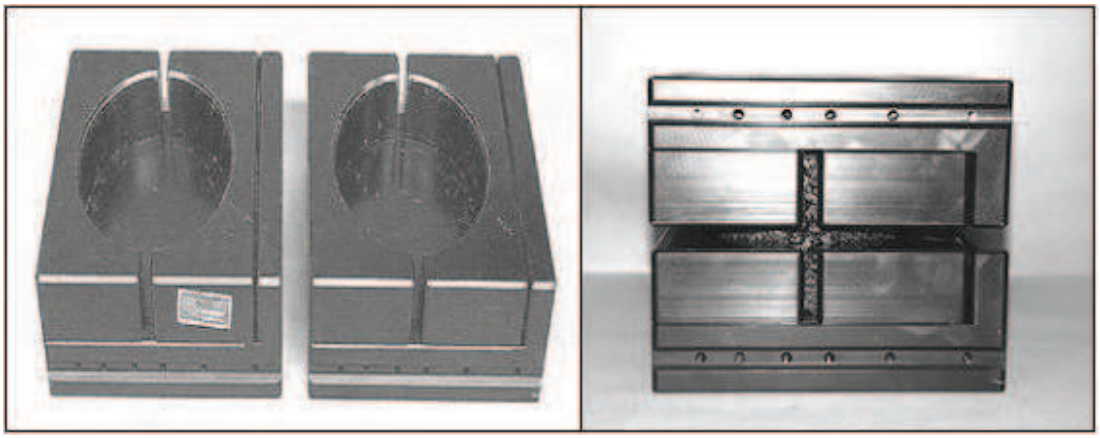

Figure 2.32 – Shearing apparatus used by Mohammad *et al*. [2002]

Romanoschi and Metcalf [2001b, 2002] performed laboratory direct shear tests at various normal load levels (138 ~ 522 kPa). They used a shear test unit as shown in Figure 2.33 on 95mm diameter asphalt cores taken from a full-scale test site. Shear loading is applied at a constant displacement rate of 12mm/min until a

total shear displacement of 12mm is reached. The shear force (F_v), normal force (F_h) and shear displacement are recorded and controlled.

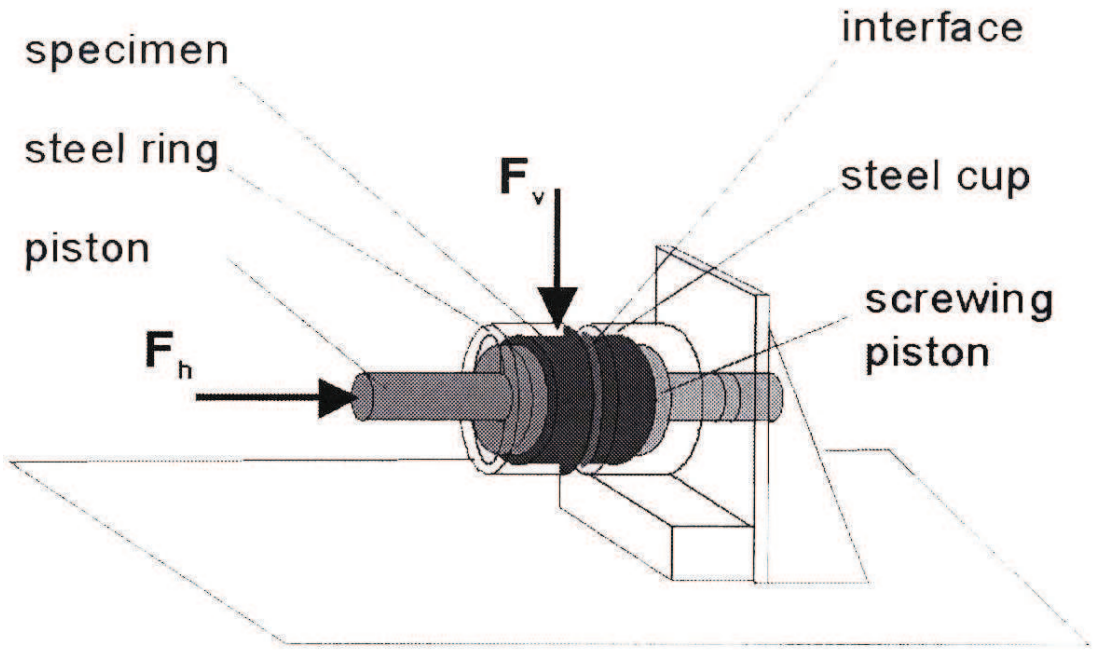

Figure 2.33 - Schematic diagram of shear test unit developed by Romanoschi and Metcalf [2002]

Because a pavement structure is subjected to repetitive loadings imposed by moving vehicles and it is unlikely that the interface would fail in a single load application, Romanoschi and Metcalf [2001b] also developed a shear fatigue test by modifying the shear test unit presented in Figure 2.33. In the shear fatigue test presented in Figure 2.34, the shear plane is positioned at an angle of 25.5º to the horizontal plane, so that the shear stress at the interface is half of the normal stress. The test is performed by applying a haversine vertical load with a frequency of 5Hz. They reported that it was difficult to determine the fatigue failure point. Therefore, they used the number of load cycles that produced an increase of permanent shear deformation of 1mm (ND1) as a parameter for a comparative evaluation of the interface fatigue properties.

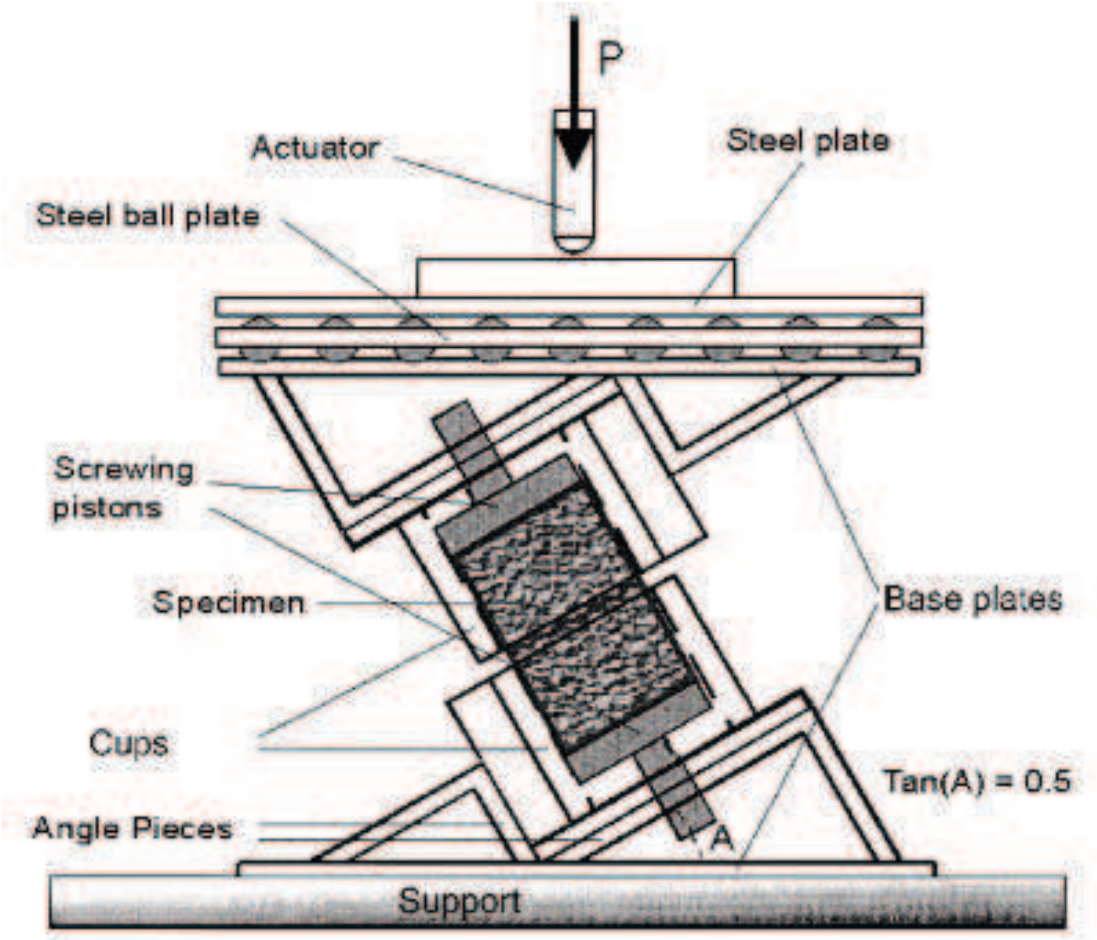

Figure 2.34 – Schematic diagram of shear fatigue test unit developed by Romanoschi and Metcalf [2001b]

The National Center for Asphalt Technology (NCAT) at Auburn University, USA designed a shear test device shown in Figure 2.35 [West *et al.*, 2005]. This device allows the application of a combined shear-normal loading on a cylindrical double layered specimen of 150mm diameter. Shear loading is applied at a constant displacement rate of 50.8mm/min, so that the test can be easily performed in a standard Marshal or CBR equipment. A screw assembly is used to apply normal loading to the front pressure plate. The applied normal loading is monitored through a load cell placed in between the screw assembly and the front pressure plate.

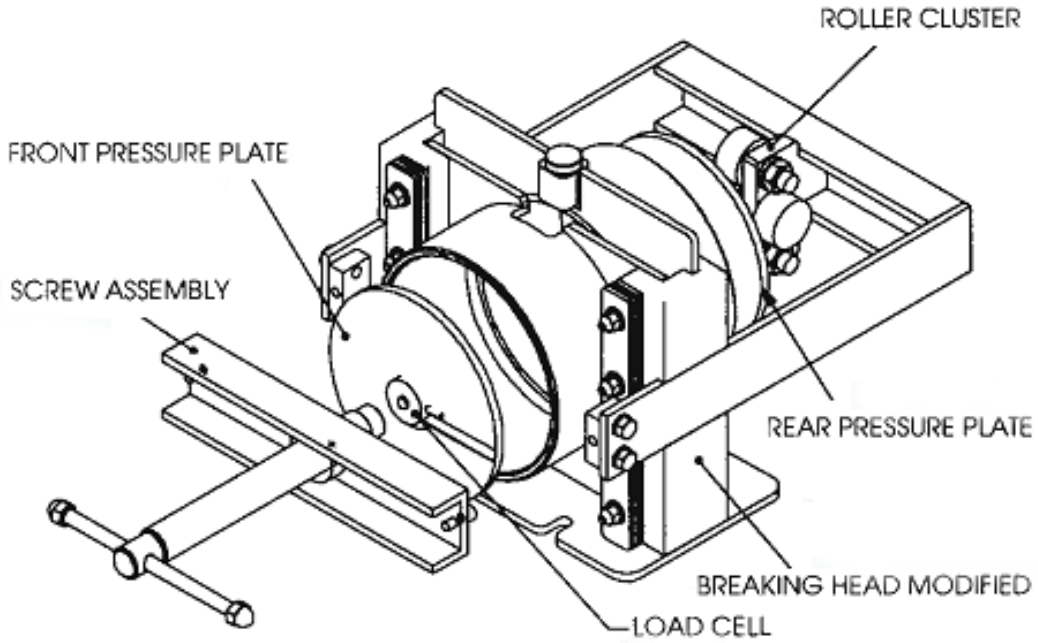

Figure 2.35 – NCAT shear test device (From West *et. al.*, 2005)

In Germany, Wellner and Ascher [2007] developed a dynamic shear testing device presented in Figure 2.36. They used the testing device to determine the dynamic shear reaction modulus of the interface between layers. The testing device uses a double layered core specimen of 100mm nominal diameter and allows the application of repeated shear displacement combined with a normal load. It was designed to perform shear testing at the following conditions: testing temperature of -25 to 65ºC, normal load of 0 to 1.1MPa, shear displacement up to 0.25mm, gap between the shearing rings of 0 to 15mm.

In addition to the laboratory shear test that has been previously mentioned, an in-situ shear test method utilising the rear truck wheel was developed by EMPA [Raab and Partl, 1999]. The test setup presented in Figure 2.37 shows that the shear loading is generated by hydraulic or pneumatic actuator(s), whilst the vertical loading is provided by the rear truck wheel load. The test is typically used to assess the interface bond of an asphalt layer laid over concrete. During the test, horizontal and vertical displacements are monitored and recorded.

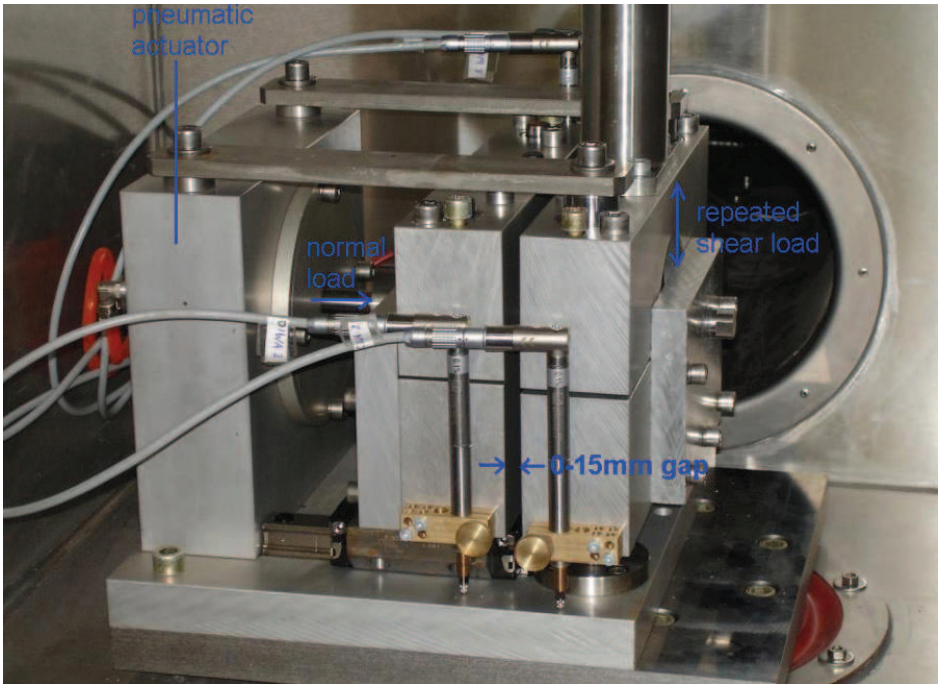

Figure 2.36 – Dynamic shear testing device developed by Wellner and Ascher [2007]

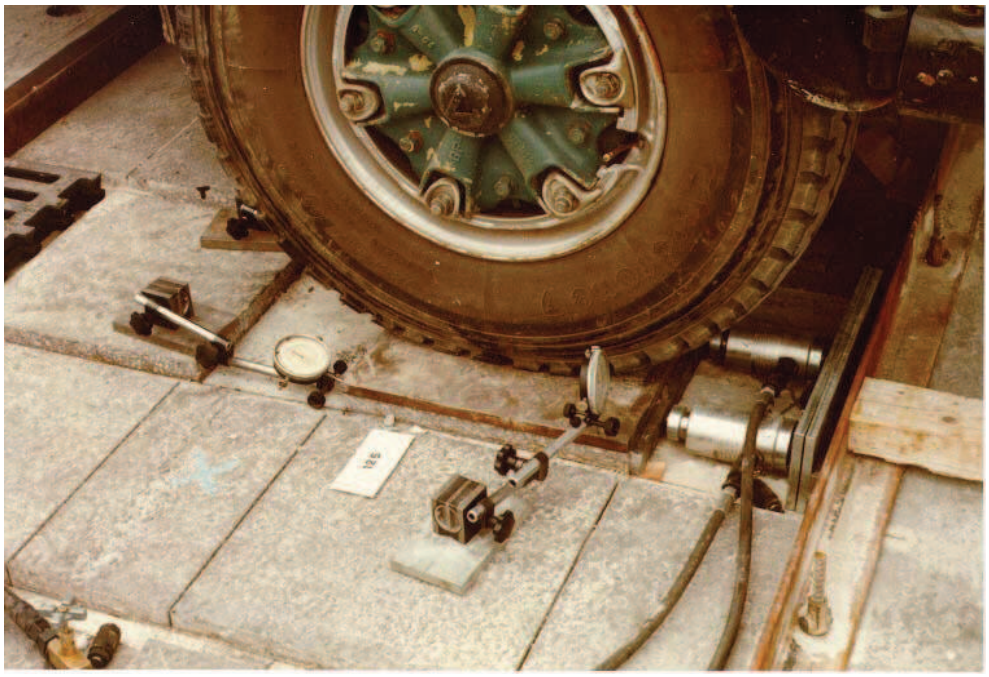

Figure 2.37 – The EMPA in-situ shear test (From Raab and Partl, 1999)

The direct shear tests where both normal and shear stresses are applied to the interface are widely used and popular. However, there are a number of limitations, for example:

- The shear stress distribution on the interface is not uniform [de Bondt, 1999; Kruntcheva *et al*., 2001],
- The experimental complexity associated with the application of a normal as well as shear load is not suitable for routine testing.

Direct shear test without normal load

Because the direct shear tests with normal load are known to have experimental complexity associated with the application of a normal as well as shear load, various direct shear tests without the application of normal load have been developed in several countries to simplify the experimental setup. It should be noted that, similar to the direct shear test with normal load, the test arrangement is also suffers from a non-uniform interface shear stress. Partl and Raab [1999] also mentioned that the loading and the resulting stress and strain distributions in the specimen is still considerably different from that of in the real pavement structure. In this test arrangement, applied shear force pushes the layer sideways across a pre-defined shear plane; whilst in real pavement structure, horizontal traffic loads are transmitted top-down from the tyre contact area on top of the surfacing to the interface between layers.

Leutner [1979] developed a simplified direct shear test named the Leutner shear test (Figure 2.38). The Leutner test is used as a standard test in Germany and included in the German Standard ALP A-Stb Teil 4 [DIN, 1999]. The test is performed on a 150 ± 2mm diameter core specimen comprising at least two layers (with a bond between them) taken either from a pavement structure or produced in the laboratory. The principle of the test is to apply a shear displacement rate across the interface without the application of a normal force to the specimen; consequently, a force perpendicular to the interface to better simulate the traffic load condition is not applied. To ensure a firm gripping of the specimen and a proper

contact between the specimen and the loading device, it is specified that the thicknesses of the layers below (lower layer) and over (upper layer) the interface should be at least 70mm and 25mm, respectively. The testing device has a range of interchangeable clamping and loading devices (i.e. lower and upper shearing rings) of different diameters (between 148 and 152mm) to cover the range of specimen diameters. The test is typically carried out at a standard displacement rate of 50 ± 3mm/min and a standard testing temperature of 20 ± 1°C. The standard displacement rate of 50 ± 3mm/min allows the test to be performed in standard Marshall or CBR loading devices which are widely available in most road testing laboratories.

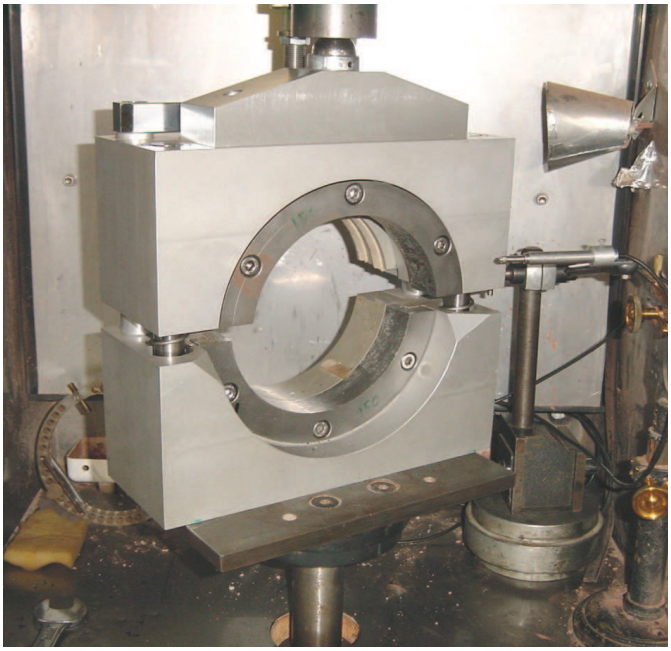

Figure 2.38 – Photograph of the Leutner shear testing device (From Choi *et al.*, 2005)

EMPA developed a modified version of the Leutner test named the LPDS (Layer Parallel Direct Shear) test, shown in Figure 2.39 [Raab and Partl, 1999, 2004a, 2004c; Partl and Raab, 1999]. Similar to the Leutner test, the LPDS test uses a core specimen of 150 ± 2mm diameter comprising at least two layers and is typically performed at a standard displacement rate of 50 ± 2mm/min and a standard testing temperature of 20 ± 1°C.

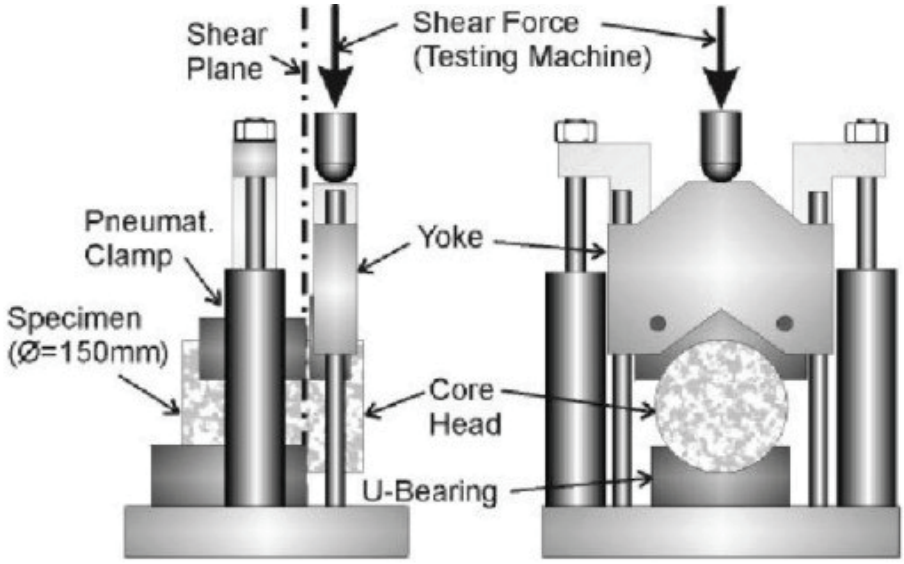

Figure 2.39 - Schematic view of the LPDS device (From Partl and Raab, 1999)

Although a range of interchangeable loading and clamping devices of different diameters are available in the LPDS to cover the range of specimen diameters, Raab and Partl [1999] considered that providing a range of loading and clamping devices could be expensive. During the development of the LPDS, they investigated several shapes of loading and clamping devices that can be used to cover the entire range of specimen diameters: V-shaped loading and clamping devices (Form B), Parallel plates (Form C) and combination between a U-shaped loading device and a V-shaped clamping device (Form D). They compared the results obtained using the modified loading and clamping devices with that of using the standard U-shaped loading and clamping devices (Form A, similar to the Leutner). Figure 2.40 shows different shapes of loading and clamping devices in the LPDS investigated by Raab and Partl [1999].

From the investigation using different shapes of loading and clamping devices, Partl and Raab [1999] found that a structurally weak layer may be locally deformed at the beginning of the test by a “snow plough” effect until sufficient local stability is reached to induce the shear stress over the whole interface plane. They recommended that it is necessary to use semicircular (U-shaped) loading and clamping devices (Form A) and the test should be restricted to temperature less than 40 ºC. Furthermore, because a test that is carried out at higher temperatures is

more variable, they recommended a testing temperature of 20ºC for routine testing. From comparative testing, they found that the results obtained using the Leutner were virtually similar to those of obtained using the LPDS with U-shaped loading and clamping devices (Form A).

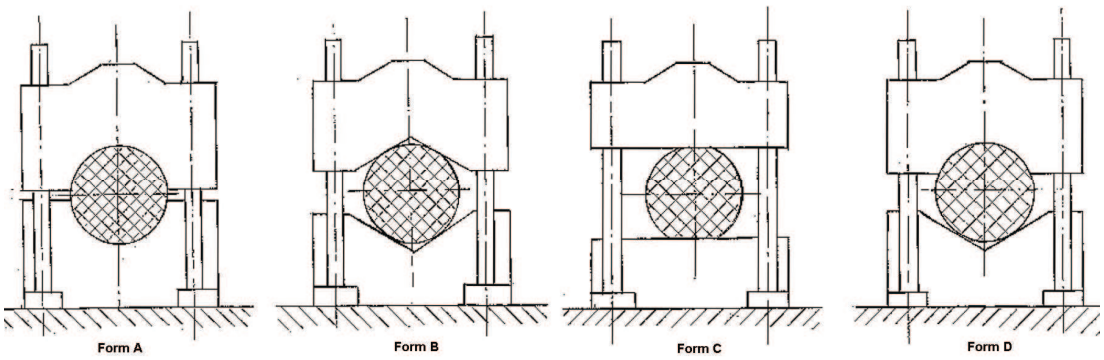

Figure 2.40 - Schematic view of different shapes of loading and clamping devices in the LPDS investigated by Raab and Partl [1999]

Partl and Raab [1999] also carried out a series of shear tests on different types of fresh asphalt pavements using the LPDS. They used the apparatus to determine the in layer and interlayer shear strength, τ and shear reaction modulus, *Ks* of 150mm diameter core specimens. The results from the in layer shear testing within a pavement layer and interlayer shear testing between pavement layers were analysed and compared. They suggested that the test is a simple and useful tool for quality assessment and inspection testing of interlayer adhesion properties of pavements immediately after construction. Since 2000, the LPDS test has been incorporated into the Swiss Standard SN 671961 [Vereinigung Schweizerischer Strassenfachleute, 2000]. Similar to the German Standard ALP A-Stb Teil 4, the Swiss Standard SN 671961 specifies that the thickness of the upper layer should be at least 25mm.

Choi *et al.* [2005] performed an investigation to develop a laboratory-based interface bond test to be used as a routine standard test in the UK. After reviewing and investigating several candidate tests, they found that the direct shear test appeared to be the most common and widely used laboratory test method to

investigate the interface properties. They considered that the application of normal force in the direct shear test requires a much more complicated testing set-up which makes it difficult to be accepted as a routine standard test. Therefore, they decided to adopt a simplified direct shear test without the application of normal load and demonstrated the suitability of the Leutner test for routine testing to determine the bond between asphalt layers. They introduced a 5mm gap between the shearing rings (i.e. loading and clamping devices) in the Leutner test frame to prevent crushing of large aggregate particles as well as to improve the repeatability of results. They developed a modified Leutner testing protocol with the 5mm gap between the shearing rings (see Appendix A.1) and a limited number of laboratory manufactured specimens as well as samples obtained from site cores were tested.

Choi *et al.* [2005] mentioned that the 5mm gap between the shearing rings was introduced after they frequently observed crushing of large aggregate particles at the sheared interface. The crushing was thought to be caused by misalignment between the specimen interface and the shear plane in the Leutner test frame. They reported that the standard Leutner test frame does not have enough tolerance in the shear plane and found it difficult to align the interface to the shear plane, especially when the specimen had an irregular interface (due to coarse aggregates interlocking or an uneven bottom layer surface). For practical reasons, a 5mm gap between the shearing rings was introduced to provide enough tolerance, so that the specimen interface can easily be aligned in the Leutner test frame. The standard Leutner test frame can easily be modified to provide a 5mm gap into the shear plane by machining the standard shearing rings.

To investigate the effect of the introduction of the 5mm gap in the Leutner test on interface stress conditions, Choi *et al.* [2005] developed a simple linear elastic three-dimensional Finite Element (FE) model. They used material properties presented in Table 2.2 in the FE analysis. They applied a vertical point load of 10 kN to the top of one half of the steel loading frame. Figure 2.41 shows the comparison between the predicted normal and shear stresses calculated along the central diameter of the interface (from top to bottom) for the two Leutner test frames (with 5mm gap and without gap). The orientation of the normal stress is perpendicular to the orientation of the interface, whereas the orientation of the shear stress is parallel

to the orientation of the interface. Because the stress conditions are not pure shear due to bending in the specimen, there is a non-zero normal stress at the interface. The predicted shear and normal stresses of the modified Leutner test frame (with 5mm gap) over the central 90mm of the specimen are virtually identical compared to the corresponding curves of the standard Leutner test frame (without gap). From the FE analysis, they also found that the introduction of the 5mm gap seemed to reduce the stress concentrations at the edge of the specimen (see the top and bottom 10mm of the specimen in Figure 2.41), which was considered to be beneficial.

Table 2.2 Material properties used in the FE model of standard and modified Leutner test frames developed by Choi *et al.* [2006]

Material	Thickness (mm)	Young's modulus (MPa)	Poisson's ratio
Upper layer	50	3000	0.35
Lower layer	70	5000	0.35
Steel frame	-	212000	0.35

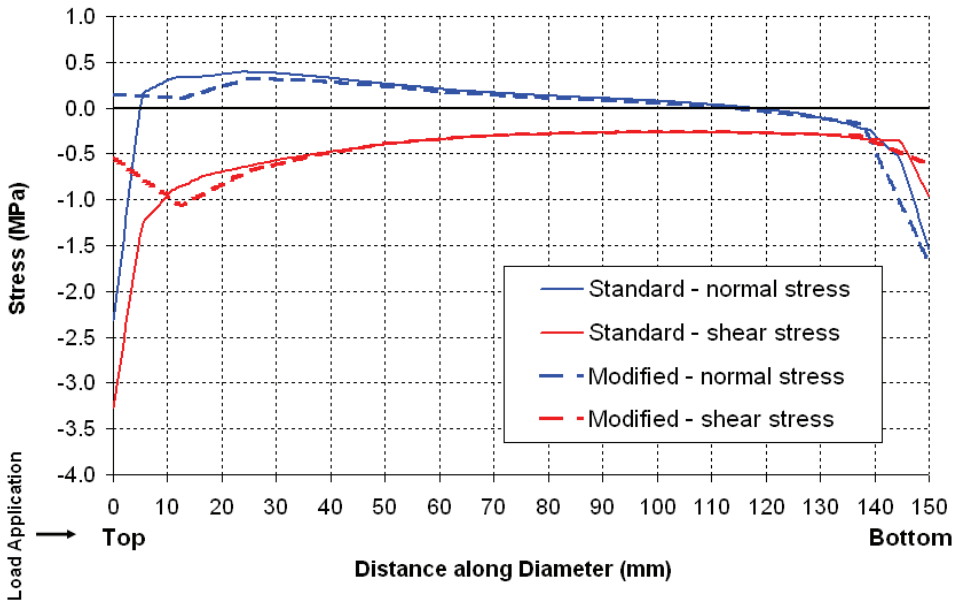

Figure 2.41 – FE stress distributions of standard and modified Leutner test frames (Adapted from Choi *et al.*, 2005)

Sutanto *et al.* [2006] reported a comparison of results obtained using the standard (without gap) and the modified (with 5mm gap) Leutner test frames on 14mm Stone Mastic Asphalt (SMA) surfacing over 20mm Dense Bituminous Macadam (20DBM) binder course specimens using two different interface conditions at a testing temperature of 20ºC. As presented in Table 2.3, they showed that the 5mm gap significantly reduced the crushing at the sheared interface. The modification also reduced the variability of results, showed by the reduced Coefficients of Variation (COVs). Following the introduction of the 5mm gap between shearing rings, alignment of the interface to the shear plane became much easier and occurrences of edge aggregate crushing at the sheared interface were virtually eliminated.

Table 2.3 Comparison between standard and modified Leutner results at a testing temperature of 20ºC (Adapted from Sutanto *et al.*, 2006)

Mixture type	Interface condition		Standard Leutner	Modified Leutner
SMA/20DBM	Tack Coat	Mean shear strength (MPa)	1.89[a]	1.78[c]
		COV (%)	18	6
	Slurry	Mean shear strength (MPa)	2.27[b]	1.96[c]
		COV (%)	20	13

[a] Four out of six specimens crushed
[b] Five out of six specimens crushed
[c] No specimen crushed

In the modified Leutner testing protocol (with the 5mm gap), Choi *et al.* [2005] specified that the specimens should be cores of 150 ± 2mm diameter comprising at least two layers and the test is performed at a standard displacement rate of 50 ± 2mm/min and a standard testing temperature of 20 ± 0.5°C. To ensure firm gripping and proper contact between the specimen and the upper shearing ring, they recommended that the minimum thickness of the lower and upper layers should be 60mm and 30mm, respectively.

Molenaar and Heerkens [1986] used a similar shear testing device (Figure 2.42) to investigate the effect of a Stress Absorbing Membrane Interlayer (SAMI) on pavement performance. They placed the shear testing device in a standard Marshall loading frame to apply a constant shear displacement rate of 51mm/min on a core specimen of 101.4mm diameter. The applied shear load and the corresponding shear displacement are recorded and used to determine the shear reaction modulus and maximum shear stress.

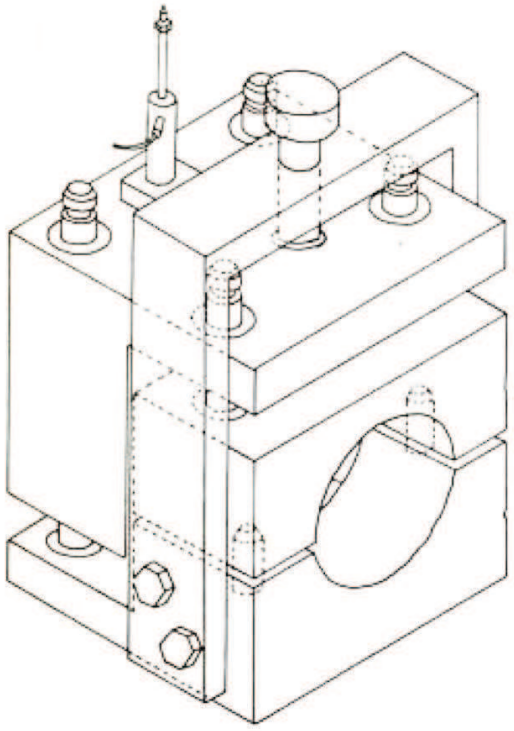

Figure 2.42 – Shear testing device used by Molenaar and Heerkens [1986]

A shear testing device, conceptually similar to the Leutner, has been developed and used as standard test in Austria. According to the Austrian Standard RVS 11.065 Teil 1 [FSV, 1999], the test is performed by applying a shear displacement rate of 50 ± 3mm/min on 100 ± 2mm diameter cores comprising of at least two bonded layers at a standard testing temperature of 25 ± 1^{o}C. Figure 2.43 shows schematic views of the shear testing device specified in the Austrian Standard RVS 11.065 Teil 1.

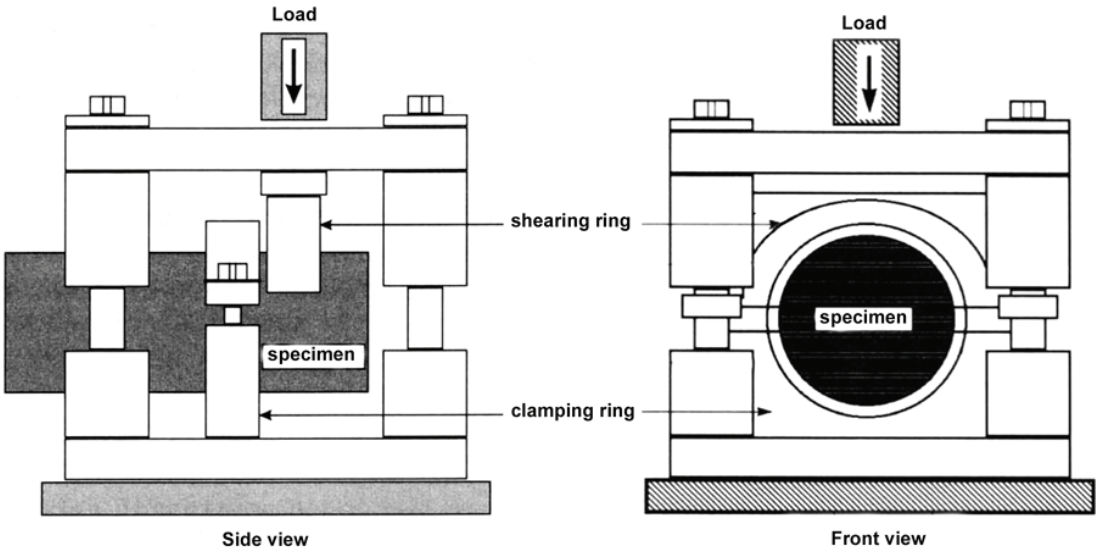

Figure 2.43 – Schematic views of shear testing device used in the Austrian Standard RVS 11.065 Teil 1 (Adapted from FSV, 1999)

At Florida Department of Transportation (FDOT) in the US, Sholar *et al.* [2004] developed a similar shear testing device (Figure 2.44). Two specimen diameters of 101.6 and 152.4mm were evaluated and the 152.4mm specimen diameter was chosen because it is usually used by the FDOT for density determination and pre-construction pavement evaluation purposes and they believed that the larger specimen diameter would provide less variable results (especially for asphalt mixtures containing a large nominal maximum aggregate size). A shear displacement rate of 50.8 mm/min was selected due to practical consideration that the test can easily be performed in a standard Marshall or CBR loading device. They also found that results obtained from testing performed at 50.8mm/min showed sufficient test value range for distinguishing the good and poor performing samples. They recommended a testing temperature of 25^{o}C because it is relatively easy to be achieved in the laboratory and they found that it becomes more difficult to distinguish the good and poor performing samples at higher testing temperature. Due to high possibility that the cores are not extracted exactly perpendicular to the pavement surface, they introduced a 4.8mm gap between the shearing platens. The 4.8mm gap was considered to be large enough to accommodate a slightly skewed interface plane and not too large to cause excessive bending to the specimen.

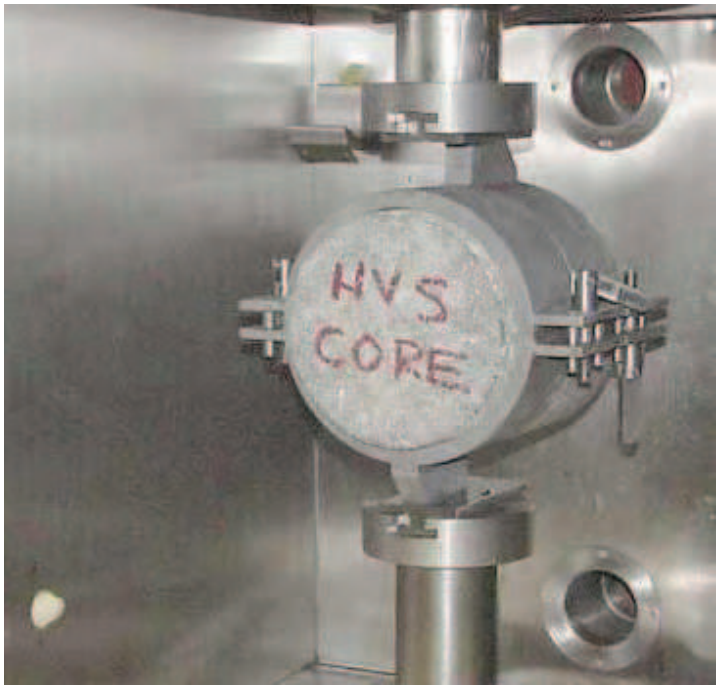

Figure 2.44 – Shear testing device developed by Sholar *et al.* [2004]

A double-shear testing device named the Modified Compact Shearing (MCS) test has been developed by the Mechanics and Modelling of Materials and Structures in Civil Engineering (3MsCE) laboratory at The University of Limoges, France. The MCS device, presented in Figure 2.45, has been used to investigate the shear fatigue behaviour of asphalt concrete mixtures and tack coat materials using a prismatic specimen (70x30x100mm^3) consisting of three parts [Diakhaté *et al*., 2006, 2007; Diakhaté, 2007]. The outside parts (70x30x30mm^{3}x2) are fully fixed using steel clamps, whereas the middle part (70x30x40mm^3) is subjected to monotonic or repeated loading until failure. The applied shear load and its corresponding shear displacement are recorded and analysed.

Considering that the MCS test frame is not rigid enough to perform shear fatigue testing at low temperature, Diakhaté [2007] developed a new double-shear testing frame (Figure 2.46) that is capable to perform a high frequency shear fatigue test at low temperature. The test is performed on a prismatic specimen of volumetric dimension 70mm by 30mm by 105mm. Steel plates (10mm thick) are glued to the specimen to ensure that shear failure occurs at the predefined shear planes.

Different gaps (5, 10 and 20mm) between the metal plates were evaluated using an FE analysis and the result revealed that specimen with the 5mm gap shows more uniform shear stress distribution at the interface.

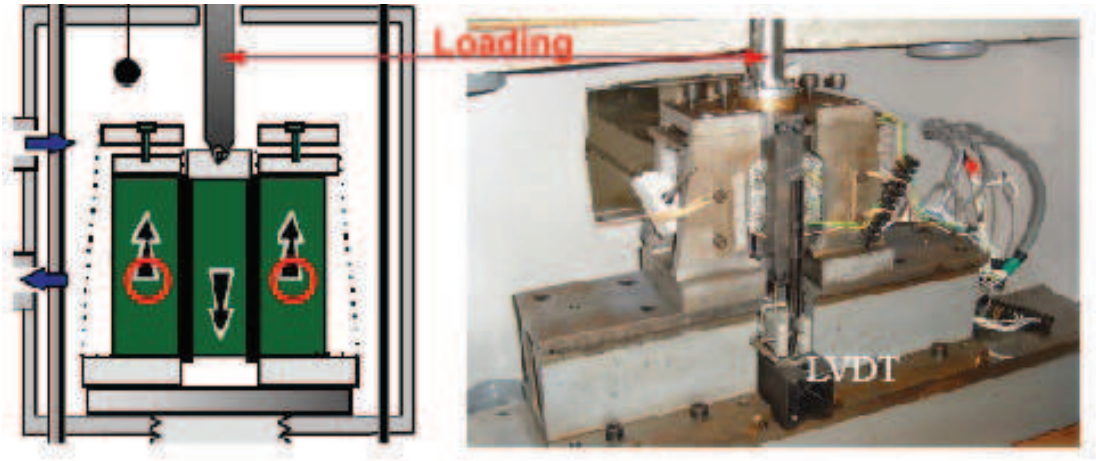

Figure 2.45 – Schematic diagram and Photograph of the MCS testing device (From Diakhaté, 2007)

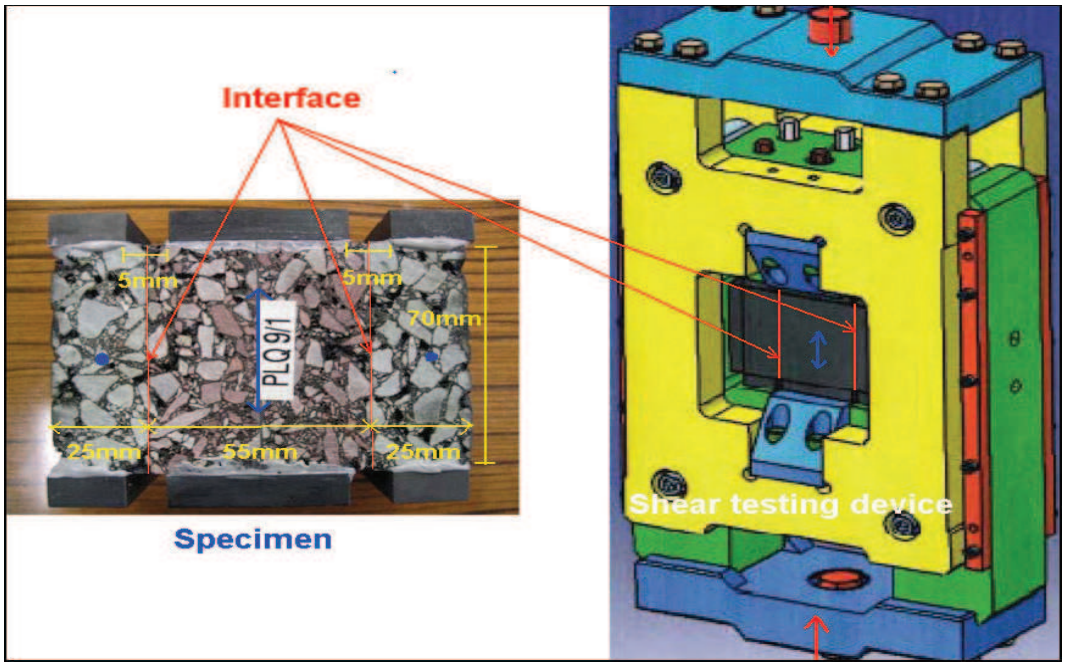

Figure 2.46 – Schematic view of the double-shear testing frame developed by Diakhaté [2007]

2.5.1.4 Other destructive tests

A three-point shear test named the Laboratorio de Caminos de Barcelona (LCB) shear test, shown in Figure 2.47, has been developed at the Technical University of Catalonia, Barcelona, Spain [Mirò Recasens *et al.*, 2005]. The test is performed by placing a cylindrical specimen of 101.6mm diameter in a mold or clamping device, so that the interface is positioned at 5mm beyond the edge of the mold. The mold (with the cylindrical specimen inside) is then placed horizontally over two semicircular supports (with 200mm spacing between them), in such way that the gap between the shearing support and the edge of the mold is 10mm and the interface is 5mm away from the shearing support (see Figure 2.47). A shear displacement rate of 1.27mm/min is applied through a loading piston positioned in the middle of the two semicircular supports. The displacement rate of 1.27mm/min was chosen because it is the typical rate of the CBR loading device used in Spain.

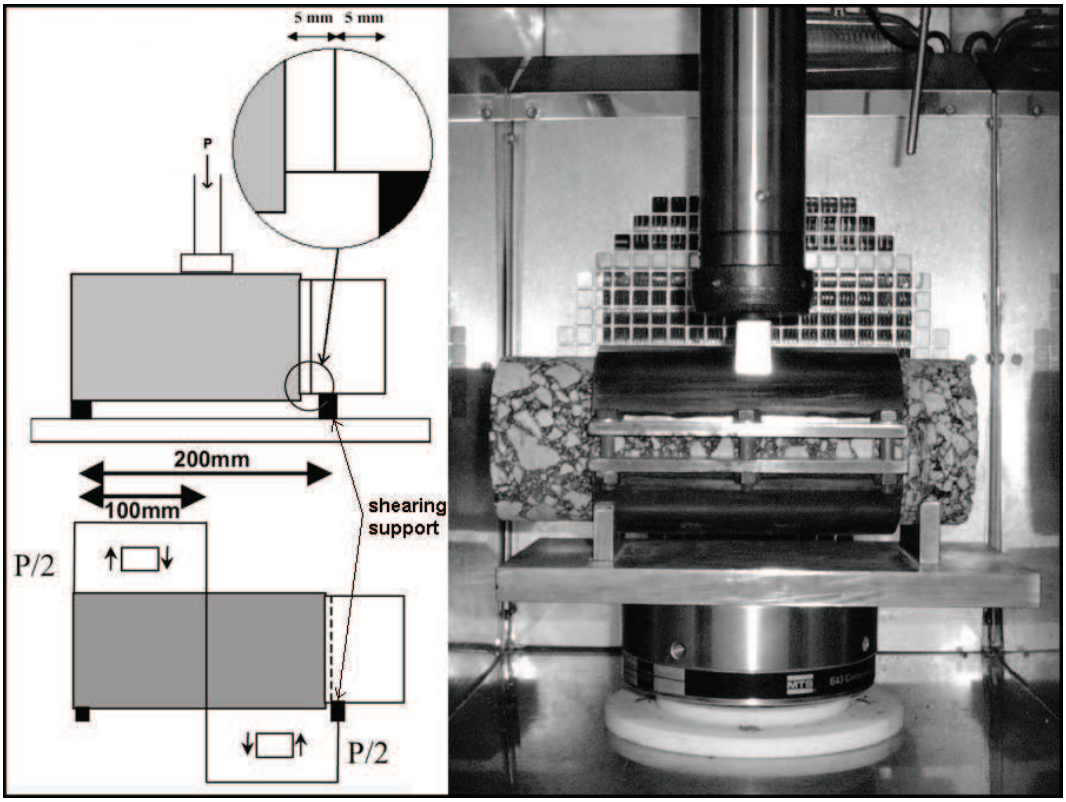

Figure 2.47 – Schematic diagram and photograph of the LCB shear testing device (Adapted from Mirò Recasens *et al.*, 2005)

The LCB shear test arrangement is quite simple and easy to be performed. However, there are a number of limitations, for example:

- The specimen still suffers from a combination of shear and bending stress.
- Due to the relatively low shear strength obtained from testing at a shear displacement rate of 1.27mm/min and considering the variability of the results, it would be more difficult to distinguish between the good and poor performing samples.
- The clamping arrangement with the 200mm spacing between shearing supports would limit the ability to test a short core specimen.

Recognising that the specimen in most interface shear tests is subjected to a combination of shear and bending stresses, de Bondt [1999] developed a four-point interface shear tester where a uniform shear stress distribution could be found (verified by an FE model). The loading configuration, shear and moment distributions and test setup of the four-point shear test are shown in Figure 2.48, 2.49 and 2.50, respectively. The shear and moment distributions (Figure 2.49) clearly show that the specimen is arranged in such a way that the interface is placed at the centre of the region where it is subjected to a shear load of $13/15F_{actuator}$ and the bending moment is zero.

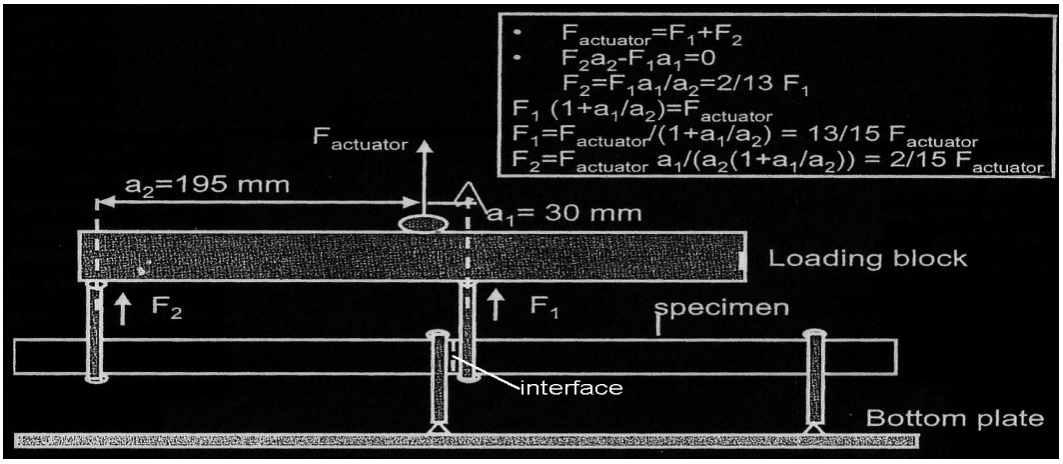

Figure 2.48 – Loading configuration in the four-point shear test (From Erkens, 2002)

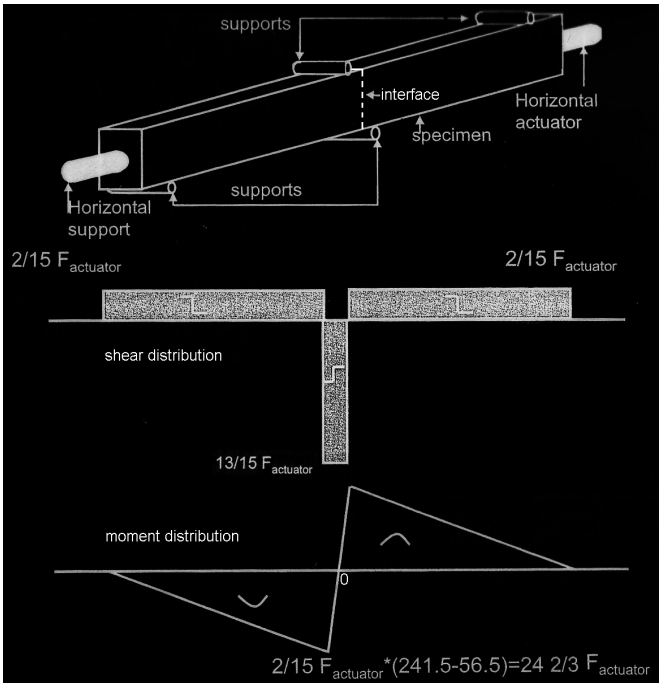

Figure 2.49 - Shear and moment distributions in the four-point shear test (From Erkens, 2002)

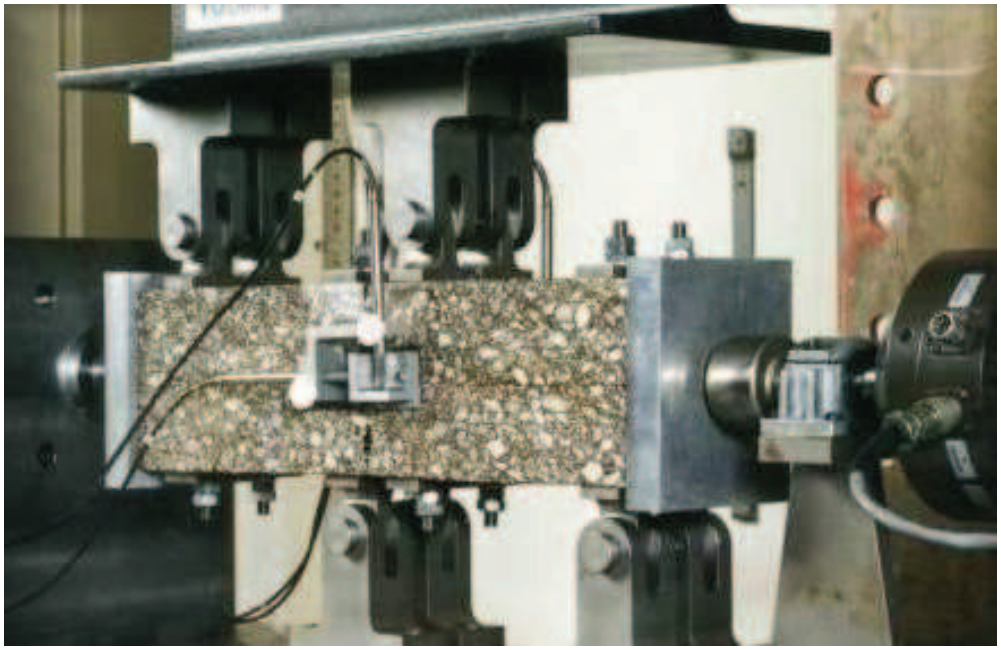

Figure 2.50 - Test setup of the four-point interface shear test developed by de Bondt [1999].

Nishiyama et al. [2005] used an indirect tensile strength test to determine the bond between concrete pavements. The test can be used to determine bond strength between asphalt layers by taking a horizontal core in such way that the interface is located at the centre of specimen diameter. A photograph of the indirect tensile strength test used by Nishiyama et al. [2005] is shown in Figure 2.51. The value of the indirect tensile strength (ITS) at the interface between layers can be calculated using the formula adapted from BS EN 12697-23 [British Standard Institution, 2003c]:

$$ITS = \frac{2P}{\pi D H} \tag{2.5}$$

where *ITS* denotes the indirect tensile strength of the interface (GPa), *P* is the applied load (kN), *D* is the diameter of the specimen (mm) and *H* is the height of the specimen (mm).

Figure 2.51 - Photograph of the indirect tensile strength test (From Nishiyama *et al.*, 2005)

Although it is possible to use the indirect tensile test to determine bond properties between asphalt layers, it should be noted that it has the following limitations:

- Specimen preparation requires considerable amount of effort.
- Because the core is extracted in such way that the interface is at the centre of the specimen diameter, the test can not be used to determine the bond beneath a thin layer. If a 100mm diameter core specimen is used, the thickness of the individual layer shall be at least 50mm.
- The test only measures tensile bond properties and can not be used to assess the effect of aggregate interlock at the interface
- Raab and Partl [1999] reported that the test showed considerable amount of scatter.

Another type of indirect tensile test named the Wedge Splitting Test (Figure 2.52) has been developed at The University of Vienna, Austria [Linsbauer and Tschegg, 1986; Brühwiler and Wittmann, 1990; Tschegg et al., 1995]. The test arrangement was originally designed to determine the fracture properties of a concrete specimen. Tschegg et al. [1995] used the test to characterise the mechanical fracture properties of bond between different asphalt layers. The principle of the test is to split a double-layered specimen at the interface between the adjacent layers. Different shapes of specimen can be used by creating a groove and a starter notch on the specimen as presented in Figure 2.52. A vertical force is applied to the metal wedge that induces horizontal forces to split the specimen. Applied vertical force and the corresponding horizontal displacement are recorded during the test. The horizontal splitting force, F_H is then calculated using the following equation:

$$F_H = \frac{F_V}{2 \tan \alpha} \tag{2.6}$$

where F_H denotes the horizontal force (kN), F_v is the vertical force (kN) and α is the wedge angle (°). A load-displacement curve (F_H-δ) can be drawn to evaluate the fracture mechanical properties of the interface. Similar to the indirect tensile test,

the Wedge Splitting test can not be used to assess the effect of aggregate interlock at the interface and the specimen preparation requires a considerable amount of effort.

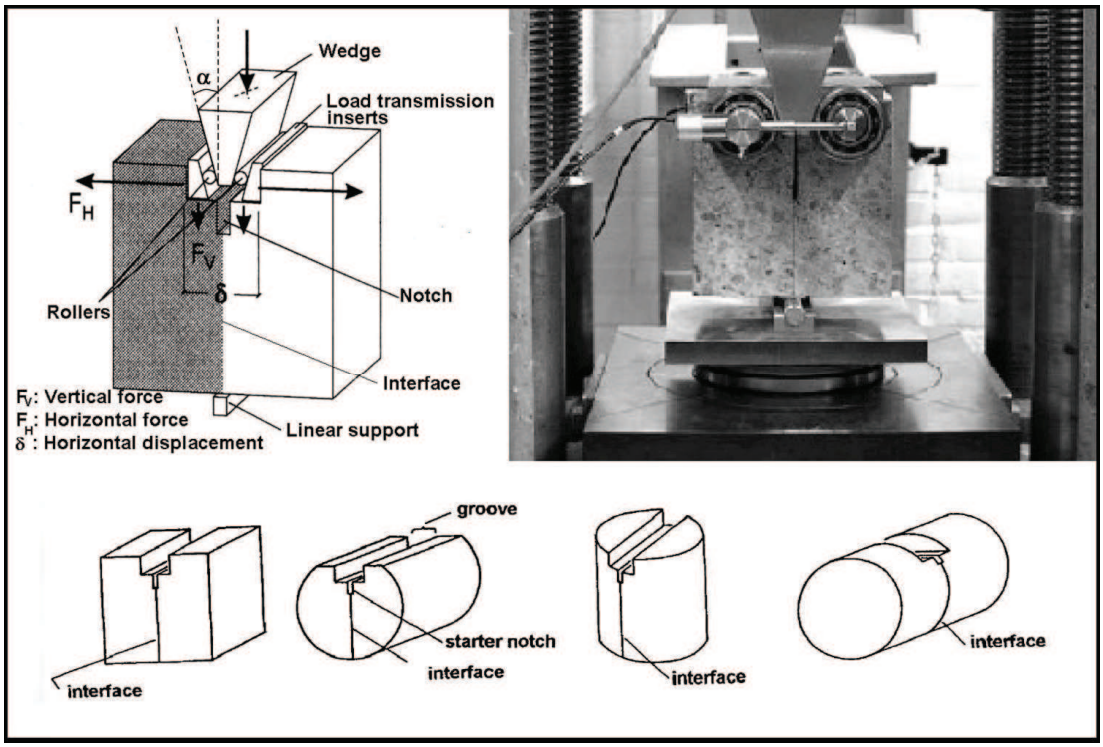

Figure 2.52 – Schematic diagram, photograph and different specimen shapes of the Wedge Splitting Test (Adapted from Linsbauer and Tschegg, 1986; Tschegg *et al*., 1995)

2.5.2 Non - Destructive Tests

Together with the development of destructive test methods, research to develop a range of non-destructive test methods to determine interlayer bond have been extensively performed.

Lepert *et al*. [1992] investigated the suitability of existing non-destructive test equipment to detect bond failure between pavement layers. The experiment was performed on a test section consisting of different interface conditions, located in the

shoulder of the A38 Motorway in France. The investigation used two measurement approaches and was performed using a number of non-destructive testing devices:

- Deflection measurement using Inclinometry, Deflectograph and Falling Weight Deflectometer (FWD).
- Dynamic measurement using Collograph, Lightweight Vibrator and radar.

The Inclinometry and the Deflectrograph are experimental devices for the measurement of pavement surface deflections as a specified axle load approaches it. The FWD equipment applies an impact load to the pavement surface and measures the surface deflections at seven radial locations. The Collograph is a device that applies a harmonic force of 2000N at 60Hz and measures the response of the pavement to this loading. The Lightweight Vibrator is a device that measures the scattering curves of surface waves in pavements. The radar is a device for transmitting electric waves to the pavement and measuring its electromagnetic response. Lepert *et al*. [1992] found that only the radar was capable of detecting bond failures. However, it should be noted that the capability of the radar is limited to the condition when the interlayer has reached the stage of a thin, possibly moist cohesionless layer.

Al Hakim [1997] developed a new back-analysis technique to determine the shear reaction modulus of the interface between asphalt layers using the FWD measured deflections. This technique consists of a two-stage back-analysis process. In the first stage, a database is developed using a combination of layer stiffnesses. A search for the best model using multiple regression analysis is then performed with the layer stifnesses as dependent variables and the deflections as independent variables. In the second stage, another database is developed for a combination of layer stiffnesses and bond conditions. The calculated deflection bowl that fits best with the measured FWD deflection is used for stiffness prediction. The foundation stiffnesses found from the first stage, along with the layer stifnesses and bond conditions found from the second stage are taken as the back-analysed pavement parameters. Although this test is non-destructive, it should be noted that a coring survey is necessary to determine the pavement parameters when a construction history is not available.

Simonin and Maisonneuve [1998] reviewed the use of a non-destructive testing equipment named "Colibry" to detect interface bond failure. This test is performed by applying a mechanical impulse to the surface of the pavement and measuring its response using a set of accelerometers. At each measurement point, the value of the transfer function between the response and the impulse at a certain frequency is determined. They stated that for a pavement whose surfacing has a bond failure at the interface, the transmitted waves are reflected from the failed interface, enhancing the pavement response and the modulus of the transfer function. They mentioned that the phenomenon was even more noticeable for waves with a frequency around 1500Hz. Although it has been found capable of detecting bond failure, this technique can only be used when other pavement defects do not interfere with the measurements.

Kruntcheva *et al.* [2000a] examined the suitability of the Portable Seismic Pavement Analyser (PSPA), as shown in Figure 2.53, to quantify the bond condition beneath a thin surfacing course system. The basic principle of the PSPA is to generate stress waves in the pavement layers and observe its response. They concluded that the device can not be used to determine the bond condition beneath a thin surfacing course system because the bituminous material strongly attenuates the high frequency wave components in the first 100mm of the pavement structure.

Kruntcheva *et al.* [2000b] considered that the new back-analysis technique using FWD test results is not the most suitable for assessment of bond condition between pavement layers in shallow interfaces. They reviewed the suitability of using defection data to quantify the interface bond. They analysed the deflection when a five-layer pavement structure, as shown in Figure 2.54, was loaded with an inclined static load of 75kN, distributed over a circular contact area with a diameter of 75mm. Three different values of the inclination angle α were considered: 1) α=0°; 2) α=22.5°; and 3) α=45°. Based on the results shown in Figure 2.55, they explained that close to the load centre, the bond condition does not significantly affect the vertical displacements. Furthermore, they stated that this condition explains why the back-analysis of the FWD data cannot be used with confidence for assessing the bond condition beneath a thin layer close to the surface.

Figure 2.53 – Photograph of the PSPA device (From Steyn and Sadzik 2007)

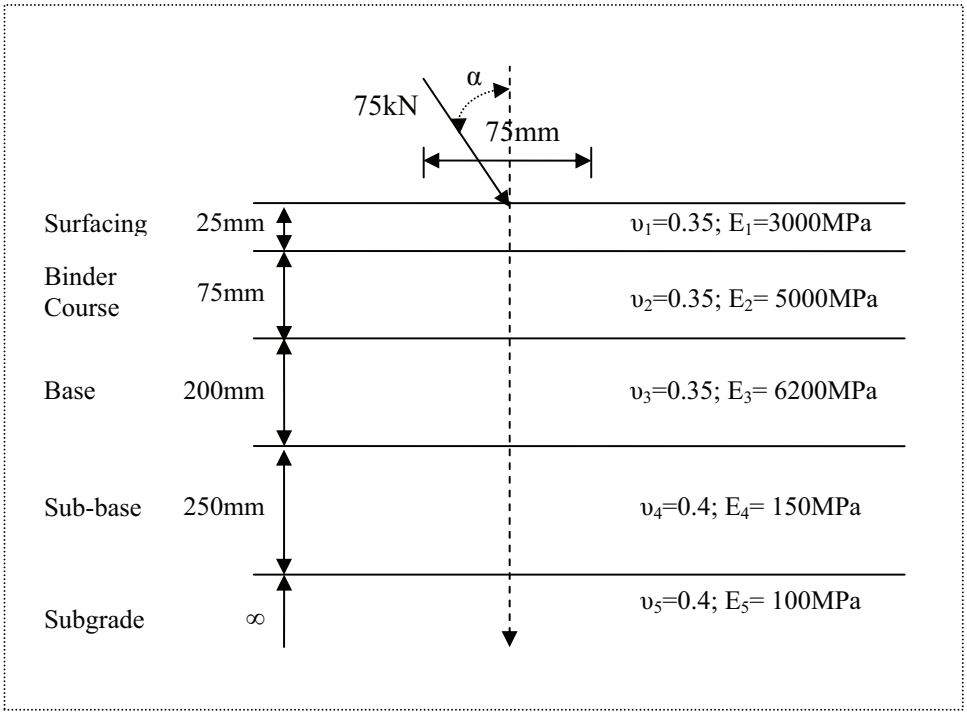

Figure 2.54 - Schematic drawing of the five layer pavement analysed by Kruntcheva *et al.* (Adapted from Kruntcheva *et al.*, 2000b)

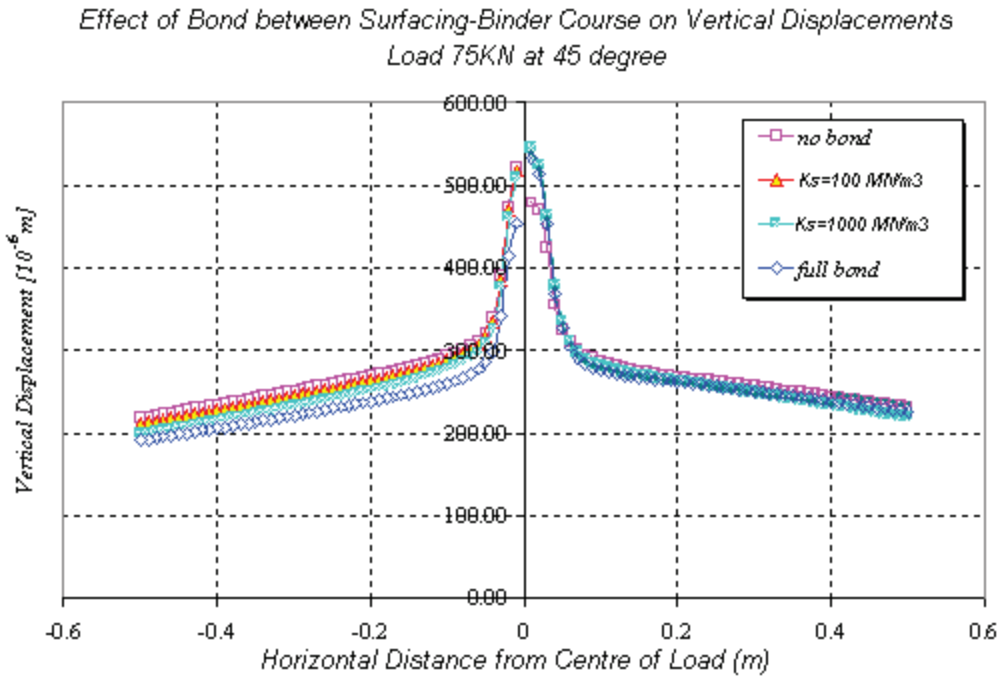

Figure 2.55 - Effects of bond on vertical displacements (From Kruntcheva *et al.*, 2000b)

Sangiorgi *et al*. [2002] performed Impulse Hammer Tests to evaluate in-situ bond condition. The Impulse Hammer is a portable non-destructive testing device that measures the vertical acceleration of a pavement surface adjacent to a point where an impulse is applied. The signal recorded from the accelerometer is then analysed. They found that the shape of the accelerometer waves of a bonded interface could be easily distinguished from the unbonded one. Instead of using the commonly used frequency-based analysis, they introduced a new data interpretation approach using Fractal Theory. Although further investigation is needed, they concluded that the Impulse Hammer Test was satisfactory to detect pavement bond condition.

2.5.3 Standardised Test Methods and Specification Limits

Roffe and Chaignon [2002] performed a worldwide survey and reported that standardised test methods for assessing bond condition of pavement structures had

been available for a pull-off test in Austria and a direct shear test without normal load (LPDS) in Switzerland. In Germany, standardised methods of the Leutner [DIN, 1999] and pull-off [DIN, 2003] tests have been published in 1999 and 2003, respectively. They specifically use the pull-off test to determine the tensile bond strength beneath a thin layer. A direct shear test method without the application of normal load, similar to the Leutner and the LPDS tests, is included in the Austrian Standard RVS 11.065 Teil 1 [FSV, 1999]. In the UK, the torque bond test has been developed into the stage where it is included as a mandatory test in the guidelines document SG3/05/234 [British Board of Agreement, 2004]. In Italy, a direct shear test method using the ASTRA device is included in the Italian Standard [UNI/TS 11214, 2007].

In Germany and Switzerland, minimum limits for shear bond strength have been proposed as national standards [Codjia, 1994; Partl and Raab, 1999; Stöckert, 2001]. In the UK, some research has been focussed to investigate the bond between asphalt layers. However, up to the present, no specification limits exist related to the shear bond strengths of a range of UK roads.

A summary of different test methods to asses the state of bond at the interface has been presented to provide a better understanding on the variation of fundamental test principles, test conditions, test configurations, specimen geometries, specimen dimensions and test equipments used in different bond test methods and their implications on the obtained test results.

2.6 Factors Affecting Bond between Asphalt Layers

Good bonding between pavement layers is desirable because it ensures a good pavement performance. Therefore, a knowledge of the factors that affect the state of bond between adjacent layers is essential. This section summarises several factors that have been identified by researchers.

An extensive investigation of slippage in the UK was conducted by the TRL in the mid-1970s [TRRL, 1976; Kennedy, 1978; TRRL, 1979; Kennedy and Lister,

1980]. The results showed that a slip plane is most likely to develop with a surfacing compacted at elevated temperature on a cold binder course laid on a foundation of inadequate stiffness. To reduce the risk of slippage, the following recommendations have been suggested: 1) improve the quality of unbound materials used in bases and sub-bases by increasing the level of compaction and 2) avoid high rolling temperature when laying the surfacing over a cold binder course. From the aforementioned recommendations, it can be summarised that level of compaction and quality of the lower layer, rolling temperature and temperature of the lower layer during the construction of a pavement structure are important factors to ensure a good bond between the adjacent layers.

Adequate level of compaction of the upper layer is also of significant importance to achieve good bond. Better compaction results in better embedment of aggregates in the upper layer to the layer underneath and sufficient contact surface between the upper and lower layers. Raab and Partl [2004c], using gyratory compacted specimens, investigated the effect of compaction effort on bond. They found that an upper layer compacted at 204 gyrations showed higher interface shear strength compared to that at 50 gyrations.

Research on the effect of compaction method on bond [Canestrari *et al.*, 2005; Mirò Recasens *et al.*, 2005; West *et al.*, 2005] revealed that although the bond at the interface of a laboratory-compacted specimen is considerably higher than the corresponding field-compacted specimen, they generally show similar trends. The results suggest that the laboratory-compacted specimen is suitable for comparative study of bond on various pavement material and interface conditions.

Several researchers [Partl and Raab, 1999; Pös *et al*., 2001; Carr, 2001; Collop and Thom, 2002; Raab and Partl, 2004c] reported that air void content of the surfacing materials significantly affects bond condition of the uppermost interface. More recently, Ferrotti [2007] performed an image analysis on the images obtained using the X-ray Computer Tomography (X-ray CT) equipment at EMPA to determine the air void content at the interface and the adjacent layers. From the investigation, Ferrotti [2007] summarised that air void content in a double-layered specimen is

concentrated at the interface and the relationship between the air void content and the interface shear strength seems to be parabolic.

Pös *et al*. [2001] and Sholar *et al.* [2004] investigated the effect of aggregate gradation in the upper and lower layer on bond. They concluded that the gradation of the upper and lower layer mixtures significantly affects the interface shear strength. In addition, Pös *et al*. [2001] drew the following conclusions:

- Asphalt mixtures with fine grained material laid on coarse grained layers provide adequate interparticle friction at the interface, and are thus more likely to have higher interface shear strength.
- The bond at the interface of an asphalt mixture with coarse grained material laid on a fine grained layer is highly affected by bitumen content and its adhesive properties.

Raab and Partl [1999] stated that the bond at the interface is also influenced by the type of the mixture used in the upper and lower layers. Collop *et al.* [2003] reported that bond strength at the interface between a 20DBM binder course and a Cement Bound Macadam (CBM) base is quite low. The low bond strength of this material combination was thought to be due to the lack of aggregate interlock at the interface (i.e. no embedment of aggregates in the DBM binder course to the stiff CBM base layer underneath). The low bond strength related to the cementious lower layer is similar to the bond failure at the interface between an asphalt surfacing and a concrete lower layer found by Raab and Partl [1999] that has been mentioned in Section 2.3 of this Chapter.

Application of bituminous bond (tack) coat at the interface has been long practiced to achieve a good state of bond between pavement layers. Hachiya and Sato [1997] found that inadequate curing of tack coat applied on a dirty interface significantly reduces the interface shear strength. Raab and Partl [2004c] and Sholar *et al.,* [2004] showed that for some material combinations, increasing the tack coat application rate increased the shear strength, while for other material combinations, there was little effect. They concluded that the use of tack coat does not always lead to higher interface shear strength.

Water is widely known to have a negative impact on an asphalt pavement structure as it reduces bitumen adhesion. Raab and Partl [2004c] and Sholar *et al.,* [2004] confirmed that the presence of water at the surface of the lower layer when laying the upper layer reduces the interface shear strength. Raab and Partl [2004a] investigated the effect of water penetration to the interface by pumping pressurised water through a small hole to the interface and immersing double-layered core specimens in water prior to shear tests. The results suggested that, using their experimental setup, the penetration of water to the interface decreases the interface shear strength by 15-27%.

During the construction of a pavement structure, it is commonly specified that the surface of the lower layer must be cleaned from any contamination (such as dirt, debris, oil) prior to laying the upper layer. Research on the effect of surface contamination of the lower layer on bond revealed that the presence of contaminants at the interface typically reduces the bond at the interface [Hachiya and Sato, 1997; Carr, 2001; Collop *et al.*, 2003; Raab and Partl, 2004c, 2007b].

Partl and Raab [1999] considered that the age of the lower layer (i.e. newly laid or old) may also affect the interface bond condition. To ensure a good bonding between adjacent pavement layers, BS 594987 [British Standard Institution, 2007] recommends different bond (tack) coat application rates for newly laid and old lower layers.

Raab and Partl [2004a] performed an investigation on the effect of a stress absorbing membrane interlayer (SAMI) on bond. They used the LPDS and the tensile bond test devices at EMPA to quantify the interface bond properties. The results demonstrated that the bond strengths at the interface were significantly lower when the SAMI was installed at the interface between adjacent layers.

Frictional resistance between the upper and lower layers is also attributed as one of the factors affecting bond at the interface between layers. Sholar et al., [2004] and West et al. [2005] found that surface texture of the lower layer significantly affects the interface bond. They showed that laying asphalt mixtures over a milled bottom layer significantly enhances the shear strength of the interface

between those layers. An investigation by Partl et al. [2006] on the effect of contact surface roughness showed that the shear strength at the interface increases as the contact surface roughness increases. Ferrotti [2007] demonstrated the effect of interlayer roughness on the measured bond strength of the interface. The interlayer roughness was quantified by performing an image analysis on the images obtained using the x-ray CT equipment. Copper wires with a diameter of 0.3mm and a density of 8.96t/m^3 were put at the interface, so that the interlayer roughness could easily be identified.

Pavement temperature varies widely depending on the geographical location and time of the year, thus an investigation into the effect of pavement temperature on bond between pavement layers is of significant importance. It is well known that asphalt behaves as a viscous material at high temperature and as an elastic material at low temperature. Many researchers found that the shear strength at the interface decreases significantly as the testing temperature increases [Uzan *et al.*,1978; Hachiya and Sato, 1997; Partl and Raab, 1999; Sholar *et al.,* 2004; Canestrari *et al*., 2005; Choi *et al*., 2005 and West *et al*., 2005]. Very low shear strength observed during testing at high temperature (>30°C) combined with the standard deviation of the test may increase the difficulties in determining the difference between materials in comparative testing. On the other hand, there is a concern regarding the capacity of a testing machine or apparatus for testing at low temperature (<15°C) as the shear strength may be higher than its capacity. Partl and Raab [1999], Sholar *et al* [2004], Choi *et al*. [2005] and West *et al*. [2005] considered an intermediate testing temperature (20-25°C) as the most suitable testing temperature due to practical application of the test whilst maintaining the testing variability and comparative testing ability.

Variation of vehicle speed significantly affects the properties of an asphalt pavement as it dictates the loading rate. Asphalt behaves as a viscous material at slow loading rate and as an elastic material at fast loading rate. Investigations on the effect of loading rate on bond found that the shear strength at the interface increases as the loading rate increases [Hachiya and Sato, 1997; Sholar *et al.,* 2004 and Choi *et al*., 2005]. A standard shear displacement rate of 50mm/min is

favourable for routine testing so that Marshall and CBR loading devices can be utilised [Sholar *et al*., 2004 and Choi *et al*., 2005].

Sholar et al. [2004] evaluated different specimen dimensions used in bond testing. After evaluating core specimens of 101.6 and 152.4mm diameters, they decided to use the 152.4mm specimen diameter because they believed that the larger specimen diameter would provide less variable results. Santagata *et al*. [2009] found that the bond strength obtained using the LPDS device is higher than that obtained using the ASTRA device. They considered that one of the factors that might contribute to the difference was the different specimen dimensions used in the LPDS and ASTRA tests.

Vertical load on a pavement structure generates normal force acting at the interface between layers. Investigations on the effect of normal load on bond found that the shear strength at the interface increases as the magnitude of the normal load increases [Uzan *et al*., 1978; Mohammad *et al*. 2002; Romanoschi and Metcalf, 2002; Canestrari *et al*., 2005; Choi *et al*., 2005 and West *et al*., 2005]. In addition, West *et al*. [2005] found that the effect of normal load is less significant on testing at low temperature. This was thought to be logical as friction between aggregates at the interface dominates the interface shear strength at high temperature and frictional resistance between aggregates is proportional to the normal force.

Raab and Partl [1999] mentioned that pavement geometry could also influence the bond between layers. Slippage cracking frequently observed on downward and upward gradients, curves and intersections indicates that the higher magnitude of horizontal load at those locations could significantly deteriorate the bond (especially at the uppermost interface).

Several researchers showed that the bond at the interface generally increases with time [Canestrari *et al*., 2005; Raab and Partl, 2007b]. However, it should be noted that the investigations were performed at a small scale in the laboratory. Stöckert [2001] evaluated the interface shear strength on pavements after one year in service and found significant improvement of shear strength (approximately 50% improvement) when the initial shear strength was approximately 1.1MPa. In

addition, sites with high initial shear (approximately 1.7MPa) showed little improvement and sites with low initial shear strength (approximately 0.55MPa) did not show any improvement.

The investigation by Stöckert [2001] was performed only one year after construction and no reference to traffic and climatic data were available. EMPA in Switzerland performed investigations on the influence of traffic and time on interface bond to investigate the long term performance of bond [Raab and Partl, 1999, 2007a, 2008, 2009; Partl and Raab, 1999]. Partl and Raab [1999] reported that after about 3-5 years in service, a slight improvement of interface shear strength was found on some material combinations. They also reported that no significant differences in the bond strength were observed for specimens inside and outside the wheel track. Raab and Partl [2007a, 2008 and 2009] performed further investigation on 14 high volume roads after about 9-13 years in service and demonstrated that:

- For new construction (new over new), the interface bond strength can be expected (but not in every case) to increase after 10 years.
- For pavement rehabilitation (new over old) or old construction (old over old), the increase of bond strength after 10 years cannot be expected.
- A high proportion of heavy vehicles over a long period of time may cause bond problems.
- Bond properties inside and outside the wheel track varied for the single sites and no trend could be derived. From the 14 investigated sites, 6 sites showed higher bond strength inside the wheel track, 2 sites showed no significant difference and 6 sites showed higher bond strength outside the wheel track.

Raab and Partl [2007a and 2008] investigated the difference between the bond properties inside and outside the wheel tracks in a stationary circular track (Figure 2.56). Compared to the case in the real road sections, the difference of bond strength inside and outside the wheel track in the circular track seemed to be more noticeable. This was thought to be logical because the trafficking in the circular track was performed in a more defined and canalised manner.

Figure 2.56 – Circular Track used by Raab and Partl [2007a and 2008].

The TRL reported that slippage failures most frequently occurred during the spring and rarely during the hot summer. From this fact, they indicated that trafficking at elevated temperature could increase the bond strength as a result of healing or re-bonding effects [Kennedy, 1978]. However, it was not clear whether the improvement was influenced by trafficking at high temperature or other unknown factors as traffic and temperature data were not available. Choi *et al*. [2005] performed pilot scale experiments at different temperatures in an accelerated testing facility to assess whether bond strength increased with trafficking. They found an indication that the bond was improved with trafficking at elevated temperature (30-35^{o}C) where the initial bond was low or intermediate (< 1MPa). It should be noted that to achieve the low initial interface bond strength, they spread an excessive amount of water/talcum powder mixture at the interface which does not represent a realistic interface condition in a real pavement structure. Additionally, because most of the cores were debonded during the coring process, only four cores at the section with the low initial interface bond strength could be tested. Due to the un-realistic interface treatment and the lack of data, further investigation is required to confirm their finding.

2.7 Discussion

The assumption that adjacent pavement layers are fully bonded together without any relative displacement between them does not represent the real condition in the pavement structure because a number of bond failures have been widely reported. When slippage occurs, the assumption of full slip is also considered as unrealistic because friction may still exist at the interface between adjacent layers. Therefore, the assumption of intermediate bond condition (i.e. between those two extreme conditions) is considered to be more realistic.

From the review on the reported bond failures, it can be summarised that most of the bond failures occurred at the interface between the surfacing and the binder course. These failures were mainly located at the locations where the horizontal forces as a result of turning, braking, ascending, descending, accelerating and decelerating were high. The presence of slippage cracking and/or horizontal permanent deformation was the most common visual evidence of bond failures at those locations. This demonstrates that poor bond condition could significantly affect the serviceability life of the pavement. Furthermore, slippage cracking will allow the penetration of water to the layer underneath, which could extent the damage to the whole pavement structure. Bond failures at the interface between the lower pavement layers have also been reported [Hakim, 2002; Raab and Partl, 2004a]. From an FWD test on a three-year old poorly bonded pavement structure, Hakim [2002] reported that although the foundation and individual layer stiffnesses were reasonably good, the effective stiffness and residual life of the pavement were low.

Because bond failures had been widely reported, several researchers performed theoretical studies to investigate the implication of bond on pavement performance. Shear, tensile and mixed shear-tensile separation modes could be used to characterise the bond failures. Although the tensile and mixed shear-tensile separation modes could also occur in a real pavement structure, the shear separation mode seems to be the most commonly found in the reported bond failures in real pavement structures (Section 2.4.1). In the theoretical studies, determination of a proper interface model is essential to represent the interface bond condition and the horizontal reaction modulus, K_s was found to be the most

commonly used by researchers because it is quite simple and can easily be incorporated into the well-known linear elastic theory or BISAR software.

Theoretical studies showed that the distribution of stresses, strains and deflections within a pavement structure is highly influenced by interface bond condition. Bond condition between binder course and base seems to be the most significant factor on the life of the overall pavement structure. Full slippage at this interface could reduce the pavement life by about 50% to 80%. Whereas the intermediate bond condition at this interface could reduce the pavement life by approximately 20% to 40%. However, it should be noted that the theoretical studies were based on the traditional assumption that the life due to fatigue is determined by fatigue cracking at the base of the asphalt layer(s) and the life due to permanent deformation is empirically determined from vertical compressive strain at the top of the subgrade; whereas recent research has suggested that in thick asphalt pavement structures, fatigue cracking could initiate from the surfacing and permanent deformation could occur within the bituminous materials. Furthermore, thick asphalt pavement structures showed no evidence of structural deterioration due to fatigue at the bottom of the asphalt layers or deformation at the top of the subgrade as long as the pavement structure had been properly maintained [Nunn *et al.*, 1997; Myers and Roque, 2001; Read and Whiteoak, 2003]. Therefore, a more detailed theoretical research on the effect of bond on structural life of a pavement structure that considers different failure mechanisms (e.g. Figure 2.57 suggested by Hakim [2002]) is required.

Investigation into the effect of horizontal load on bond revealed that the maximum horizontal tensile strain on the pavement surface is located just outside the contact area and the direction is 180 degrees from the direction of the applied horizontal load. The high magnitude of horizontal tensile strains along the edge of the contact area as a result of horizontal load application can lead to progressive failure around the back edge of the contact area. This behaviour agrees with the crescent-shaped (slippage) crack phenomenon.

Investigation into the effect of surfacing thickness on bond showed that the reduction of surfacing thickness tends to increase the horizontal shear stress at the

bottom of the surfacing, which may cause the bond condition between the surfacing and the binder course becomes more critical. If slippage occurs within this interface, the maximum horizontal tensile strain at the bottom of the surfacing becomes excessive and the value may exceed the horizontal tensile strain at the bottom of the bituminous layer and cause a rapid surfacing failure. This condition becomes worse when a significant horizontal load exists.

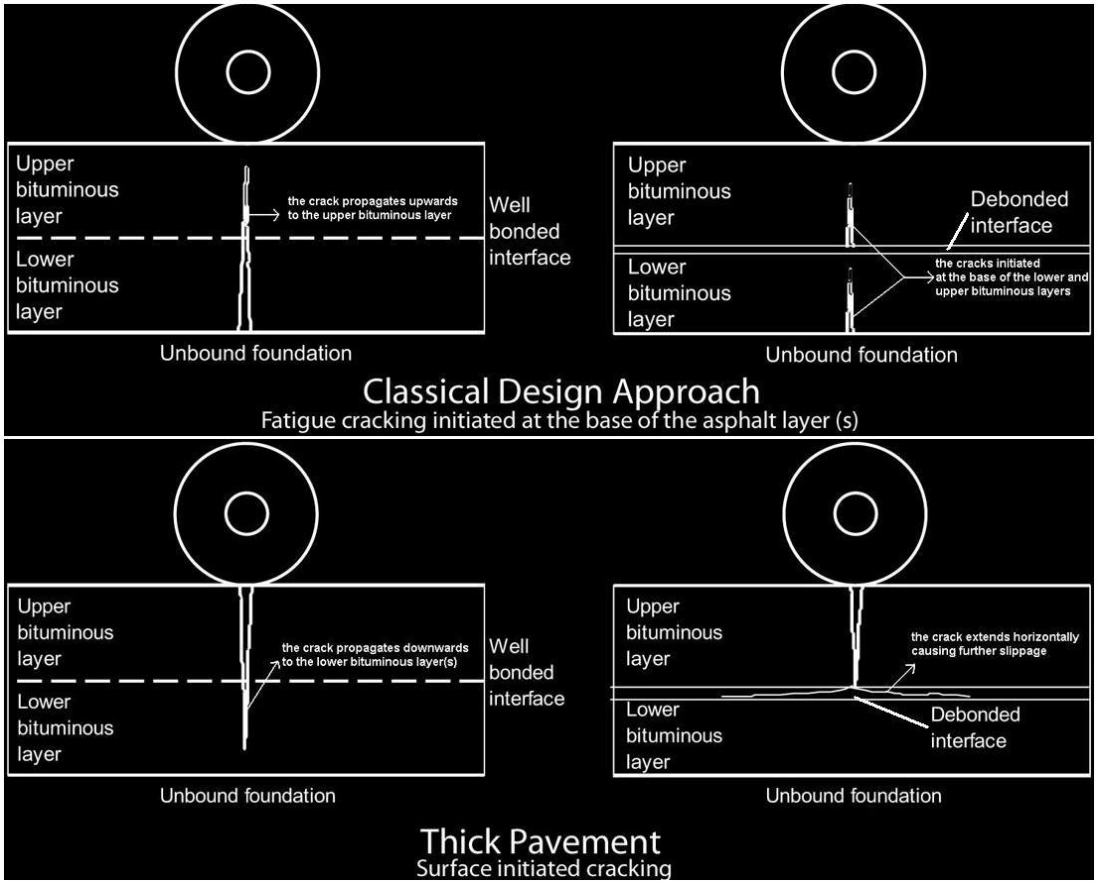

Figure 2.57 – Effect of bond on crack initiation and propagation (Adapted from Hakim, 2002).

Considering the importance of bond, several test methods have been developed in different countries to evaluate the mechanical properties of bond. A comprehensive summary of existing test methods for assessing bonding conditions has been presented and discussed briefly in Section 2.5 of this Chapter. The tests can be broadly divided into two main categories: destructive and non-destructive

bond tests. The destructive test is typically associated with coring or cutting processes that cause damage to the pavement structure, whilst the non-destructive test does not include any process that may cause damage to the pavement structure.

Clearly, the non-destructive test method has the advantage of not causing damage to the pavement structure. However, it should be noted that apart from the new FWD back-analysis method developed by Al Hakim [1997], the existing non-destructive test methods are only capable to detect bond failure and have not been able to determine the state of bond at the interface. The new FWD back-analysis method developed by Al Hakim [1997] seems to be the most useful non-destructive technique to date. However, it is also considered to have the following limitations:

- When construction history is not available, a destructive coring survey needs to be undertaken in order to determine pavement parameters to be used in the analysis.
- The FWD analysis is sensitive to layer thicknesses. Inaccurate input of layer thicknesses in the analysis may cause erroneous results.
- Kruntcheva *et al.* [2000b] found that the test is not suitable to determine the state of bond at shallow interfaces.

Considering the aforementioned disadvantages, the non-destructive test method is not discussed further in this research.

Along with the development of the non-destructive test methods, various destructive test methods have also been developed by many researchers. Considering that those destructive test methods utilise various test principles, test conditions, test configurations, specimen geometries, specimen dimensions and test equipments, they render different test results. According to the loading mechanism, the destructive bond test method could be classified into the following types (Figure 2.58):

(a) Tensile bond test
(b) Torque bond test

(c) Direct shear bond test

(c.1.) Direct shear bond test with normal load

(c.2.) Direct shear bond test without normal load

(d) Other destructive bond test

(d.1.) Three-point shear bond test

(d.2.) Four-point shear bond test

(d.3.) Indirect tensile bond test

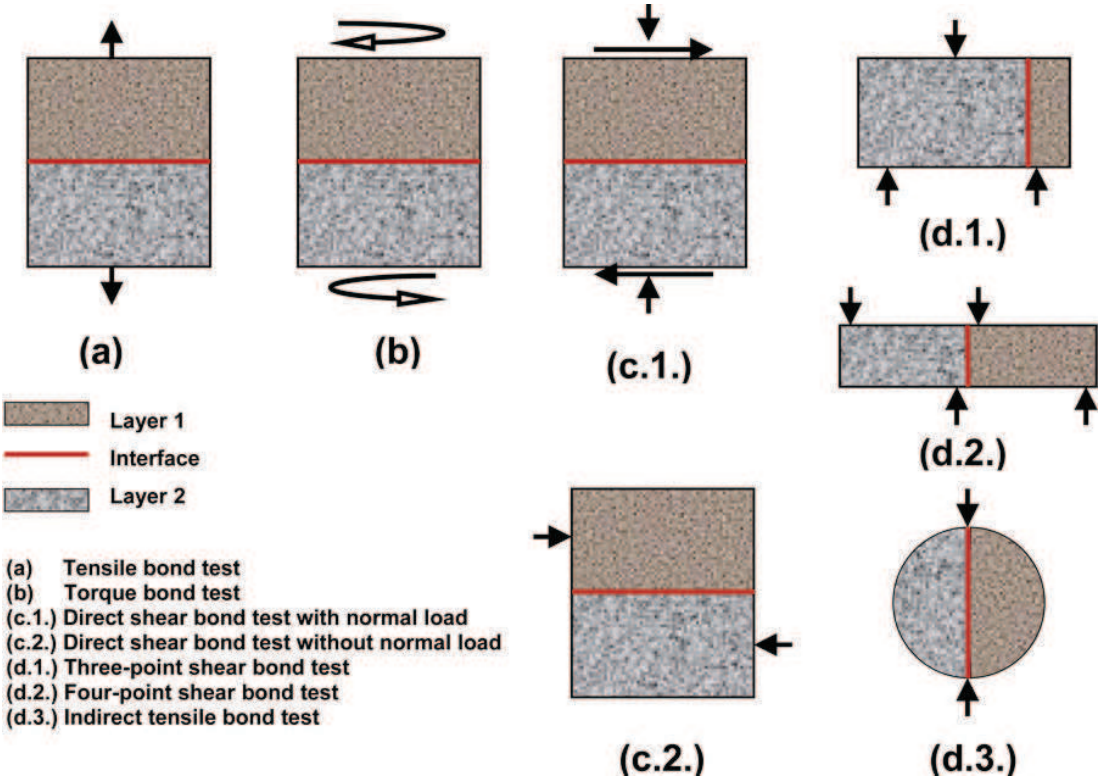

Figure 2.58 – Main types of destructive bond test methods.

The tensile and indirect tensile bond test methods (types (a) and (d.3.)) are considered to be useful for determining the tensile bond properties. The tensile bond tests are available in both laboratory and in-situ variants, whilst the indirect tensile bond tests are only available in a laboratory variant. It should be noted that although it could occur in a real pavement structure, the tensile separation mode employed by the tensile and indirect tensile bond test methods seems to be rarely found in the reported cases of bond failure (Sections 2.3 and 2.4.1). Several researchers also

considered that the representation of a realistic interface loading condition in the field by the tensile and indirect tensile bond tests is dubious [Raab and Partl, 1999; Kruntcheva *et al.*, 2000b; Choi *et al.*, 2005; Ferrotti, 2007]. Furthermore, both the direct and indirect tensile tests are known to have several limitations related to the scattering of results, the inability to determine the interface tensile strength when it is higher than that of the asphalt layer and the inability to assess the effect of aggregate interlock. Due to the aforementioned considerations, the tensile and indirect tensile test methods seems not suitable for determining the bond properties of an interface between pavement layers.

The other test methods (types b, c.1., c.2., d.1. and d.2.) utilise the shear separation mode that appears to be the most commonly found in the reported bond failures in the field. In terms of uniformity of the induced shear stress at the interface, the four-point shear bond test (type d.2.) seems to be pre-eminent for a detailed research because it renders a uniform shear stress distribution and eradicates bending at the interface. Furthermore, the test can be performed with and without the application of a normal load. However, due to the complexity related to specimen preparation and experimental setup, the four-point shear bond test is considered not suitable for routine testing of bond.

The direct shear tests with (type c.1.) and without (type c.2.) the applications of a normal load seem to be the most common and widely used laboratory test methods to investigate the bond properties. Both of them are known to suffer from non uniform shear stress distribution at the interface. The direct shear test with normal load is considered more suitable for a detailed research than the direct shear test without normal load because it can be used to asses the effect of normal load and dilatancy. However, the application of normal load requires a much more complicated testing set-up, and it is thus more difficult for it to be accepted as a routine test. The direct shear test without normal load (type c.2.) seems to be the most suitable laboratory-based test for routine testing of bond due to several considerations, including:

- Simpler experimental setup due to the absence of normal load application.

- Simpler specimen preparation because it does not require specimen gluing and the test typically uses a core specimen which is widely used for pavement evaluation purposes and can easily be retrieved from a pavement structure or a laboratory manufactured slab.
- Shear load applied in a pre-defined shear plane, so that failure would not occur within the asphalt layer.
- Quicker duration.
- Good precision in test results, as demonstrated by [Raab and Partl, 1999; Stöckert, 2001; Sholar *et al.*, 2004; Choi *et al.*, 2005; Ferrotti, 2007].

Furthermore, several testing protocols of the direct shear test without normal load have been included (in Germany, Austria and Switzerland) or proposed (in the UK and USA) as laboratory-based standard tests in different countries [DIN, 1999; FSV, 1999; Vereinigung Schweizerischer Strassenfachleute (VSS), 2000; Sholar et al., 2004; Choi et al., 2005].

The three-point shear test (type d.1.) is quite similar to the direct shear tests. It also suffers from non-uniform shear stress distribution at the interface. Although a normal load can also be applied, the test is typically performed without normal load. In terms of popularity, the test seems to be less popular than the direct shear tests and only a few researchers (Mirò Recasens *et al.*, 2005; Vacin *et al.*, 2005) use this test arrangement. It should be noted that due to its specific supports and loading arrangements, the test would require a longer core specimen and a higher capacity of loading machine than that of the direct shear test without normal load. Therefore, the test (type d.1.) would be less favourable for routine bond testing than the direct shear test without normal load (type c.2.).

In the torque bond test (type b), shear failure at the interface is induced by twisting a core specimen at a constant rate. The test can be performed by applying the torque manually or mechanically and is available in both in-situ and laboratory variants. Normal load can also be applied in several variants of this test. Although a clamping mechanism can also be used, metal platen(s) glued on top (and bottom) of the core specimen are typically used to transfer the torque into the core specimen. The main drawback of this test is that the failure would occur within the asphalt layer

when the shear strength of the asphalt layer is lower than that of the interface. Therefore, this test might not be suitable for specimens containing a structurally weak surfacing material such as porous asphalt. This drawback could be eliminated by clamping the core specimen in such way that the edge(s) of the clamp(s) forms a pre-defined shear plane at the interface. However, Raab and Partl [1999] mentioned that the clamping could be problematic because insufficient gripping would cause slipping, whilst over tightening may cause damage to the specimen. Furthermore, they reported that the standard deviation of the measured torque strengths in the torque bond test could be as high as 20% of the average value. Due to the issues related to shear failure within the asphalt layer and the scattering of results, the torque bond test would be less accurate than the other tests that utilise the shear separation principle (types c.1., c.2., d.1. and d.2.). Furthermore, because it typically requires gluing of specimen (or gripping if a clamping mechanism is used) the torque bond test would be less suitable for a laboratory-based routine testing of bond than the direct shear test without normal load (type c.2.) and the three-point shear test (type d.1.).

Due to the importance of bond and to provide more assurance that the construction of roads complies with the design requirements, the availability of a standardised bond test method for routine testing in the UK is essential. *Choi et al.* [2005] performed an investigation to develop a laboratory-based standard test for routine testing of bond in the UK and demonstrated the suitability of the Leutner test (a type of direct shear test without normal load) for routine testing of bond. They introduced a 5mm gap between the Leutner shearing rings to eliminate crushing of large aggregate particles at the interface and to improve the repeatability of the test (discussion on the effect of the 5mm gap has been presented in Section 2.5.1.3 of this Chapter). They developed a modified Leutner testing protocol (with the 5mm gap) and utilised it to perform bond tests on a limited number of laboratory prepared specimens and field cores. It should be noted that because the modified Leutner testing protocol requires the upper layer thickness to be tested it should be at least 30mm (Appendix A.1); it could not be used to determine the bond beneath a thin surfacing layer less than 30mm in thickness.

Due to this limitation, the modified Leutner test (with 5mm gap) needs to be further modified to cover bond strength measurement underneath a thin surfacing layer less than 30mm in thickness. Such modification to the LPDS test (similar to the modified Leutner test) to allow the determination of bond properties beneath thin surfacings by means of steel plate extension has been performed at EMPA by Raab and Partl [2004b, 2005]; however, the effects of upper layer thickness and the steel plate extension on the measured bond strengths have not been investigated thoroughly. Further modification to the modified Leutner test to allow the determination of bond strengths beneath thin surfacing layers (<30mm in thickness) was carried out as a part of this research. This modification is discussed in more detail in Chapter 3, where results from an experimental investigation on the effect of upper layer thicknesses and extensions as well as a discussion on an FE analysis performed by Dr. S. Wang (a research associate at The University of Nottingham) are presented. Furthermore, to be accepted as a robust method to determine interface bond properties, the modified Leutner test needs to be utilised to perform bond testing on a wide range of UK material combinations and bond conditions. Therefore, a bond database using the modified Leutner test was developed in this research study and the details will be discussed in Chapter 6.

The manual torque bond test is widely used in the UK due to the fact that it is included as a mandatory test in the guidelines document SG3/05/234 [British Board of Agreement, 2004] as part of the assessment and certification of thin surfacing course systems. The test is performed manually and no normal load is applied. Although it can be performed in the laboratory, the manual torque bond test is typically performed in-situ and generally restricted to the uppermost interface. Because it is typically performed by taking a partial core followed by gluing a metal platen on top of the core and then applying a torque manually using a handheld torque wrench, the manual torque bond test is considered as a relatively cheap and simple method to determine bond strength underneath a thin surfacing layer. Although it has several drawbacks that may affect the accuracy of results; due to its low cost, portability and practicality the manual torque bond test seems to be the most suitable alternative for in-situ routine testing of bond underneath a thin surfacing layer, providing that the in-layer shear strength of the surfacing is higher than the shear strength of the interface underneath the surfacing.

It is interesting to note that Choi *et al.* [2005] performed the manual torque bond test at a constant torque rate of 600Nm/minute, whilst the guidelines document SG3/05/234 [British Board of Agreement, 2004] requires the test to be performed at a constant rotation rate of 180°/min. Because rotation rate at the interface may be affected by adjacent layer thicknesses and stifnesses, performing the test at a constant rotation rate may affect the variability of results. A series of experimental tests to investigate the effect of the two different loading rates (600Nm/min and 180°/min) used in the manual torque bond test on the variability of results were part of this research study and the findings are presented and discussed in Chapter 4.

To achieve a good state of bond at the interface, many researchers performed investigations on the factors that affect interface bond conditions. Several factors that have been identified in this literature review are compaction level and quality of lower layer material, rolling temperature, lower layer temperature during construction, compaction level of upper layer material, compaction method, air void content of the mixture, gradation of upper and lower layer mixtures, mixture type, application of bituminous bond (tack) coat at the interface, appearance of water at the surface of lower layer, water penetration to the interface, contamination (e.g. dirt, debris, oil) at the surface of lower layer, age of lower layer, application of stress absorbing membrane interlayer (SAMI) at the interface, surface texture of lower layer material, interlayer roughness, pavement temperature, loading rate, specimen dimension, normal load, pavement geometry, time, combination of traffic and time and trafficking at elevated temperature.

One of the factors that may affect interface bond conditions is trafficking at elevated temperature. After performing pilot scale experiments in an accelerated testing facility at different temperatures on the same pavement construction, Choi *et al*. [2005] indicated that when initial bond strength was low or intermediate (<1MPa), the bond strength increased with trafficking at 30-35^{o}C. However, further investigation is required to confirm this because only a very limited number (4) of cores were successfully tested and the interface treatment they used was very un-realistic. Therefore, an investigation into the effect of trafficking at an elevated temperature on bond with a particular emphasis on situations where the initial bond

is below 1MPa was performed during the research of this thesis and the details are presented in Chapter 5.

Along with the availability of a standardised test method, a specification limit of bond strength is also essential. At the moment, no specification limit of bond strength for UK road constructions is available. Lack of information regarding the value of bond strength to be achieved would cause dilemmas during construction. This issue becomes more important due to the extensive use of thin surfacing course systems in the UK, because a thinner surfacing layer is associated with a higher shear stress at the interface beneath the surfacing, which may result in a more critical bond condition at this interface. Further details regarding the recommendation of specification limits of bond strength in the UK will be discussed in Chapter 7.

Chapter 3

MODIFICATION TO THE LEUTNER TEST

3.1 Introduction

As discussed in Chapter 2, the direct shear test without normal load seems to be the most suitable for routine testing of bond. Choi *et al*. [2005] have also demonstrated the suitability of the Leutner test (a simplified direct shear test without normal load) to determine the bond between asphalt layers. They introduced a 5mm gap between the shearing rings to improve the repeatability of the results and developed a modified Leutner testing protocol (with the 5mm gap, see Appendix A.1). They proposed the modified Leutner testing protocol as a laboratory-based specification test method to determine bond properties of an interface between asphalt layers in the UK. To ensure a proper contact with the upper shearing ring, they recommended in the modified Leutner testing protocol that the minimum thickness of the upper layer should be 30mm. Consequently, the modified Leutner test should not be used to determine the bond strength beneath thin surfacing course systems less than 30mm in thickness.

This Chapter presents further modification to the modified Leutner test (with 5mm gap) to accommodate testing of thin surfacing course systems having layer thickness less than 30mm. Raab and Partl [2004b, 2005] have performed such modification to the LPDS test (similar to the modified Leutner test) by attaching a steel platen to the surface of a core specimen to enable the measurement of bond properties at the interface beneath a thin asphalt layer. However, the effects of surfacing thicknesses and extensions on the measured bond strength have not been investigated.

3.2 Comparison between Standardised Test Methods

As discussed earlier in Chapter 2, several testing protocols of direct shear test without normal load have been included or proposed as standard tests for routine testing of bond in different countries. A comparison between the testing protocols is presented in Table 3.1.

Table 3.1 Comparison between different standard testing protocols of direct shear test without normal load

	Source				
	DIN [1999]	**FSV [1999]**	**VSS [2000]**	**Sholar *et al.* [2004]**	**Choi *et al.* [2005]**
Standard	DIN2312 ALP A-Stb Teil 4	RVS 11.065 Teil 1	SN 671961	proposed	proposed
Apparatus	Leutner	Austrian Shear Tester	LPDS/Leutner (1)	FDOT Shear Tester	Modified Leutner
Country	Germany	Austria	Switzerland	USA	UK
Specimen	Core 150 ± 2mm diameter	Core 100 ± 2mm diameter	Core 150 ± 2mm diameter	Core 150 ± 2mm diameter	Core 150 ± 2mm diameter
Displacement rate	50 ± 3mm/min	50 ± 3mm/min	50 ± 3mm/min	50.8mm/min	50 ± 2mm/min
Testing temperature	20 ± 1°C	25 ± 1°C	20 ± 1°C	25°C	20 ± 0.5°C
Clamping mechanism	Manually tightened	Manually tightened	Hydraulic or manually tightened (3)	Manually tightened	Manually tightened
Gap between shearing rings	No gap	N/A	Maximum 2mm (2)	4.8mm	5mm
Maximum deviation of specimen surface	5mm	N/A	2mm	N/A	N/A
Minimum upper layer thickness	25mm	N/A	25mm	N/A	30mm
Minimum lower layer thickness	70mm	N/A	N/A	N/A	60mm

(1) Both LPDS and Leutner apparatus are compatible [Raab and Partl, 1999]
(2) No gap when Leutner apparatus is used or 2mm gap when LPDS apparatus is used [Raab and Partl, 1999; Wellner and Ascher, 2007].
(3) Hydraulic when LPDS apparatus is used or manually tightened when Leutner apparatus is used [Raab and Partl, 1999]

All standard testing protocols listed in Table 3.1 use a core specimen, a nominal displacement rate of 50mm/min and an intermediate nominal testing temperature of 20 or 25°C. The core specimen seems to be favourable because it is widely used and retrieval of the specimen can be performed easily. The nominal displacement rate of 50mm/min allows the test to be carried out in the widely available standard Marshall and CBR loading devices. The intermediate testing temperature of 20 or 25°C could easily be achieved in the laboratory and has been preferred by several researchers [Partl and Raab, 1999; Sholar *et al.*, 2004; Choi *et al.*, 2005; West *et al.*,2005]. Apart from the Austrian standard RVS 11.065 Teil 1, all the standard testing protocols use a nominal specimen diameter of 150mm, which appears to be widely used in pavement evaluation purposes and could be expected to render less variable results compared to that of the 100mm nominal diameter.

The German [DIN, 1999], Swiss [VSS, 2000], USA [Sholar *et al.,* 2004] and UK [Choi *et al.,* 2005] testing protocols specify a gap between shearing rings of 0mm, maximum 2mm, 4.8mm and 5mm respectively. The gap provides a certain level of tolerance to accommodate testing of a slightly skewed or uneven interface. It is worth noting that the gap should not be too large or it may cause excessive bending stresses due to the cantilever effect of unsupported specimen edges. The maximum 2mm gap specified in the Swiss testing protocol allows both the commercially available standard Leutner apparatus with no gap and the more versatile LPDS apparatus with a 2mm gap to be used in this testing protocol. Assuming the deviation of the specimen surface is equal to that of the interface; the maximum interface deviation in the Swiss protocol would be 2mm, which could easily be accommodated by the 2mm gap in the LPDS apparatus. It should be noted that the 2mm maximum interface deviation would be a little bit difficult to accommodate if the standard Leutner apparatus with no gap is used in the Swiss protocol. This difficulty would arise in the German protocol, where a maximum surface deviation of 5mm is specified and a standard Leutner apparatus with no gap is used.

The gap specified in the USA protocol is approximately equal to that of the UK protocol. As previously discussed in Chapter 2, the 5mm gap between shearing rings in the modified Leutner apparatus used in the UK protocol was introduced

because Choi *et al.* [2005] frequently observed crushing of large aggregate particles at the edge of the specimen and found it difficult to align the interface in the standard Leutner apparatus. The effect of the 5mm gap has also been discussed comprehensively in Chapter 2. Although the maximum deviation of specimen surface is not specified in the UK testing protocol, BS EN 12697-36 [British Standards Institution, 2003f] recommends that the axis of a core specimen should be within 5° of the normal axis to the pavement, which may cause an interface deviation in a 150mm diameter core specimen of up to 13mm. Although the 5mm gap in the UK protocol would not fully accommodate an interface deviation of up to 13mm, it is considered to be wide enough because providing a 13mm gap to fully accommodate the interface deviation would increase the risk of excessive bending stresses.

The German and Swiss protocols require a minimum upper layer thickness of 25mm, whilst the UK protocol requires an upper layer thickness of at least 30mm. The minimum upper layer thicknesses were specified because too little contact between the upper layer specimen and the upper shearing ring would cause higher stress concentrations at the contact area and may results in a “snow plough” effect at the edge of the specimen as mentioned by Raab and Partl [1999], especially when the upper layer material is structurally weak or when testing specimens at an elevated temperature. Considering the minimum upper layer thickness, the presence of a gap between shearing rings and that the interface is assumed to be aligned at the middle of the gap; the minimum effective width of the contact area between the specimen and the upper shearing ring in the Leutner, the LPDS and the modified Leutner apparatus would be 25mm, 24mm and 27.5mm respectively (Figure 3.1).

To ensure a proper specimen clamping, the German and UK protocols require a minimum lower layer thickness of 70mm and 60mm respectively. Although the Swiss protocol does not specify the minimum lower layer thickness, the clamping arrangement of the LPDS apparatus, shown in Figure 3.1, would provide better specimen clamping than those of the Leutner and modified Leutner apparatuses.

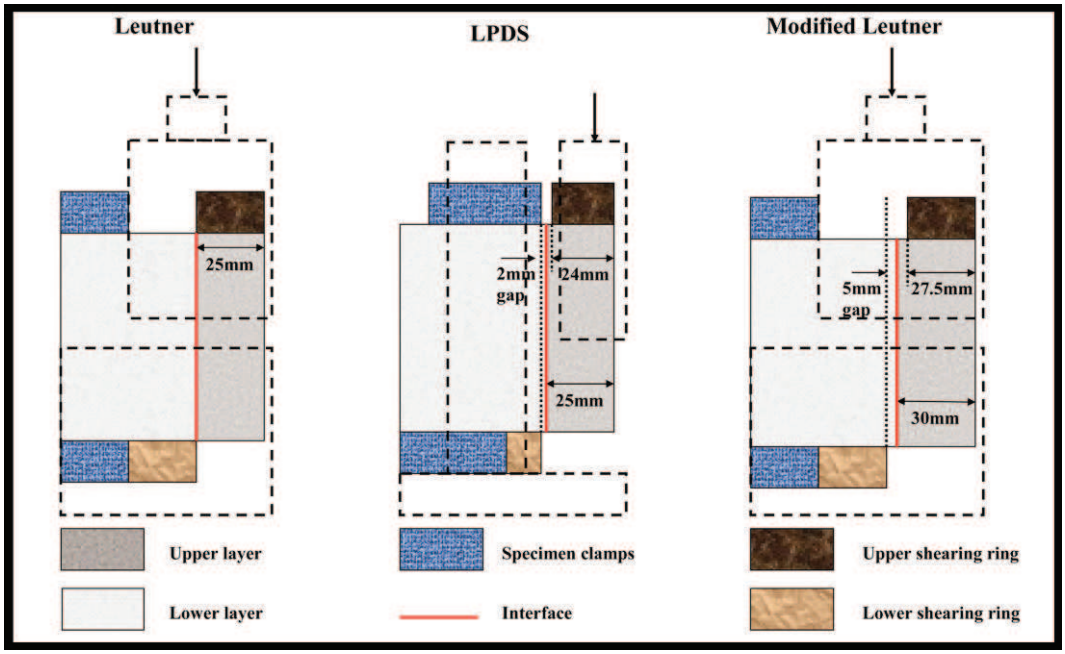

Figure 3.1 - Comparison of gap, minimum upper layer thickness and minimum contact width between different equipments (Adapted from DIN [1999], VSS [2000] and Choi *et al.* [2005]).

3.3 Experimental Programme

3.3.1 Materials

Two types of surfacing materials consisting of a 14mm Stone Mastic Asphalt (SMA) and 10mm proprietary Thin Surfacing (TS1) were used as the upper layer in this study. A typical binder course material consisting of a 20mm Dense Bituminous Macadam (20DBM) was used as the lower layer. A gritstone aggregate was used for the SMA and TS1 mixtures and a limestone aggregate was used for the DBM mixture. All materials were designed according to the relevant Standards [British Standards Institution, 2005a and 2006b]. Details of the mixtures are given in Table 3. 2.

Table 3. 2. Mixture characteristics

Mixture type	Binder grade	Binder content (% mass)	Air void content	Max. density (Mg/m3)	Compacted layer thickness (mm)
20mm DBM	30/45pen	4.7%	5.5%	2.490	60
14mm SMA	40/60pen	6%*	4%	2.501	40
10mm TS1	150pen	4.9%	4%	2.554	15/25/35

* includes 0.3% cellulose fibres by mass of total mixture

Slabs of plan dimensions 305mm by 305mm, each comprising of two layers, were manufactured in a Cooper CRT-RC slab 'roller' compactor [Cooper Technology, 2009] in accordance with BS EN 12697-33 [British Standards Institution, 2003d] to simulate site compaction conditions as closely as possible. The roller compactor presented in Figure 3.2 is capable of compacting a 305mm by 305mm slab with a target thickness of 40-100mm. It is equipped with a steel wheeled roller segment of 800mm diameter and 305mm width, a sliding table that is able to move back and forth beneath the roller and a pneumatic system which allows a 30kN roller load to be applied. The compaction is performed by placing a mould containing a loose asphalt mixture on the sliding table, applying a compaction force (without vibratory mode) to the roller and moving the sliding table back and forth until the target specimen thickness is achieved.

The material for the lower layer, once mixed, was placed in the mould and compacted to the desired thickness (60mm). The layer was allowed to cool to room temperature and the surface was then treated to give one of the desired interface conditions:

(a) For the SMA surfacing, a 'standard' amount of tack coat, comprising K1-40 emulsion was spread on the lower layer surface using a clean brush to give an average of 200 g/m^2 residual bitumen. The emulsion was allowed to break before laying the upper layer.

(b) For the TS1 surfacing, a polymer modified bond coat was spread on the lower layer surface to give an average of 300 g/m^2 residual bitumen.

The tack coat and bond coat application rates used in this investigation were chosen according to recommendations from the industry and the Road Emulsion Association (REAL) Ltd. After the interface had been prepared, the material for the upper layer was then mixed and compacted on top of the lower layer to the desired thickness. From each slab, two 150mm cores were obtained for Leutner testing. Six identical tests were undertaken for each test condition.

Because the minimum compacted thickness of the SMA mixture is 40mm, some of the SMA/20DBM cores were trimmed to get surfacing thickness of 15mm and 25mm as needed for the surfacing thickness investigation.

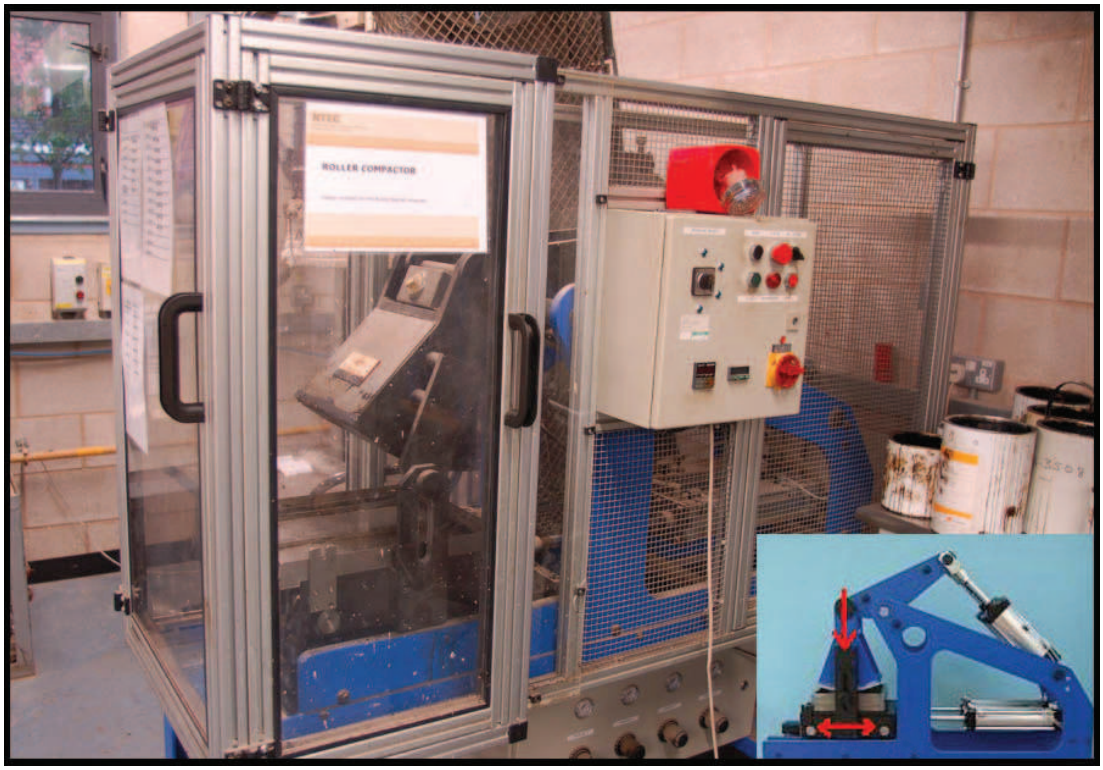

Figure 3.2 - Photograph of the slab roller compactor

3.3.2 Modified Leutner Test Procedure

After the cores had been produced, they were conditioned in a temperature-controlled cabinet prior to testing. Cores were then placed into the modified Leutner apparatus and the interface properly aligned with the shear axis. The modified Leutner shear test was performed according to the testing protocol developed by Choi et al. [2005], presented in Appendix A.1. As presented in Table 3.1, the test is typically performed on a 150 ± 2mm core specimen at a displacement rate of 50 ± 2mm/min and a testing temperature of 20 ± 0.5°C. Because it is commonly found in the field that the deviation of a core diameter could be up to 5mm, the modified Leutner testing protocol presented in Appendix A.1 recommends having at least 5 sets of various interchangeable shearing rings from 145 to 155mm in diameter to cover the range of specimen diameters. The shear force is measured using a load cell and the shear displacement is measured using a Linear Variable Differential Transformer (LVDT) incorporated into the hydraulic testing machine (i.e. load-line displacement). Figure 3.3 shows a photograph and schematic diagram of the modified Leutner apparatus used in this investigation.

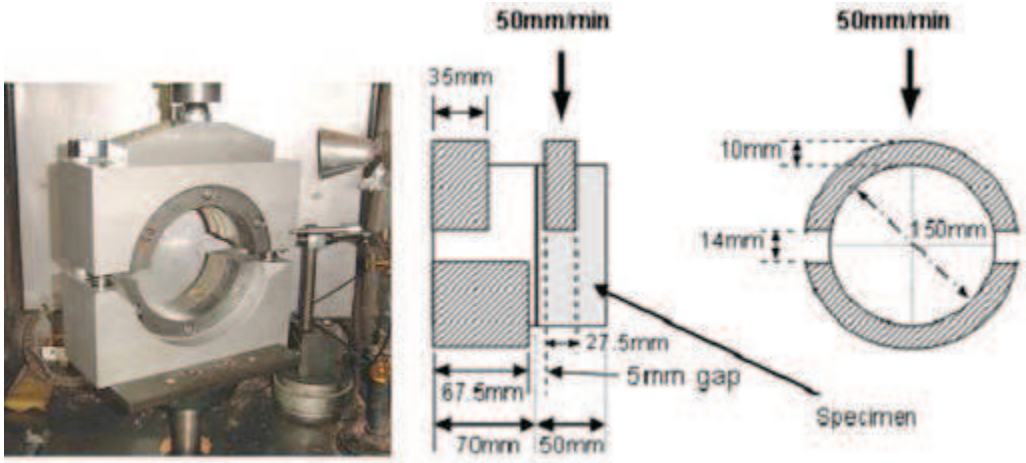

Figure 3.3 - Photograph and schematic diagram of modified Leutner apparatus (From Choi *et al.*, 2005)

3.4 Effect of Surfacing Thickness

The objective of this first phase of the investigation was to study the effect of surfacing thickness on shear strengths of the interfaces. Two layer specimens using varying upper layer thickness and material types were investigated. The experimental data were evaluated for outlying points using boxplot analysis to find an unusually large or small observation known as outlier. The appearance of outliers in the data being analysed may result in misleading data interpretation.

The boxplot analysis is a graphical analysis and known to be one of the easiest and quickest methods to identify outliers. In this analysis, the median and the interquartile range (25^{th} and 75^{th} percentile) were determined. MINITAB software was used to perform the boxplot analysis. MINITAB identifies outliers on boxplot analysis by labelling observations that are at least 1.5 times the interquartile range from the edge of the box [Minitab Inc., 2007]. Clearly, boxplots of the experimental data used in this investigation do not show outlying observations (Figure 3.4).

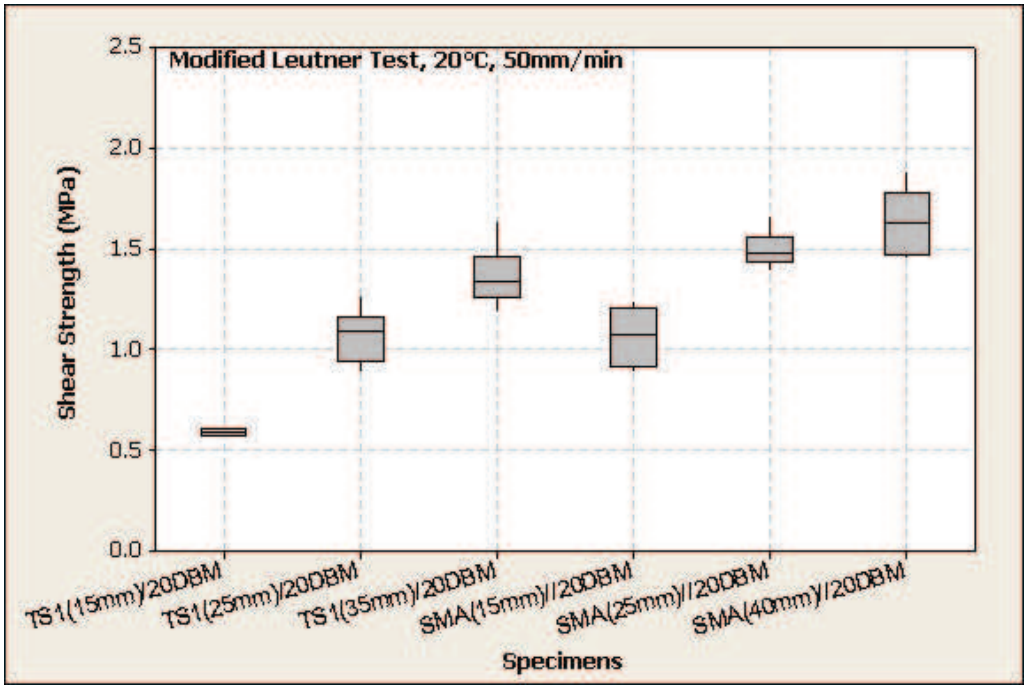

Figure 3.4 – Boxplots of the experimental data used in the effect of surfacing thickness investigation.

Figure 3.5 shows the shear strength measured from the SMA/20DBM specimens (SMA thickness of 15, 25 & 40mm) and the TS1/20DBM specimens (TS1 thickness of 15, 25 & 35mm) together with 95% confidence limits. The results shown in Figure 3.5 demonstrate that the difference in shear strengths for surfacing having thickness greater than 25mm is relatively small. For both the SMA/20DBM and the TS1/20DBM combinations, the shear strengths decrease significantly when the thickness of the surfacing is reduced to 15mm.

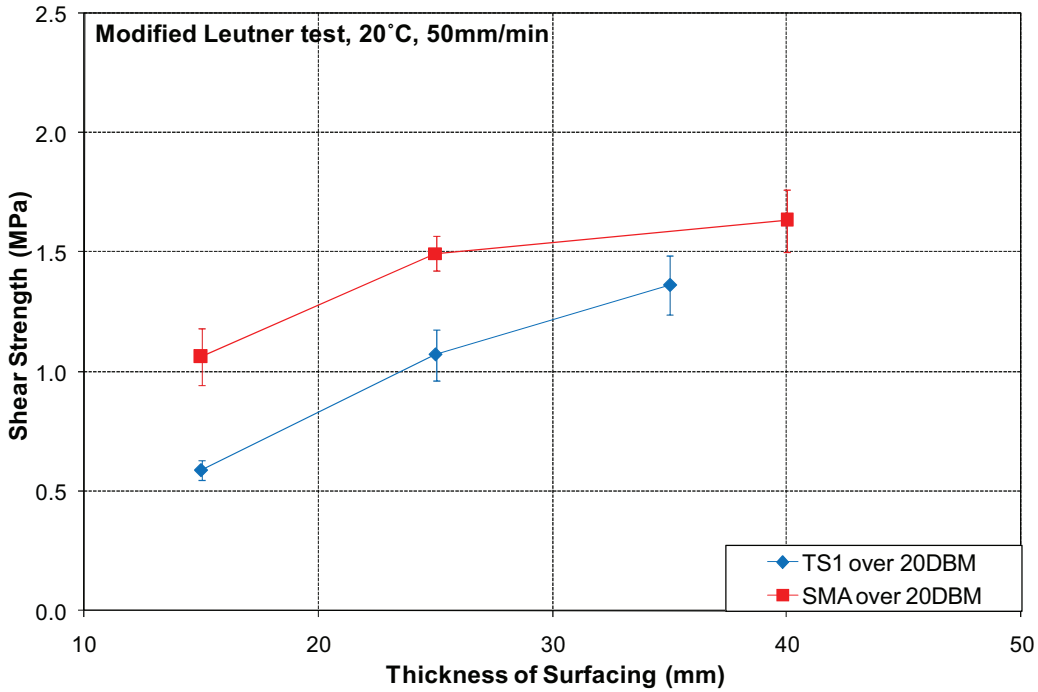

Figure 3.5 - Effect of surfacing thickness on interface shear strength

To investigate the mode of failure and attempt to explain the lower bond strengths obtained from the specimens containing the thinner upper layer material, the profiles of the specimens' surface were measured using a profile comb and the cores were inspected. The photographs of the TS1/20DBM and the SMA/20DBM specimens after testing and the profiles of the specimens' surface are shown in Figures 3.6 and 3.7, respectively. Figure 3.6 shows that for the TS1/20DBM specimen with the 15mm thick surfacing, the crack is not restricted entirely to the interface but extends into the surfacing mixture. The crack shows that the interface

is only partially failed (approximately 50% of the diameter) and the other part is still intact. Assuming that the shear plane area is equal to the failed area, using the whole diameter as a basis for calculating shear plane area leads to lower measured shear strength. Figure 3.7 shows that there is significant bulging at the top half of the surface of the TS1/20DBM and the SMA/20DBM specimens with the 15mm thick surfacings. For the TS1/20DBM and SMA/20DBM specimens with the 25mm thick surfacings, the crack is restricted to the interface and the bulging appears to be less significant (Figures 3.6 and 3.7).

The bulging is thought to be due to a number of factors including bending stresses in the specimen due to the fact that the shear force is applied a short distance away from the interface resulting in tensile stresses and strains in the top half of the specimen perpendicular to the plane of the interface, compression in the surfacing material resulting in lateral expansion due to Poisson's ratio effects and local buckling of the surfacing material. Some of these factors were verified with Finite Element (FE) models developed by Dr. S Wang (a research associate at The University of Nottingham) and the details are discussed in Section 3.8.

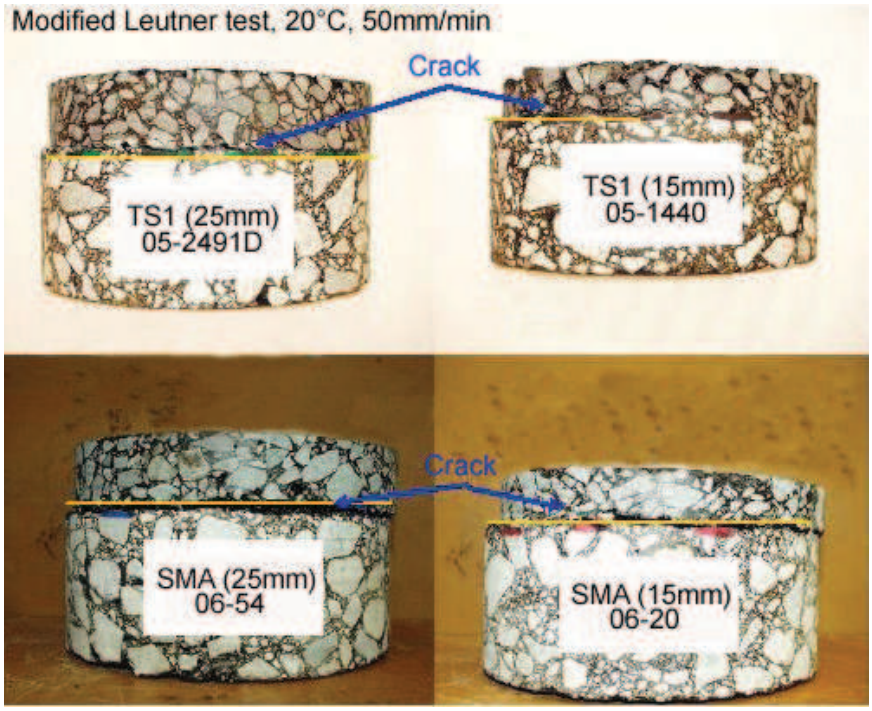

Figure 3.6 – Cores after testing

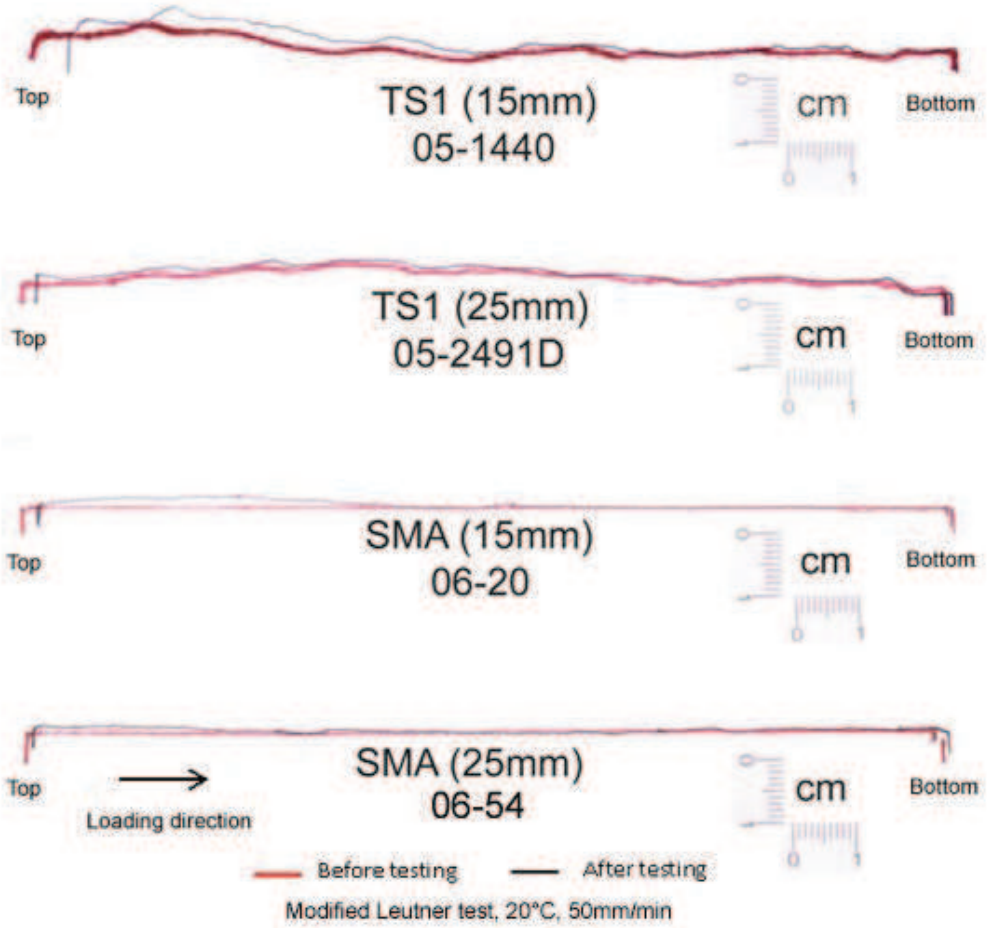

Figure 3.7 – Profiles of the specimens' surface, before and after modified Leutner testing

It can be seen in Figure 3.5 that the measured interface shear strength for the specimens containing SMA surfacing appears to be less sensitive to surfacing thickness than that for the specimens containing TS1 surfacing. Furthermore, Figure 3.6 shows that for all the combinations containing SMA surfacing the crack is restricted to the interface and for some of the combinations containing TS1 surfacing the crack is not restricted entirely to the interface but also extends into the surfacing mixture. In theory, the extent of crack would depend on the state of bond at the interface to allow cracking over the entire interface and the structural integrity of the surfacing to prevent cracking within the surfacing mixture. The effect of surfacing thickness on interface shear strength would be less significant when the interface shear strength is relatively low and the surfacing is relatively stiff (e.g. when a stiff

surfacing is laid over a concrete) because it would be easier to shear the interface off to allow cracking over the entire interface rather than in the stiff surfacing. On the other hand, the effect of surfacing thickness on interface shear strength would be more significant when the stiffness of the surfacing is relatively low (e.g. when the temperature is relatively high) and the interface is relatively strong because the crack would not be restricted entirely to the interface but may also extend into the soft surfacing mixture. The effect of surfacing stiffness on the extent of crack at the interface was also verified by an FE model developed by Dr. S Wang that will be discussed more detail in Section 3.8.

3.5 Effect of Surfacing Extension

In order to minimise bulging in the top half of the specimen and provide a larger area for the modified Leutner loading frame to apply the load, the thin surfacing materials were artificially extended using either a 150mm diameter cylindrical core of SMA (varying thickness) or a 150mm diameter flat surface cylindrical metal (aluminium) platen with a thickness of 30mm which were glued to the thin surfacing prior to modified Leutner testing. Raab and Partl [2004b, 2005] have used a similar approach in the LPDS test by gluing a cylindrical steel platen on top of a thin surfacing layer.

According to information gained from the industry, a stiff adhesive epoxy resin such as Araldite 2011 [Huntsman, 2007] or Epiglass® HT9000 [Marshall *et al.*, 2004] has been found suitable to glue an aluminium platen on top of an asphalt surfacing in the widely used manual torque bond test in the UK. The Epiglass® HT9000 has interlaminar shear strength of 25.9MPa and is suitable for temperatures between 10 and 35˚C. Therefore, Epiglass® HT9000 was used to glue the extension materials to the thin surfacings. Thin films of Epiglass® HT9000 of approximately 0.2 - 0.5mm (estimated by eye) were applied at the interface between the surfacings and the extension materials.

After modified Leutner testing, all the specimens failed at the bond between the 20DBM and the surfacing material when the SMA cores were attached to the

surfacing. In contrast, all the specimens failed at the glued interface between the surfacing and the aluminium when the flat aluminium platens were attached to the surfacing. Because the stiffness of aluminium at 69GPa is significantly higher than the stiffness of any asphalt material, a relatively high stress condition would occur at the aluminium extension. This condition together with the state of bond at the interface between the surfacing and the layer underneath may affect the state of shear stress at the glued interface between the surfacing and the aluminium extension. Therefore, it is necessary to investigate the interface shear strength between the surfacing and the layer underneath and that between the surfacing and the aluminium extension in order to find the reason why the specimens failed at the glued interface between the surfacing and the aluminium.

It is mentioned in the Epiglass® Manual [Marshall *et al.*, 2004] that Epiglass® HT9000 has interlaminar shear strength (shear strength between layers of laminated materials) of 25.9MPa. However, it should be noted that the interlaminar shear strength was obtained from a flexural beam test on a laminated material at a temperature and a loading condition that are different to that of the modified Leutner test. Therefore a series of modified Leutner tests was performed to determine the interface shear strengths at the glued interfaces of TS1/SMA and TS1/Flat-Aluminium. Three identical tests were performed for each combination. Boxplots of the experimental data do not show outlying observations (Figure 3.8). Results are shown in Figure 3.9 where it can be seen that the shear strength for the TS1/Flat-Aluminium interface is significantly lower than the shear strength for the TS1/SMA interface. Assuming that the interface shear strengths of the 35mm thick TS1/DBM of 1.36MPa shown in Figure 3.5 represents the 'true' interface shear strength of the TS1/20DBM combination, the interface shear strength for the TS1/Flat-Aluminium of 1.24MPa shown in Figure 3.9 is lower than that for TS1/20DBM. This, in conjunction with the relatively high stress conditions at this interface, could explain why the specimens failed at the glued interface between the surfacing and flat aluminium platen rather than at the stronger binder course and surfacing interface. In addition, the interface shear strength for the TS1/SMA of 1.970MPa, which is higher than that for TS1/20DBM, may also explain why the TS1/20DBM specimens with SMA extensions failed at the interface between the surfacing and the binder course.

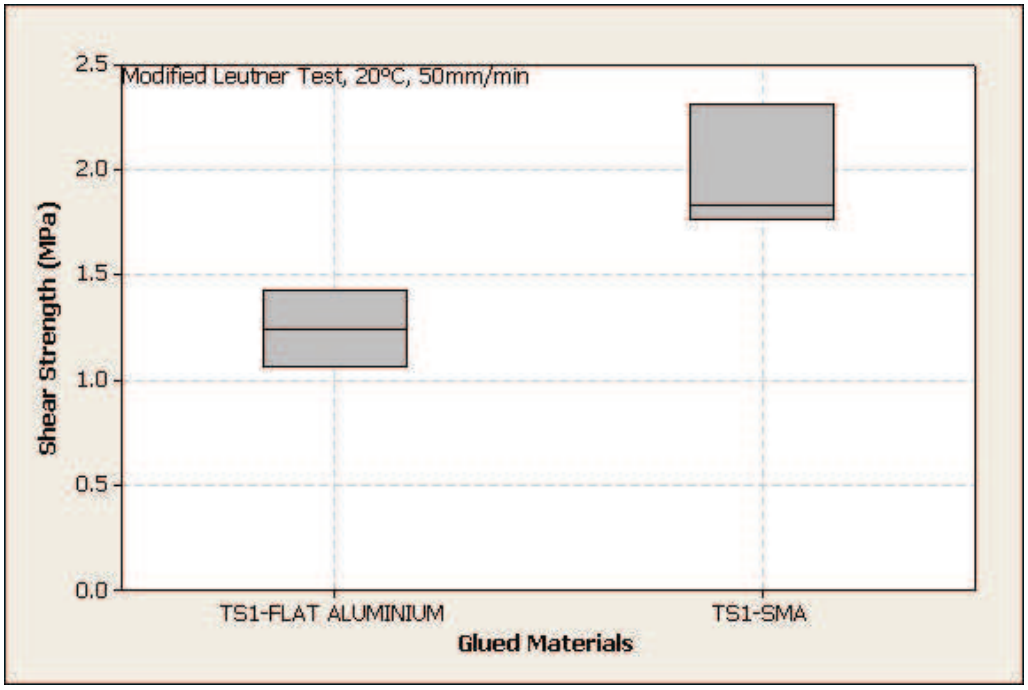

Figure 3.8 - Boxplots of the experimental data used in the effect of glued materials investigation

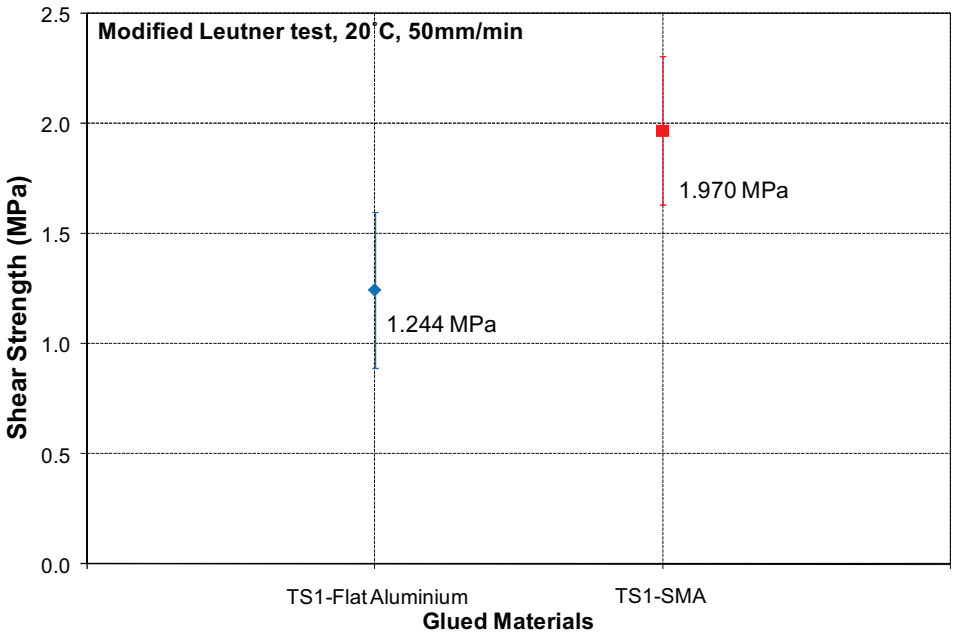

Figure 3.9 - Shear strengths at the interface between glued materials

It is also interesting to note that Raab and Partl [2004b, 2005] have successfully used a flat steel extension to determine the interface shear strength beneath a thin surfacing layer in the LPDS test and they did not report glue failure at the interface between the surfacing and the flat steel extension. This may be because the interface shear strength of the glued interface between the surfacing and flat steel extension they used was relatively higher than that beneath the thin surfacing they investigated. Assuming that a similar type of glue (stiff epoxy resin) was used and the interface shear strength between the surfacing and steel extension (used by Raab and Partl [2004b, 2005]) is similar to that of TS1/Flat-Aluminium of 1.24MPa (Figure 3.9), the interface shear strength between the surfacing and steel extension would be relatively higher than the interface shear strengths beneath the thin surfacings investigated by Raab and Partl [2004b, 2005] of between 0.9 and 1.13MPa (16 – 20kN over 150mm diameter cores).

To strengthen the interface between the aluminium and the surfacing, the platen was modified by grooving its surface to increase the effective contact area. This was found to be successful as it restricted failures to the interface of interest between the surfacing and layer below. Figure 3.10 shows a photograph and schematic diagram of the grooved aluminium platen.

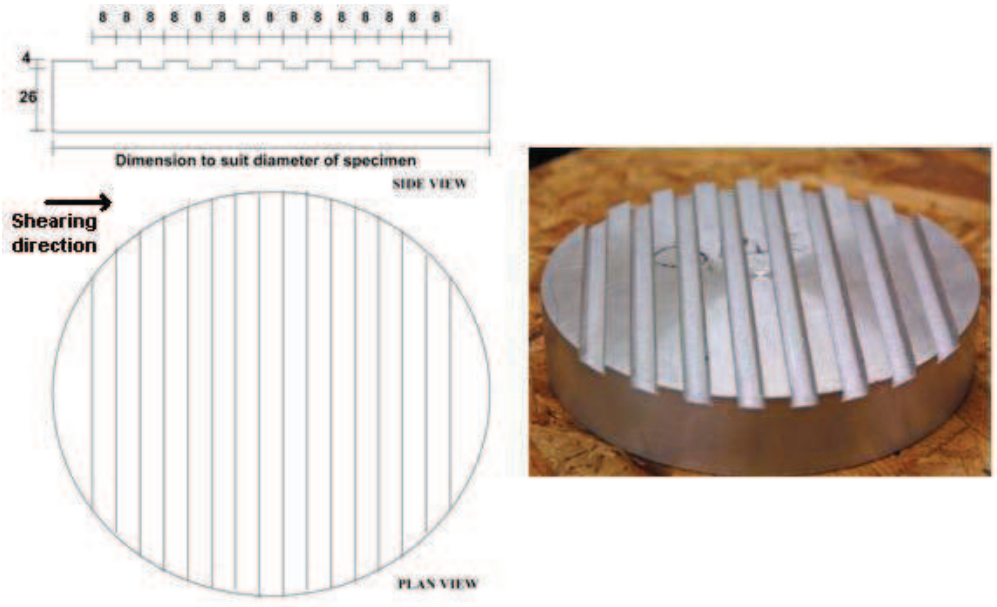

Figure 3.10 – Grooved aluminium platen

A series of investigations involving different extending materials of various thicknesses was performed. Six identical tests were performed for each combination. Boxplot analysis has been performed to scrutinise any outlying observation. The boxplots shown in Figure 3.11 demonstrate that the experimental data do not show outlying observations. Figure 3.12 shows the shear strength of the TS1/20DBM interface plotted against the thickness of extending material (SMA asphalt mixture or aluminium plate), together with the 95% confidence limits. It can be seen from this figure that for the TS1/20DBM specimens with the 25mm thick surfacing, the thickness of the SMA extending material does not significantly affect the shear strength. However, for the TS1/20DBM specimens with the 15mm thick surfacing, the shear strengths increase significantly as SMA extending material of 10mm of thickness is attached (results using 40mm thick SMA extending material do not show significant difference). The shear strengths measured from the TS1/20DBM specimens with 15mm and 25mm surfacings and 30mm grooved aluminium as the extending material show approximately equal values to the results using the 40mm thick SMA extending material.

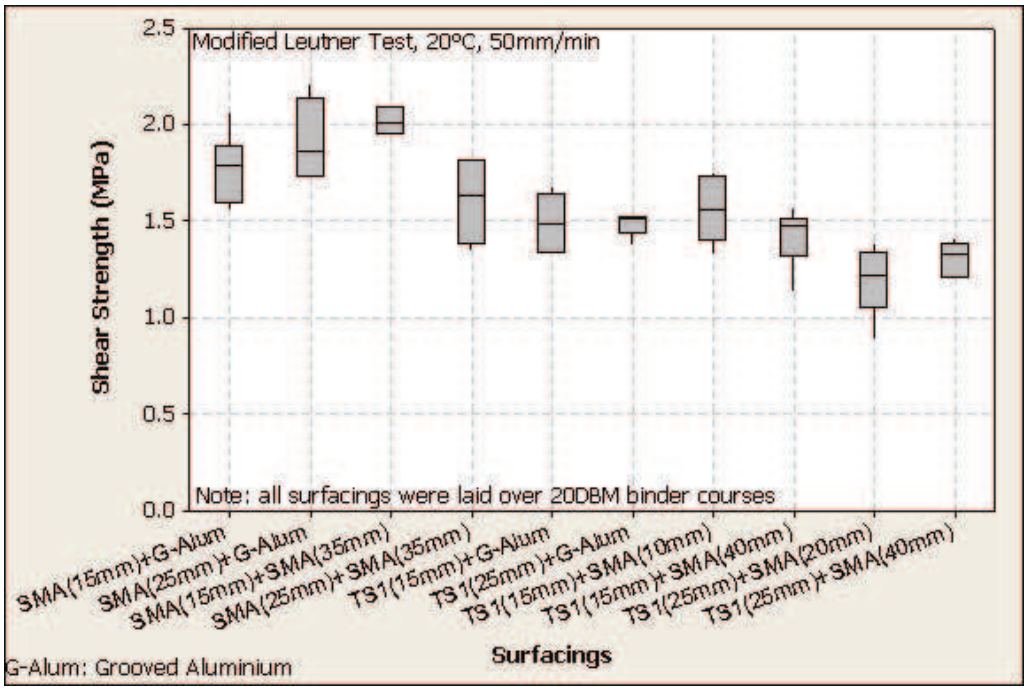

Figure 3.11 - Boxplots of the experimental data used in the effect of surfacing extension investigation

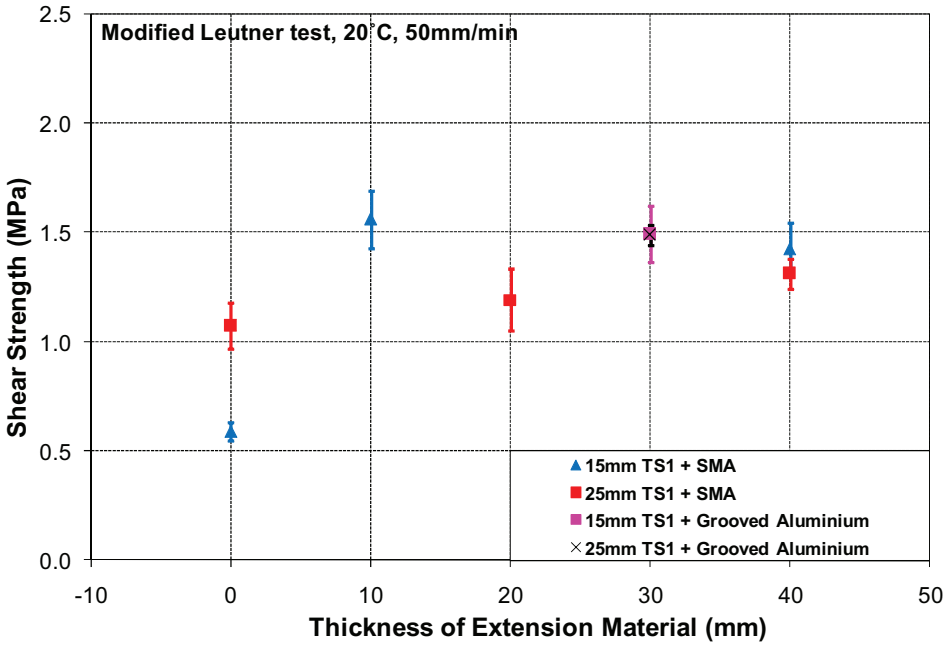

Figure 3.12 - Effect of extending material on TS/DBM specimen

Figure 3.13 shows the shear strength at the interface between the SMA surfacing and the 20DBM binder course plotted against the thickness of SMA extending material, together with the 95% confidence limits. It can be seen from this figure that for the SMA/20DBM specimens where a 25mm thickness surfacing material was used over DBM, the thickness of SMA extending material does not significantly affect the shear strength. However, for the 15mm thick SMA over 20DBM the interface shear strength increases significantly as the 35mm thick SMA extending material is attached. The shear strength of the SMA/20DBM interface for the 15mm SMA/20DBM and 25mm SMA/20DBM with aluminium as the extending material are comparable to the results from the standard 40mm thick SMA/20DBM specimen.

Results from the SMA/20DBM specimens shown in Figure 3.13 show similar trends to those for the TS1/20DBM specimens (Figure 3.12) where the shear strengths do not differ significantly as various thickness of extending material are attached on top of the 25mm thick surfacing. However, the shear strengths are

found to increase significantly when the extending material is attached to the 15mm thick surfacing.

It can be seen from Figures 3.12 and 3.13 that similar effects are found when using either the SMA or grooved aluminium as the extending material and, for practical purposes, it has been decided to adopt the grooved aluminium as it can be easily cleaned and re-used.

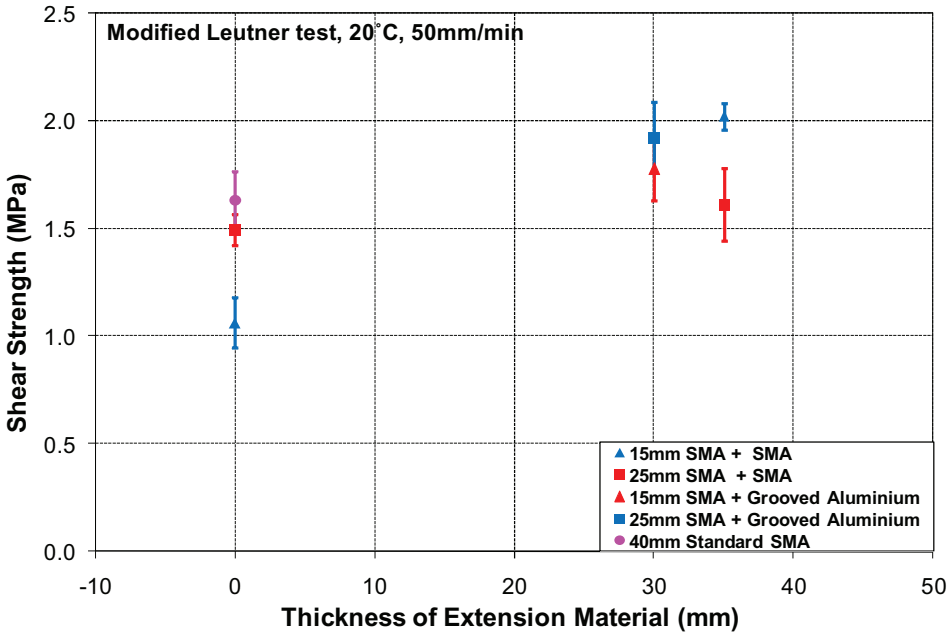

Figure 3.13 - Effect of extending material on SMA/20DBM specimen

3.6 Temperature Effect

To investigate the effects of temperature on shear strength, a series of modified Leutner tests was performed on two ultra thin surfacing course systems (15mm thick surfacing material) at temperatures of 30°C and of 15°C in addition to the standard temperature of 20°C. The 30mm thick grooved aluminium platen was used as the extending material for the TS1/20DBM and the SMA/20DBM specimens. As in the previous investigation, boxplot analysis has been performed to detect the outliers. The boxplots as presented in Figure 3.14 do not show any outliers. Average values of

shear strength together with the 95% confidence limits are plotted against test temperature in Figure 3.15. The results from a 40mm thick standard SMA/20DBM specimen obtained by Choi *et al*. [2005] are also presented for comparison.

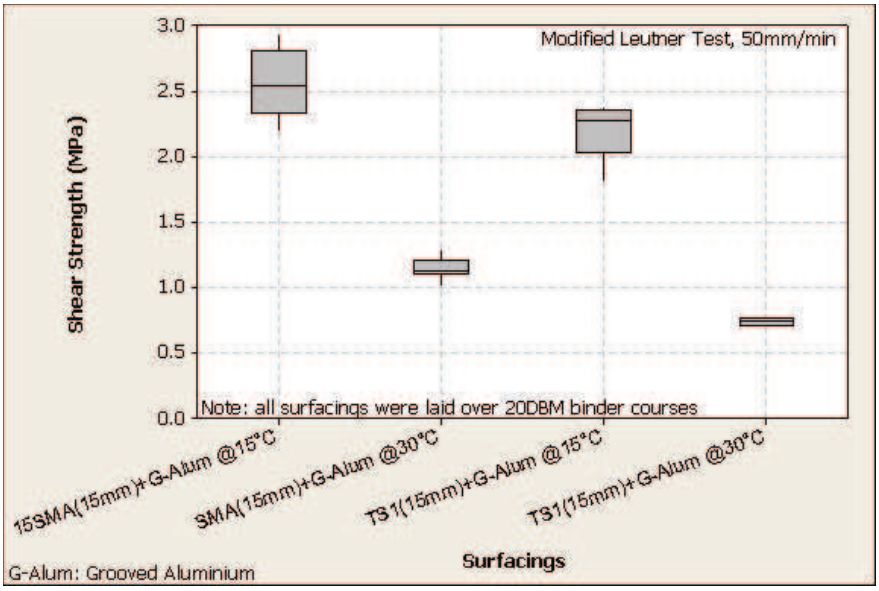

Figure 3.14 – Boxplots of the experimental data used in the effect of temperature investigation

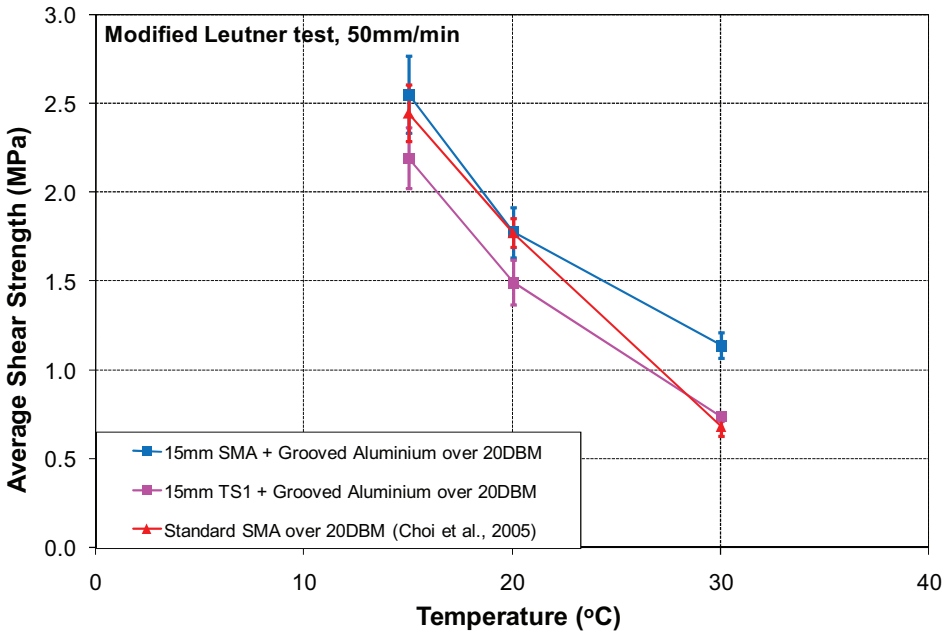

Figure 3.15 - Temperature effect on shear strength

As expected, Figure 3.15 shows that the shear strength decreases as the temperature increases. Results at 15°C and 20°C from the 15mm thick SMA/20DBM specimen extended with aluminium are approximately equal to the results from the 40mm thick standard SMA/20DBM specimen. However, at 30°C the result for the 40mm thick standard SMA/20DBM specimen is lower which may be due to specimen bulging caused by the reduction of surfacing stiffness as the temperature increases.

3.7 Displacement Rate Effect

Modified Leutner tests at different displacement rates were also conducted to investigate displacement rate effects on interface shear strength. A series of modified Leutner tests was performed on two ultra thin surfacing course systems at a higher loading rate of 100mm/min and a lower loading rate of 10mm/min in addition to the standard rate of 50mm/min. The boxplots that show no appearance of outliers are shown in Figure 3.16.

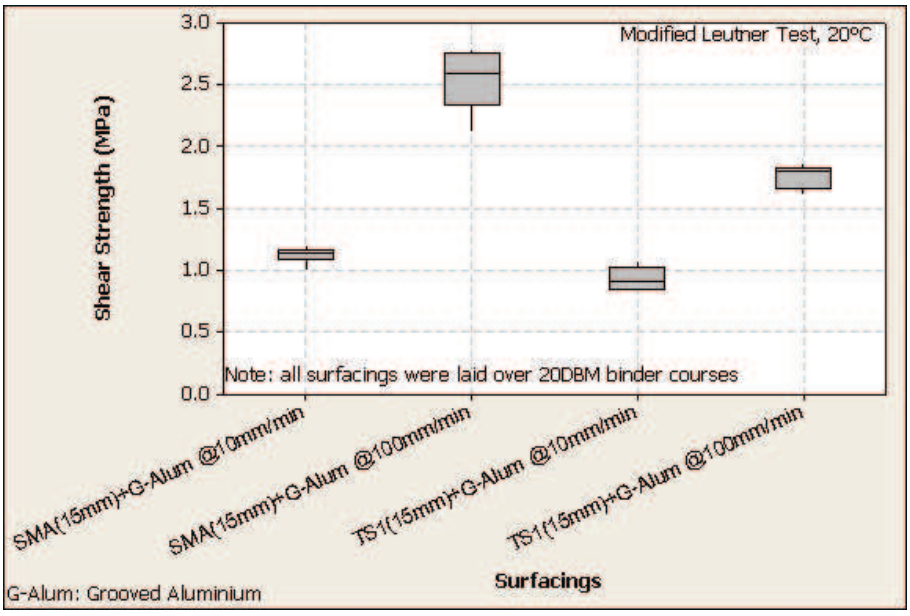

Figure 3.16 - Boxplots of the experimental data used in the effect of displacement rate investigation

Average values of shear strength together with 95% confidence limits are plotted versus displacement rate in Figure 3.17. As in the previous investigation, results were compared to those from 40mm thick standard SMA/20DBM specimens [Choi *et al*., 2005]. It should be noted that only three tests were performed on the 40mm thick standard SMA/20DBM specimens at 10mm/min and 100mm/min.

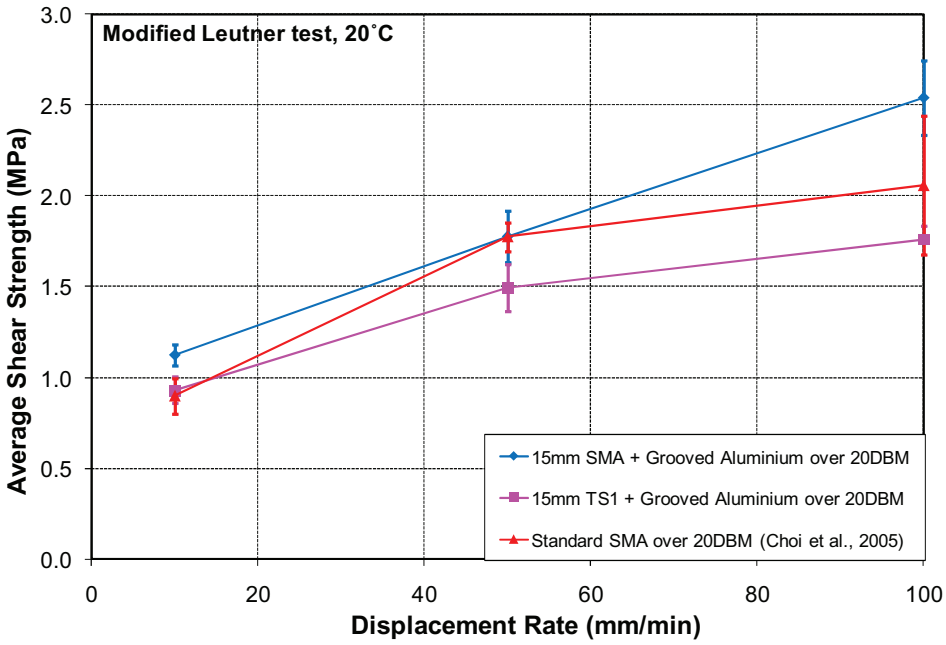

Figure 3.17 - Effect of displacement rate

It can be seen from Figure 3.17 that, as expected, the shear strength increases as the displacement rate increases. Results for 15mm thick SMA/DBM specimens extended with aluminium at 50 mm/min shows similar values to the results for the 40mm thick standard SMA/DBM specimens. The difference in results at 10 mm/min is believed to be due to the same phenomenon attributed to the difference in shear strength at high temperatures.

3.8 Finite Element Modelling

(Developed by Dr. S. Wang)

During experimental investigations, the occurrence of bulging and local material failure at the top half of the thin asphalt surfacings was linked to the lower measured shear strength at the interface below the layer. A modification by extending the thickness of the surfacing layer using an aluminium platen or an additional asphalt mixture layer successfully eliminated the bulging and restricted bond failure to the interface beneath the surfacing.

To achieve better understanding regarding the bulging at the top half of the surfacing material and the failure at the interface, an investigation using analytical methods by means of FE analysis was necessary. FE models were developed to investigate the distribution of damage at the interface induced by shear loading in the modified Leutner test. The analysis focussed on the modified Leutner test for a thin surfacing layer and the utilisation of surfacing extension during the test. The FE analysis was performed by Dr. S Wang (a research associate at The University of Nottingham) and the results are discussed in this section to verify the findings of the experimental investigation.

A typical relationship between shear stress at the interface and the corresponding shear displacement as seen in Figure 3.18 is approximately linear until the shear stress reaches the maximum bond strength of the interface. Beyond that point, the shear stress decreases in approximately exponential form until the specimen fails along the interface. This kind of constitutive relationship can be modelled using a Cohesive Zone Model (CZM) in ABAQUS software [Hibbitt, Karlsson and Sorensen, Inc., 2004].

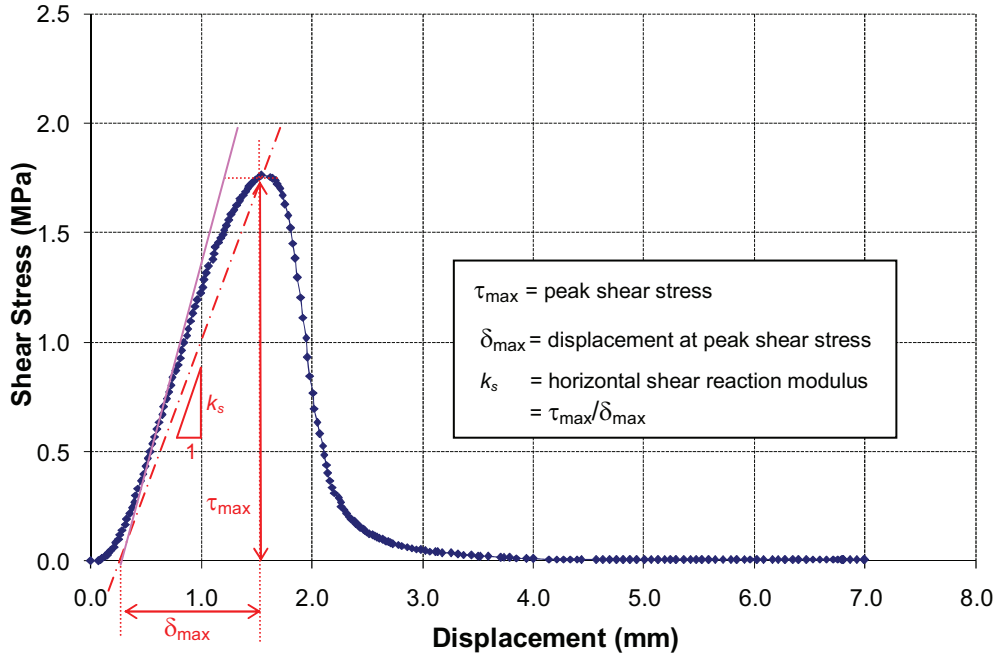

Figure 3.18 – Typical shear stress versus shear displacement plot from the modified Leutner test

3.8.1 Model Description

In the CZM model, the traction separation behaviour of the interface prior to damage initiation is described as linear elastic in terms of a penalty stiffness that degrades under tensile and/or shear loading, but is unaffected under pure compression. The following un-coupled linear elastic traction-separation constitutive relationship was used in the analysis:

$$\begin{Bmatrix} t_n \\ t_s \\ t_t \end{Bmatrix} = \begin{bmatrix} K_{nn} & & \\ & K_{ss} & \\ & & K_{tt} \end{bmatrix} \begin{Bmatrix} \delta_n \\ \delta_s \\ \delta_t \end{Bmatrix} \tag{3.1}$$

where t_n is the normal stress, t_s and t_t are the shear stresses in two directions (longitudinal and transverse), K_{nn} is the normal reaction modulus, K_{ss} and K_{tt} are the

shear reaction moduli in two directions, δ_n is the normal displacement, and δ_s and δ_t are the shear displacements in two directions.

Assuming that the initiation of damage (crack) and the corresponding softening process can be predicted using a quadratic failure criterion [Cui *et al.*, 1992], the damage will initiate if the following quadratic criterion is met:

$$\left\{\frac{\langle t_n \rangle}{t'_n}\right\}^2 + \left\{\frac{t_s}{t'_s}\right\}^2 + \left\{\frac{t_t}{t'_t}\right\}^2 = 1 \tag{3.2}$$

where t'_n is the tensile strength, and t'_s and t'_t are the shear strengths in both directions. The Macaulay bracket symbol <> is used to signify that pure compressive deformation or stress state does not initiate damage.

The damage is represented by a damage value, D and the following exponential softening evolution law [Camanho and Davila, 2002] was used:

$$D = 1 - \left\{\frac{\delta_m^0}{\delta_m^{\max}}\right\}\left\{1 - \frac{1 - \exp\left(-\alpha\left(\frac{\delta_m^{\max} - \delta_m^0}{\delta_m^f - \delta_m^0}\right)\right)}{1 - \exp(-\alpha)}\right\} \tag{3.3}$$

$$\delta_m = \sqrt{\langle \delta_n \rangle^2 + \delta_s^{\,2} + \delta_t^{\,2}}$$

where D is the damage value, δ_m is the total mixed mode relative displacement, α is a non-dimensional parameter that defines the rate of damage evolution, $\delta_m^{\max}$ is the maximum value of the total mixed mode relative displacement attained during the loading history, δ_m^f is the total mixed mode relative displacement at complete failure, and δ_m^0 is the total mixed mode relative displacement at damage initiation. The damage value, D initially has a value of 0 and monotonically evolves to 1 upon further loading after the damage initiates.

ABAQUS version 6.5 was used in the Finite Element (FE) analysis and linear hexahedral brick element C3D8 was chosen. It is a three dimensional (3D) element, with eight nodes and each has three translational degrees of freedom, U1, U2, U3 along X, Y, Z directions. This element is less affected by the size of element and usually gives higher accuracy in 3D stress analysis if compared with other elements, such as the tetrahedral element. Cohesive element COH3D8 was used for the interface layer.

Continuous research at the University of Nottingham records that the horizontal shear reaction modulus and shear strength at the interface range from 0.5 to 1MPa/mm and 0.5 to 2.0MPa, respectively. In the FE analysis, the horizontal shear reaction modulus and shear strength at the interface were taken as K_{ss}= K_{tt}= 0.657MPa/mm and t'_s= t'_t= 1.15MPa, respectively. To avoid numerical difficulties and maintain contact during post damage analysis, both the tensile strength, t'_n and normal reaction modulus, K_{nn} were assumed ten times as high as the corresponding values for shear. The total mixed mode relative displacement at complete failure, δ_m^f was taken as 6mm. The tensile and shear strengths and their corresponding stifnesses together with the state of stresses that met the damage initiation criterion in equation (3.2) were used to calculate the total mixed mode relative displacement at damage initiation, δ_m^0. The non-dimensional parameter was taken as two to approach the post damage behaviour of an experimental investigation performed by Collop *et al.* [2003]. The shear stress-displacement relationship of the interface used in the FE analysis is presented in Figure 3.19

Material properties used for the FE analysis are given in Table 3.3. Core specimens of 150 mm diameter were prepared in two or three layers of different thicknesses (Figure 3.20 and Table 3.4). Since the setup of modified Leutner test is symmetric about its central vertical plane, only half of the model was investigated.

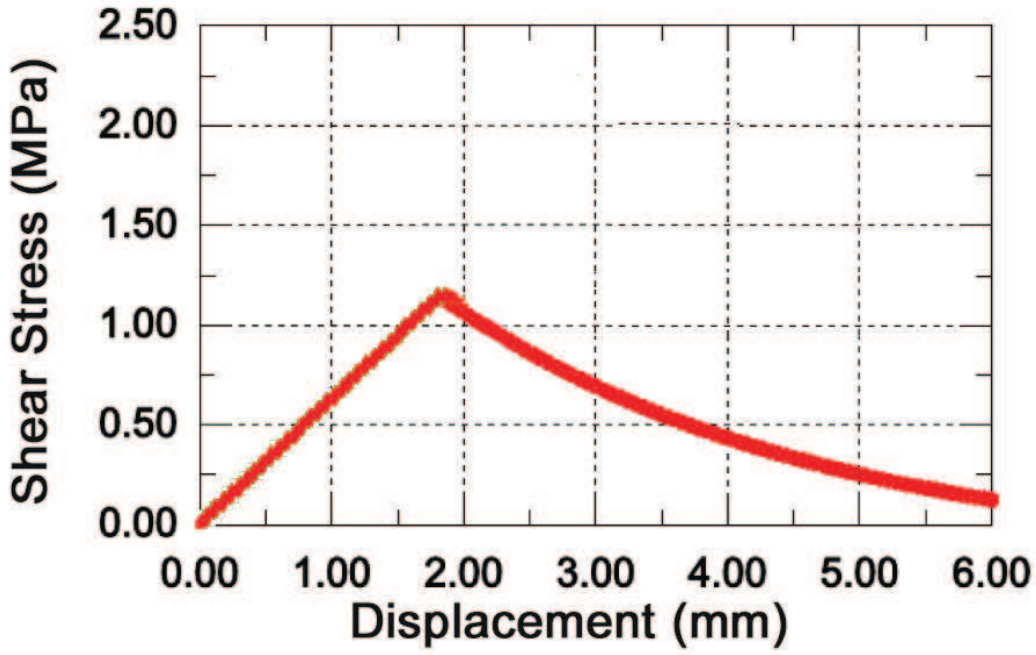

Figure 3.19 – Interface shear stress versus interface shear displacement plot of the FE model

Table 3.3. Material properties

Material	Young's modulus, (MPa)	Poisson's ratio
Binder Course 1 (B1)	5,000	0.35
Surfacing 1 (S1)	1,500	0.35
Surfacing 2 (S2)	3,000	0.35
Metal (steel)	212,000	0.35

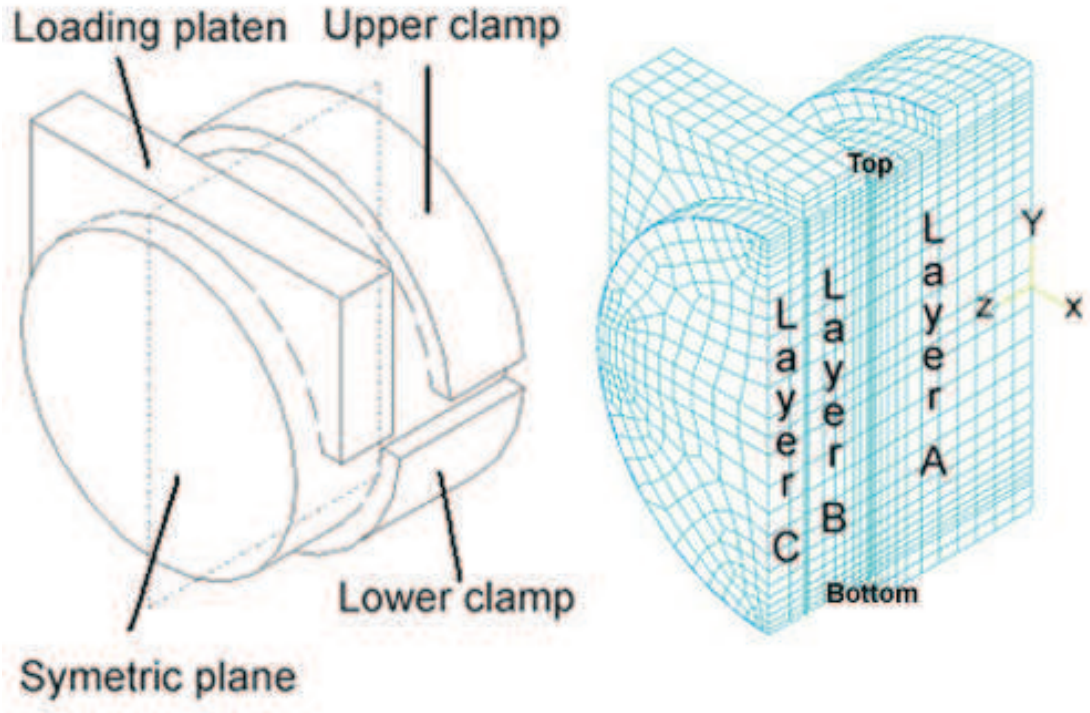

Figure 3.20 – FE specimen

Table 3.4. Model definitions

Model	Layer A		Layer B		Layer C	
	Thickness (mm)	Material	Thickness (mm)	Material	Thickness (mm)	Material
1	70	B1	15	S1	-	-
2	70	B1	25	S1	-	-
3	70	B1	45	S1	-	-
4	70	B1	15	S2	-	-
5	70	B1	25	S1	20	S2
6	70	B1	25	S1	20	Metal

3.8.2 Analysis of Damage at the Interface

3.8.2.1 Effect of surfacing thickness

Examination of TS1/20DBM specimens during experimental investigations revealed that for the 15mm thick surfacings, the crack was not restricted entirely to the interface but extended into the surfacing mixture. Whilst the 25mm thick surfacings showed that the crack was restricted entirely to the interface. To investigate the extent of damage across the interface for different thickness of upper layer, FE analyses were performed on two layer specimens of three upper layer thicknesses (15, 25 and 45mm) defined as model 1, 2 and 3 in Table 3.4.

The distributions of damage at the interface at peak loading as shown in Figure 3.21 demonstrate that the damaged portion increases as the upper layer thickness increases. The damage at the interface of the thin upper layer specimen (model 1) is more concentrated at the top part of the specimen's diameter. The thicker specimens (model 2 and 3) show higher proportion of damage along the specimen's diameter. It is interesting to note that the damaged portion of the specimen with 25mm thick surfacing (model 2) does not show significant difference compared to the specimen with 45mm thick surfacing (model 3). This explains the difference in crack pattern examined during experimental investigations.

3.8.2.2 Effect of surfacing extension

Experimental investigations demonstrated that attaching either SMA or aluminium to the thin surfacing material successfully restricted the failure entirely to the interface between the thin surfacing and binder course. To achieve better understanding regarding the effect of surfacing extensions on failure patterns at the interface beneath the thin surfacing, FE analyses were performed on 25mm thick S1 surfacing material with either 20mm S2 or 20mm metal extension materials defined as model 5 and 6 in Table 3.4. Please note that the metal extension used the FE model is steel, not aluminium as used in the experimental investigation.

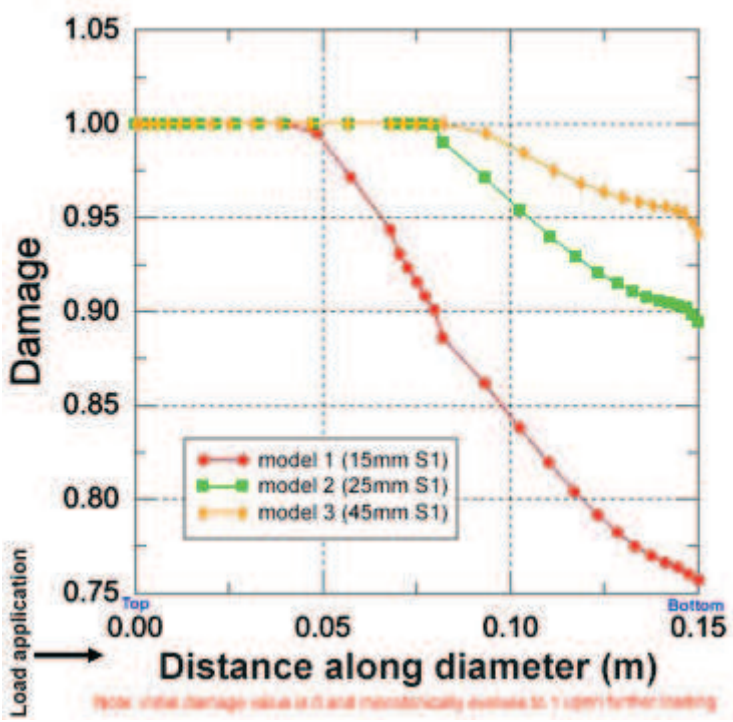

Figure 3.21 – Distributions of damage across the interface at peak loading for specimens with different surfacing thickness

The distributions of damage at the interface beneath the thin layer at peak loading are presented in Figure 3.22. Significant damage across the interface is observed when either S2 or metal extension material is attached to the surfacing. The metal extension performs better in inducing a larger portion of damage at the interface. This demonstrates the effect of surfacing extension on failure patterns at the interface beneath the thin surfacing during experimental investigations.

3.8.2.3 Effect of surfacing stiffness

Observations on failed specimens after testing during experimental investigations (Figure 3.6) revealed that for the 15mm thick TS1/20DBM specimen, the crack was not restricted entirely to the interface and extended to the surfacing material. Whilst for the 15mm thick SMA/20DBM specimen, the crack was restricted entirely to the interface. Because the interface shear strength of the TS1/20DBM is lower than the interface shear strength of the SMA/20DBM, it is considered that the proportion of

damage at the TS1/20DBM interface should be higher than the proportion of damage at the SMA/20DBM interface. However, the observations on failed specimens showed the opposite. One of the factors that were thought to contribute to this different failure pattern was the stiffness of the surfacing material. FE analyses were performed to investigate the effect of material stiffness on the distribution of damage across the interface. Two specimens with 15mm thick surfacing of S1 and S2 materials defined as model 1 and model 4 in Table 3.4 were investigated.

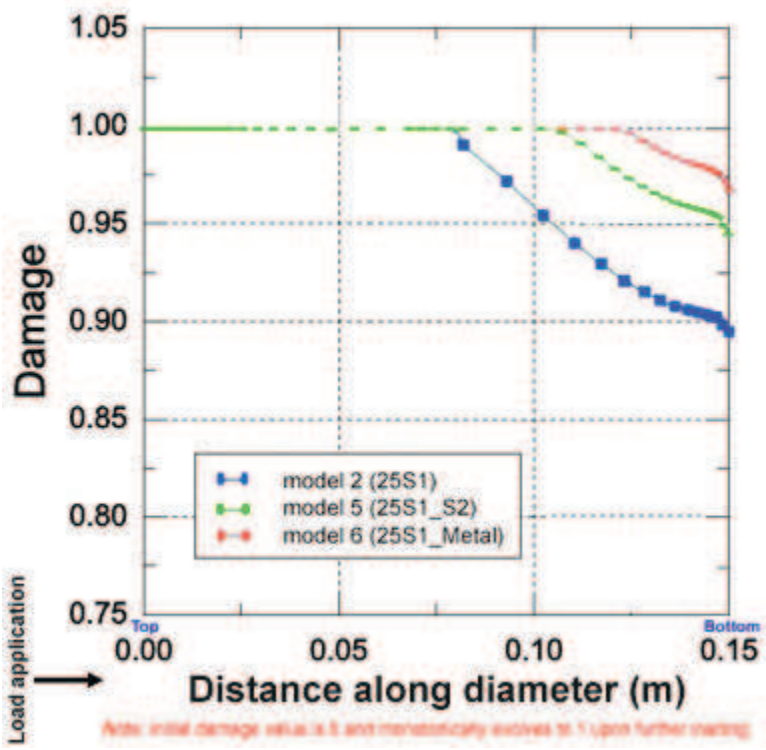

Figure 3.22 – Effect of surfacing extension on the distribution of damage across the interface at peak loading

Figure 3.23 shows the damage distributions at the interface of specimen models 1 and 4. Clearly, specimen model 4 with higher surfacing stiffness shows a higher proportion of damage compared to that of specimen model 1. Damage is more concentrated in a small area for the softer surfacing specimen (model 1) and a wider spread of damage across the interface is induced by the stiffer surfacing

specimen (model 4). This explains the difference of crack distributions in TS1/20DBM and SMA/20DBM specimens during experimental investigations.

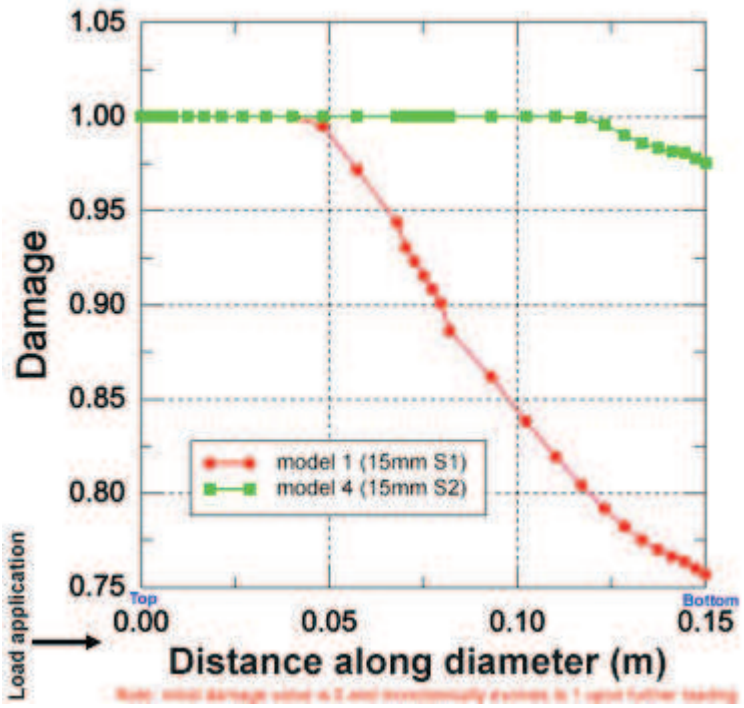

Figure 3.23 - Effect of surfacing stiffness on the distribution of damage across the interface at peak loading

3.8.3 Analysis of Bulging at the Top of the Surface

Observations from failed specimens containing thin surfacings revealed that a significant amount of bulging had taken place at the specimen's surface. The bulging was thought to be due to a number of factors including bending stresses in the specimen due to the fact that the shear force is applied a short distance away from the interface resulting in tensile stresses and strains in the top half of the specimen perpendicular to the plane of the interface, compression in the surfacing material resulting in lateral expansion due to Poisson's ratio effects and local buckling of the surfacing material.

FE analyses were performed to investigate the effect of Poisson's ratio of the surfacing material and normal stiffness (tensile stiffness perpendicular to the shear plane) of the interface on lateral deformation at the specimen's surface (bulging). The effect of local buckling of the surfacing material was not investigated because it was beyond the capability of the model.

Figure 3.24 shows the lateral deformations at the surface of the model 1 specimen. Clearly, the top portion of the specimen's diameter is bulged significantly and the bottom portion of the specimen's diameter is compressed. Although the compressed part at the bottom portion of specimen's diameter shown in Figure 3.24 is not clearly observed in the experimental results shown in Figure 3.7, the FE model confirms the appearance of bulging at the top of the specimen's surface.

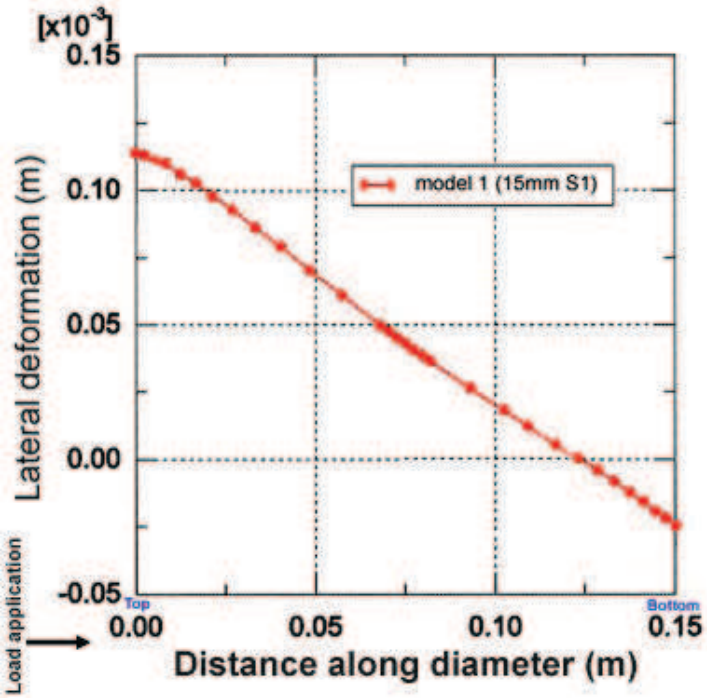

Figure 3.24 – Lateral deformation at the surface of thin surfacing

The effect of Poisson's ratio (ν) of the surfacing material on lateral deformation at the specimen's surface is presented in Figure 3.25. Three Poisson's ratio values of 0.00, 0.25 and 0.45 were used. The Poisson's ratio value of 0.00 was selected in order to determine a reference point when no lateral expansion associated with the

Poisson's ratio exists, so that the effects of Poisson's ratio and bending can be distinguished. The figure shows that the effect of Poisson's ratio is quite obvious at the top portion of the specimen's diameter and gradually becomes less obvious at the bottom portion of the specimen's diameter. This also indicates that higher vertical compression occurs at the top portion of the specimen's diameter. The higher vertical compression at the top portion of the specimen's diameter could lead to a more significant buckling effect in that portion. From the reference lateral deformation (v=0.00), it can be seen that the effect of Poisson's ratio on the lateral deformation at the specimen's surface is not as significant as the effect of bending.

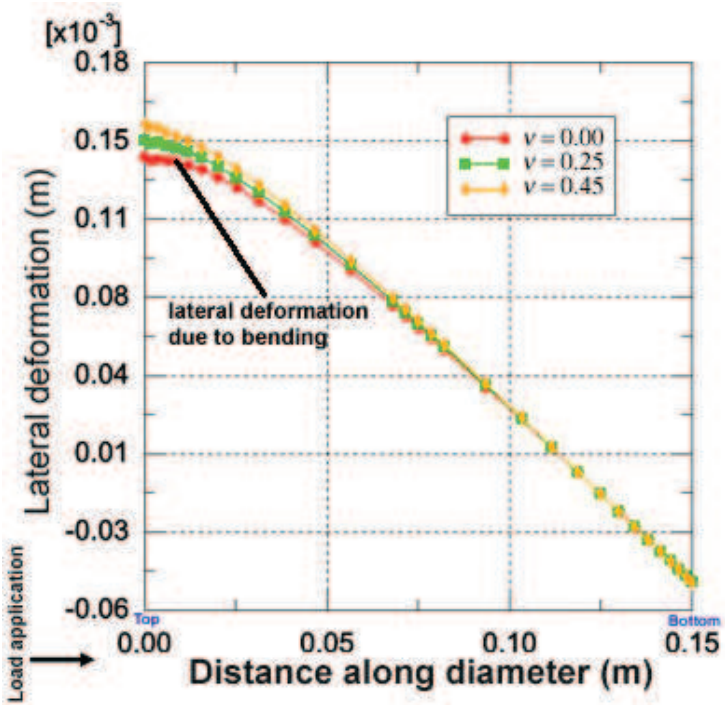

Figure 3.25 – Effect of Poisson's ratio on lateral deformation at the surface of thin surfacing

It is interesting to note that the magnitudes of the lateral deformations observed in the FE model results shown in Figures 3.24 and 3.25 are quite small compared to those observed during experimental investigation (see Figure 3.7). This difference is thought to be due to the assumption of interface normal stiffness used in the model and the effect of local buckling which can not be analysed using the present model. The interface normal stiffness was assumed to be ten times as high

as the interface shear stiffness in order to avoid numerical difficulties and maintain the contact during post damage analysis.

FE analyses were performed to investigate the effect of interface normal stiffness on lateral deformation at the surface of the specimen. Various interface normal stiffness ratios (ratio of interface normal stiffness over interface shear stiffness) of 0.01, 0.1, 1 and 10 were used. The results as presented in Figure 3.26 show that the lateral deformations increase as the interface normal stiffness ratio decreases. The magnitude of the lateral deformation can be up to nine times as high when the interface normal stiffness ratio is changed from 10 to 0.01. The typical normal stiffness ratio for bitumen is 1. However, because the shear stiffness of the interface is affected by bitumen adhesion and aggregate interlock, whilst the tensile stiffness is only affected by bitumen adhesion; the shear stiffness would be higher than the tensile stiffness when the interlocking of aggregate is quite significant. The normal stiffness ratio would be 1 for a perfectly flat bonded interface and less than 1 for a rough interface.

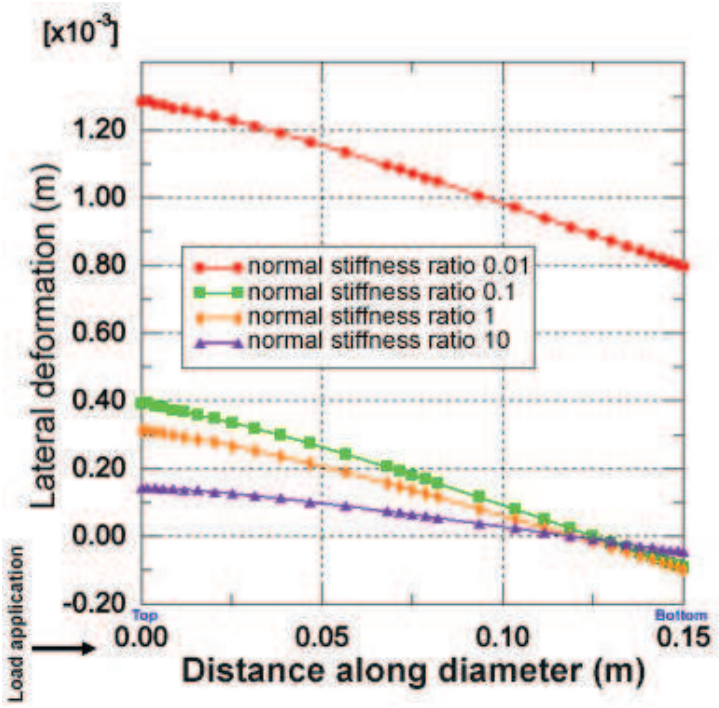

Figure 3.26 – Effect of interface normal stiffness ratio on lateral deformation at the surface of thin surfacing

3.9 Conclusion

The further modification to the modified Leutner test to enable the measurement of the bond strength beneath thin asphalt surfacing has been described. The following key points can be derived from the study:

1. The shear strength measured using the modified Leutner test before the further modification depends on surface layer thickness where the thickness of the surfacing is less than approximately 25mm.
2. Observations from failed specimens containing thin surfacings revealed that a significant amount of bulging had taken place in the top half of the specimen. It was also observed that for the TS1/20DBM specimen with the 15mm thick surfacings, the crack is not restricted entirely to the interface but extends into the surfacing mixture.
3. A further modification to the modified Leutner test that involves attaching a 30mm thick, 150mm diameter grooved metal plate to the thin surfacing significantly reduces the effect of surfacing thickness on measured shear strength.
4. The measured shear strength increases as the temperature is decreased and the loading rate is increased.
5. FE models developed by Dr. S Wang have been discussed to verify the findings of the experimental investigation.

Chapter 4

TORQUE TEST INVESTIGATION

4.1 Introduction

The manual torque bond test has been widely used in the UK because it is included as a compulsory test in the certification of thin surfacing course systems in the UK. The test is performed manually by twisting the top of a 100 ± 5mm diameter core specimen using a handheld torque wrench at a constant rate, inducing a twisting shear failure at the interface. The 100mm diameter specimen is used in the manual torque bond test because the force required to fail a larger 150mm is greater than that which an operator using a reasonable size of twisting arm could apply. Although a laboratory testing procedure is available, the test is typically performed in-situ and generally limited to the uppermost interface.

In the in-situ testing procedure, a partial core is taken to a depth of 20mm below the interface to be tested. A metal platen is then glued on top of the thin surfacing layer and the glue is allowed to gain sufficient strength before the manual torque bond test is performed. In the laboratory testing procedure, the core specimen is trimmed to a length suitable for mounting. The core is then placed in a mould so that the interface to be tested is 20 ± 10mm above the rim of the mould. The mould is then filled with mortar/grout trimmed flush with the mould rim. A metal plate is then glued on top of the specimen. The test can be performed after the glue and the mortar/grout have gained sufficient strength.

The initial testing protocol for the manual torque bond test, the guidelines document SG3/98/173 [British British Board of Agreement, 2000], requires the test to be performed at a constant torque rate to cause failure in 60 ± 30 seconds (See Appendix A.3). As previously mentioned in Section 2.5.1.2 of Chapter 2, Choi *et al.* [2005] found it difficult to control the aforementioned loading rate. Therefore, they

used a constant torque rate of 600Nm/min which was achieved by synchronising the movement of the torque dial gauge in the torque wrench with the second hand of an analogue clock. In 2004, this testing protocol was superseded by the new guidelines document SG3/05/234 [British Board of Agreement, 2004]. The new testing protocol requires the test to be performed at a constant rotation rate so that the torque wrench sweeps an angle of 90° within (30±15) seconds (See Appendix A.4). It should be noted that because the torque wrench is twisting the top of the core and the actual rotation at the interface could be affected by the stiffnesses and thicknesses of the adjacent pavement layers (See Section 4.2), the variability of results obtained from the test at a constant rotation rate would be affected by the variability of the adjacent pavement layers' stiffnesses and thicknesses. To provide a better understanding regarding the difference between the constant torque rate (600Nm/min) used by Choi *et al.* [2005] and the constant rotation rate (180°/min) required by the guidelines document SG3/05/234 [British Board of Agreement, 2004], it is necessary to conduct an investigation using an apparatus that is able to control the loading rate accurately and is performed in a well controlled environment.

Diakhaté et al. [2006, 2007] developed a mechanically controlled torque bond test apparatus that is able to overcome the issues related to the manual torque bond test mentioned earlier in Section 2.5.1.2 of Chapter 2. The apparatus is able to control the loading rate accurately, ensure the planarity of the loading system and eliminate the appearance of lateral shear. However, because of the chain-sprocket mechanism used in the apparatus, the force can be applied in one direction only and the apparatus is therefore not suitable for applying a cyclic zero-mean torsional load.

An automatic torque bond apparatus, similar to the apparatus developed by Diakhaté et al. [2006, 2007], was developed in this research study in order investigate the two different loading rates (600Nm/min and 180°/min) used in the manual torque bond test in a more controlled environment and loading condition. Although quite similar to the apparatus developed by Diakhaté *et al*. [2007], the apparatus developed in this research study uses a rack and pinion mechanism and is capable of transferring either tensile or compressive force to generate negative or positive torsional load, hence it can be used to perform a cyclic zero-mean torsional load and was later used to perform a series of repeated torque bond tests.

4.2 Basic Formulae

Consider the interface in a torque bond specimen as divided into ring elements of radius *r* and thickness *δr* (Figure 4.1). Each element is subjected to a shear stress τ'. The force acting on each element is given by:

$$\delta F = \tau' 2\pi r \delta r \tag{4.1}$$

This force will produce a moment about the centre axis of the specimen, providing a torque δT on each element:

$$\delta T = \tau' 2\pi r^2 \delta r \tag{4.2}$$

The total torque for a torque bond specimen of radius *R* will then be the sum of all contributions of the elements:

$$T = \int_0^R \tau' 2\pi r^2 \delta r \tag{4.3}$$

Two approaches can then be considered:

- Considering a plastic-limit type of approach, the shear stress at the interface is assumed to be constant over the radius *R* and equal to the shear strength (i.e. $\tau' = \tau$), calculating the integration in equation (4.3) gives:

$$T_{plastic} = \frac{2\pi\tau R^3}{3} \tag{4.4}$$

- Considering an elastic-limit type of approach, the shear stress at the interface is assumed to vary linearly over the radius *R*, so that the shear stress at the centre of the disc is zero and the shear stress at the outside radius *R* is equal to the shear strength (i.e. $\tau' = \tau r/R$), calculating the integration in equation (4.3) gives:

$$T_{elastic} = \frac{\pi \tau R^3}{2} \tag{4.5}$$

In a torque test, the torque T and radius R of a specimen can be determined so that the shear strength τ of the specimen can be calculated using equation (4.4) or (4.5).

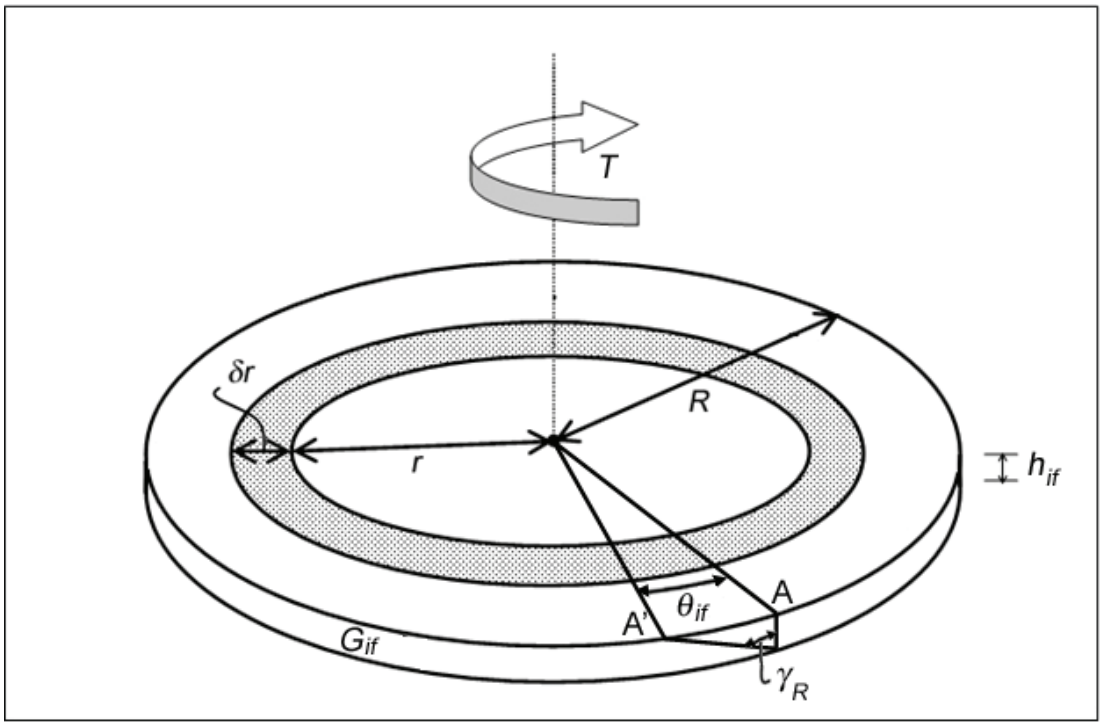

Figure 4.1 – Interface in a torque bond specimen

Consider the interface of a torque bond specimen with a shear modulus G_{if}, thickness h_{if} and radius R subjected to a torque T at the top end and the bottom end being fixed (Figure 4.1). Because of the action of the torque, a radial line at the free top end of the interface twists through an angle of θ_{if}, point A shifts to A' and induces an angle γ_R at the fixed bottom end. The angle γ_R reflects the shear strain at the outside radius R of the interface:

$$AA' = R\theta_{if} = h_{if}\gamma_R$$
$$\gamma_R = \frac{R\theta_{if}}{h_{if}} \tag{4.6}$$

Considering the interface as divided into ring elements of radius *r*, the shear strain γ' acting on each element is given by:

$$\gamma' = \frac{r\theta_{if}}{h_{if}} \tag{4.7}$$

The shear modulus G_{if} and the shear reaction modulus K_s are given by:

$$G_{if} = \frac{Shear\ Stress}{Shear\ Strain} = \frac{\tau}{\gamma} = \frac{\tau'}{\gamma'} \tag{4.8}$$

$$Ks = \frac{G_{if}}{h_{if}} \tag{4.9}$$

Equations (4.7), (4.8) and (4.9) can be combined to define the shear stress τ' acting on each element given by:

$$\tau' = G_{if}\gamma' = \frac{G_{if} r\theta_{if}}{h_{if}} = K_s r\theta_{if} \tag{4.10}$$

Substituting equation (4.10) into equation (4.3), gives:

$$\begin{aligned} T &= \int_0^R K_s r\theta_{if} 2\pi r^3 \delta r = \frac{K_s \theta_{if} \pi R^4}{2} \\ K_s &= \frac{2T}{\theta_{if} \pi R^4} \end{aligned} \tag{4.11}$$

Equation (4.11) can be used to determine the interface shear reaction modulus K_s in a torque test, providing that the torque *T*, angle of twist of the interface θ_{if} and radius of the specimen *R* are known.

Consider a torque bond specimen as shown in Figure 4.2, consisting of: 1) a lower layer material with shear stiffness G_1 and thickness h_1; 2) a thin interface layer

material with shear reaction modulus K_s; and 3) an upper layer material with shear stiffness G_2 and thickness h_2. The specimen is subjected to a torque T at the top end and the bottom end is fixed. The torque T will induce angles of twist θ_1, θ_{if} and θ_2, giving a total angle of twist θ_{total}. The angle of twist of the interface θ_{if} can be defined by:

$$\theta_{if} = \theta_{total} - (\theta_1 + \theta_2) \tag{4.12}$$

Using a simple theory of torsion [Hearn, 1997] given by:

$$\frac{T}{J} = \frac{G\theta}{h} \tag{4.13}$$

where T is the torque, J is the second moment of area of the specimen's cross section, G is the shear modulus, θ is the angle of twist, and h is the thickness of the specimen. For a solid cylindrical shape, J is defined as $\pi R^4 / 2$.

The angles of twist θ_1 and θ_2 can then be defined by:

$$\theta_1 = \frac{T\,h_1}{J\,G_1} = \frac{2T\,h_1}{\pi R^4 G_1} \tag{4.14}$$

$$\theta_2 = \frac{T\,h_2}{J\,G_2} = \frac{2T\,h_2}{\pi R^4 G_2} \tag{4.15}$$

Substituting equations (4.14) and (4.15) into equation (4.12) gives:

$$\theta_{if} = \theta_{total} - \frac{2T}{\pi R^4}\left(\frac{h_1}{G_1} + \frac{h_2}{G_2}\right) \tag{4.16}$$

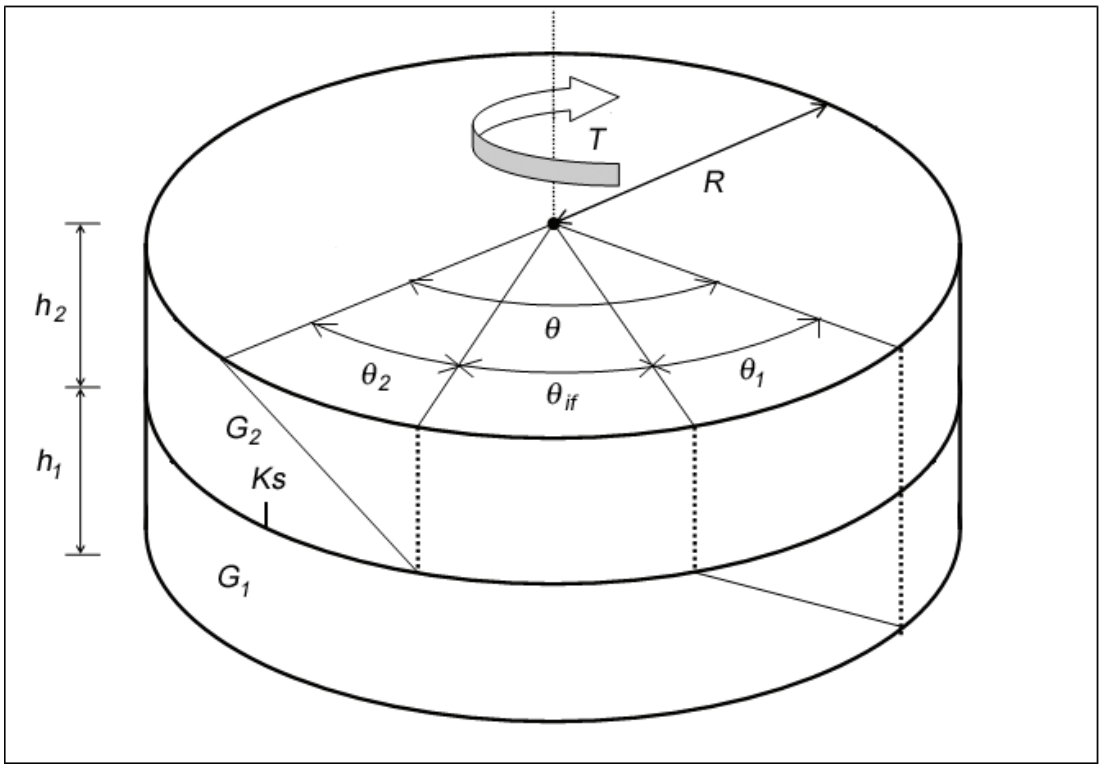

Figure 4.2 – Torque bond specimen

Combining equations (4.11) and (4.16) gives:

$$K_s = \frac{2T}{\pi R^4 \left(\theta_{total} - \frac{2T}{\pi R^4} \left(\frac{h_1}{G_1} + \frac{h_2}{G_2} \right) \right)} \tag{4.17}$$

Equation (4.17) can then be used to determine the interface shear reaction modulus K_s in a torque bond specimen.

4.3 Automatic Torque Bond Test

In order to investigate the two different loading rates in the manual torque bond test in a more accurate way, it is necessary to perform the torque bond test using

equipment that is able to control the loading rate accurately. Therefore, an automatic torque bond apparatus was developed in this research study.

4.3.1 Design and Manufacture of the Apparatus

Considering laboratory constraints associated with time and budget, the apparatus was designed to meet the following:

- It should be incorporated into an existing testing machine and data acquisition system.
- It should be relatively simple to be manufactured in the Civil Engineering Department workshop.
- It should allow easy and quick test setup.
- It should be relatively economical.

The loading machine to be used in this study was an INSTRON servo-hydraulic testing machine (Figure 4.3). The INSTRON testing machine is able to apply a vertical compressive or tensile force under static or cyclic mode. It comprises of a temperature controlled cabinet with a range of temperatures between -5 and 40˚C, a 100kN servo hydraulic actuator, an axially mounted load cell and a Linear Variable Differential Transformer (LVDT). The hydraulic power for the actuator is supplied by an external hydraulic pump. A Rubicon digital servo control system is used to operate the machine and a Rubicon data acquisition software is used to continuously monitor signals from the load cell and the LVDT to be stored in a computer as well providing feedback signals to the control system. Because the testing machine is only capable to apply a vertical load or displacement, a simple rack and pinion mechanism is used in the automatic torque bond apparatus (Figure 4.4) to transfer the applied load or displacement and convert it into a torque or rotation respectively. Because the rack and pinion mechanism is able to transfer either tensile or compressive force to generate negative or positive torsional load, the apparatus is also able to perform a cyclic zero-mean torsional load. The force and linear displacement of the rack are measured using the load cell and LVDT incorporated in the testing machine.

Figure 4.3 – INSTRON testing machine

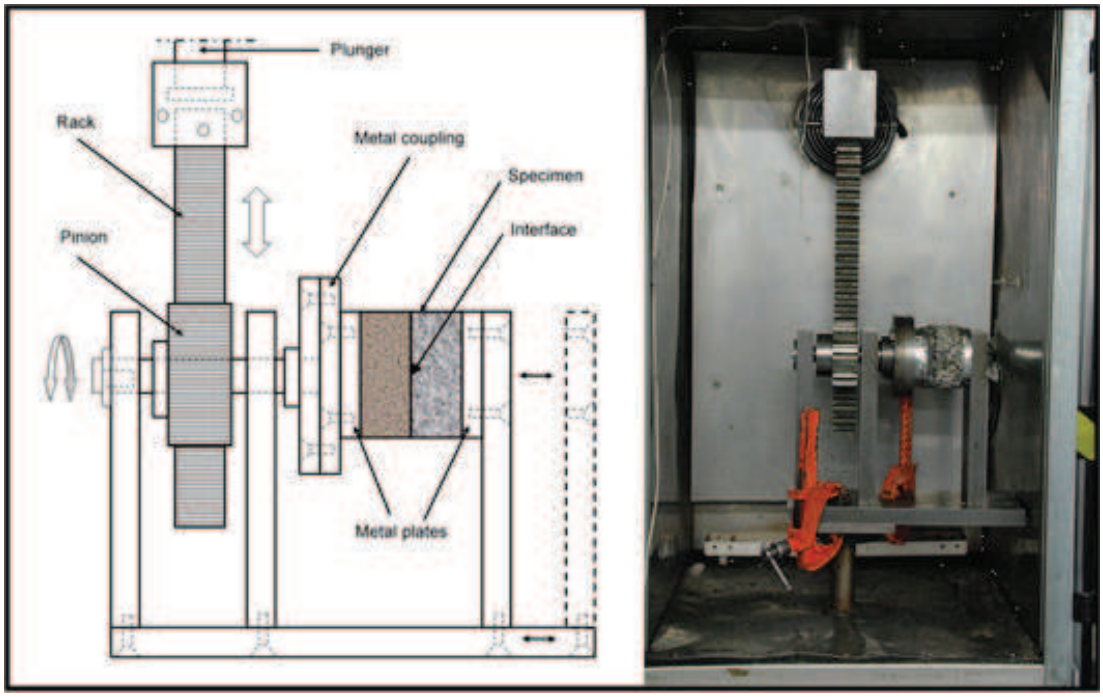

Figure 4.4 – Schematic and photograph of the automatic torque bond apparatus.

The torque, torque rate, angular rotation and rotation rate are calculated using the following equations:

$$T = FR, \quad \dot{T} = \dot{F}\,R \tag{4.18}$$

$$\theta = \frac{\delta}{R}, \quad \dot{\theta} = \frac{\dot{\delta}}{R} \tag{4.19}$$

where T is the torque, F is the force applied through the rack, R is the pitch circle radius of the pinion gear, $\dot{T}$ is the torque rate, $\dot{F}$ is the loading rate of the rack, θ is the angular rotation of the pinion gear, δ is the linear displacement of the rack, $\dot{\theta}$ is the rotation rate of the pinion gear and $\dot{\delta}$ is the displacement rate of the rack.

The dimension of the specimen to be tested dictated the dimension of the apparatus. Because the apparatus was intended to investigate the loading rates used in the manual torque bond test, it was decided to use a core specimen of 100mm nominal diameter. Choi *et al.* [2005] showed that the interface torque strength obtained from a manual torque bond test on a 100mm diameter core specimen at a constant torque rate of 600Nm/min and a temperature of 10˚C could be up to 400Nm. Therefore, the automatic torque bond apparatus was designed with a maximum capacity of 600Nm to allow testing of a stronger interface or at a lower temperature. The designed maximum capacity dictated the dimension of the weakest point in the apparatus and it was found that the minimum diameter of a steel pin that locks the pinion gear into its shaft should be 5mm. To allow quick and easy test setup, 100mm diameter and 10mm thick cylindrical metal platens were to be glued on top and bottom of the specimen so that the specimen can be easily placed into the test frame by bolting the metal platens. The apparatus as well as a number of cylindrical metal platens were manufactured in the Civil Engineering Department workshop, at the University of Nottingham

4.3.2 Specimen Preparation

The test requires a double-layered cylindrical specimen of 100mm nominal diameter. A trial test (to be discussed in Section 4.3.3 of this Chapter) revealed that the specimen needs to be trimmed at 20mm below the interface in order to prevent failure at the bottom part of the specimen as well as to better simulate the position of the interface in the manual torque bond test. Prior to testing, the diameter of the cylindrical specimen is carefully measured using a vernier calliper. Metal loading platens are glued to the top and bottom surfaces of the specimen. A jig as shown in Figure 4.5 is used to ensure parallel alignment of the metal platens and the specimen. To protect the specimen and the interface from glue spillage, adhesive foils are wrapped around the interface and the glued metal loading platens. The specimen is left until the glue hardens and gains sufficient strength.

Figure 4.5 – Jig for gluing the loading platens to the torque specimens

4.3.3 Automatic Torque Bond Test Procedure

After a double-layered specimen has been prepared by gluing cylindrical metal platens to both ends of the specimen and the glue has gained sufficient strength, it is conditioned in a temperature-controlled cabinet for at least 5 hours prior to testing. The cylindrical metal platens are bolted to the automatic torque bond apparatus and a thread sealant is used to ensure that the bolts do not loosen during testing. The specimen and the apparatus are then placed inside a temperature-controlled cabinet and attached into an axial testing machine. To perform testing at a constant torque rate, a constant vertical force is applied into the rack of which the rate can be calculated using equation (4.18). For testing at a constant rotation rate, the rack is subjected to a constant vertical displacement rate calculated using equation (4.19). The vertical force and its corresponding displacement are measured using a load cell and an LVDT incorporated into an axial testing machine respectively. The applied torque is calculated from the measured vertical force using equation (4.18), while the corresponding rotation is calculated from the measured vertical displacement using equation (4.19).

4.3.4 Calibration of the Apparatus and Trial Tests

After the automatic torque bond apparatus (Figure 4.4) had been manufactured, it was attached to the testing machine to calibrate the torque and its corresponding rotation and to check whether any play and/or friction existed within the system that may affect the accuracy of the results. The applied torque was calibrated by attaching a torque meter into the apparatus. A number of vertical forces were applied and the resultant torque readings from the torque meter were recorded. The applied torques were calculated from the applied vertical forces using equation (4.18) and then calibrated with the readings from the torque meter. The rotation of the pinion gear was calibrated by applying vertical displacements into the rack and the corresponding rotations of the metal coupling (shown in Figure 4.4), connected by a shaft into the pinion gear, were measured using an angle meter. The applied rotations were calculated from the applied vertical displacements using equation (4.19) and then calibrated with the rotations of the metal coupling.

The presence of any play within the system was checked by performing trial tests on a number of SMA/20DBM specimens of 100mm nominal diameter using two different loading rates (600Nm/min and 180˚/min) at a temperature of 20˚C. Details of the mixtures are given in Table 3.2 in chapter 3. Six identical tests were carried out for each test condition. Following the trial tests, a slip was found in the attachment of the rack to the actuator and a small modification to the attachment was carried out. A slight play was also found between the rack and the pinion gear and a support was then added at the back of the rack (Figure 4.6) in order to eliminate the play. The presence of any friction within the bearing system was checked by applying a set of displacements into the rack without any specimen placed in the apparatus and monitoring the resistant forces. It was found that the resistant forces were less than 0.04% of the of the maximum design load, which was considered very small and not significant.

It is interesting to discuss that for the trial testing at 180˚/min, some of the specimens failed at the bottom part of the 20DBM binder course. A visual observation on the 20DBM layer revealed that its bottom part appeared to be highly voided. The air void content of the 20DBM was then measured by slicing a number of 20DMB cores (60mm thick) into 3 parts (bottom, middle, and top) and it was found that the air void content at the bottom part was higher than that at the middle and upper parts. The relatively high air void content at the bottom part of the 20DBM appeared to weaken the torque strength of the material. Trimming the specimen at 20mm below the interface of interest to discard the relatively high voided bottom part was found to successfully prevent failure within the asphalt layer. Besides preventing failure within the relatively high voided bottom part of the specimen, the trimming at 20mm below the interface was chosen in order to better the simulate the manual torque bond test because both the guidelines documents SG3/98/173 and SG3/05/234 [British Board of Agreement, 2000, 2004] require the specimen to be held at 20mm below the interface. The finding regarding the relatively low structural integrity of the relatively high voided bottom part of the specimen also indicates that the torque bond test appears to be not suitable for a double layered specimen containing a highly voided asphalt layer (e.g. porous asphalt) because the specimen may fail within the asphalt layer rather than at the interface between the adjacent layers.

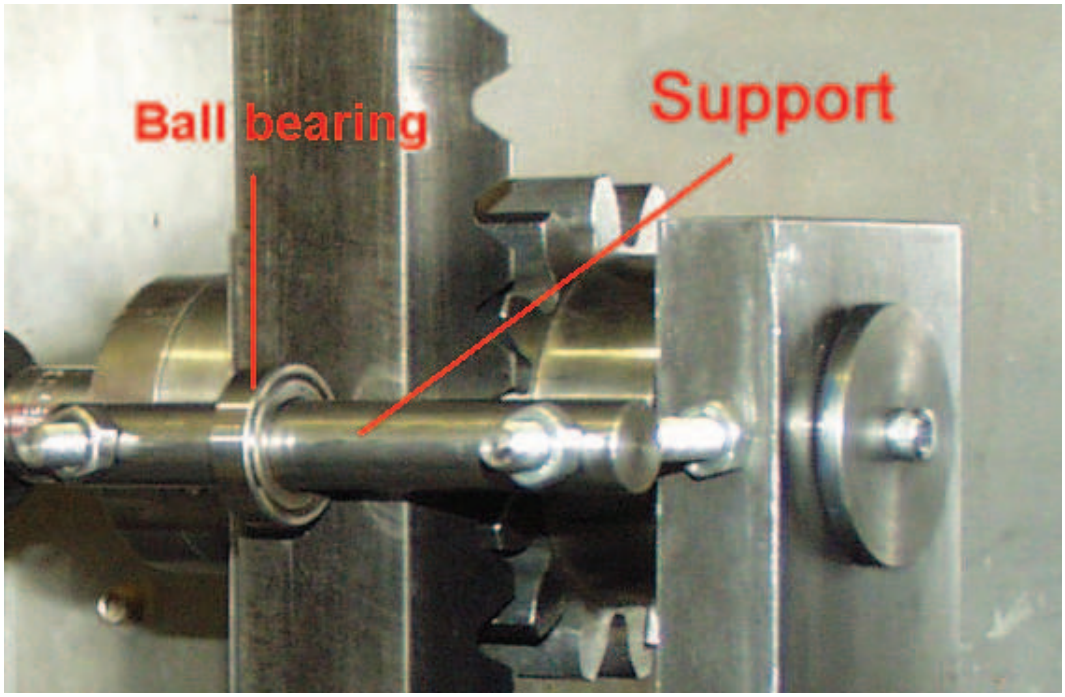

Figure 4.6 – Support at the back of the rack

4.4 Comparison between Manual and Automatic Torque Bond Tests

After the automatic torque bond apparatus had been developed, it was necessary to compare the results obtained from the automatic torque bond test to those of the manual torque bond test. A series of manual and automatic torque bond tests were performed on SMA/20DBM and TS1/20DBM specimens of 100mm nominal diameter. Details of the mixtures are given in Table 3.2 in chapter 3. The tests were performed at a target torque rate of 600Nm/min and temperature of 20°C. Five identical tests were undertaken for each material combination and test equipment. In the automatic torque bond tests, the specimens were prepared according to Section 4.3.2 and the tests were performed according to the procedure presented in Section 4.3.3.

Apart from the loading rate (600Nm/min) and the gripping mechanism (Figure 4.7), the manual torque bond test was performed according to the guidelines

document SG3/98/173 [British Board of Agreement, 2000] presented in Appendix A.3. The loading rate of 600Nm/min was chosen in this investigation because as mentioned earlier in Section 2.5.1.2 of Chapter 2 and Section 4.1 of this Chapter, Choi *et al.* [2005] found it difficult to control the loading rate specified in the guidelines document SG3/98/173. The clamping unit shown in Figure 4.7 was used because it allows easier and quicker setup than placing the specimen in a mould and then filling the mould with mortar/grout to hold the specimen as required in the guidelines document SG3/98/173.

Figure 4.7 – Laboratory manual torque bond test equipment used by Choi *et al*. [2005]

It should be noted that in the clamping unit shown in Figure 4.7, the specimen has to be clamped properly to give a firm grip so that it does not rotate during testing and it should not be over tightened to avoid damage to the specimen. Similar clamping issues have also been mentioned by Raab and Partl [1999]. To provide better gripping, a number of small welding patches can be applied into the inner surface of the clamping unit (Figure 4.8). To avoid inaccuracy due to the clamping issue, the result was to be discarded if the specimen rotates during testing and/or the clamping mechanism damages the specimen. A handheld torque wrench (Figure 4.7) equipped with a built-in torque gauge which can measure a torque over a range of 0-400Nm with a scale readable to 10Nm was used to apply the torque.

Figure 4.8 – Small welding patches applied into the inner surface of the clamping unit

Figure 4.9 shows a comparison of the nominal shear strength from the manual and automatic torque bond tests. The nominal shear strength is calculated from the measured peak torque using the elastic limit state approach in equation (4.5). Because the torque rate is considered to be less accurate, the results from the manual torque bond test, as expected show higher Coefficients of Variation (COVs) than that shown by the results from the automatic torque bond test of the corresponding material combination. It is interesting to note that the results of the automatic torque bond test are 20-30% higher than the results of the manual torque bond test. The difference was thought to be due to several drawbacks associated with the manual torque bond test: inaccurate torque rate, the appearance of lateral shear due to the absence of a lateral support at the top part of the specimen and axial bending on the specimen due to the application of a torque that is not parallel to the interface. To investigate the accuracy of the applied torque rate in the manual torque bond test, nominal torque rate is plotted against nominal shear strength from the manual torque bond test and the plot is presented in Figure 4.10. The nominal torque rate of the manual torque bond test is defined as the measured peak torque divided by the recorded time to failure.

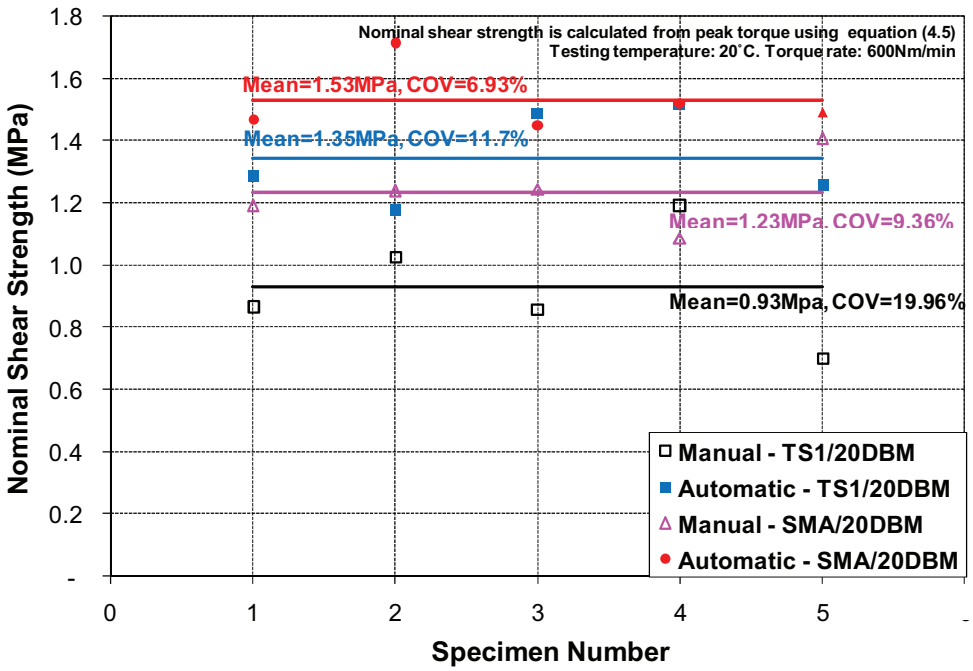

Figure 4.9 – Comparison between manual and automatic torque bond tests

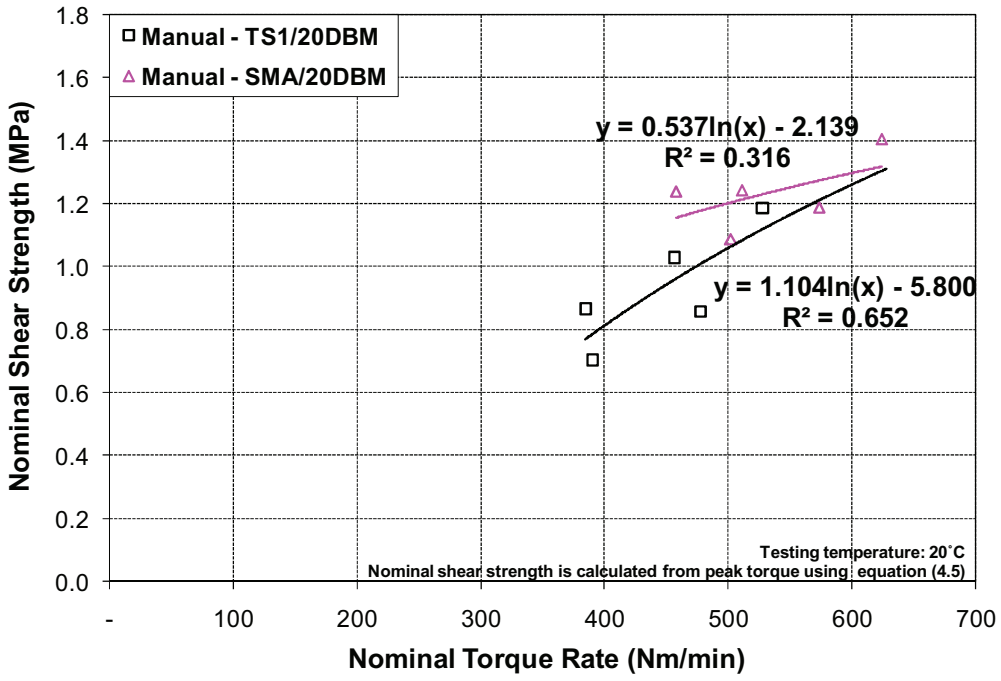

Figure 4.10 – Nominal torque rate versus nominal shear strength plot from the manual torque bond test

Figure 4.10 shows that most of the nominal torque rates from the manual torque bond test are below the target torque rate of 600Nm/min. The figure also demonstrates that the nominal shear strength increases as the nominal torque rate increases. The trends of the data demonstrate that applying a nominal torque rate of 600Nm/min would give nominal shear strength values of approximately 1.262MPa for the TS1/20DBM specimen and approximately 1.296MPa for the SMA/20DBM specimen. It should be noted that the actual torque rate could fluctuate during the test because there is a possibility that the operator would apply a high torque rate at the beginning of the loading and that the torque rate would gradually decrease as the force needed to induce the torque gradually increased.

Because there is no lateral support at the top part of the specimen in the manual torque bond test (see Figure 2.25 in Chapter 2); lateral shear would appear at the interface (Figure 4.11), in addition to the measured torque. To investigate the significance of the lateral shear in the manual torque bond test, nominal lateral shear was calculated from the measured peak torque using the equation presented Figure 4.11. The length of the twisting arm of 0.8m was used in the calculation. The results presented in Table 4.1 demonstrate that the values of the nominal lateral shear are very small compared to the nominal shear strengths presented in Figure 4.9. Considering the variability of nominal shear strengths shown in Figure 4.9, the appearance of lateral shear would not significantly affect the shear strength.

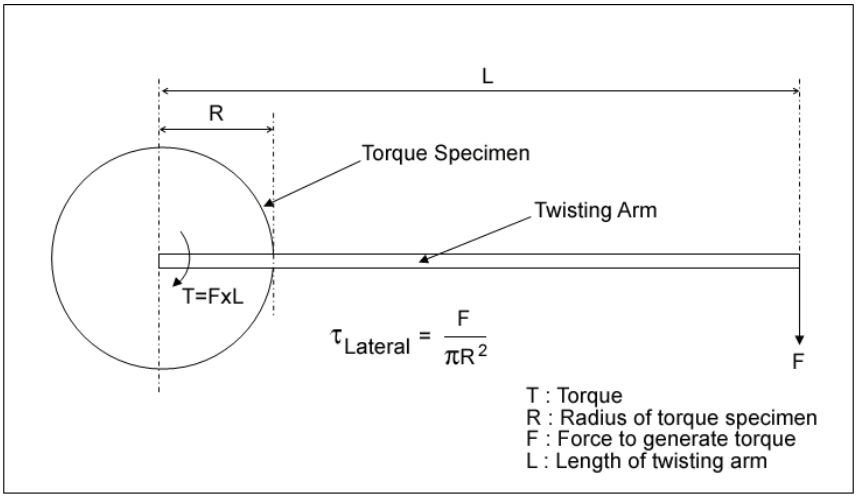

Figure 4.11 – Lateral shear acting at the interface

Table 4.1. Nominal lateral shear in the manual torque bond test

Specimen	Peak Torque (Nm)	Nominal Lateral Shear (MPa)
TS1/20DBM-1	160	0.0066
TS1/20DBM-2	190	0.0079
TS1/20DBM-3	159	0.0066
TS1/20DBM-4	220	0.0091
TS1/20DBM-5	130	0.0054
SMA/20DBM-1	220	0.0091
SMA/20DBM-2	229	0.0095
SMA/20DBM-3	230	0.0095
SMA/20DBM-4	201	0.0083
SMA/20DBM-5	260	0.0108

4.5 Automatic Torque Bond Test Series

A series of automatic torque bond tests were performed over a range of temperatures using either a constant torque rate of 600Nm/min or a constant rotation rate of 180°/min. Please note that in order to reflect the condition in the manual torque bond test, the rotation rate was based on the rotation at the top of the specimen. Leutner tests were also performed at a standard displacement rate of 50mm/min for comparison with results from the automatic torque bond test.

4.5.1 Materials

One hundred twenty six cores of 100mm nominal diameter were tested using the automatic torque test and sixty three cores of 150mm nominal diameter were tested using the Leutner test. The cores were part of the RILEM TC 206 ATB/TG4 - Interlaboratory Test on Interlayer Bonding of Asphalt Pavements and obtained from a trial section constructed in Macerata, Italy by the Universita Politechnica delle Marche (see Piber *et al.* [2009] for further details). The lower layer was a 50mm

thick 16mm Asphalt Concrete mixture (AC16) and the upper layer was a 30mm thick 11mm Asphalt Concrete mixture (AC11). Limestone and basalt aggregates were used in the AC16 and AC11 mixtures respectively. Three different interface conditions were used:

- No bitumen emulsion was applied at the interface and the pavement was constructed hot on hot (Pavement 1)
- A modified bitumen emulsion was applied to give an application rate of approximately 150gr/m^2 residual bitumen (Pavement 2).
- A cationic bitumen emulsion was applied to give an application rate of approximately 150gr/m^2 residual bitumen (Pavement 3).

The cores were conditioned in a temperature-controlled cabinet prior to testing. Seven identical tests were undertaken for each test condition.

4.5.2 Effect of Testing Temperature

Figure 4.12 shows the nominal shear strength together with 95% confidence limits plotted against the testing temperature for the three different interface conditions and two different loading rates. The results of the modified and cationic emulsions tested at a temperature of 10°C and a constant rotation rate of 180°/min are not presented because the specimens did not fail until the torque reached the maximum capacity of the testing frame. As expected, the nominal shear strength increases as the testing temperature decreases. The results at high temperature (i.e. 30°C) generally show lower variability compared to the results at low or intermediate temperatures. However, at high testing temperature, it becomes more difficult to distinguish the nominal shear strength values between specimens of different interface conditions. The results at low temperature (i.e. 10°C) generally show higher variability compared to the results at intermediate temperature (i.e. 20°C). Furthermore, testing at low temperature requires higher force to induce torque failure at the interface. If the low testing temperature is used in the manual torque bond test, the required higher force to induce failure at interface would increase the

risk of strains and falls to the operator. According to the aforementioned considerations, a testing temperature of 20°C is recommended.

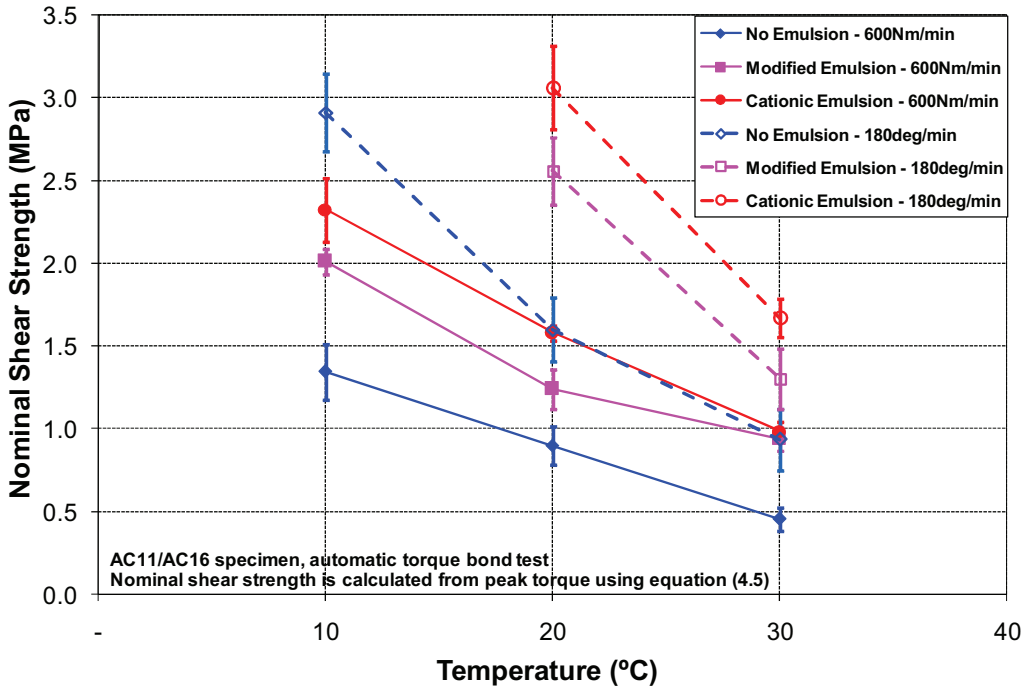

Figure 4.12 – Effect of testing temperature on nominal shear strength obtained from the automatic torque bond test

Figure 4.13 shows the nominal interface shear reaction modulus together with 95% confidence limits plotted against the testing temperature. Equation (4.11) was used to calculate the nominal interface shear reaction modulus. The results show that the nominal shear reaction modulus increases as the temperature decreases. It is interesting to note that the effect of interface treatment on the nominal interface shear reaction modulus at a constant torque rate of 600Nm/min is less obvious than that at a constant rotation rate of 180°/min. It seems that at a constant rotation rate of 180°/min the bitumen becomes stiffer and the effect of interface treatment becomes more dominant compared to the effect of aggregate interlock.

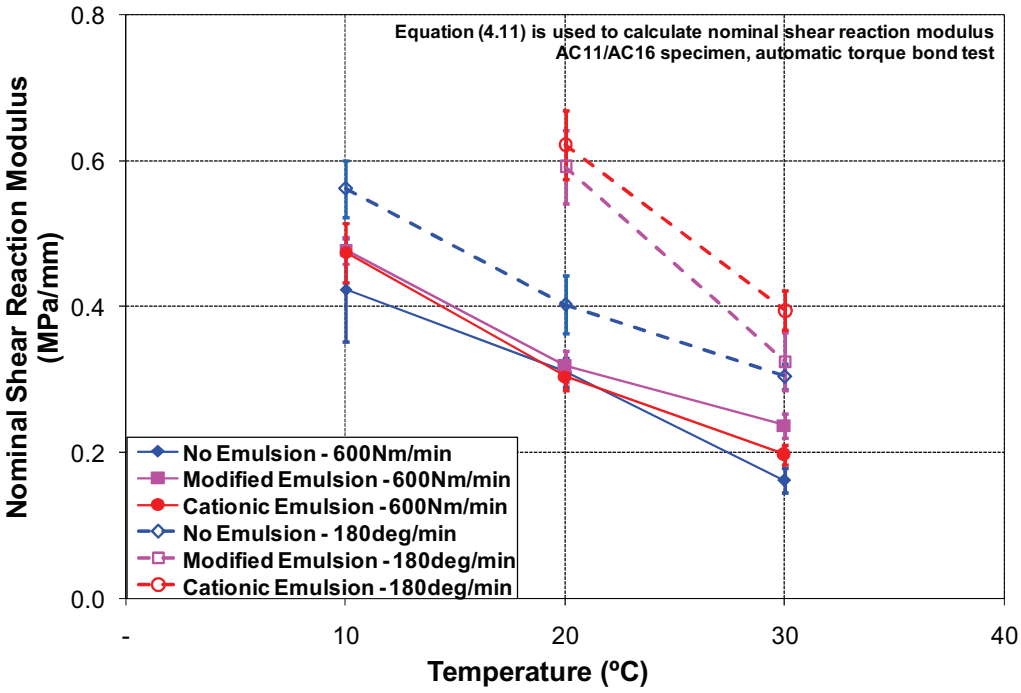

Figure 4.13 - Effect of testing temperature on nominal shear reaction modulus obtained from the automatic torque bond test

4.5.3 Effect of Loading Rates

Figure 4.14 shows a comparison between the nominal shear strength from the test performed at a constant torque rate of 600Nm/min and the nominal shear strength from the test performed at a constant rotation rate of 180°/min together with 95% confidence limits. The nominal shear strength is calculated from peak torque using equation (4.5). Seven identical tests were performed for each test condition. It can be seen from this figure that there is a reasonably good correlation between results from the two tests. The nominal shear strength of the test performed at 180°/min is approximately 1.9 times as high as the nominal shear strength of the test performed at 600Nm/min. The error bars clearly show that the variability of the test performed at a constant rotation rate of 180°/min is higher than the variability of the test performed at a constant torque rate of 600Nm/min. The higher variability found on the test performed at a constant rotation rate is considered to be due to the fact that

the rotation rate is based on the rotation at the top of the specimen, whilst the actual rotation of the interface would depend on the thickness and the stiffness of the upper and lower layer materials.

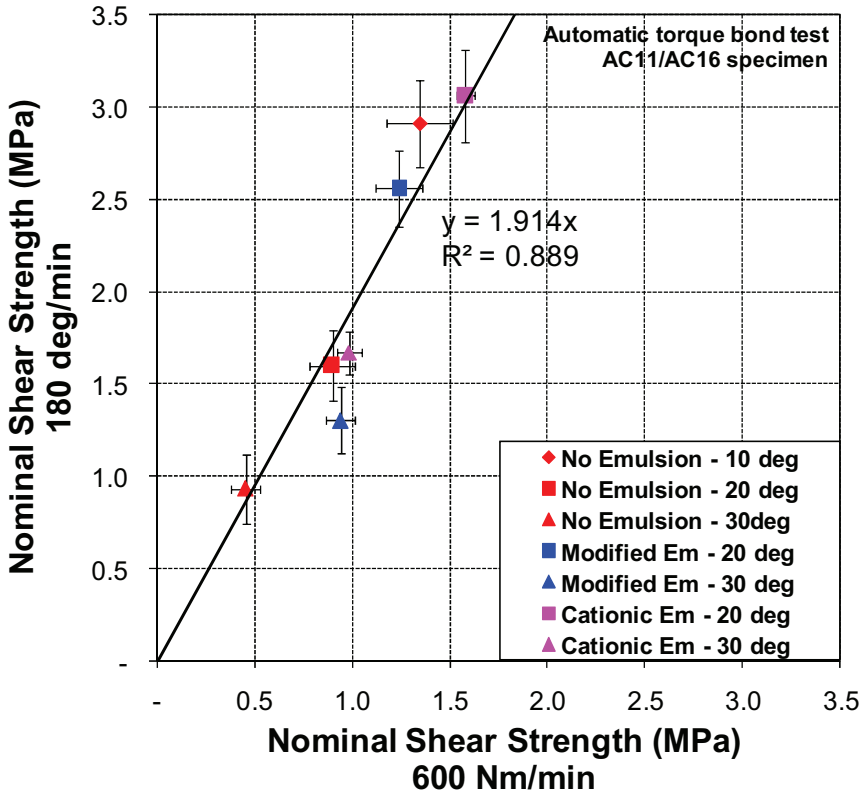

Figure 4.14 – Comparison of nominal shear strength from tests at different loading rates

Figure 4.15 shows a comparison between the nominal shear reaction modulus from the test performed at a constant torque rate of 600Nm/min and the nominal shear reaction modulus from the test performed at a constant rotation rate of 180°/min together with 95% confidence limits. Again, equation (4.11) was used to calculate the nominal interface shear reaction modulus. It can be inferred from this figure that the correlation is not as good as the correlation of the nominal shear strength. Apart from the specimen with no emulsion at the interface and tested at 10°C, the error bars suggest that the variability of the test performed at a constant rotation rate of 180°/min is higher than the variability of the test performed at a

constant torque rate of 600Nm/min. Although the coefficient of correlation is not sufficiently high, the nominal shear reaction modulus of the test performed at 180°/min is approximately 1.6 times as high as the nominal shear reaction modulus of the test performed at 600Nm/min.

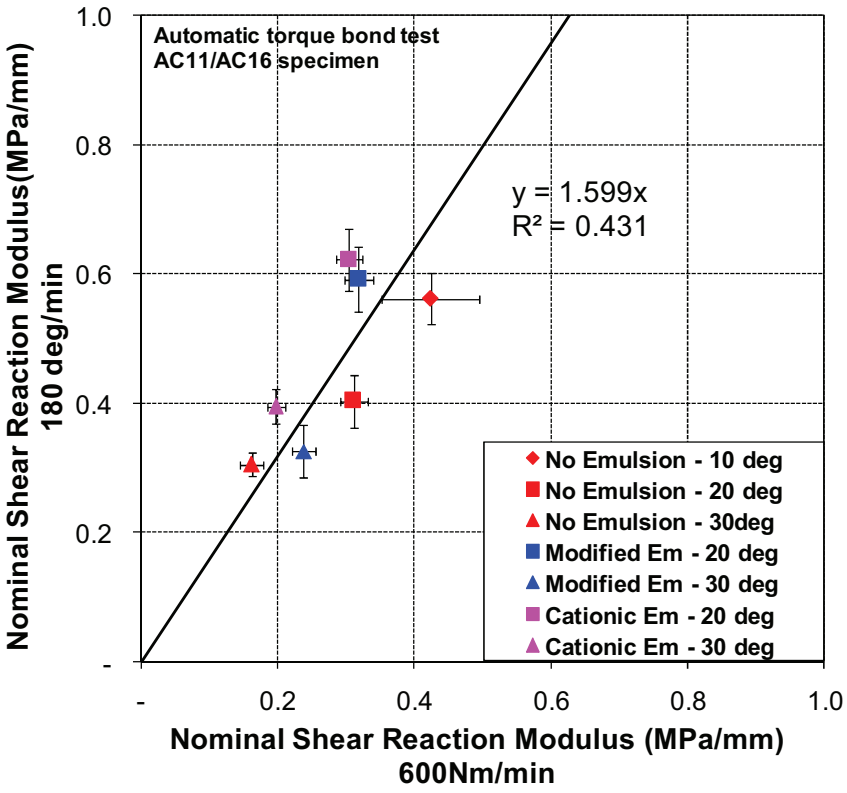

Figure 4.15- Comparison of nominal shear reaction modulus from tests at different loading rates

4.5.4 Rotation at Nominal Shear Strength

Figures 4.16 and 4.17 show the nominal shear strength plotted against the rotation at nominal shear strength together with 95% confidence limits for the automatic torque bond tests performed at a constant torque rate of 600Nm/min and a constant rotation rate of 180˚/min respectively. The results of the modified and cationic

emulsions from testing at 10°C are not presented in Figure 4.17 because the specimens did not fail until the maximum torque capacity of the testing frame.

It can be seen in Figures 4.16 and 4.17 that the rotations at nominal shear strength range between approximately 3˚ and 7˚. The rotation at shear strength for the test at 600Nm/min (Figure 4.16) appears to be relatively independent of the testing temperature and dependent on the interface treatment. The rotation at shear strength for testing at 180˚/min (Figure 4.17) appears to be more dependent on the testing temperature and less dependent on the interface treatment compared to that for testing at 600Nm/min. It can also be seen that for testing at 180˚/min (Figure 4.17), the rotation at shear strength increases as the testing temperature decreases. Read and Whiteoak [2003] showed that when bitumen is very soft, strain at break of the bitumen is less sensitive to temperature and more sensitive to penetration index of the bitumen. Therefore, for testing at a constant torque rate of 600Nm/min; the bitumen probably becomes very soft so that the rotation at shear strength is relatively not affected by the testing temperature and on the other hand becomes more dependent on the bitumen penetration index of the interface treatment.

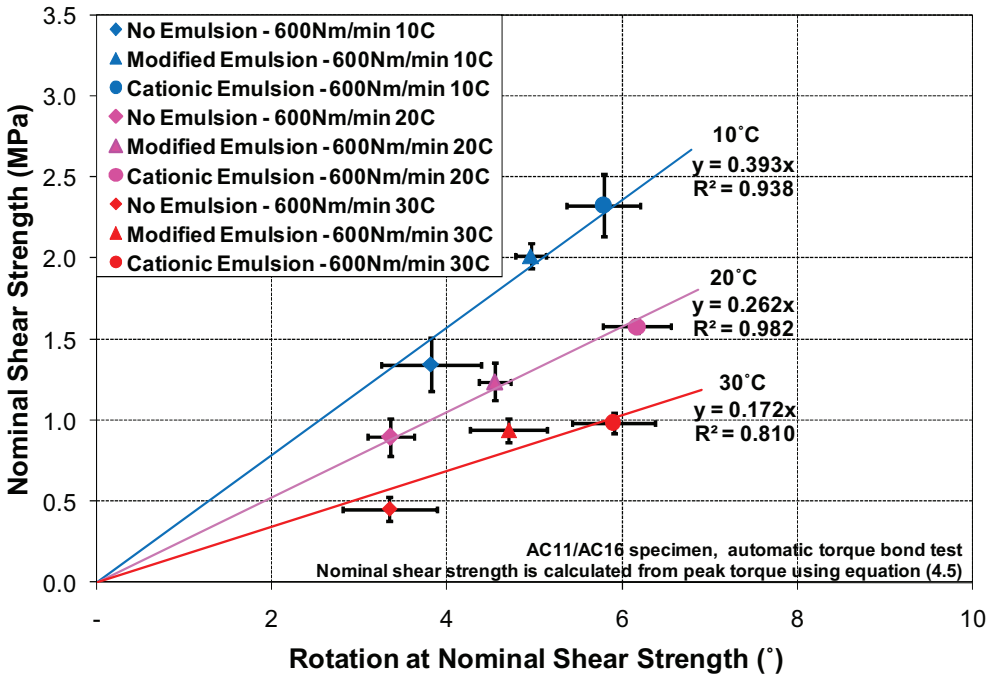

Figure 4.16 - Rotation at nominal shear strength for automatic torque bond test performed at 600Nm/min

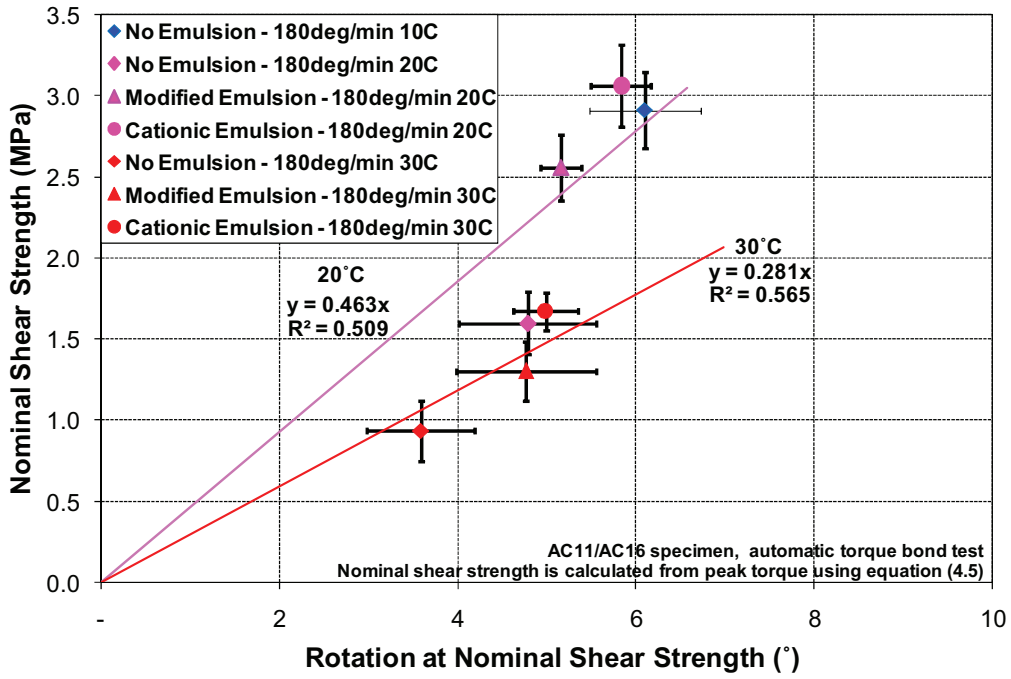

Figure 4.17 - Rotation at nominal shear strength for automatic torque bond test performed at 180˚/min

The gradients of lines joining particular points of different interface treatments at the same temperature to the origin in Figures 4.16 and 4.17 can be considered to be the secant modulus for those testing temperatures. The term secant modulus is used here in order to distinguish it from the nominal shear reaction modulus presented in Figures 4.13 and 4.15, because the secant modulus is presented in units of MPa/˚, whereas the nominal shear reaction modulus is presented in units of MPa/mm. Both of the tests at 600Nm/min and 180˚/min show that the secant modulus is dependent on the testing temperature. It is interesting to note that the gradients for the test at 600Nm/min show higher coefficients of correlation than those for the test at 180˚/min, which indicate that the secant modulus for the tests at 600Nm/min is more independent of the interface treatment than that for the test at 180˚/min. This confirms the finding presented in Section 4.5.2 that the effect of interface treatment on the nominal shear reaction modulus for the test at 600Nm/min is less obvious than that at 180˚/min.

4.5.5 Time to Failure

To investigate the applicability of the two loading rates (600Nm/min and 180˚/min) in the manual torque bond test, it is necessary to investigate the amount of time required to induce torque failure at the interface (time to failure). In the manual torque bond test, a relatively short time to failure may cause it to be difficult to control the loading rate accurately whilst a relatively long time to failure may cause a strain injury to the operator. In order to investigate the time to failure in a more accurate way, the automatic torque bond test was used to perform testing at the two different loading rates (600Nm/min and 180˚/min).

Figures 4.18 and 4.19 show the time to failure together with 95% confidence limits plotted against the testing temperature for the automatic torque bond tests performed at a constant torque rate of 600Nm/min and a constant rotation rate of 180˚/min respectively. As expected, the time to failure increases as the testing temperature decreases.

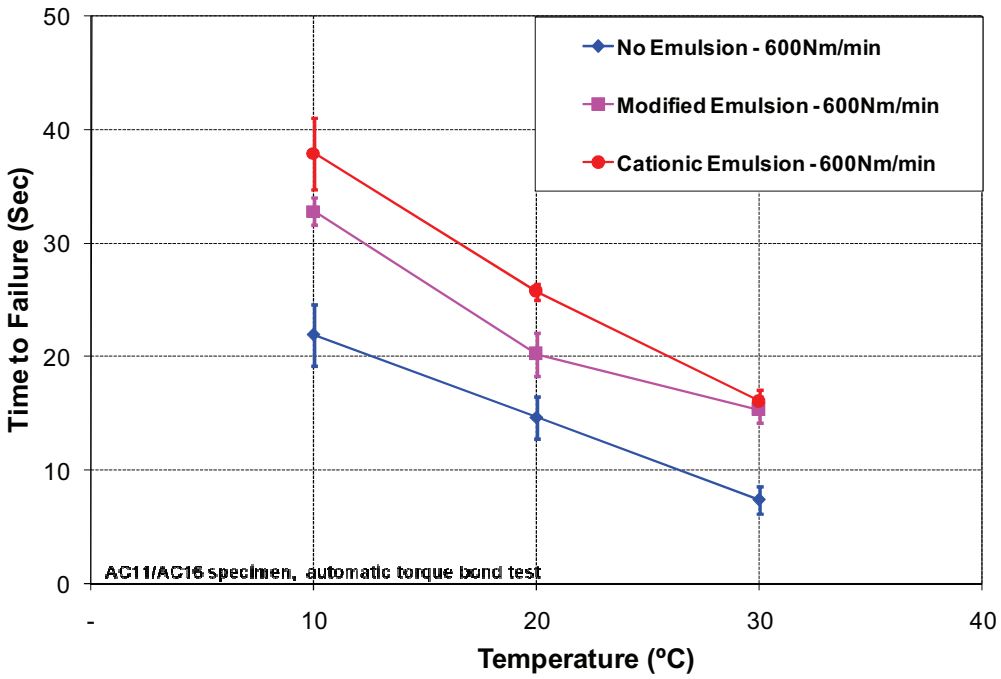

Figure 4.18 – Time to failure for automatic torque bond test performed at 600Nm/min

It can be seen in Figure 4.18 that the amount of time required to induce torque failure for the automatic torque bond test at 600Nm/min ranges between approximately 7 and 42 seconds. Because the time to failure is not relatively short, the loading rate of 600Nm/min would be relatively easy to controll if it is used in the manual torque bond test. However, as mentioned earlier, applying a static force for a relatively long period of time may cause a strain injury to the operator. Therefore, the force required to induce torque failure as well as its duration needs to be assessed.

The maximum nominal shear strengths from the automatic torque bond test at a constant torque rate of 600Nm/min and at testing temperatures of 10, 20 and 30˚C (Figure 4.12) are approximately 2.5, 1.7 and 1.2MPa respectively. Assuming that the nominal shear strength of the manual torque bond test is 20 - 30% lower than that of the automatic torque bond test (Section 4.4), the length of the twisting arm used in the manual torque bond test is 0.8m and equation (4.5) is used to calculate the peak torque values; the maximum force required in the manual torque bond test at 600Nm/min to induce torque failure at testing temperatures of 10, 20 and 30˚C would be 47, 32 and 23kgf respectively. Assuming that the maximum duration of force application in the manual torque bond test at 600Nm/min could be predicted from the corresponding time to failure in the automatic torque bond test presented in Figure 4.18, the maximum duration of force application at testing temperatures of 10, 20 and 30˚C would be approximately 42, 27 and 18seconds respectively. According to Kerschhagl [2009] and considering that the posture of the operator while performing the manual torque bond test is bad as it includes a twisting movement, applying a 47kgf force for 42seconds (at 10˚C testing temperature) may cause a physical overload. The physical overload is unlikely to happen when a 32kgf force is applied for 27seconds (at 20˚C testing temperature) or a 23kgf force is applied for 18seconds (at 30˚C testing temperature). Therefore, performing the manual torque bond test at a constant torque rate of 600Nm/min and at a testing temperature of 10˚C should be avoided because it may cause a strain injury to the operator.

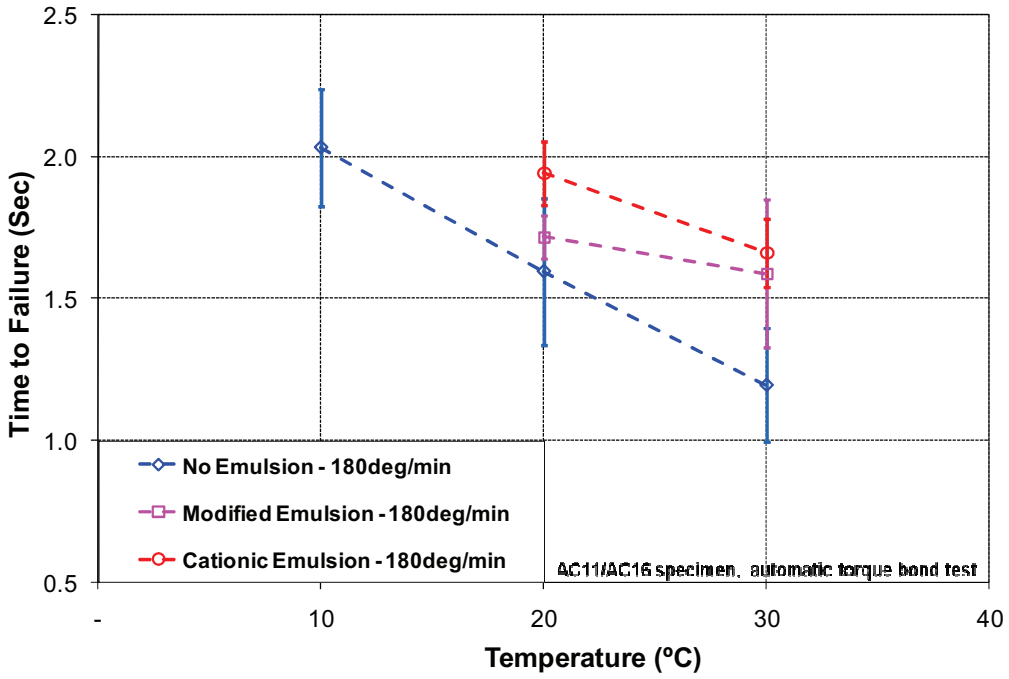

Figure 4.19 – Time to failure for automatic torque bond test performed at 180˚/min

Figure 4.19 demonstrates that the time to failure for the automatic torque bond test at 180˚/min ranges between approximately 1 and 2.25seconds. Because the rotations at nominal shear strength for the automatic torque bond test at 180˚/min (Figure 4.17) are very small (approximately 3 to 7˚) and the failure for the test at 180˚/min would occur in less than 3 seconds, the loading rate would be difficult to controll accurately if the constant rotation rate of 180˚/min is used in the manual torque bond test.

4.5.6 Comparison between modified Leutner and Automatic Torque Bond Tests

A series of modified Leutner tests was performed for comparison with results from the automatic torque bond test. The tests were performed at a displacement rate of 50mm/min and temperatures of 10, 20 and 30°C.

Figure 4.20 shows a comparison between the average shear strengths obtained from the modified Leutner test at a displacement rate of 50mm/min and the average nominal shear strengths obtained from the automatic torque bond tests at a constant torque rate of 600Nm/min and at a constant rotation rate of 180°/min. It can be seen from this figure that the results from the Leutner test show a reasonably good correlation to the results from the automatic torque test at a constant torque rate of 600Nm/min. Because the variability of the automatic torque test performed at a constant rotation rate of 180°/min has been found to be higher, the correlation to the Leutner test is not as good as the correlation of the test performed at a constant torque rate of 600Nm/min.

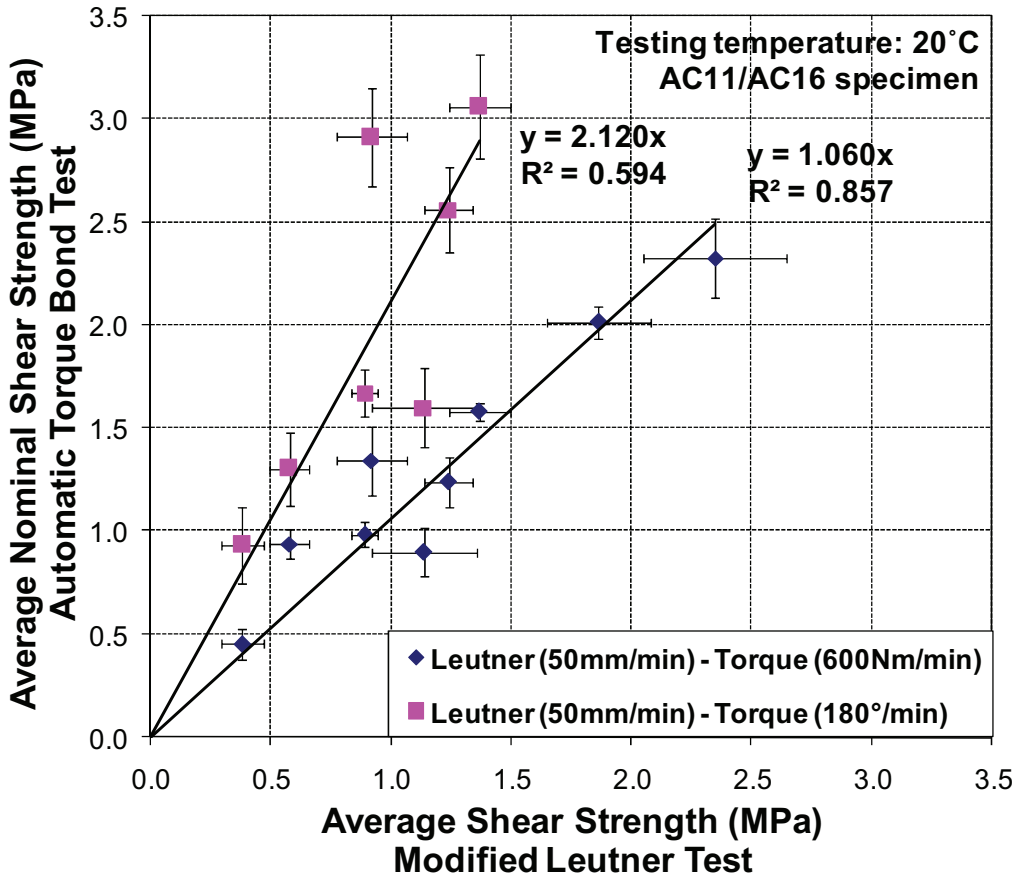

Figure 4.20 - Correlation between modified Leutner and automatic torque bond tests

4.5.7 Recommendation for the Manual Torque Bond Test

The results from the automatic torque bond tests on AC16/AC11 specimens performed at two different loading rates of 600Nm/min and 180°/min, at three different temperatures and three different interface treatments lead to the following considerations related to the manual torque bond test:

- A very high torsional force is needed to perform the test at a constant rotation rate of 180°/min.
- The test at 30˚C shows the lowest variability of nominal shear strength, followed by the test at 20°C and then the test at 10°C. However, at the 30°C testing temperature, it becomes more difficult to distinguish the nominal shear strengths between specimens of different interface treatments.
- The variability of the nominal shear strength and shear reaction modulus obtained from the test performed at a constant rotation rate of 180°/min are generally higher than that from the test performed at a constant torque rate of 600Nm/min.
- The time to failure for the testing at 600Nm/min ranges between approximately 7 and 42 seconds, hence the loading rate of 600Nm/min would be relatively easy to controll if it is used in the manual torque bond test.
- Performing the manual torque bond test at a constant torque rate of 600Nm/min and at a testing temperature of 10˚C may cause a strain injury to the operator.
- For the test at 180˚/min, the rotations at nominal shear strength are very small (approximately 3 to 7˚) and the time to failure is very short (less than 3 seconds). Therefore, the loading rate would be very difficult to controll accurately if the constant rotation rate of 180˚/min is used in the manual torque bond test.
- In the manual torque bond test, the typical maximum capacity of the torque wrench is 350Nm. According to the automatic torque test results shown in Figure 4.12 and the comparison between the automatic and manual torque test presented in Section 4.4, there is a high possibility that the torque

strength measured using the manual torque test at 20°C and a constant rotation rate of 180°/min would be higher than 350Nm and the torque can not be measured using the typical torque wrench.

According to the aforementioned considerations, it is recommended to perform the manual torque bond test at a constant torque rate of 600Nm/min and a testing temperature of 20°C.

4.6 Comparison between Modified Leutner and Manual Torque Bond Tests on Thin Surfacing Specimens

A series of manual torque bond tests was performed on SMA/20DBM and TS1/20DBM thin surfacing specimens for comparison with results from the modified Leutner test presented in Section 3.6 of Chapter 3. Details of the mixtures are given in Table 3.2 in chapter 3. The modified Leutner and manual torque bond tests were performed at a target displacement rate of 50mm/min and a target torque rate of 600Nm/min respectively. The tests were performed at three different temperatures of 15, 20 and 30^{o}C. Cores were conditioned in a temperature controlled cabinet prior to testing.

Figure 4.21 shows a comparison between the average shear strengths measured with the Leutner test at a displacement rate of 50mm/min and the average nominal shear strengths obtained from the manual torque bond test at a constant torque rate of 600Nm/min. It can be seen from this figure that there is a reasonably good correlation between results from the two tests. Note that, in addition to the thin surfacing results, data from a previous research study performed at the same loading rates [Choi *et al*., 2005] have also been included. Results from the current study at all temperatures compare well to previous results at 20^{o}C. In the previous study, a slightly different correlation was found at 30^{o}C which may have been due to the bulging phenomenon discussed in Chapter 3.

It is interesting to note that the correlation gradient of the manual torque bond test performed at 600Nm/min shown in Figure 4.21 is approximately 30% lower than

the correlation gradient of the automatic torque bond test performed at 600Nm/min shown in Figure 4.20. This supports the finding that the results of the automatic torque bond test are 20-30% higher than the results of the manual torque test and the reason for this has been discussed in Section 4.4.

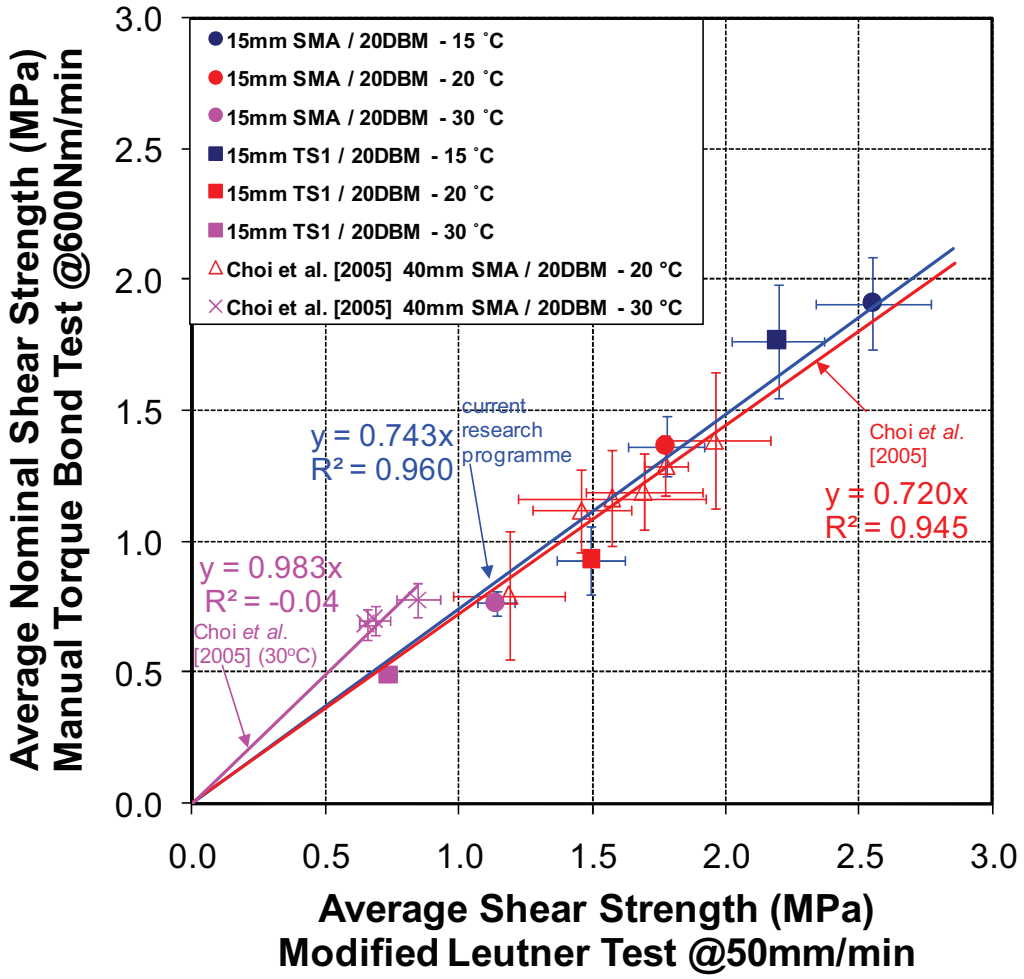

Figure 4.21 - Correlation between modified Leutner and manual torque bond tests

4.7 Repeated Loading

In a real pavement structure, a single load application is unlikely to cause the interface to fail. Therefore, it is important to investigate the behaviour of the interface under repeated loading. The automatic torque test is capable of transferring either tensile or compressive force to generate negative or positive torsional load, hence it is suitable to perform a cyclic zero-mean torsional load.

4.7.1 Materials

To investigate the effect of repeated loading on bond, a 14mm Stone Mastic Asphalt (SMA) surfacing material and a 20mm Dense Bitumen Macadam (20DBM) binder course material were used. A gritstone aggregate was used for the SMA and a limestone aggregate was used for the 20DBM mixtures. All materials were designed according to the relevant Standards [British Standard Institution, 2005 and 2006b]. Details of the mixtures are given in Table 4.2.

Table 4.2. Mixture characteristics for repeated loading investigation

Mixture type	Binder grade	Binder content (% mass)	Air void content	Max. density (Mg/m3)	Compacted layer thickness (mm)
20mm DBM	30/45pen	4.7%	5.5%	2.490	60
14mm SMA	40/60pen	6%*	4%	2.501	40

* includes 0.3% cellulose fibres by mass of total mixture

The interface was treated to give one of the following interface conditions:

a) A K1-40 emulsion, 200g/m^2 average spread rate of residual bitumen (TC).
b) A polymer modified bond coat, 300g/m^2 average spread rate of residual bitumen (BC).

The specimens were produced by manufacturing a number of 305mm by 305mm double layered slabs (with a bond between them) in the slab roller compactor (Figure 3.2). From each slab, five 100mm cores were obtained for repeated automatic torque bond testing. After the specimens had been cored, they were prepared according to Section 4.3.2 and the tests were performed according to the procedure presented in Section 4.3.3.

4.7.2 Test Conditions

A trial run was performed at various loading frequencies and a frequency of 2Hz was chosen because of safety consideration. The tests were performed at two different temperatures of 20 and 30°C. Testing at lower temperature was not performed as it would require higher torsional load, beyond the capacity of the testing frame. Strengthening the testing frame is recommended to enable tests at higher loads and frequencies. However, due to time limitation and major modification requirement, the strengthening of the testing frame was not carried out during this research study.

The repeated automatic torque test can be performed in either stress controlled (constant torque) or strain controlled (constant rotation) modes. There has not been any research investigating the actual mode of loading at the interface of an actual pavement. Stress controlled mode was chosen due to the consideration that the torque over the height of the specimen would be equal regardless of the thicknesses and properties of the upper and lower layer materials.

4.7.3 Test Results

Figure 4.22 shows typical results from tests at three different shear stress levels (0.89MPa, 0.69MPa and 0.47MPa). In Figure 4.22, the shear reaction modulus normalised against the initial shear reaction modulus is plotted versus the number of loading cycles. Equations (4.5) and (4.11) were used to calculate the shear stress

and the shear reaction modulus of the interface. It can be seen from Figure 4.22 that the normalised shear reaction modulus decreases significantly as the specimen approaches failure. Ideally, similar to a typical stress controlled fatigue test for an asphalt mixture, the fatigue failure point is determined as the number of load cycles that corresponds to the specimen being completely fractured. However, because the instrumentation to detect complete fracture of the interface was not available, the failure point was arbitrarily determined as the number of cycles that corresponds to the normalised shear reaction modulus of 0.5.

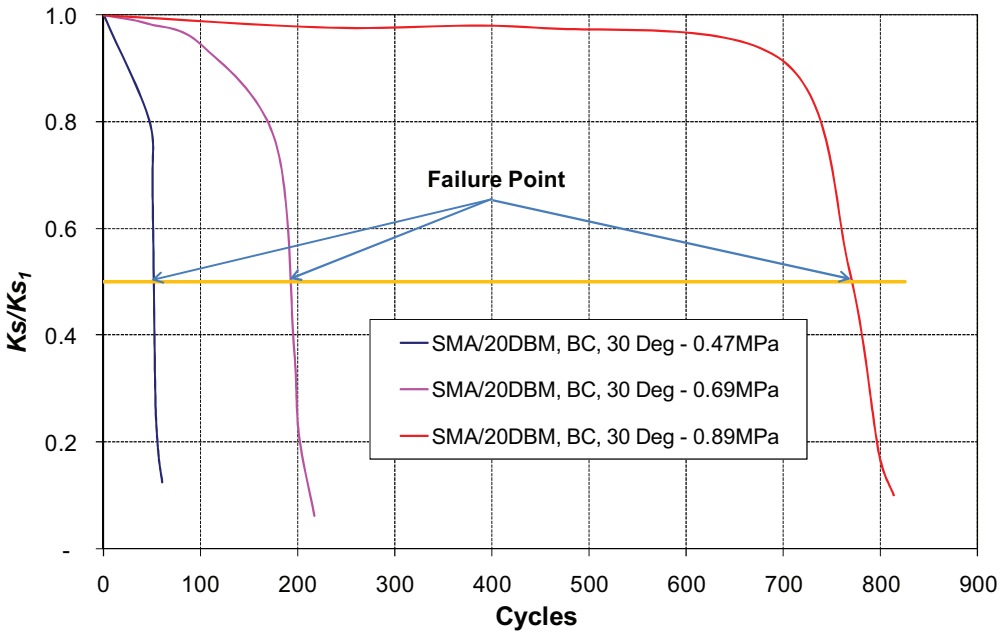

Figure 4.22 – Typical plot of the normalised shear reaction modulus versus the number of loading cycles

A series of repeated automatic torque tests were performed on SMA/20DBM, TC and SMA/20DBM, BC at 20 and 30°C. Figure 4.23 shows the shear stress plotted against the number of cycles to failure. It can be inferred from Figure 4.23 that there is no significant difference between results for the TC and BC interfaces (also checked with a statistic test). Also, the lines at 20°C are almost parallel to the lines at 30°C. From the reasonably good coefficients of correlation shown in Figure 4.23, the automatic torque bond test demonstrates the suitability for investigating the

interface behaviour under repeated loading. Strengthening the testing frame is recommended to enable tests at higher loads and frequencies.

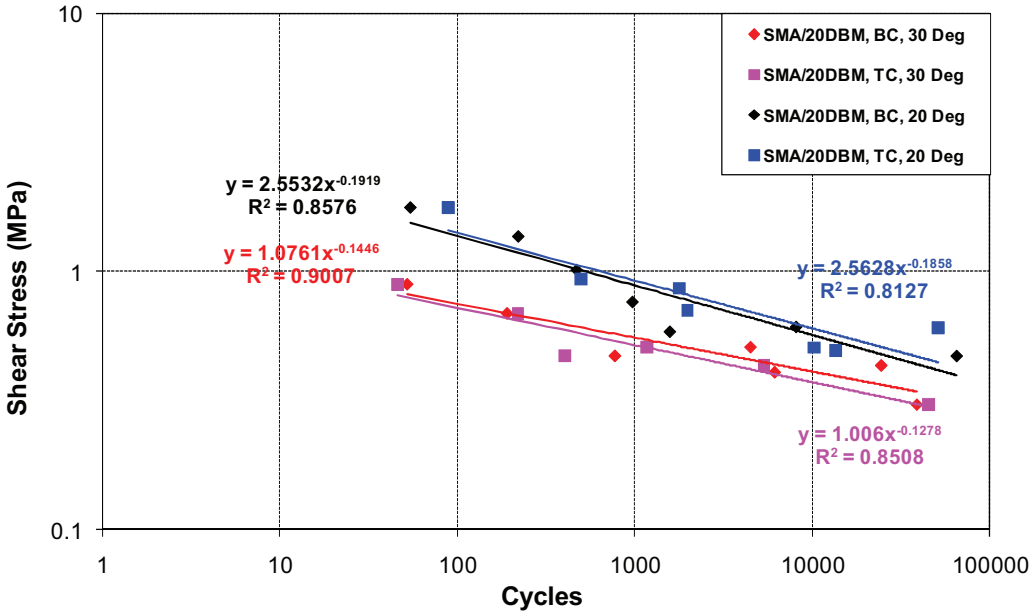

Figure 4.23 – Effect of repeated loading on shear stress

4.8 Conclusion

An investigation into the measurement of interface bond properties using the torque bond test principle has been described. Basic formulae for calculating the shear stress and the shear reaction modulus of the interface using the torque test principle have been briefly explained. The following key points can be derived from the study:

1. At a constant torque rate of 600Nm/min, the shear strength measured using the automatic torque test is higher than the shear strength measured using the manual torque bond test.
2. The nominal loading rate of the manual torque test performed at 600Nm/min has been found to be lower than the target loading rate, hence leading to the lower measured shear strength compared to the automatic torque test.

3. The results of the manual torque test on SMA/20DBM and TS1/20DBM specimens performed at 600Nm/min and using a twisting arm of 0.8m in length show that the values of nominal lateral shear are very small and not significant compared to that of the nominal shear strength.
4. The shear strength of the automatic torque test performed at a constant rotation rate of 180°/min is approximately 1.9 times as high as the shear strength performed at a constant torque rate of 600Nm/min.
5. Considering the variability of results, the force needed to induce the torsional load, the possibility to control the loading rate accurately and the ability to distinguish the effect of different interface treatments; it is recommended that the manual torque bond test is performed at an intermediate temperature (i.e. 20ºC) and a constant torque rate of 600Nm/min.
6. For the range of specimens that have been tested, there is a reasonably good correlation between the average shear strength measured from the modified Leutner test at a constant displacement rate of 50mm/min and the average nominal shear strength measured from the automatic and manual torque bond tests performed at a constant loading rate of 600Nm/min.
7. The automatic torque bond test demonstrates the suitability for investigating the interface behaviour under repeated loading. Strengthening the testing frame is recommended to enable tests at higher loads and frequencies.

Chapter 5

TRAFFICKING INVESTIGATION

5.1 Introduction

Good bonding at the interface between pavement layers is essential to ensure that the pavement fulfils the design requirement. To achieve the good bond condition, it is important to understand several factors that may affect the state of bond at the interface. The literature review in Chapter 2 identified that trafficking is one of the factors that may affect the state of bond at the interface. In the UK, the effect of trafficking on bond was first mentioned by the TRL. Because they found that bond problems were most frequently observed during the spring and very few during the hot summer, they indicated that trafficking when the temperature is high during the hot summer could improve the bond due to healing and re-bonding effects [Kennedy, 1978]. However, this indication was not followed by any substantial research by the TRL to investigate the effect of trafficking at elevated temperature on bond.

Partl and Raab [1999] investigated the development of bond in a number of in-service roads in Switzerland and found a slight improvement of bond in some material combinations after the roads had been about 3-5 years in service. Stöckert [2001] evaluated the bond strengths of a number of pavements in Germany after they had been one year in service. The researcher found significant, little and no improvements of bond strength when the initial bond strength was intermediate (approximately 1.1MPa), high (approximately 1.7MPa) and low (approximately 0.55MPa) respectively. More recently, Raab and Partl [2007a, 2008 and 2009] investigated the development of bond in 14 high volume roads in Switzerland after 9-13 years in service. They concluded that for a newly constructed pavement (new over new), the bond strength can be expected (but not always) to increase after 10 years; whereas for a rehabilitated pavement (new over old) the bond strength

cannot be expected to increase after 10 years. They also demonstrated that a high proportion of heavy vehicles over a long period of time could deteriorate the bond. From the previously mentioned findings, it appears that the development of bond in an in-service road over a period of time is affected by many factors such as time, temperature, traffic volume, load magnitude, initial bond condition, and material (mixture) combination. Some other factors such as chemical and physical properties of the interface as well as the adjacent pavement layers, ageing, moisture and climate may also have an influence.

Choi *et al.* [2005] performed a more specific investigation into the combined effect of trafficking, initial bond condition and trafficking temperature on the development of bond strength in an accelerated pavement testing facility. They performed two pilot scale experiments at different temperatures on the same pavement construction containing a range of interface bond conditions. They found an indication that the bond was improved with trafficking at elevated temperature (30-35°C) where the initial bond was low or intermediate (<1MPa). However, due to the lack of data, further testing was required to confirm this. Additionally, only one material combination had been tested and they achieved the initially low or intermediate bond condition by spreading an excessive amount of water/talcum powder mixture at the interface which is clearly un-realistic in an actual pavement system.

This chapter presents an investigation into the development of bond with trafficking at elevated temperature. Because material combination appears to affect the development of bond with trafficking, the investigation was performed on a wider range of UK material combinations. Particular emphasis was placed on situations where the initial bond condition is low or intermediate since results of the investigation performed by Choi *et al.* [2005] have shown the potential for improvement. The investigation was performed using a more realistic interface condition in two different laboratory trafficking procedures. To cover a wider range of material combinations and considering time constraints, a simple approach was used in the first laboratory trafficking procedure where a 150mm core specimen was confined in a Percentage Refusal Density (PRD) mould [British Standards Institution, 2005b] and trafficking was simulated by applying a vertical stress until a

set number of cycles. After the trafficking had been performed, a modified Leutner test was then performed on the 150mm core specimen to determine the interface shear strength. The combinations that showed improvement in the first trafficking procedure were then used in the second trafficking procedure where a rolling wheel load was applied using a French Wheel Tracker (FWT) machine [British Standards Institution, 2003b] on a double layered prismatic specimen confined in a steel mould until a set number of wheel passes. After the trafficking in the FWT had been performed, two 150mm diameter core specimens were then extracted from each prismatic FWT specimen prior to modified Leutner testing.

5.2 Poor Bond Investigation

As noted above, Choi *et al.* [2005] used an un-realistic interface treatment in order to achieve the low initial bond condition. Therefore, a series of Leutner tests incorporating various interface conditions was performed during this research study to achieve an initially low or intermediate bond condition in a more realistic way .

5.2.1 Materials and Specimen Preparation

To investigate the interface conditions that produce an initially low or intermediate bond condition, a 14mm Stone Mastic Asphalt (SMA) surfacing material was used as the upper layer and a 20mm Dense Bitumen Macadam (20DBM) binder course material was used as the lower layer. Gritstone and limestone aggregates were used for the SMA and DBM mixtures, respectively. All materials were designed according to the relevant Standards [British Standards Institution, 2005a and 2006b]. Details of the mixtures are given in Table 5.1.

Slabs of plan dimensions 305mm by 305mm, each comprising 2 layers, were manufactured in the Cooper CRT-RC slab 'roller' compactor (Figure 3.2) in accordance with BS EN 12697-33 [British Standards Institution, 2003d] to simulate site compaction conditions as closely as possible. The material for the lower layer,

once mixed, was placed in the mould and compacted to the desired thickness. The surface was then treated to give one of the following interface conditions:

(a) The lower layer was allowed to fully cool to room temperature. A 'standard' amount of tack coat, comprising K1-40 emulsion, was spread on the lower layer surface using a clean brush to give an average of 200 g/m^2 residual bitumen.

(b) The lower layer was chilled at 5^{o}C for 16±1 hours prior to interface preparation. A slurry mixture comprising 16g of limestone filler and 32g of water was applied on the 305mm × 305mm area of the lower layer surface.

(c) The lower layer was chilled at 5^{o}C for 16±1 hours prior to interface preparation. A quantity of water (48g) was applied on the 305mm × 305mm area of the lower layer surface.

(d) The lower and upper layers were designed using the minimum permissible binder content. The lower layer surface was 'scuffed' with an abrasive to remove surface bitumen then chilled at 5^{o}C for 16±1 hours prior to interface preparation. A slurry mixture comprising 16g of limestone filler and 48g of water was applied on the 305 mm × 305 mm area of the lower layer surface.

Table 5.1. Mixture characteristics for poor bond investigation

Mixture type	Binder grade	Binder content (% mass)	Air void content	Max. density (Mg/m3)	Compacted layer thickness (mm)
14mm SMA	40/60pen	6%*	4%	2.501	40
14mm SMA-MB**	40/60pen	5.7%*	4%	2.531	40
20mm DBM	30/45pen	4.7%	5.5%	2.490	60
20mm DBM-MB**	30/45pen	4.1%	5.5%	2.504	60

* Includes 0.3% cellulose fibres (of mixture weight)
** Designed using minimum permissible binder content (only for case d)

Case (a) can be considered to be 'best' current practice where a known amount of tack coat is applied to a clean surface. Case (b) was designed to simulate

the condition where an upper layer is laid over a dirty lower layer after a drizzle during a chilly morning and no tack coat is applied. Case (c) was designed to simulate the condition where an upper layer is laid over a clean lower layer after a heavy rain during a chilly morning and no tack coat is applied. Case (d) can be considered to be the 'worst' condition and was designed to simulate the situation where both layers are using the minimum permissible binder content, the surface of the lower layer has had the surface bitumen removed due to hauling traffic (see Figure 5.1), the upper layer is laid over a dirty lower layer after a heavy rain during a chilly morning and no tack coat is applied.

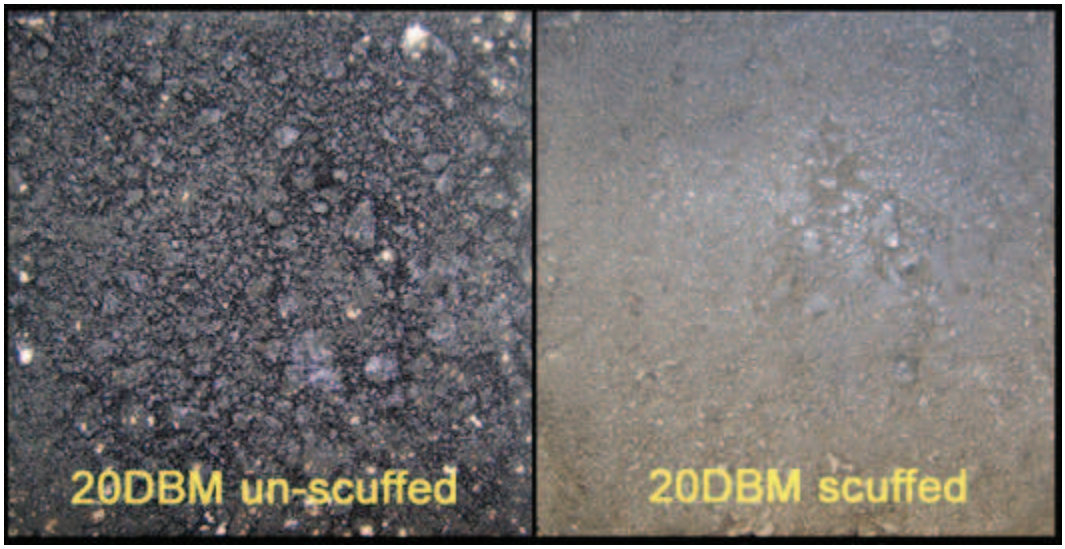

Figure 5.1 – Un-scuffed and scuffed surfaces of 20DBM

Although the condition in Case (d) is relatively extreme, it is considered to be more realistic than the interface treatment used by Choi *et al.* [2005] because of the following reason:

- The application of minimum permissible binder contents in both layers could be found during the construction of a real pavement structure.
- Hauling traffic may cause surface bitumen stripping in a newly laid lower layer.

- In bad construction practice, tack coat is often not applied at the interface when an upper layer is laid over a new lower layer.
- The compaction of an upper layer over a cold, dirty and very wet lower layer may also be found in bad construction practice.

After the interface had been prepared, the material for the upper layer was mixed and compacted on top of the lower layer to the desired thickness. From each slab, two 150mm diameter cores were obtained for modified Leutner testing. Nominally six identical tests were undertaken for each test condition.

5.2.2 Results

Figure 5.2 shows the shear strength of the various interface conditions. The error bars represent the 95th percentile confidence limits. It can be seen from Figure 5.2 that only interface condition (d) shows an average shear strength of less than 1MPa indicating an intermediate/poor bond. Interface condition (d) was therefore used as the interface condition in the trafficking investigation.

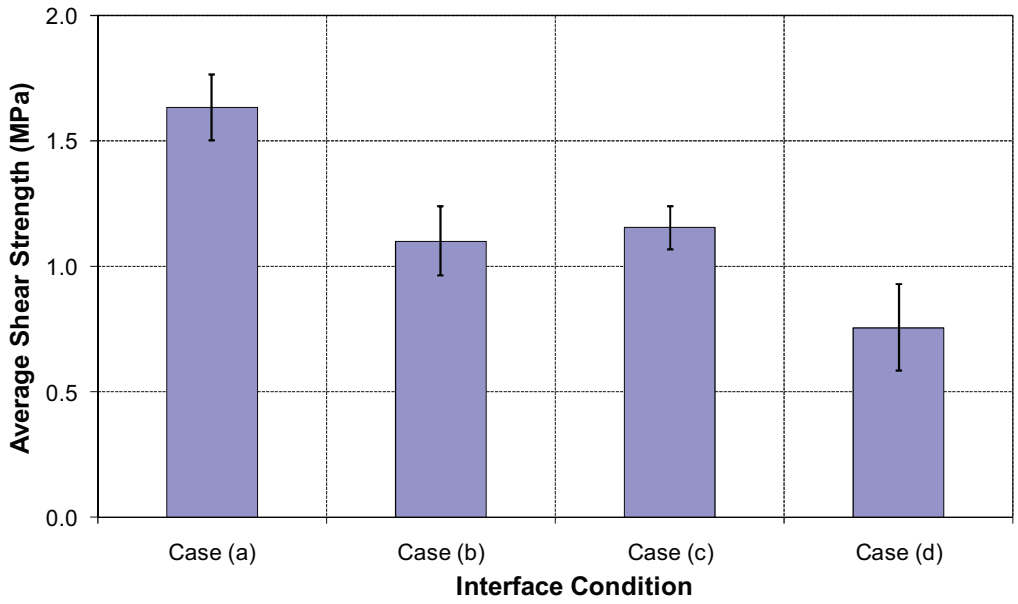

Figure 5.2 – Average shear strength of various interface conditions

5.3 Simulated Trafficking Using Percentage Refusal Density (PRD) Mould

It has been mentioned earlier in the introduction to this Chapter that a simple approach was used in this first laboratory trafficking procedure in order to cover a wider range of material combinations and considering the time constraint. The trafficking was simulated by applying a repeated vertical stress into a 150mm diameter specimen. In order to prevent lateral deformation, a steel mould of 150mm diameter was to be used to confine the specimen. A steel split mould (Figure 5.3) commonly used for a Percentage Refusal Density (PRD) test to determine the percentage refusal density of core samples of 150mm nominal diameter cut from compacted bituminous mixtures [British Standards Institution, 2005b] was then used to confine the specimen. The PRD mould consists of a base plate with latches and a steel split mould body of 150mm nominal diameter and 170mm height with two clamp screws to adjust the diameter of the mould body with the diameter of the specimen.

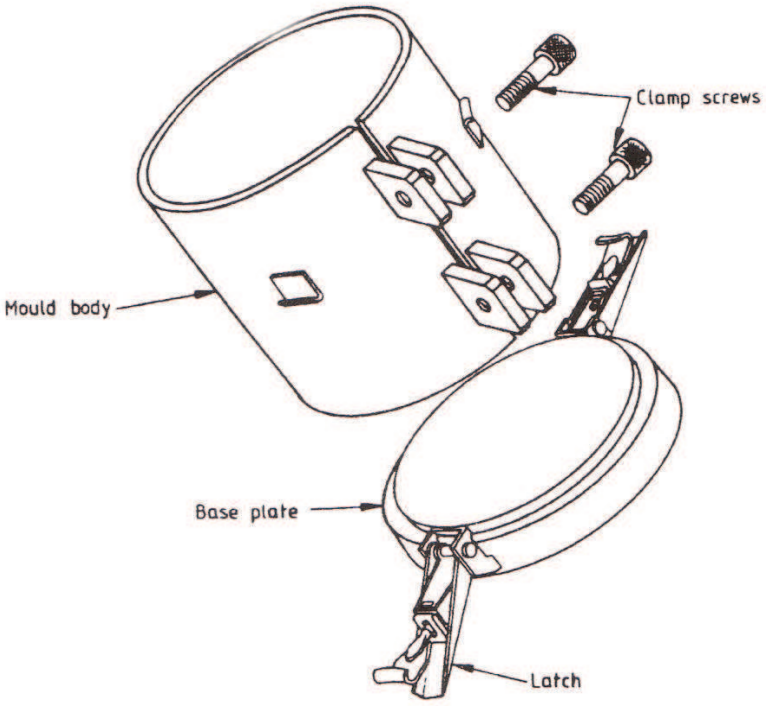

Figure 5.3 – PRD mould (From British Standards Institution, 2005b)

It should be noted that the stress conditions associated with a rolling wheel loading in a real pavement structure are extremely complex and cannot be precisely replicated in a laboratory trafficking procedure. There are some notable differences between the condition in the PRD mould trafficking and that in a real pavement structure, for example:

- Lateral confinement in the PRD mould is significantly higher than that in the field.
- Movement of large aggregate particles close to the specimen circumference is constrained by the significantly high lateral confinement of the PRD mould.
- Loading in the PRD mould is applied axially, hence it cannot simulate the rotation of principal stresses related to rolling wheel loading in the field.
- Loading in the PRD mould is applied continuously using specific temperature and loading conditions; whereas the temperature and loading conditions in the field are randomly distributed.

5.3.1 Materials and Trafficking Setup

In the simulated trafficking investigation using the PRD moulds, two surfacing materials (14mm Stone Mastic Asphalt (SMA) and a proprietary Thin Surfacing (TS1)), two binder course materials (20mm Dense Bitumen Macadam (DBM) and 0/14 Enrobé à Module Élevé (14EME)) and one base material (0/20 EME (20EME)) were used. A gritstone aggregate was used for the SMA, TS1 and EME and a limestone aggregate was used for the DBM mixtures. All materials were designed according to the relevant Standards [British Standards Institution, 2005a and 2006b; Sanders and Nunn, 2005] using the minimum permissible binder contents. Details of the mixtures are given in Table 5.2. Slabs with the interface condition (d) were prepared and cored in the same manner as the specimens described in Section 5.2.1.

Table 5.2. Mixture characteristics for simulated trafficking investigation

Mixture type	Binder grade	Binder content (% mass)	Air void content	Max. density (Mg/m3)	Compacted layer thickness (mm)
14mm SMA	40/60pen	5.7%**	4%	2.531	40
10mm TS1	150pen	4.6%	4%	2.454	15
20mm DBM	30/45pen	4.1%	5.5%	2.504	60
0/14 EME	10/20pen	5.4%	5%	2.522	60
0/20 EME	10/20pen	5.2%	5%	2.530	80

* Minimum permissible binder content is used
** Includes 0.3% cellulose fibres (of mixture weight)

It should be noted that in order to achieve the targeted layer thickness and air void content of the 14EME over 20EME material combination, a bigger slab size (500mm by 500mm plan dimension) and a bigger laboratory roller compactor (Figure 5.4) were used. The big roller compactor can be used to compact a 500mm by 500mm slab with a target thickness of 40-200mm. It consists of a steel wheeled roller segment of 1000mm diameter and 500mm width, a sliding table, a pneumatic system which allows up to 50kN roller load and a 0-50Hz vibrator. The compaction was performed in accordance with BS EN 12697-33 [British Standards Institution, 2003d].

Figure 5.5 shows the setup for the simulated trafficking using the PRD moulds. The specimen (core of 150mm diameter) was placed in a percentage refusal density (PRD) mould, which provides lateral confinement to the specimen. To prevent friction between specimen circumference and inner surface of the PRD mould, silicon grease was applied to the inner surface of the mould. A sinusoidal loading with a frequency of 5 Hz and 600 kPa peak contact pressure was then applied to the specimen surface through a loading platen to simulate traffic loading. Hard rubber discs were placed between the specimen surfaces (top and bottom) and the loading platens. The trafficking was performed at elevated temperature (35°C). The modified Leutner test was performed after 0, 1,000, 10,000 and 100,000 cycles.

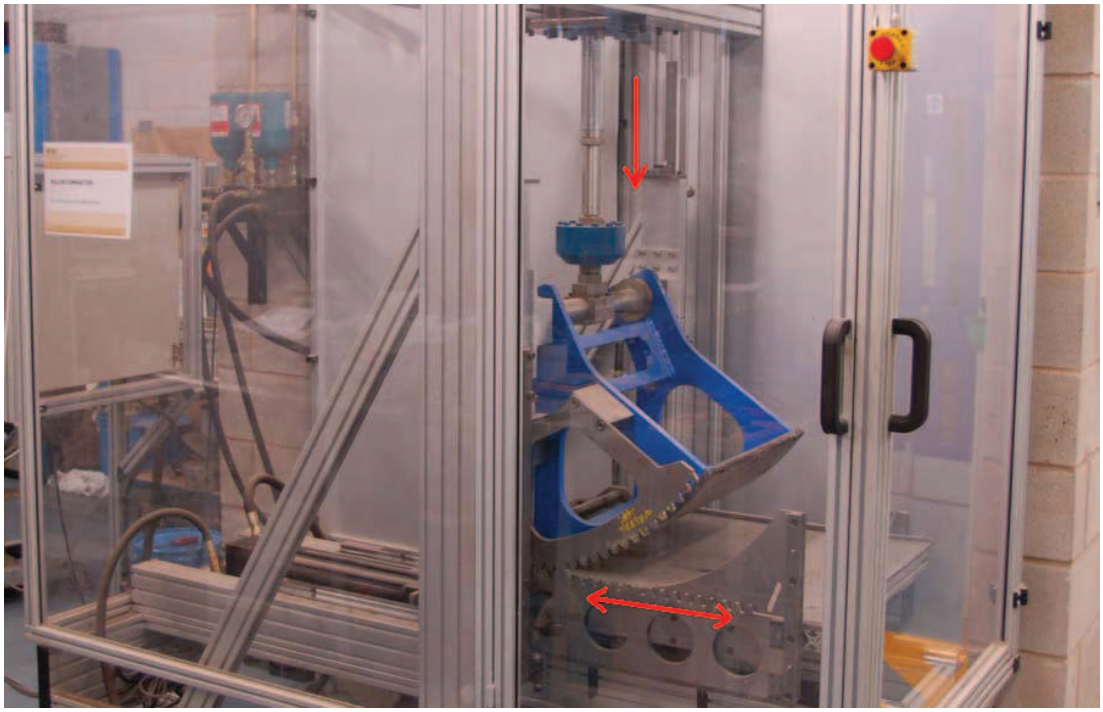

Figure 5.4 – Photograph of the big slab roller compactor

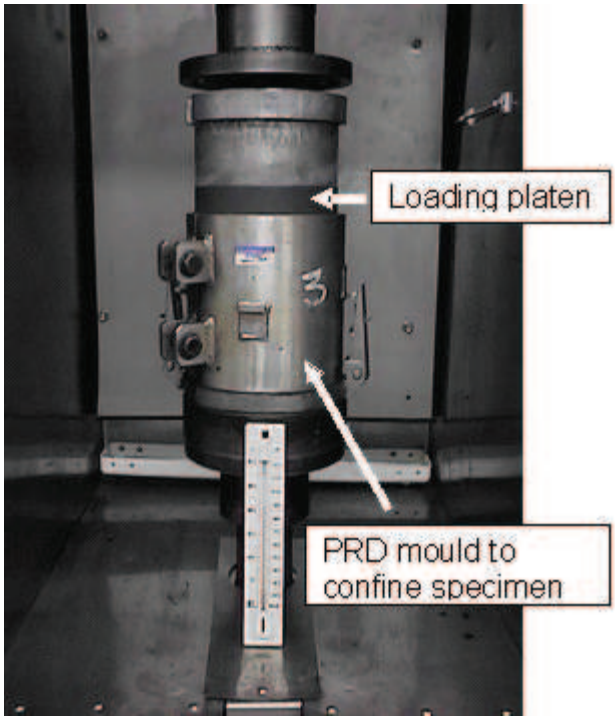

Figure 5.5 – Setup of simulated trafficking using PRD mould

An investigation by Thom [2007] showed that the average maximum pavement temperature measured in the car park area at the University of Nottingham during the summer is approximately 33˚C (Figure 5.6), hence the trafficking temperature of 35˚C used in the trafficking investigation is considered to be reasonable.

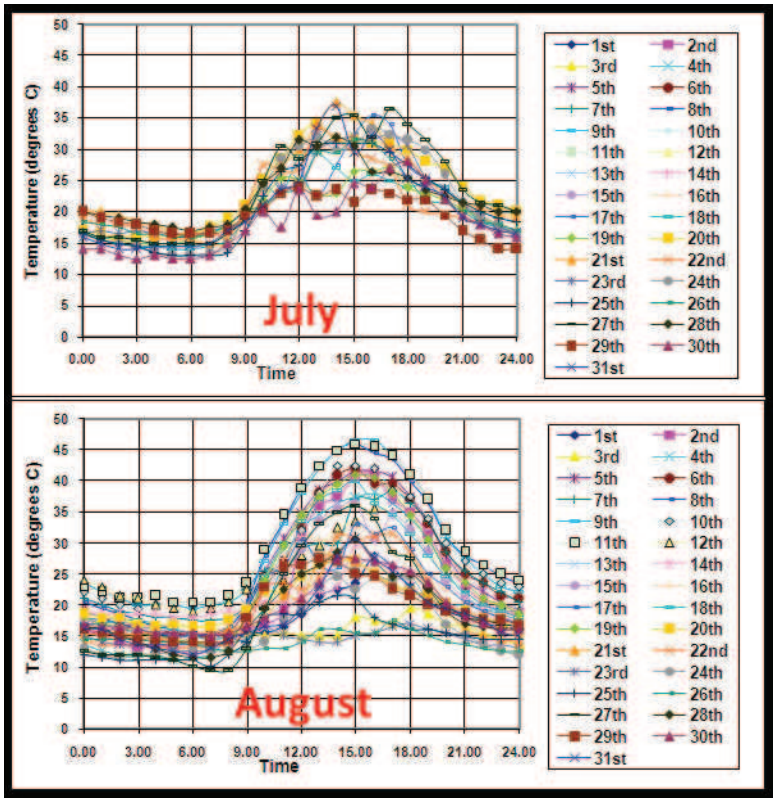

Figure 5.6 – Pavement temperature variations during the summer (From Thom, 2007)

5.3.2 Results of Simulated Trafficking Using PRD Mould

Figure 5.7 shows interface shear strength obtained from the modified Leutner test after the PRD trafficking plotted against the number of trafficking cycles for all material combinations. The error bars represent the 95th percentile confidence limits. It should be noted that some of the TS1/14EME and SMA/14EME specimens were un-bonded immediately after coring (these are noted in the figure). The initial

interface shear strengths range from approximately 0.3MPa for the SMA/14EME combination to approximately 1.4MPa for the TS1/20DBM combination.

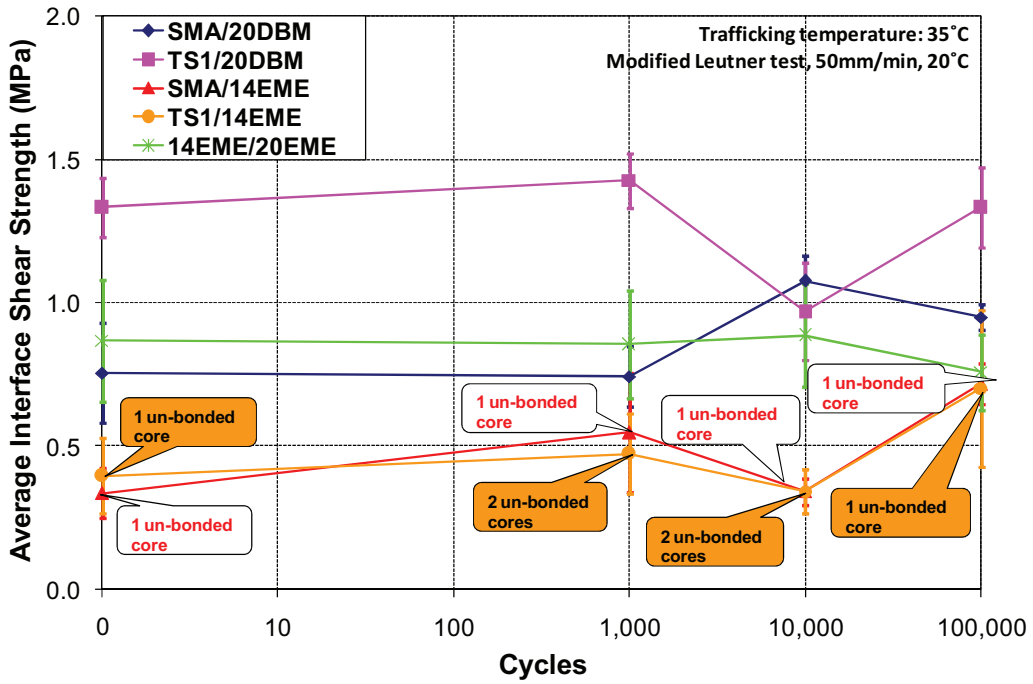

Figure 5.7 – Results of simulated trafficking using PRD mould

Figure 5.7 shows that, in general, three stages could be observed in terms of change in interface shear strength. The first stage is when the bond strength increases up to a certain initial peak point, which may have been caused by densification of the upper layer material and its additional embedment into the layer underneath (Figure 5.8(a)). The second stage is when the bond strength decreases after reaching the initial peak point, which may have been caused by aggregate reorientation (Figure 5.8(b)). The third stage is when the bond strength starts to increase again up to its maximum point, which may be assumed as the condition where the material is reaching the optimum packing condition (Figure 5.8(c)). Between 1,000 and 10,000 cycles, 3 of the 5 material combinations showed a decrease in bond strength with only the SMA/20DBM material combination showing any significant improvement. However, between 10,000 and 100,000 cycles the same three combinations that previously showed a decrease in bond strength, now show significant increases whereas the combination that previously showed an

increase in bond strength now shows a slight decrease in bond strength. Overall, the SMA/14EME, TS1/14EME, SMA/20DBM combinations showed increases in bond strength after 100,000 cycles of approximately 130%, 80% and 30% respectively, with the TS1/20DBM and 14EME/20EME combinations showing no improvement.

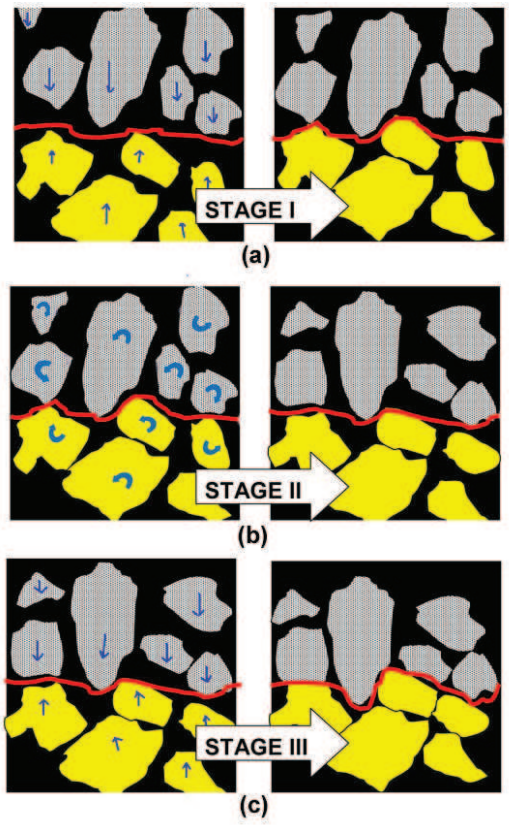

Figure 5.8 – Idealised Scenario of three stages that may occur during PRD simulated trafficking

As mentioned above, the interface bond strength of the TS1/20DBM combination in Figure 5.7 does not show any improvement after 100,000 cycles. Because the TS1 surfacing is quite thin (15mm) and the initial bond strength of the TS1/20DBM combination is relatively high (approximately 1.4MPa), the optimum density of the TS1 surfacing and the optimum embedment of the TS1 surfacing into the 20DBM binder course may have been achieved immediately after compaction in the slab roller compactor and additional compaction by the PRD trafficking seems

not capable of generating further densification in the TS1 surfacing and additional embedment of the TS1 surfacing into the 20DBM binder course. The case of the 14EME/20EME combination that also does not show any improvement after 100,000 cycles appears to be caused by the low bitumen penetration grade, continuous aggregate gradation and relatively low air void content used in the 14EME and 20EME materials that may affect the capability of the PRD trafficking to generate densification in the 14EME material and additional embedment of the 14EME material into the 20EME material.

It has been noted previously that a small number of samples for the TS1/14EME and SMA/14EME combinations were initially un-bonded immediately after coring and could not be subjected to Leutner testing. An additional investigation was carried out using these specimens by reassembling them in their original compaction orientations and performing simulated trafficking, to compare the results with the initially bonded specimens. The results are shown in Figure 5.9 where it can be seen that all of the initially un-bonded specimens developed a bond after trafficking for 1,000, 10,000 and 100,000 cycles, although the bond strengths were less than 0.4MPa and typically lower that the initially bonded specimens.

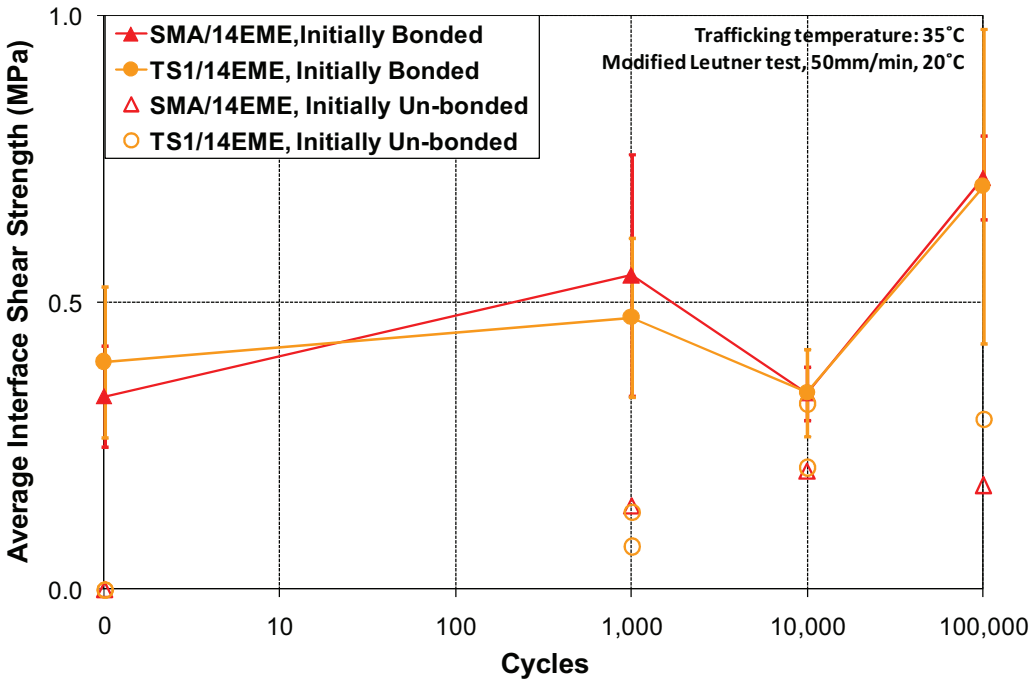

Figure 5.9 – Effect of simulated trafficking on un-bonded specimens

It is interesting to note in Figure 5.7 that the initial shear strengths of the combinations incorporating the 20DBM binder course (TS1/20DBM and SMA/20DBM) are higher than the corresponding combinations incorporating the 14EME binder course (TS1/14EME and SMA/14EME). The shear strengths after trafficking are also significantly different, even though the same surfacing materials have been used and the grading of the 20DBM binder course mixture is similar to the grading of the 14EME binder course mixture. Considering that the grading of the 20DBM mixtures is quite close to the grading of the 14EME mixture, it was thought that the difference in shear strength could have been caused by the different bitumen penetration grade used in the lower layer mixtures. This difference might affect the embedment of the upper layer aggregates into the underlying layer. Therefore, a set of SMA/14EME specimens was produced, using a softer binder (30/45 pen, as used in 20DBM lower layer) in the 14EME lower layer. The results presented in Figure 5.10 show that the shear strengths of the SMA/14EME specimens made using 30/45 pen binder are approximately similar to those of the SMA/20DBM specimens which indicates that the binder grade used in the lower layer is likely to be a reasonably significant factor, although additional testing would be required to confirm this.

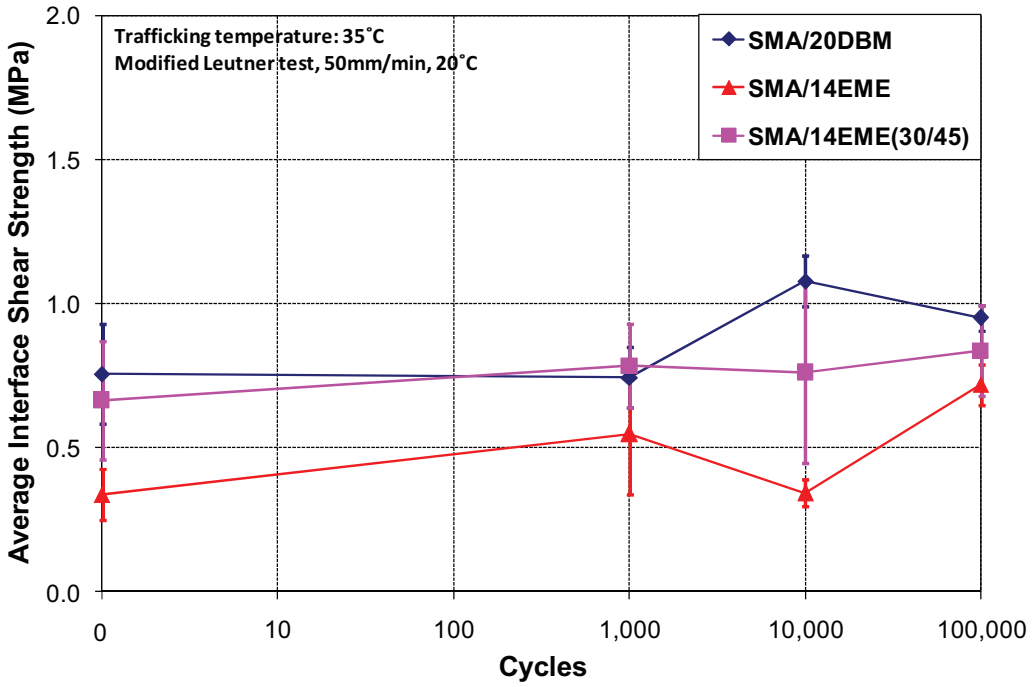

Figure 5.10 – Effect of binder penetration grade on average shear strength

5.4 Simulated Trafficking Using the French Wheel Tracker (FWT)

Although some of the material combinations showed overall increases in bond strength after simulated trafficking in the PRD moulds, the results were not conclusive and the mechanism for simulating the trafficking was un-realistic. For example, the specimens were contained in a PRD mould which will apply significantly more lateral confinement than that experienced in the field, while the loading was applied axially so more complex effects related to rolling wheel loading such as rotation of principal stresses were not included. It was therefore decided to undertake more realistic experiments using the French Wheel Tracker [British Standards Institution, 2003b] to more closely simulate in situ conditions. Although the French Wheel Tracker (FWT) trafficking could be expected to more closely simulate the field condition than the PRD mould trafficking; it is still considerably different to the field condition, for example:

- Rolling wheel loading in the FWT moves back and forth and shoves the material in the longitudinal direction in an un-realistic way compared to the field condition where the rolling wheel loading moves only in the direction of traffic.
- Trafficking in the FWT is more canalised than the randomly distributed field condition.
- Trafficking in the FWT is performed at defined temperature and loading conditions, which are considerably different to the randomly distributed temperature and loading conditions in the field.

The SMA/20DBM, SMA/E14ME and TS1/14EME combinations were used in the FWT trafficking because they had shown improvement in the PRD trafficking. Although the 14EME/20EME combination did not show improvement in the PRD trafficking, it was also used in the FWT trafficking in order to asses whether the trafficking in the FWT that includes rolling wheel movement was able to improve the interface bond strength of the stiff 14EME/20EME combination.

5.4.1 Materials, Specimen Preparation and Trafficking Setup

All materials were designed according to the relevant Standards [British Standards Institution, 2005a and 2006b; Sanders and Nunn, 2005] using the minimum permissible binder contents. Details of the mixtures are the same as those listed in Table 5.2. The same sample preparation procedure as used with the PRD trafficking tests was used with the exception that larger slabs (500mm × 500mm) were produced using a bigger laboratory roller compactor (Figure 5.4), so that the prismatic specimens required for the FWT (see Figure 5.11) could be obtained. Typically two prismatic shape specimens were obtained from one slab.

Two identical prismatic specimens were then placed in the FWT steel moulds which were then fixed to the machine. The trafficking setup for the FWT is shown in Figure 5.12. Sinusoidal loading with a frequency of 2Hz and a peak tyre contact pressure of 720 kPa was then applied to the specimen surface through the pneumatic rubber tyres. The trafficking was performed at elevated temperature (35^{o}C). Two 150mm diameter cores were taken from each of the prismatic specimens after they had been trafficked for 0, 1,000, 10,000 and 100,000 wheel passes for modified Leutner testing. Four cores obtained from the two prismatic specimens were used for each trafficking condition. The modified Leutner tests were performed on the core specimens in such a way that the direction of force application in the modified Leutner tests is parallel to the direction of rolling wheel in the FWT.

Figure 5.11 – Prismatic specimen used in FWT

Figure 5.12 – Trafficking setup for FWT

5.4.2 Results of Simulated Trafficking Using the French Wheel Tracker

Figure 5.13 shows interface shear strength after FWT trafficking plotted against the number of trafficking cycles for all the material combinations. As before, the error bars show the 95th percentile confidence limits. It should be noted that some of the specimens were found to be un-bonded immediately after coring (these are noted in the figure). It can be seem from Figure 5.13 that apart from the 14EME/20EME combination, all of the material combinations show a greater improvement in interface shear strength with trafficking compared to the PRD results (Figure 5.7). For example, the SMA/14EME and SMA/20DBM material combinations show improvements of approximately 380% and 200% after 100,000 passes compared to approximately 80% and 30% respectively from simulated

trafficking undertaken using the PRD moulds. Similar to the PRD result, simulated trafficking using the FWT on 14EME/20EME combination showed no improvement.

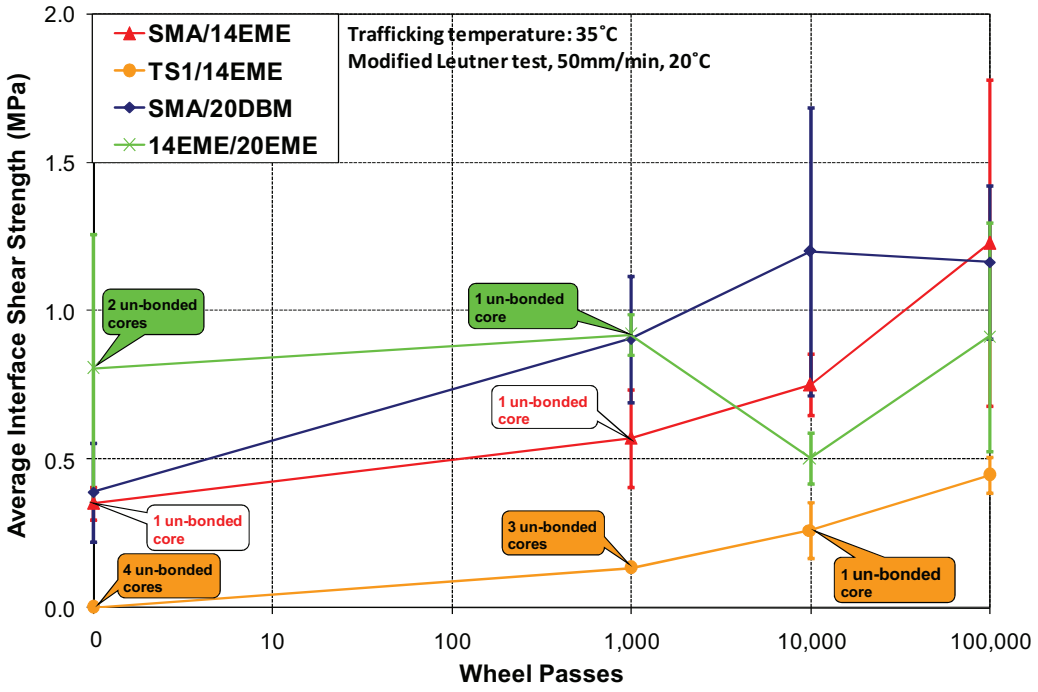

Figure 5.13 – Results of trafficking with FWT

It is interesting to note that apart from the 14EME/20EME binder course/base combination, the second and third stages in terms of change in shear strength that appeared in the PRD trafficking are not clearly observed during the FWT trafficking. This may have been caused by the rolling wheel movement of the FWT in relation to the aggregate reorientation stage.

Figure 5.13 shows that the bond strengths of the TS1/14EME combination are lower than the bond strengths of the same material combination shown in Figure 5.7. This may have been caused by the bigger laboratory roller compactor that was used to prepare the FWT specimens. Because the TS1 surfacing is quite thin (15mm) and the 14EME is considered to be quite stiff, the compaction effort of the bigger laboratory roller compactor may have damaged the aggregates in the TS1 surfacing.

The proportions of cores that were found to be un-bonded immediately after coring seem to increase when the interface shear strength of the corresponding material combinations is below 0.5MPa (Figures 5.7 and 5.13). This may indicate that, when the interface shear strength of the interface is below 0.5MPa, there is a possibility that the core would be un-bonded immediately after coring

5.5 Conclusion

The following key points can be derived from the study:

1. A more realistic poor bond condition was achieved by using interface condition (d), which comprised:
   - using the minimum permissible binder content for both layers,
   - 'scuffing' the bottom layer surface and then chilling at 5^{o}C for 16$\pm$1 hours,
   - treating the lower layer surface with a slurry mixture comprising 16g of limestone filler and 48g of water
2. Results from the PRD mould-based simulated trafficking showed that the bond strengths for the SMA/14EME, TS1/14EME and SMA/20DBM combinations increased after 100,000 cycles by approximately 130%, 80% and 30% respectively whereas the TS1/20DBM and 14EME/20EME combinations showed no improvement. It was also found that initially un-bonded specimens showed some bond development with trafficking and the use of a softer binder in the 14EME asphalt mixture improved the bond strength.
3. Results from the more realistic FWT-based simulated trafficking showed that all of the surfacing/binder course material combinations show a greater improvement in interface shear strength with trafficking compared to the PRD results. For the SMA/14EME and SMA/20DBM material combinations, this improvement in interface shear strength corresponded to increases of approximately 380% and 200% after 100,000 passes.
4. Similar to the PRD result, simulated trafficking using the FWT on 14EME/20EME binder course/base combination showed no improvement.

Chapter 6

DEVELOPMENT OF BOND DATABASE ON MODIFIED LEUTNER TEST

6.1 Introduction

Choi *et al.* [2005] demonstrated the suitability of the modified Leutner test to determine the bond strength at the interface between asphalt layers. During this research study, a further modification to the modified Leutner test has been performed to enable determination of the bond strength beneath thin surface course systems less than 30mm in thickness. The modified test has then been used to measure the bond strength over a range of temperatures and loading rates. Details regarding the modification have been presented and discussed in Chapter 3. Comparisons between the modified Leutner test and the manual as well as automatic torque bond tests have been presented and discussed in Chapter 4. To be accepted as a robust method for determining the bond between asphalt layers, a more comprehensive investigation and the development of a bond database measured using the modified Leutner test for a wide range of UK material combinations (including thin surface course systems) and bond conditions need to be performed.

This chapter presents the development of a bond database for UK materials and constructions measured using the modified Leutner test. Modified Leutner tests on a wide range of UK material combinations and bond conditions have been performed on cores taken from laboratory prepared slabs as well as field coring. Laboratory investigations on the effect of ageing and moisture on bond have also been performed. To cover testing of specimens containing thin surfacings, the tests were performed according to the new modified Leutner testing protocol presented in Appedix A.2.

6.2 Materials and Specimen Preparation

6.2.1 Laboratory Manufactured Specimens

To build up a comprehensive database of bond between the upper two interfaces for a wide range of UK material combinations and bond conditions, four typical surfacing materials (14mm Stone Mastic Asphalt (SMA), two proprietary Thin Surfacings (TS1 and TS2) and 30/14 Hot Rolled Asphalt (HRA)), two binder course materials (20mm Dense Bitumen Macadam (20DBM) and 0/14 Enrobé à Module Élevé (14EME)) and two base materials (28mm DBM (28DBM) and 0/20 EME (20EME)) were used. A gritstone aggregate was used for the SMA, TS1, TS2, HRA and EME and a limestone aggregate was used for the DBM mixtures. All materials were designed according to the relevant Standards [British Standards Institution, 2005a, 2006a and 2006b; Sanders and Nunn, 2005]. Details of the mixtures are given in Table 6.1.

Table 6.1. Mixture characteristics for laboratory manufactured specimens

Mixture type	Binder grade	Binder content (% mass)	Air void content	Max. density (Mg/m3)	Compacted layer thickness (mm)
14mm SMA	40/60pen	6%*	4%	2.501	40
10mm TS1	150pen	4.9%	4%	2.554	15/35
14mm TS2	70/100pen	5.5%	4%	2.420	20
30/14 HRA	50pen	7.2%	5%	2.368	40
20mm DBM	30/45pen	4.7%	5.5%	2.490	60/40
0/14 EME	15pen	5.4%	5%	2.522	60
28mm DBM	30/45pen	4%	6%	2.498	60
0/20 EME	15pen	5.2%	5%	2.530	80

* Includes 0.3% cellulose fibres (of mixture weight)

Slabs of plan dimensions 305mm by 305mm, each comprising of two layers, were manufactured in a slab 'roller' compactor (Figure 3.2) in accordance with BS

EN 12697-33 [British Standards Institution, 2003d] to simulate site compaction conditions as closely as possible. The material for the lower layer, once mixed, was placed in the mould and compacted to the desired thickness. The layer was allowed to cool to room temperature and the surface was then treated to give one of the following interface conditions:

(a) A 'standard' amount of tack coat, comprising K1-40 emulsion, was spread on the lower layer surface using a clean brush to give an average of 200 g/m^2 residual bitumen. The emulsion was allowed to break before laying the upper layer (TC).
(b) A polymer modified bond coat was spread on the lower layer surface to give an average of 300 g/m^2 residual bitumen. Except when the TS1 surfacing was used, the emulsion was allowed to break before laying the upper layer (BC).
(c) No tack (bond) coat was applied (NE).

After the interface had been prepared, the material for the upper layer was mixed and compacted on top of the lower layer to the desired thickness. From each slab, two 150mm diameter cores were obtained for Leutner testing. The cores were obtained using a wet coring method. Nominally six identical tests were undertaken for each test condition to assess variability. It should be noted that to achieve the targeted layer thickness and air void content of the 14EME over 20EME material combination, a bigger slab size (500mm by 500mm plan dimension) and a bigger laboratory roller compactor (Figure 5.4) were used.

6.2.2 Field Cores

A number of 150mm diameter cores were taken from thirty in-service roads in the UK and the information of the sites is presented in Table 6.2. Note that the traffic for Sites #1 to #4 and #6 shown in Table 6.2 are average values and in many cases construction and traffic details were not available. The binder course and base on most of the sites were believed to be more than 20years old.

Table 6.2. Site details

Site	Road Class	Material			Nominal layer thickness (mm)			Construction/Comments	Traffic	Climate*		
		S	Bin	B	S	Bin	B			MAT (˚C)	W-MDMin (˚C)	S-MDMax (˚C)
#1	Two-lane A-road	10TS	14HRA	20HRA	40	50	60	Surfacing laid in June 2002	4060 veh/day northbound, 3811 veh/day southbound	9-10.5	1	19-22.5
#2	Two-lane A-road	10TS	20DBM	CBM	45	45	50	Surfacing laid in April 2002	4895 veh/day eastbound, 6044 veh/day westbound	9-10.5	1	19-22.5
#3	Two-lane B-road	10TS	14HRA	20HRA	30	30	40	N/A	3355 veh/day northbound, 3111 veh/day southbound	9-10.5	1	19-22.5
#4	B-road	14TS	14DBM	40DBM	50	45	55	Surfacing laid in August 2003	2700 vehicles/day **	9-10.5	1	19-22.5
#5	Two-lane C-road	10TS	20HRA	20HRA	45	50	60	Surfacing laid in September 2003	2204 veh/day eastbound, 1969 veh/day westbound	9-10.5	1	19-22.5
#6	Two-lane C-road	14TS	20HRA	20DBM	30	40	40	Surfacing laid in June 2002	3746 veh/day eastbound, 3373 veh/day westbound	9-10.5	1	19-22.5
#7	A-Road	-	20DBM	28DBM	-	80	120	Surfacing had not been laid when the cores were taken	N/A	9	2.5	19
#8	A-Road	14HRA	20HRA	14HRA	35	70	40	Constructed in 1978	13 million standard axles (msa) in lane 1 between 1983 and 2003.	8.5-9.5	(-0.5)-1.5	16-21
#9	Motorway	14HRA	20HRA	20HRA	50	50	70	N/A	92600 veh/day **	9-11	0.5-3	20-22.5
#10	Motorway	14TS	20DBM	20DBM	50	80	100	N/A	92600 veh/day **	9-11	0.5-3	20-22.5
#11	A-Road	14HRA	20DBM	28DBM	40	60	100	N/A	19800 veh/day **	8-10	0-1.5	22
#12	A-Road	14HRA	20DBM	28DBM	50	60	60	N/A	18100 veh/day **	8-10	0-1.5	22
#13	Two-lane B-road	10TS	20DBM	-	20	60	-	Surfacing laid in August 2005	Medium	9-11	0.5-3	20-22.5
#14	Two-lane D-road	10TS	20DBM	-	40	70	-	Surfacing laid in July 2005	Light to medium residential	9-11	0.5-3	20-22.5
#15	Two-lane B-road	10TS	20DBM	-	25	70	-	Surfacing laid in April 2005	Medium	9-11	0.5-3	20-22.5
#16	Two-lane D-road	14TS	20DBM	-	50	70	-	Surfacing laid in June 2005	Light to medium	9-11	0.5-3	20-22.5
#17	Two-lane D-road	10TS	10HRA	-	50	35	-	Surfacing laid in June 2005	Rural light	9-11	0.5-3	20-22.5
#18	Two-lane D-road	6TS	20DBM	-	30	100	-	Surfacing laid in October 2005	Very light residential	9-11	0.5-3	20-22.5
#19	A-Road	-	EME	Concrete	-	70	70	Surfacing had not been laid when the cores were taken	N/A	9-11	0.5-3	20-22.5
#20	Motorway	-	EME	HMB15	-	50	70	Surfacing had not been laid when the cores were taken, binder course laid in December 2005, base laid in 2000	N/A	9-10	0-2	17-21
#21	Motorway	14HRA	14HRA	28DBM	50	40	60	N/A	70300 veh/day **	9-11	0.5-3	20-22.5
#22	Two-lane A-road	14HRA	10SMA	10SMA	50	25	60	N/A	2700 veh/day **	9-10.5	1	19-22.5
#23	Two-lane A-road	10TS	14HRA	14HRA	30	40	60	Layer 2-3 un-bonded, glassgrid between layer 2&3	2700 veh/day **	9-10.5	1	19-22.5
#24	Two-lane A-road	10TS	20HRA	14SMA	40	45	40	Layer 1-2 un-bonded, glassgrid between layer 1&2	2700 veh/day **	9-10.5	1	19-22.5
#25	Two-lane A-road	10TS	14HRA	14HRA	30	60	45	Layer 2-3 un-bonded, glassgrid between layer 2&3	2700 veh/day **	9-10.5	1	19-22.5
#26	Two-lane C-road	14HRA	10HRA	-	35	55	-	N/A	2700 veh/day **	9-10.5	1	19-22.5
#27	Two-lane A-road	10TS	20HRA	-	50	40	-	N/A	2700 veh/day **	9-10.5	1	19-22.5
#28	Two-lane A-road	10TS	20HRA	-	50	50	-	N/A	2700 veh/day **	9-10.5	1	19-22.5
#29	Motorway	14HRA	28HRA	28HRA	40	60	40	N/A	79000 veh/day **	8-10	0-1.5	22
#30	Motorway	14HRA	28HRA	14HRA	50	60	40	N/A	94900 veh/day **	8-10	0-1.5	22

* According to regional air temperature data from Met Office [2009] for the corresponding site location

** According to regional traffic statistic from Department for Transport [2006] for the corresponding site location and road class

TS : Thin Surfacing
HRA : Hot Rolled Asphalt
DBM : Dense Bituminous Macadam
CBM : Cement Bound Macadam
HMB : High Modulus Base
SMA : Stone Mastic Asphalt
EME : Enrobé à Module Élevé

S : Surfacing
Bin : Binder course
B : Base
MAT : Mean annual temperature
W-MDMin : Mean daily minimum temperature during the winter
S-MDMax : Mean daily maximum temperature during the summer

The sites were selected from various road classes across the UK in order to cover a wider range of material combinations. Following the number of specimens required in the manual torque bond test procedure in the guidelines documents SG3/98/173 and SG3/05/234 [British Board of Agreement, 2000, 2004] that have been widely used in the UK, nominally six cores were obtained from each site. A wet coring method was used to retrieve the cores. In the wet coring method, the drill bit is cooled using water; therefore the coring had to be undertaken carefully and the use of an excessive amount of water had to be avoided in order to prevent the penetration of water into the interface. The cores were taken inside the left wheel path at the straight run of the roads at an equal spacing of 100m. The location inside the wheel path was chosen in order to allow future investigation regarding the effect of traffic and age on bond. In order to minimise disruption to the traffic, no core inside the right wheel path was taken. The site coring was performed at ambient temperature according to the Design Manual for Roads and Bridges (DMRB) HD29/99 [The Highways Agency, 1999].

6.3 Modified Leutner Test Results

6.3.1 Modified Leutner Test on Laboratory Manufactured Specimens

The modified Leutner test was performed at a standard displacement rate of 50mm/min and a standard testing temperature of 20°C. Six individual tests were performed for each combination to assess variability. The test results have been evaluated for outlying tests using boxplot analysis to scrutinise the outliers. Boxplot analyses of the test results are presented in Appendix B. Table 6.3 shows a summary of test results together with the Coefficients of Variation (COVs) for all the material and interface combinations tested. It can be seen from this table that the shear strengths range between 1.12MPa and 2.68MPa, the displacements determined at the shear strength range from 1.05mm to 2.40mm and the shear reaction modulus ranges from 0.48MPa/mm to 1.90MPa/mm.

Table 6.3. Summary of test results from the laboratory manufactured specimens

Material Combination	Bond Condition	Interface Shear Strength		Interface Displacement*		Interface Shear Reaction Modulus**	
		Average (MPa)	COV (%)	Average (mm)	COV (%)	Average (MPa/mm)	COV (%)
SMA/20DBM	TC	1.63	10.0	2.40	7.8	0.68	6.6
	BC	1.93	7.9	2.30	10.8	0.84	8.0
	NE	2.35	10.9	2.10	6.8	1.12	8.1
SMA/14EME	TC	1.86	11.0	1.96	9.3	0.95	11.4
	BC	1.20	16.0	1.84	4.2	0.65	16.1
	NE	1.52	18.8	1.75	8.0	0.87	13.5
TS1/20DBM	TC	1.43	10.8	1.96	12.0	0.74	20.7
	BC	1.50	10.7	1.77	10.1	0.86	20.1
	NE	1.64	8.4	2.18	14.1	0.76	11.9
TS1/14EME	TC	1.86	13.6	1.89	17.1	1.01	20.0
	BC	2.09	11.9	1.82	13.4	1.17	19.0
	NE	1.16	23.7	1.45	13.2	0.80	15.9
TS2/20DBM	TC	1.37	20.2	2.17	28.9	0.68	31.5
	BC	1.48	4.7	1.91	4.6	0.78	7.3
	NE	1.57	12.3	1.77	10.3	0.89	10.8
TS2/14EME	TC	1.56	13.4	1.53	8.4	1.03	19.5
	BC	1.27	27.7	1.53	7.5	0.83	27.5
	NE	1.21	9.8	1.24	10.8	0.98	16.8
HRA/20DBM	TC	1.12	14.3	2.36	6.4	0.48	15.5
	BC	1.50	11.6	2.04	7.4	0.74	14.1
HRA/14EME	TC	1.37	18.9	1.61	13.5	0.87	22.5
	BC	1.22	12.3	1.57	8.5	0.78	12.8
	NE	1.54	12.1	1.55	7.9	1.00	13.1
14EME/20EME	TC	1.75	21.0	1.31	12.4	1.33	11.3
	BC	2.32	25.6	1.48	16.1	1.56	17.7
	NE	2.68	13.4	1.42	8.4	1.90	13.9
20DBM/28DBM	TC	1.65	12.6	1.05	12.0	1.58	5.2

* Determined at the shear strength.

** Shear strength divided by displacement at the shear strength.

Figure 6.1 shows the interface shear strengths for all the material and bond combinations together with the 95th percentile confidence limits. Table 6.3 and Figure 6.1 show that all the surfacing/binder course combinations containing the 20DBM binder course show the highest shear strengths when no emulsion is applied at the interface and the lowest shear strengths when tack coat is applied at the interface. An after-testing observation on surfacing/binder course specimens containing the 20DBM binder course revealed that there is a significant embedment of the surfacing material into the binder course material, which could be expected to provide a significant aggregate interlock at the interface. Additionally, although no emulsion was applied at the interface, a thin film of bitumen actually appeared at the interface because the lower layer is newly made and the bitumen which uniformly covers the aggregates at the surface of the lower layer is not stripped. Due to the fact that a thin film of bitumen already appeared at the interface, the application of bond or tack coat at the interface may have caused an excessive amount of bitumen at the interface so that the aggregate interlock became less significant and the interface became more deformable. The more deformable interface condition could be noticed from the typical reduction of the shear reaction modulus when the tack or bond coat is applied. The SMA/20DBM combination shows the highest interface shear strength among all the surfacing/binder course combinations containing the 20DBM binder course. This is thought to be due to the high stone content of the SMA surfacing, which may have created a more significant embedment of the surfacing material into the binder course material.

Two of the four surfacing/binder course combinations containing the 14EME binder course (SMA/14EME, TS2/14EME) showed the highest shear strength with tack coat at the interface whereas the other two combinations showed the highest shear strength with either nothing at the interface (HRA/14EME) or bond coat at the interface (TS1/14EME). An after-testing observation on surfacing/binder course specimens containing the 14EME binder course revealed that the embedment of the surfacing material into the binder course material is not significant. Therefore, it could be assumed that the interlocking of aggregates at the interface of the surfacing/binder course combinations containing the 14EME is not significant and the bond strength would depend on the thickness and the cohesion properties of the bitumen at the interface. Probably, the optimum thickness and cohesion of the

bitumen at the interface of the SMA/14EME and TS2/14EME combinations is achieved when 200g/m^2 residual bitumen of tack coat is applied at the interface. Therefore, the application of either 300g/m^2 residual bitumen of bond coat or nothing at the interface of those combinations may have caused either an excessive or insufficient bitumen thickness at the interface. Because the bitumen content of the HRA surfacing mixtures is high, the application of either tack coat or bond coat at the interface of the HRA/14EME combination may have caused an excessive bitumen thickness at the interface.

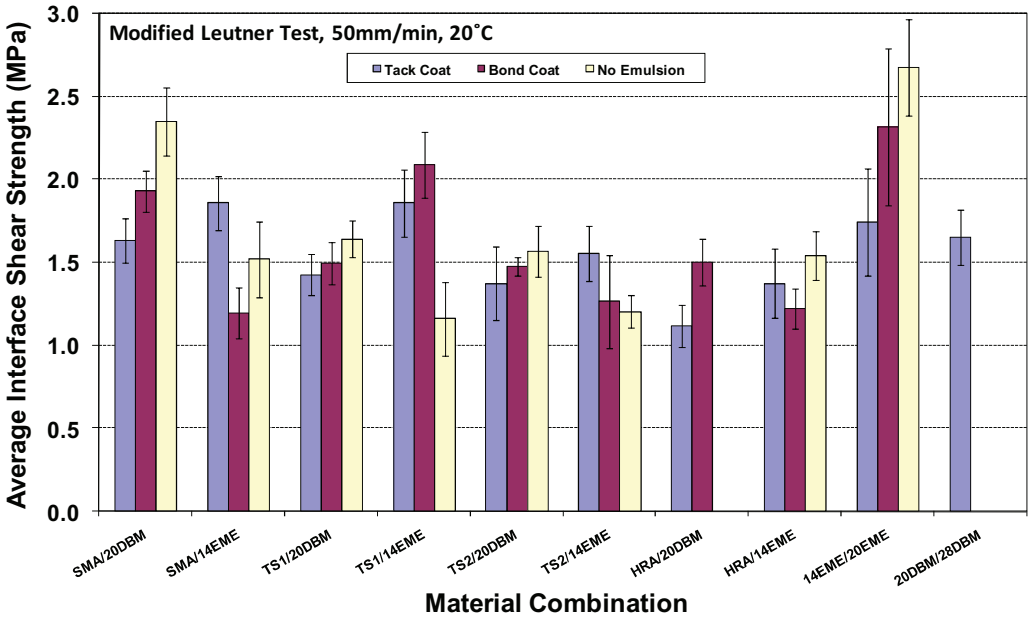

Figure 6.1 – Interface Shear strengths of UK material combinations and bond conditions

It is interesting to note that among all the combinations presented in Figure 6.1 the 14EME/20EME binder course/base combination with nothing at the interface shows the highest interface shear strength. The rough nature of the 20EME base together with the smaller nominal aggregate size of the 14EME binder course compared to that of the 20EME may have created a significant aggregate interlock at the interface of this combination. The effect of the significant aggregate interlock may have also been further amplified by the stiff nature of both the 14EME and 20EME layers due to the low bitumen penetration grade, creating a very stiff and strong interface. The application of either tack coat or bond coat at the interface of

this combination may have caused an excessive amount of bitumen at the interface so that the aggregate interlock became less significant and the interface became more deformable. Similar to the case of the surfacing/binder course combinations containing the 20DBM, the more deformable interface condition of the 14EME/20EME binder course/base combination could be noticed from the typical reduction of the shear reaction modulus when the tack or bond coat is applied (Table 6.3).

6.3.2 Ageing and Moisture Damage on Laboratory Manufactured Specimens

Age hardening (ageing) and moisture damage are known as the factors affecting the durability of a bituminous material. Ageing is commonly associated with hardening of bitumen due to the loss of volatile components as well as oxidation of the bituminous material during construction (short term ageing) and during its service life (long term ageing). Some other factors such as steric hardening of the bitumen and ultraviolet radiation have also been linked to ageing. Ageing is manifested as an increase in bituminous material stiffness, which could be expected to improve its load transfer capability and give better resistance to deformation. However, excessive ageing may cause embrittlement of the bituminous material where it becomes more vulnerable to cracking, reducing its ability to withstand traffic and thermally induced stresses and strains. Moisture can significantly degrade the structural integrity of bituminous material through loss of cohesion of the bituminous material and adhesive failure between the bitumen and aggregate. Those factors will reduce the strength and stiffness of the bituminous material, reducing its capability to support traffic and thermally induced stresses and strains.

Many research projects have been performed by researchers to develop accelerated laboratory ageing and moisture damage procedures on compacted bituminous materials in order to assess their relative durability performance. In the UK, Scholz [1995] developed the LINK (Bitutest) long term oven ageing and water sensitivity test protocols. These protocols are widely used in the UK because they

are included in the guidelines document SG3/05/234 [British Board of Agreement, 2004] as part of the assessment and certification of thin surfacing course systems [Read and Whiteoak, 2003].

The LINK long term oven aging procedure comprises of ageing a compacted specimen in a forced-draft oven at a temperature of 85 ± 1˚C for 120 ± 0.25hours. The oven is switched off at the end of the ageing period and the specimen is left in the oven to cool to room temperature. After the specimen has been cooled to room temperature, it is conditioned in a temperature controlled cabinet at a designated testing temperature prior to a stiffness test. Scholz [1995] showed that the LINK long term ageing procedure is effective to simulate the effect of long term ageing as measured by increase of bituminous material stiffness modulus. The procedure is relatively sensitive to difference of volumetric proportions of bitumen and air void content in the bituminous material and can be used confidently for comparative purposes.

In the LINK water sensitivity test procedure, a compacted specimen is subjected to saturation under a partial vacuum of 510 mmHg (68 kPa) at 20˚C for 30 minutes. After the saturation under a partial vacuum has been performed, the specimen is then subjected to a number of thermal conditioning cycles. Each cycle comprises of immersing the specimen in water at 60°C for 6 hours, 5˚C for 16 hours and finally 20˚C for 2hours. A stiffness test is performed after each cycle has been completed. Scholz [1995] demonstrated that the LINK water sensitivity test procedure is suitable to investigate the effects of volumetric proportions of bitumen and air void content in the bituminous material and could possibly be used to assess the relative durability performance of bitumen and/or mixture types.

Because the accelerated laboratory durability procedures were typically designed to investigate ageing or moisture damage only and considering that, in long term service condition, the pavement is likely to undergo both ageing and moisture damage together; Choi [2005] developed the Saturation Ageing Tensile Stiffness (SATS) test which can investigate the combined ageing and moisture damage effect. The SATS test consists of initial moisture saturation of 100mm diameter cylindrical specimens by a vacuum system, followed by conditioning of the

specimens at a temperature of 85˚C and a pressure of 2.1MPa in the presence of moisture for 65hours.

Most durability testing procedures have been designed to assess the relative durability performance of bitumen, loose bituminous mixtures or compacted bituminous mixtures. Raab and Partl [2004a], using the LPDS apparatus, investigated the effect of moisture on interface bond strengths of specimens taken from a 20 year old pavement structure using two moisture damage testing procedures. The first procedure is by immersing the specimens in a waterbath at 40˚C together with pumping water at a given pressure into the interface for a given amount of time (Figure 6.2). The second procedure is simply by immersing the specimens in the waterbath at 40˚C for 75hours. For the tested specimens, they showed that the reduction of interface shear strength of approximately 27% after immersing the specimens in the waterbath at 40C for 8 hours and applying a pressure of 0.5bar (0.05MPa) is approximately similar to that after immersing the specimens in the waterbath at 40˚C for 75hours. Therefore, they recommended using immersion at 40˚C for 75hours rather than pressure.

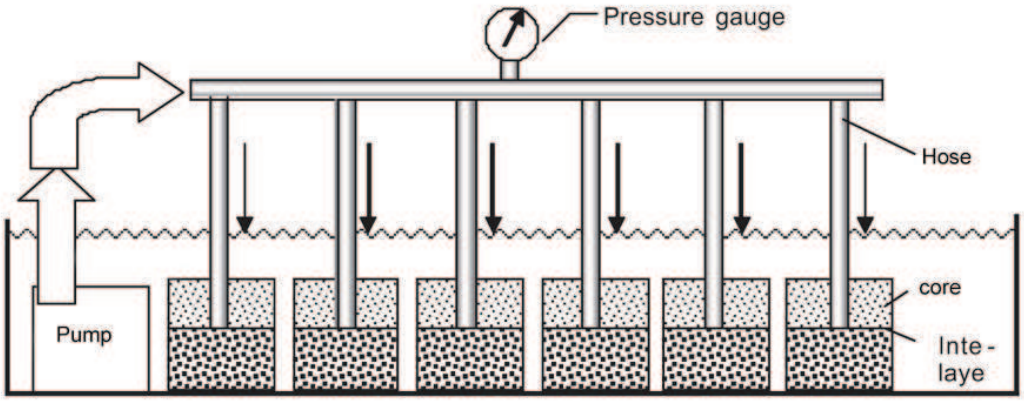

Figure 6.2 – Moisture damage procedure performed by Raab and Partl [2004a]

A series of modified Leutner tests on a number of surfacing/binder course combinations were performed to investigate the effect of ageing and moisture damage on bond. The SATS procedure seems to be pre-eminent because it represents the combined effect of ageing and moisture damage. However, the size

of the SATS pressure vessel was designed for 100mm diameter specimens; hence it is not sufficiently large to accommodate the 150mm diameter specimens used in the modified Leutner test. Furthermore, although the interface bond test can also be performed on 100mm diameter specimens using the automatic torque bond test, it requires gluing metal platens on top and bottom of the specimens. Gluing the metal platens after the SATS testing would not be possible because of the wet specimen surface, whilst gluing the metal platens prior to the SATS testing would significantly affect the results because it would hinder the penetration of moisture into the interface. Therefore, the LINK long term oven ageing and water sensitivity test protocols were used because they have been found suitable for bituminous mixtures in the UK. The LINK water sensitivity test protocol requires less complicated experimental setup than the procedure that includes pressure performed by Raab and Partl [2004a]. Furthermore, because the LINK water sensitivity test protocol includes thermal conditioning at an elevated (60˚C) and low (5˚C) temperatures, it appears to be more suitable to represent the warm and cold climatic conditions than the waterbath immersion at an elevated temperature.

6.3.2.1 Effect of Ageing

The investigation into the effect of ageing on interface bond properties was carried out by performing the LINK long term oven ageing protocol on a number of 150mm diameter specimens prior to the modified Leutner testing. Nominally six cores were tested for each material combination and test condition. The results shown in Figure 6.3 demonstrate that the ageing process increases the interface shear strength by 16 to 41%. It can also be seen that the shear reaction modulus generally increases for the aged specimens. Those expected typical increase in interfaces shear strength and shear reaction modulus could have been caused by the bitumen hardening as a result of the ageing process. It is interesting to note that the increase of interface shear strength and interface shear reaction modulus after ageing for the combinations containing thin surfacings (TS1 and TS2) are generally higher than those for the corresponding combinations containing HRA or SMA surfacing. The thinner surfacing may have caused a more severe age hardening of the bitumen at the interface.

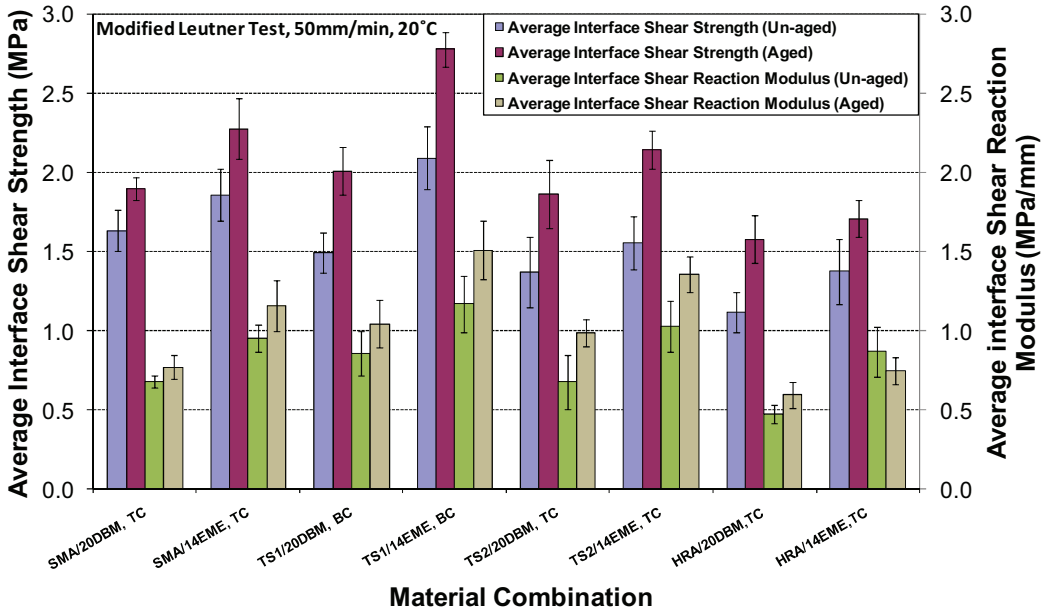

Figure 6.3 – Effect of ageing

6.3.2.2 Effect of Moisture Damage

Choi [2005] showed that the stiffness of a 28mm DBM specimen with 15pen bitumen decreased by approximately 15% after it had been moisture conditioned using the LINK protocol for 4 cycles. The researcher also demonstrated a slight increase of the stiffness at 1 cycle. The increase of stiffness at early conditioning was also observed by Scholz [1995] and was attributed to partial age hardening caused by the elevated temperature of 60˚C used in the moisture conditioning process. To investigate the effect of conditioning cycles, a set of SMA/20DBM-TC specimens were produced and moisture conditioned using the LINK protocol for 0, 1, 5, and 15 cycles prior to modified Leutner tests. Nominally six cores were tested for each test condition. The result is presented in Figure 6.4 together with the 95th percentile confidence limits. Figure 6.4 demonstrates that the interface shear strength increases after 1 cycle and then decreases after 5 and 15 cycles to a value that is approximately equal to the initial interface shear strength. A similar trend is shown by the interface shear reaction modulus where it increases by approximately 36% after 1 cycle and then decreases after 5 and 15 cycles to values that are approximately 14% and 20% lower than the initial interface shear reaction modulus

respectively. The initial increases of interface shear strength and interface shear reaction modulus at 1 cycle are similar to the initial increases of stiffness found by Scholz [1995] and Choi [2005] mentioned earlier and are likely to be because of partial age hardening in the specimens.

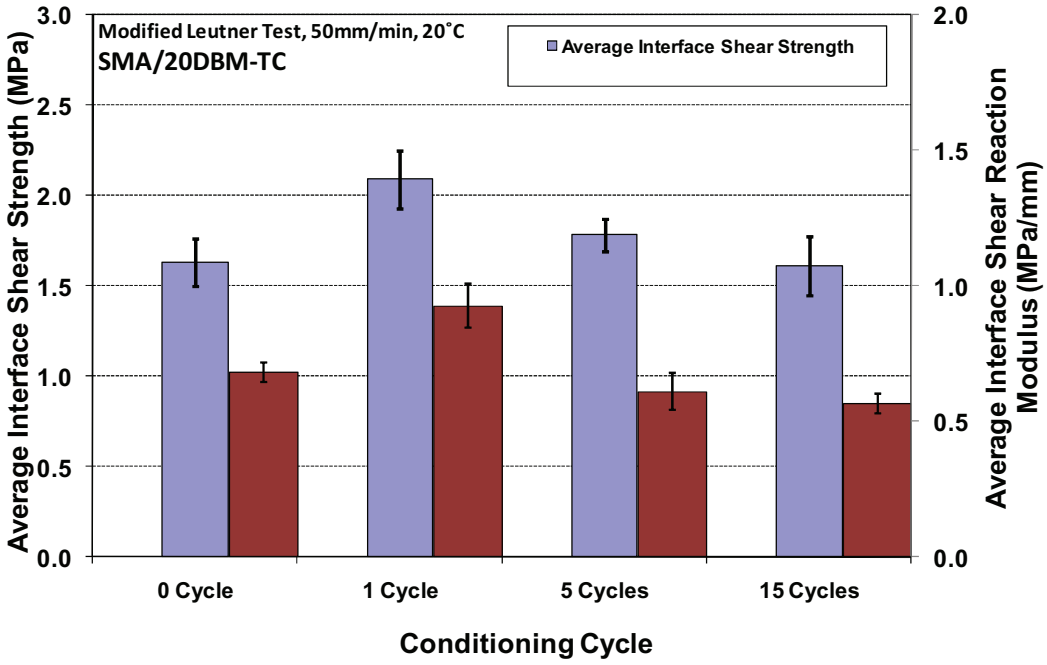

Figure 6.4 – Effect of conditioning cycle

The result in Figure 6.4 also demonstrates that the degradation of the interface shear reaction modulus appears to be more rapid than that of the interface shear strength. Considering that 5 conditioning cycles has reduced the interface shear reaction modulus of the SMA/20DBM-TC specimens by approximately 14%, performing the LINK water sensitivity test protocol for 5 cycles is thought to be sufficient to assess the relative effect of moisture damage on interface shear reaction modulus of different material combinations.

Performing the modified Leutner test on a specimen containing thin surfacing requires gluing a grooved aluminium platen on top of the thin surfacing layer. Gluing the aluminium platen after moisture conditioning procedure would not be possible because the specimen surface is wet. On the other hand, gluing the platen prior to

moisture conditioning procedure would hinder the penetration of moisture into the interface. To investigate the effect of the glued aluminium platen, a set of TS1/20DBM-BC with a 15mm thick surfacing material (TS1) and a grooved aluminium platen as well as a set of TS1/20DBM-BC with a 35mm thick TS1 and no aluminium platen were produced and moisture conditioned for 5 cycles. The result is shown in Figure 6.5 together with the 95th percentile confidence limits. Figure 6.5 shows that, after 5 cycles, the interface shear reaction modulus for the specimens with aluminium platens increases by approximately 24% whereas that for the specimens without aluminium platens decreases by approximately 50%. The increase of interface shear reaction modulus for the specimens with aluminium platens may have been caused by the partial age hardening which typically occurs at the early conditioning cycle. The significantly greater reduction of interface shear reaction modulus for the specimens without aluminium platens compared to those with aluminium platens could be used to indicate that the aluminium platen may have significantly hindered the subsequent water penetration, slowing down the degradation of the interface shear reaction modulus. Therefore, moisture conditioning the thin surfacing specimens with a glued aluminium platen is not recommended.

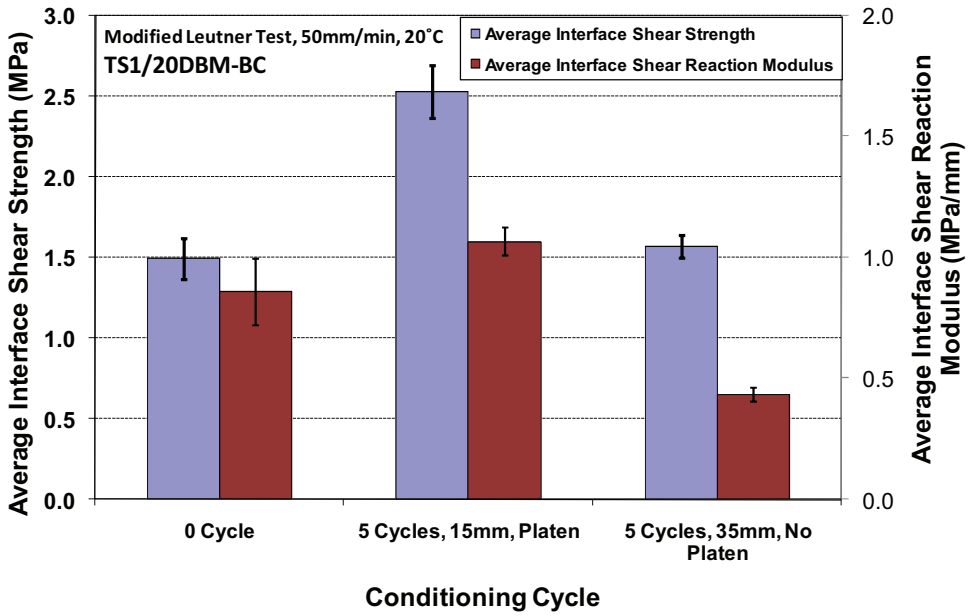

Figure 6.5 – Effect of glued aluminium platen

To investigate the effect of moisture damage on different material combinations, a set of SMA/20DBM-TC, SMA/14EME-TC, HRA/20DBM-TC and HRA/14EME-TC specimens were produced and moisture conditioned using the LINK protocol for 0 and 5 cycles prior to modified Leutner tests. Nominally six cores were tested for each test condition. The result is presented in Figure 6.6 together with the 95th percentile confidence limits. Figure 6.6 shows that apart from the HRA/20DBM-TC combination, the moisture conditioning reduces the interface shear reaction modulus by 14 to 18%. The interface reaction modulus for the HRA/20DBM-TC combination appears to be less sensitive to moisture damage than that for the other combinations. This may have been caused by the high bitumen content of the HRA surfacing mixture and the relatively high bitumen penetration grade of the 20DBM binder course mixture compared to that of the 14EME binder course mixture.

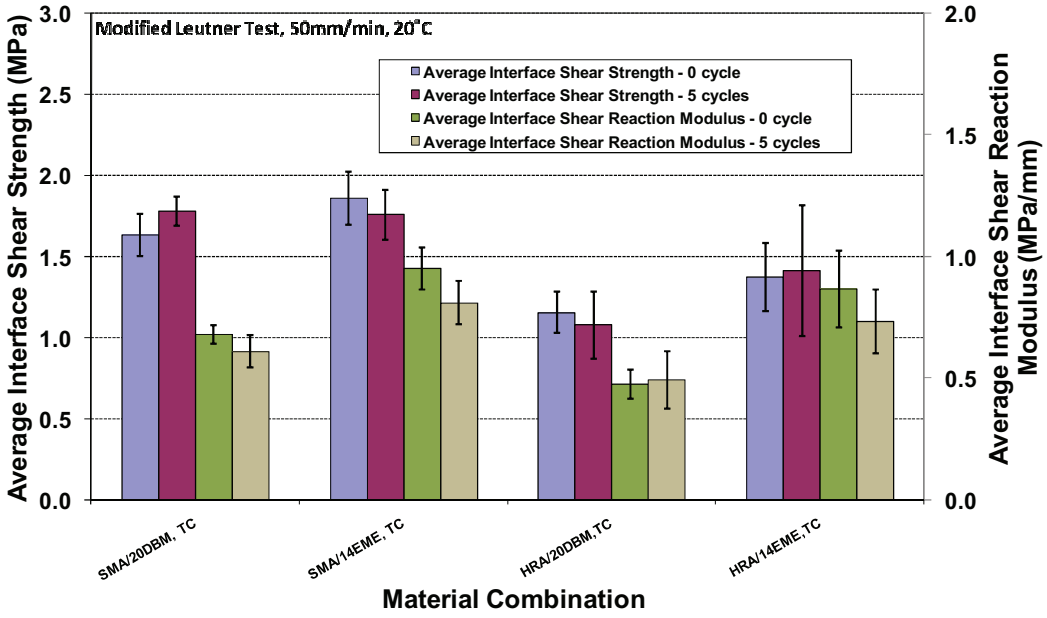

Figure 6.6 – Effect of moisture damage

It is also interesting to note that, in Figure 6.6, the combinations containing the 14EME binder course seem to be more sensitive to moisture damage than the combinations containing the 20DBM binder course. This may have been caused by the higher bitumen penetration grade of the 20DBM binder course mixture

compared to the bitumen penetration grade of the 14EME binder course mixture. From the result in Figure 6.6, it appears that the reduction of interface shear reaction modulus after it has been moisture conditioned using the LINK protocol for 5 cycles could be used confidently to assess the relative effect of moisture damage on interface shear reaction modulus of different material combinations.

It can also be seen in Figure 6.6 that the interface shear strengths of some combinations increase, whilst those of other combinations decrease. As mentioned earlier, the increase of interface shear strength may have been caused by partial age hardening at early conditioning . Because Figure 6.6 shows that an increase of interface shear strength for some combinations still occurs after 5 conditioning cycles and Figure 6.4 shows that the interface shear strength of the SMA/20DBM does not show any significant reduction from the initial condition even after 15 conditioning cycles, it seems that the LINK protocol is not suitable for assessing the relative effect of moisture damage on interface shear strength of different material combinations.

6.3.3 Modified Leutner Test on Field Specimens

Table 6.4 shows a summary of test results from five different classes of road (Motorway, A-road, B-road, C-road and D-road). The average values of shear strength, displacement at shear strength and shear reaction modulus for each class of road for the surfacing/binder course interface (S/Bin) and the binder course/base interfaces (Bin/B), together with their Coefficients of Variation (COVs) are presented. It can be seen from Table 6.4 that the average shear strengths range from 0.9MPa to 1.67MPa, the average displacements determined at the shear strength range from 1.87mm to 3.18mm and the average shear reaction modulus ranges from 0.56MPa/mm to 0.82MPa/mm.

It should be noted that there is a considerable amount of scatter in the data as shown by the Coefficients of Variation (COVs) in Table 6.4. The COVs range from 20.4 to 44.3% for the average shear strength, from 22.3 to 47.1% for the average displacement at shear strength and from 30.5 to 57.5% for the average shear

reaction modulus. The COVs also tend to be slightly higher for the lower class roads and lower interface positions. A considerable amount of scatter was also found by Partl and Raab [1999] during their field investigation on Swiss roads, where the COVs range from 3 to 50% for the shear strength and 9.5 to 47% for the shear reaction modulus. The COVs would be lower if the data is classified by the mixture type. However, because there are so many variants of mixture available in the UK (especially for the proprietary thin sufacings), the data was classified by the road classes.

Table 6.4. Summary of test results from field specimens

Road Class		Average Shear Strength		Average Displacement*		Average Shear Reaction Modulus**	
		Average (MPa)	COV (%)	Average (mm)	COV (%)	Average (MPa/mm)	COV (%)
Motorway	S/Bin	1.67	20.4	3.18	22.3	0.67	35.8
	Bin/B	1.65	29.7	2.68	36.1	0.82	50.5
A-Road	S/Bin	1.40	37.5	3.04	42.5	0.66	57.5
	Bin/B	1.15	40.4	1.87	33.0	0.76	36.3
B-Road	S/Bin	1.32	32.4	3.15	30.4	0.59	42.8
	Bin/B	0.98	44.3	2.45	42.8	0.62	30.5
C and D-Roads	S/Bin	1.16	31.4	2.63	41.7	0.59	43.3
	Bin/B	0.90	35.9	2.27	47.1	0.56	44.0

* Determined at the shear strength.

** Shear strength divided by displacement at the shear strength.

Table 6.4 shows that as the class of the road increases, the average shear strength and the average shear reaction modulus increase. It can be seen from the data in this table that the average shear strength tends to be greater for the surfacing/binder course interface (S/Bin) compared to the binder course/base interface (Bin/B). It seems that the higher traffic induced stresses at the shallower interface may have

caused greater additional embedment of aggregate into the layer underneath, causing the higher shear strength at the shallower interface. It is interesting to observe from the data in Table 6.4 table that the average shear reaction modulus tends to be smaller for the surfacing/binder course interface (S/Bin) compared to the binder course/base interface (Bin/B). Because the binder course and base on most of the sites were believed to be more than 20years old and most of the surfacing was relatively new, the binder course/base interface (Bin/B) may have been more severely aged than the surfacing/binder course interface (S/Bin).

It is interesting to note from the site information in Table 6.2 that the interfaces containing glassgrid reinforcements from sites #23, #24 and #25 were found to be un-bonded immediately after coring. This supports the finding of Raab and Partl [2004a], who reported that the bond strengths at the interface containing stress absorbing membrane interlayer (SAMI) were significantly low.

Figure 6.7 shows the results of the modified Leutner tests on cores from the Motorways. The different sites and the position of the interface are identified in the key. The shear strength in the majority of cases seems to be in the range 1.2 to 2.2MPa.

Figure 6.8 shows the results of the modified Leutner tests on cores from the A-roads. It can be seen that, for most combinations, the shear strengths of the interfaces between surfacing and binder course are between 1.0 and 2.4MPa which are typically higher than the shear strengths of the interfaces between binder course and base, which are between 0.5 and 1.5MPa. However, the majority of surfacing/binder course interfaces from Sites #27 and #28 shows below 1MPa shear strength. After testing, observation of the interfaces revealed that a thin layer of surface dressing appeared between the 10TS surfacing and the HRA binder course. It seems that the surface dressing layer was not removed when the new 10TS surfacing was applied.

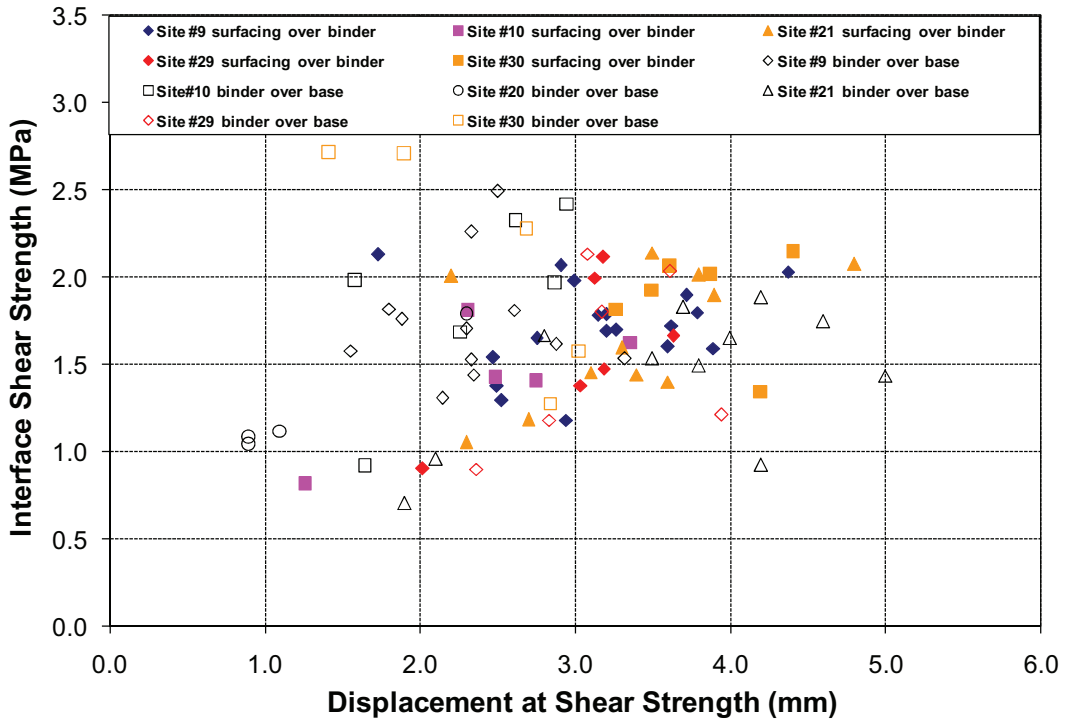

Figure 6.7 – Modified Leutner test results from Motorway cores

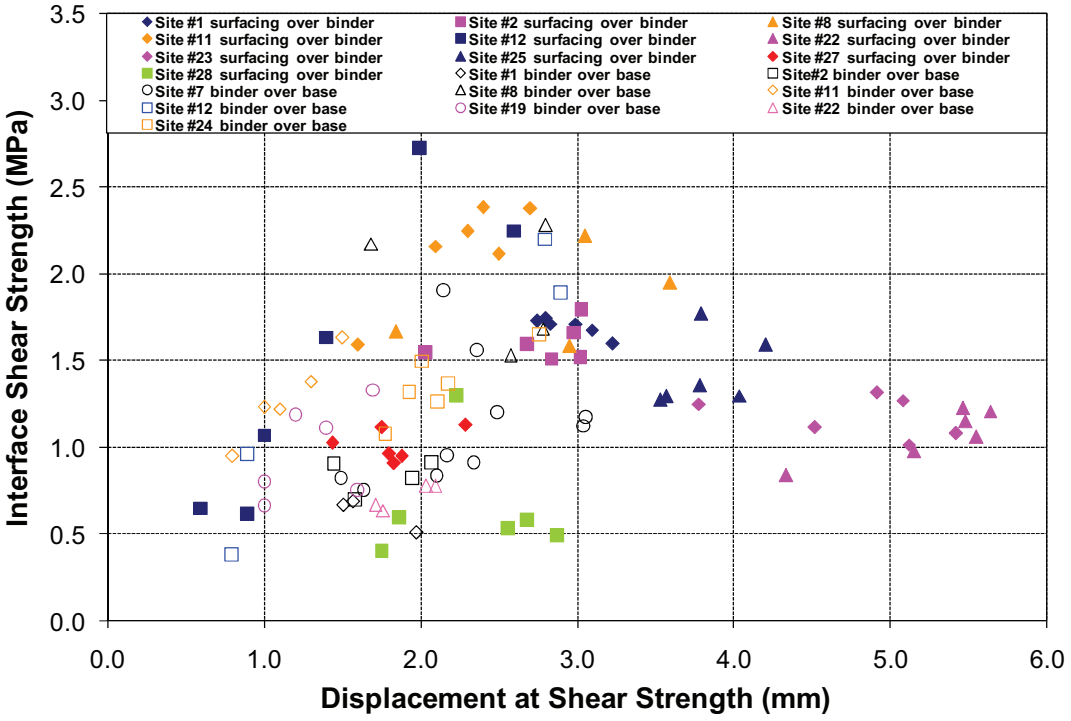

Figure 6.8 – Modified Leutner test results from A-road cores

Figure 6.9 shows the results of the modified Leutner tests on cores from the B-roads. The shear strengths of the interfaces on Site #4 are quite low (between 0.5MPa and 1.2MPa). After testing, inspection of the interface revealed that the material appeared quite soft and there appeared to be evidence of kerosene (detected by smell). This may indicate that the low shear strengths are because a cutback bitumen was used either at the interface or in one of the adjacent materials.

Figure 6.10 shows the results of the modified Leutner tests on cores from the C and D-roads. The shear strength of the majority of results seems to be in the range 1.0 to 1.8MPa. However, the majority of surfacing/binder course interfaces from Site #26 show below 1MPa shear strength. After testing, observation of the interfaces revealed that the 14mm HRA surfacing was laid over a 10mm gravel HRA binder course. Because the maximum aggregate size of the surfacing material is smaller than the maximum aggregate size of the binder course material, the interface appeared flat with no signs of aggregate interlock at the interface.

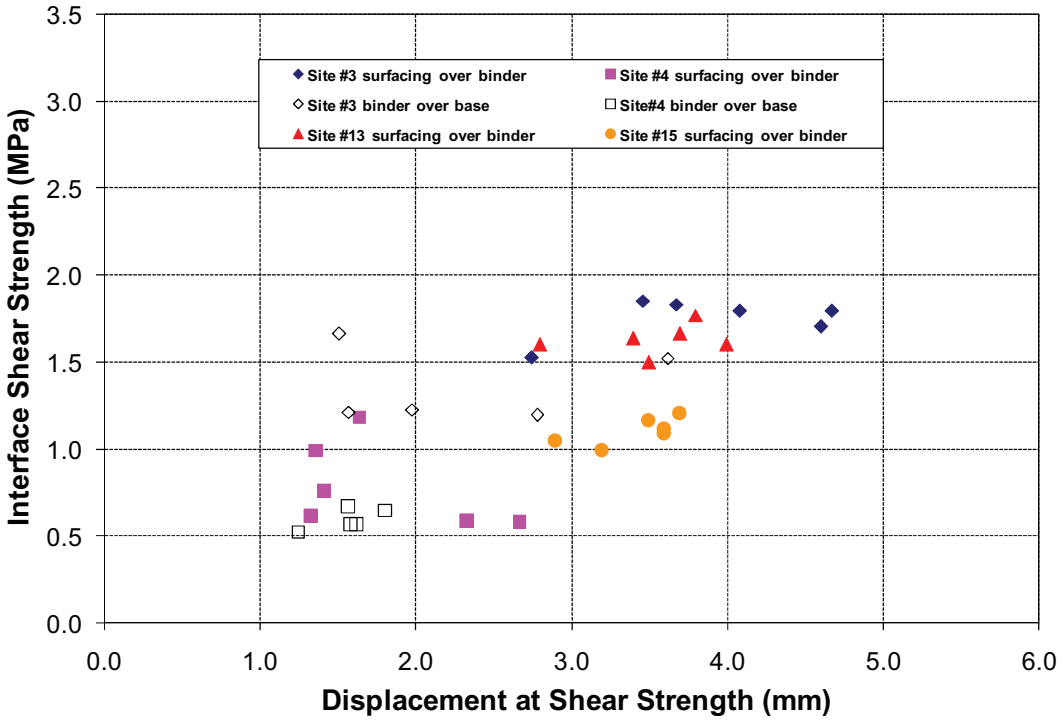

Figure 6.9 – Modified Leutner test results from B-road cores

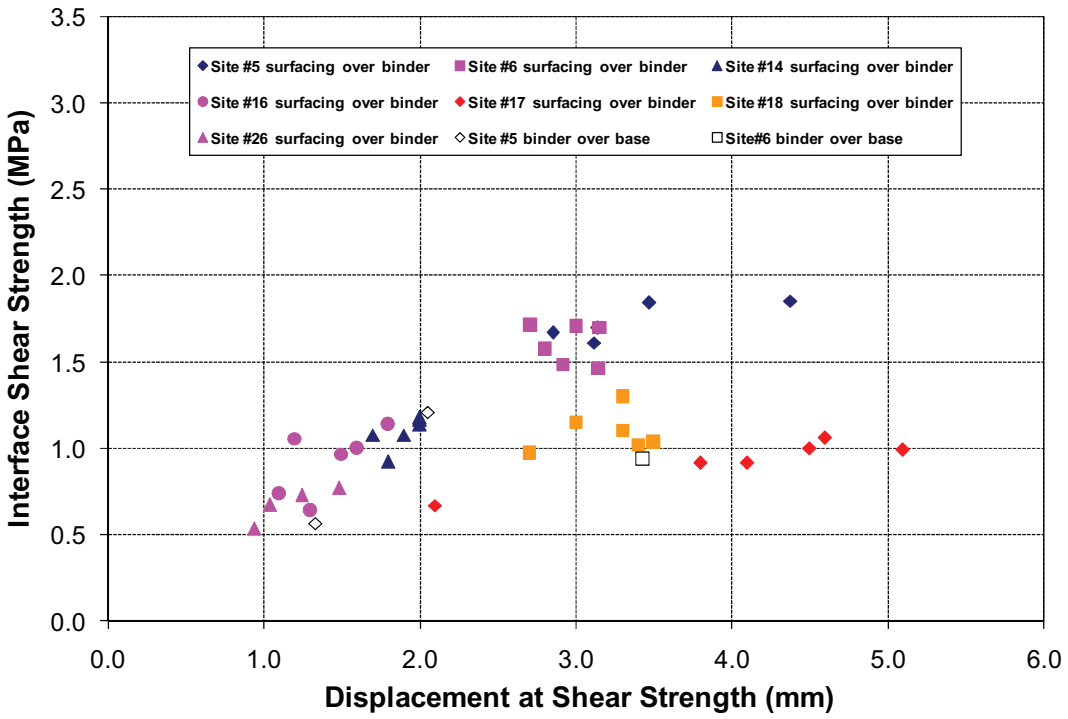

Figure 6.10 – Modified Leutner test results from C and D-road cores

6.4 Conclusion and Recommendation

The following key points can be derived from the study:

- From the modified Leutner testing on laboratory manufactured specimens, it is found that the shear strengths range from 1.12MPa to 2.68MPa, the displacements determined at the shear strength range from 1.05mm to 2.40mm and the shear reaction modulus ranges from 0.48MPa/mm to 1.90MPa/mm.
- Ageing the laboratory manufactured specimens in the oven at 85°C for 120 hours increases the shear strength by 16 to 41%.
- Relative effect of moisture damage on interface shear reaction modulus of different material combinations could be assessed by moisture conditioning specimens using the LINK water sensitivity test protocol for 5 cycles.

- The LINK water sensitivity test protocol appears to be not suitable for assessing relative effect of moisture damage on interface shear strength of different material combinations.
- From the modified Leutner testing on field specimens, it is found that the average shear strengths range from 0.9MPa to 1.67MPa, the average displacements determined at the shear strength range from 1.87mm to 3.18mm and the average shear reaction modulus ranges from 0.56MPa/mm to 0.82MPa/mm.
- Because most of the modified Leutner tests in this research study were performed using 6 specimens and the results have shown a reasonably good variability, it is recommended that 6 specimens should be used to perform the modified Leutner test.

Chapter 7

SPECIFICATION LIMITS

7.1 Introduction

Typical current practice to achieve a good state of bond at the interface is to apply a thin film of bituminous bond (tack) coat at the interface. The British Standard BS 594987 [British Standard Institution, 2007] recommends different bond (tack) coat application rates to be applied at the interface. However, these recommendations are typically born out of experience and not based on the mechanical properties of the interface. Furthermore, The Highways Agency [2006] mentioned that particular attention should be paid to specifying and achieving good bond beneath a thin surfacing layer. Therefore, it is necessary to assess the state of bond according to the mechanical properties of the interface, not only relying on the recommendations of tack (coat) application rates. At the moment, no specification limits of bond strength for UK road constructions are available; whilst in Germany and Switzerland, minimum limits for shear bond strength have been proposed as national standards by several researchers [Codjia, 1994; Partl and Raab, 1999; Stöckert, 2001]. In Switzerland, minimum limits of shear bond strength have been included in the Swiss Standard SN 640430B [VSS, 2008].

This chapter is dedicated to recommend specification limits of shear bond strength for UK roads measured using the modified Leutner test. The measured bond strengths obtained from the bond database presented in Chapter 6 were used to estimate the achievable values of shear bond strength for UK roads. The values were then compared to the predicted required shear bond strengths of typical UK road constructions obtained from a simple analysis and other standards in Germany and Switzerland to recommend specification limits of shear bond strength for UK roads.

7.2 Measured Shear Bond Strength for UK Roads

To estimate the achievable values of shear bond strength for UK road construction, the database of shear bond strength obtained from field cores presented in Chapter 6 was summarised and examined. Table 7.1 shows a summary of results from different classes of road (Motorway, A-road, B-road, C-road and D-road) where the values of shear strength are given for the entire set of specimens as well as for each class of road for the surfacing/binder course interface (S/Bin) and the binder course/base interface (Bin/B) together with their statistical parameters. Figure 7.1 and Figure 7.2 show the average shear strengths from individual sites for the surfacing/binder course interface and the binder course/base interface respectively together with the 95th percentile confidence limits.

Table 7.1. Summary of shear bond strength from field cores

Statistic Parameter	Interface Shear Strength									
	All Roads		Surfacing/Binder Course				Binder Course/Base			
	S/Bin	Bin/B	Motorway	A-Road	B-Road	C&D-Roads	Motorway	A-Road	B-Road	C&D-Roads
Average (MPa)	1.41	1.34	1.67	1.40	1.32	1.16	1.65	1.15	0.98	0.90
Standard Deviation (Mpa)	0.47	0.54	0.34	0.52	0.43	0.36	0.49	0.46	0.43	0.32
Coefficient of Variation (%)	33.12	40.40	20.39	37.53	32.37	31.43	29.71	40.41	44.33	35.88
5%-ile (MPa)	0.61	0.57	1.09	0.57	0.59	0.67	0.92	0.64	0.54	0.60
15%-ile (MPa)	0.95	0.75	1.37	0.93	0.86	0.76	1.10	0.69	0.56	0.68
25%-ile (MPa)	1.06	0.91	1.43	1.06	1.03	0.95	1.30	0.78	0.58	0.75
33%-ile (MPa)	1.14	1.01	1.53	1.13	1.10	0.99	1.50	0.83	0.65	0.81
50%-ile (MPa)	1.44	1.26	1.70	1.31	1.35	1.08	1.66	1.09	0.93	0.94

Considering that the shear stress at the shallower interface would be higher than that of at the deeper interface and the average interface shear strength for the surfacing/binder course interface (Figure 7.1) is typically higher than that for the corresponding binder course/base interface (Figure 7.2), different values of specification limit would need to be applied to the surfacing/binder course and binder course/base interfaces.

Although the results presented in Table 7.1 demonstrate that the average interface shear strength increases as the class of road increases, there is a considerably high variability shown by the Coefficient of Variation (COV). Furthermore, the average values of interface shear strength from individual sites in

Figures 7.1 and 7.2 do not show distinct differences between different road classes. Therefore, a single value of specification limit could be applied to all classes of roads.

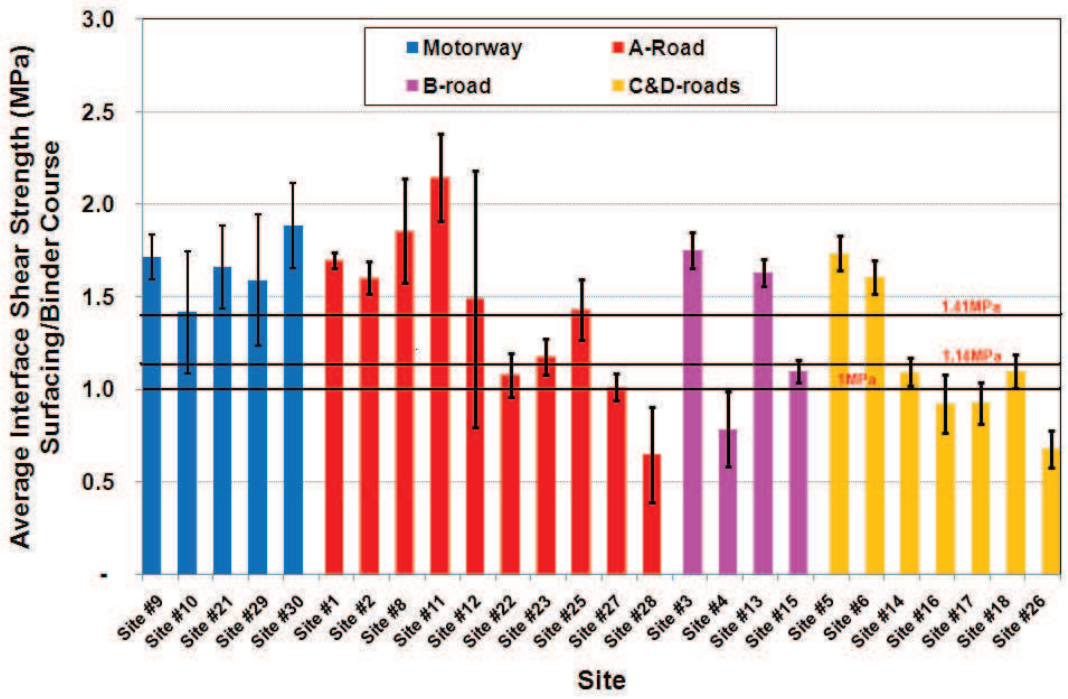

Figure 7.1 – Average shear strength for surfacing/binder course interface

Table 7.1 shows that the average shear strengths for the S/Bin and Bin/B interfaces of the entire set of specimens are 1.41 and 1.34MPa respectively. Applying a minimum limit of 1.41MPa for the S/Bin interface to the average values from individual sites shown in Figures 7.1 would exclude 4 sites from A-road (Sites #22, #23, #27 and #28), 2 sites from B-road (Sites #4 and #13) and 5 sites from C&D roads (Sites #14, #16, #17, #18 and #26). Whereas applying a minimum limit of 1.34MPa for the Bin/B interface to the average values from individual sites shown in Figure 7.2 would exclude 1 site from Motorway (Site #20), 6 sites from A-road (Sites #1, #2, #7, #11, #19 and #22), 1 site from B-road (Site #4) and 1 site from C&D roads (Site #5). Because too many sites would fail to meet the specifications, those values are considered to be too high

The specification limits proposed by Partl and Raab [1999] and Stöckert [2001] excluded approximately 33 – 35 % of the results they obtained. If the 33rd

percentile values of 1.14 and 1.01MPa presented in Table 7.1 are used as the minimum limits and applied to the average values from individual sites shown in Figures 7.1 and 7.2, 10 sites (Sites #4, #14, #15, #16, #17, #18, #22, #26, #27 and #28) would fail to meet the S/Bin specification of 1.14 MPa and 6 sites (Sites #1, #2, #4, #5, #19 and #22) would fail to meet the Bin/B specification of 1.01 MPa. Because many sites would still fail to meet the specifications, lower limits should be considered.

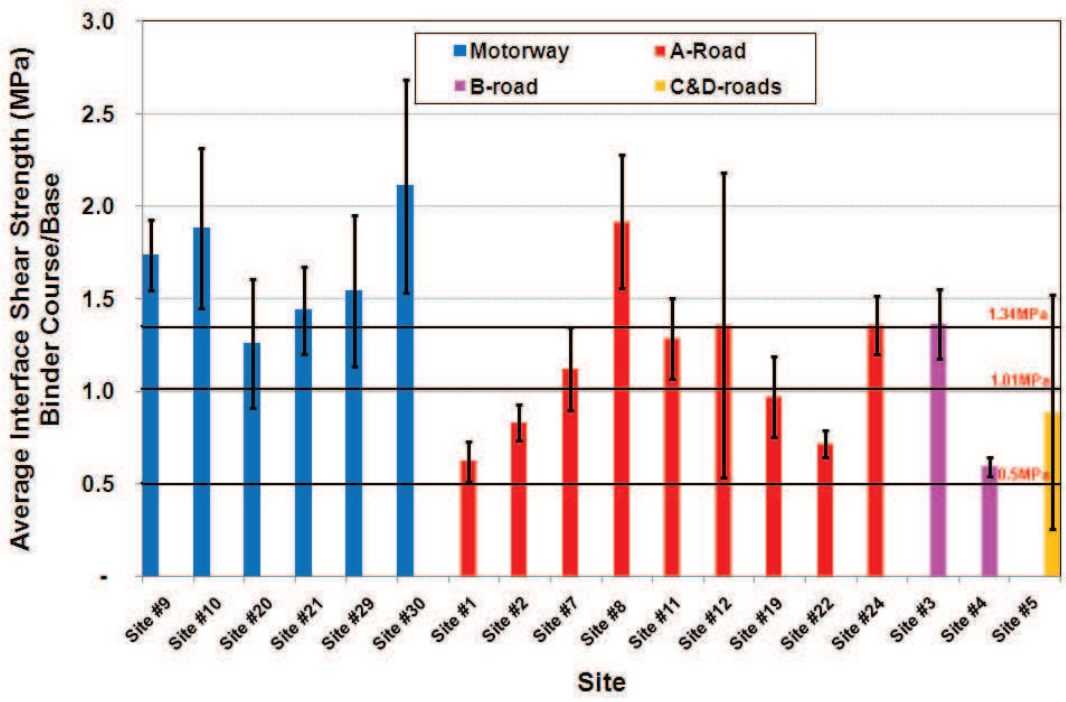

Figure 7.2 – Average shear strength for binder course/base interface

Figures 7.1 and 7.2 show that, for the S/Bin interface, only 5 sites (Sites #4, #16, #17, #26 and #28) show average interface shear strength below 1MPa. Whereas for the Bin/B interface, the average interface shear strengths of all sites are above 0.5MPa. It should be noted that although the average shear strength for the Bin/B interface of all individual sites would meet a minimum requirement of 0.5MPa, the error bars suggest that a number of individual specimens show interface shear strength below 0.5MPa. Figures 7.3 and 7.4 show the histograms for the entire set of S/Bin and Bin/B specimens obtained from field cores respectively. It can be seen from those figures that minimum limit values of 1MPa for

S/Bin interface and 0.5MPa for Bin/B interface are approximately equal to the 18th percentile of S/Bin specimens and 6th percentile of Bin/B specimen respectively. Therefore, it is highly possible to achieve shear strengths of 1MPa and 0.5MPa at the S/Bin and Bin/B interfaces respectively.

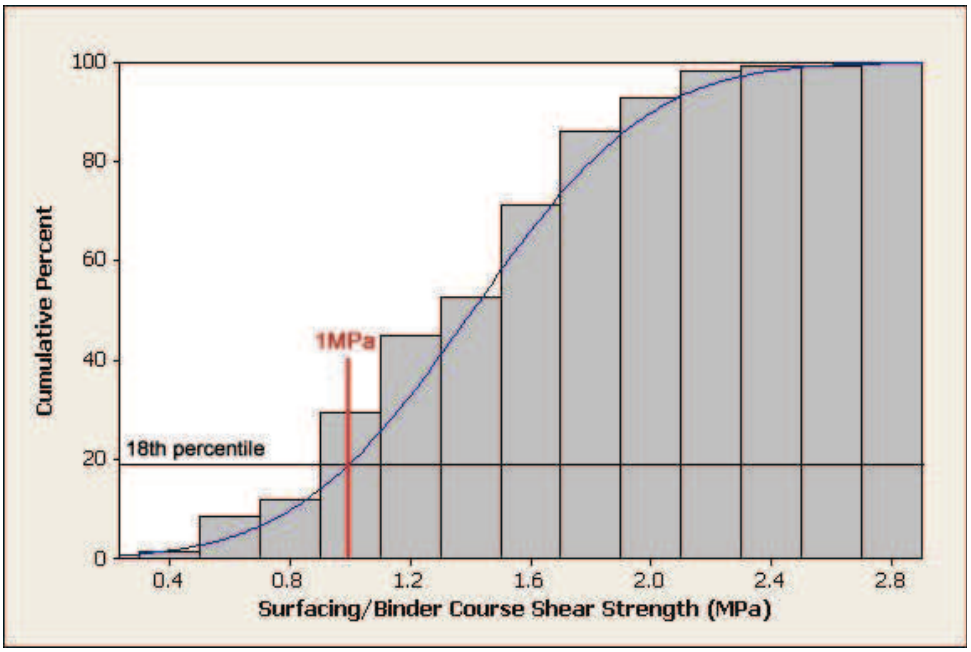

Figure 7.3 – Histogram for surfacing/binder course specimens from field cores

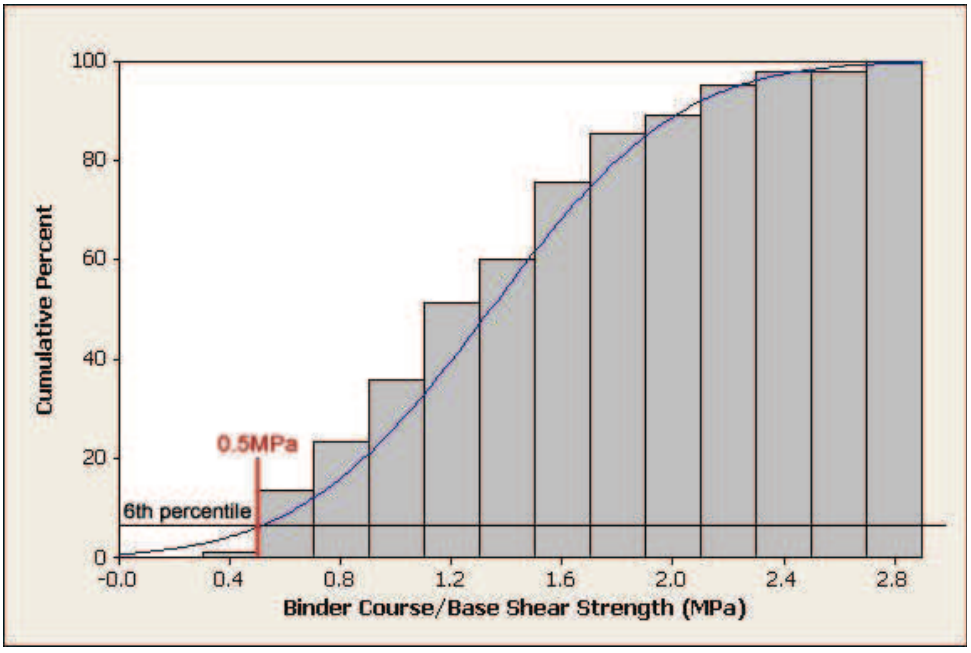

Figure 7.4 – Histogram for binder course/base specimens from field cores

7.3 Prediction of Required Bond Strength at the Interface

A simple analysis to predict the required bond strength at the interface is presented in this section. The analysis in this research study was performed using the available data, which in some cases is very limited. The approach used in the analysis might not be the best way to predict the required interface bond strength; but, it could be considered as one of the possible approaches. It should be noted that because field verification was not performed, the results from this analysis should be applied with due caution.

7.3.1 Calculation of Stresses at the Interface

An initial investigation was carried out by analysing fourteen theoretical pavement structures (comprising five or six layers) to represent a wide range of UK asphalt pavement constructions. The aim of this initial investigation was to identify the structure that suffered from the highest interface shear stresses (particularly at the two uppermost interfaces). The layer thicknesses and type of materials used were designed according to the relevant standards [The Higways Agency, 2006 and British Standards Institution, 2007] and typical current practice in the UK. The pavement structures are summarised in Table 7.2. To simplify the analysis in this initial investigation, the interfaces between layers were assumed to be fully bonded.

A value of tyre contact pressure of 600kPa with 105mm contact radius was used to represent traffic loading. According to Barber [1962], the magnitude of the horizontal load is driven by the friction coefficient between the tyre and the pavement surface, which may vary according to pavement and tyre conditions up to a limiting value of 0.8. Therefore, to simulate the worst case scenario of a locked wheel on a dry road surface, a horizontal load in the direction parallel to the traffic comprising 70% of the magnitude of the vertical load was used. Because pavement design is traditionally carried out at a reference temperature of 20˚C [The Highways Agency, 2006], the analysis was carried out at a temperature of 20˚C. The horizontal shear stresses under the centre of the wheel load at the surfacing/binder course (S/Bin) and binder course/base (Bin/B) interfaces were calculated using BISAR and are

presented in Table 7.3. It can be seen from Table 7.3 that structure #7 shows the highest shear stresses and can be considered as the worst case scenario. Therefore, structure #7 was used in the subsequent analysis.

In the subsequent analysis, an intermediate bond condition was used at the interface between bituminous layers and an approximately full bond condition was used at the interface between granular layers in order to represent a more realistic interface condition. Shear reaction modulus, K_s, was used to characterise the interface bond condition because it can easily be incorporated into the BISAR analysis and seems to be the most widely used by researchers (See Section 2.4.2 of Chapter 2). Al Hakim [1997] classified *Ks* value between 0.01 and 100 MPa/mm as intermediate bond condition. Therefore, in the subsequent analysis, three different *Ks* values of 0.1, 1 and 10 MPa/mm were used at the interfaces between bituminous layers of structure #7 (Table 7.4).

Table 7.2. Theoretical pavement structures

Structure	Layer	Material	Thickness	Stiffness (MPa)	Poisson's Ratio	Structure	Layer	Material	Thickness	Stiffness (MPa)	Poisson's Ratio
#1	Surfacing	Thin Surfacing	15mm	1500	0.35	#2	Surfacing	SMA	50mm	3000	0.35
	Binder Course	DBM 50	60mm	4700	0.35		Binder Course	DBM 50	50mm	4700	0.35
	Base	DBM 50	135mm	4700	0.35		Base	DBM 50	100mm	4700	0.35
	Sub-base	Type 2	175mm	100	0.35		Sub-base	Type 2	175mm	100	0.35
	Subgrade	-	~	50	0.35		Subgrade	-	~	50	0.35
#3	Surfacing	Thin Surfacing	15mm	1500	0.35	#4	Surfacing	SMA	50mm	3000	0.35
	Binder Course	DBM 50	60mm	4700	0.35		Binder Course	DBM 50	60mm	4700	0.35
	Upper Base	DBM 50	100mm	4700	0.35		Upper Base	DBM 50	100mm	4700	0.35
	Lower Base	DBM 50	150mm	4700	0.35		Lower Base	DBM 50	150mm	4700	0.35
	Sub-base	Type 2	400mm	100	0.35		Sub-base	Type 2	400mm	100	0.35
	Subgrade	-	~	50	0.35		Subgrade	-	~	50	0.35
#5	Surfacing	Thin Surfacing	15mm	1500	0.35	#6	Surfacing	SMA	50mm	3000	0.35
	Binder Course	EME	60mm	8000	0.35		Binder Course	EME	60mm	8000	0.35
	Base	EME	125mm	8000	0.35		Base	EME	90mm	8000	0.35
	Sub-base	Type 3	200mm	200	0.35		Sub-base	Type 3	200mm	200	0.35
	Subgrade	-	~	50	0.35		Subgrade	-	~	50	0.35
#7	Surfacing	Thin Surfacing	15mm	1500	0.35	#8	Surfacing	SMA	50mm	3000	0.35
	Binder Course	EME	60mm	8000	0.35		Binder Course	EME	60mm	8000	0.35
	Upper Base	EME	100mm	8000	0.35		Upper Base	EME	100mm	8000	0.35
	Lower Base	EME	150mm	8000	0.35		Lower Base	EME	150mm	8000	0.35
	Sub-base	Type 3	300mm	200	0.35		Sub-base	Type 3	300mm	200	0.35
	Subgrade	-	~	50	0.35		Subgrade	-	~	50	0.35
#9	Surfacing	SMA	25mm	3000	0.35	#10	Surfacing	SMA	25mm	3000	0.35
	Binder Course	DBM 50	50mm	4700	0.35		Binder Course	EME	60mm	8000	0.35
	Base	DBM 50	125mm	4700	0.35		Base	EME	115mm	8000	0.35
	Sub-base	Type 2	175mm	100	0.35		Sub-base	Type 3	200mm	200	0.35
	Subgrade	-	~	50	0.35		Subgrade	-	~	50	0.35
#11	Surfacing	SMA	25mm	3000	0.35	#12	Surfacing	SMA	25mm	3000	0.35
	Binder Course	DBM 50	60mm	4700	0.35		Binder Course	EME	60mm	8000	0.35
	Upper Base	DBM 50	100mm	4700	0.35		Upper Base	EME	100mm	8000	0.35
	Lower Base	DBM 50	150mm	4700	0.35		Lower Base	EME	150mm	8000	0.35
	Sub-base	Type 2	400mm	100	0.35		Sub-base	Type 3	300mm	200	0.35
	Subgrade	-	~	50	0.35		Subgrade	-	~	50	0.35
#13	Surfacing	SMA	35mm	3000	0.35	#14	Surfacing	SMA	40mm	3000	0.35
	Binder Course	EME	60mm	8000	0.35		Binder Course	EME	60mm	8000	0.35
	Upper Base	EME	100mm	8000	0.35		Upper Base	EME	100mm	8000	0.35
	Lower Base	EME	150mm	8000	0.35		Lower Base	EME	150mm	8000	0.35
	Sub-base	Type 3	300mm	200	0.35		Sub-base	Type 3	300mm	200	0.35
	Subgrade	-	~	50	0.35		Subgrade	-	~	50	0.35

Table 7.3. Horizontal shear stress at the interface

Structure	Interface	Shear Stress (MPa)	Structure	Interface	Shear Stress (MPa)
#1	1-2 (S/Bin)	0.382	#2	1-2 (S/Bin)	0.173
	2-3 (Bin/B)	0.070		2-3 (Bin/B)	0.018
#3	1-2 (S/Bin)	0.385	#4	1-2 (S/Bin)	0.193
	2-3 (Bin/B)	0.095		2-3 (Bin/B)	0.039
#5	1-2 (S/Bin)	0.396	#6	1-2 (S/Bin)	0.210
	2-3 (Bin/B)	0.067		2-3 (Bin/B)	0.004
#7	1-2 (S/Bin)	0.398	#8	1-2 (S/Bin)	0.227
	2-3 (Bin/B)	0.097		2-3 (Bin/B)	0.045
#9	1-2 (S/Bin)	0.297	#10	1-2 (S/Bin)	0.332
	2-3 (Bin/B)	0.066		2-3 (Bin/B)	0.044
#11	1-2 (S/Bin)	0.307	#12	1-2 (S/Bin)	0.339
	2-3 (Bin/B)	0.071		2-3 (Bin/B)	0.077
#13	1-2 (S/Bin)	0.293	#14	1-2 (S/Bin)	0.271
	2-3 (Bin/B)	0.062		2-3 (Bin/B)	0.056

Table 7.4. Different interface bond condition for structure #7

Structure	Interface	*Ks* (MPa/mm)	Bond Condition
#7-A	1-2 (S/Bin)	0.1	Intermediate bond
	2-3 (Bin/B)	0.1	Intermediate bond
	3-4 (B/LB)	0.1	Intermediate bond
	4-5 (LB/SB)	10^5	Approximately full bond
	5-6 (SB/SG)	10^5	Approximately full bond
#7-B	1-2 (S/Bin)	1	Intermediate bond
	2-3 (Bin/B)	1	Intermediate bond
	3-4 (B/LB)	1	Intermediate bond
	4-5 (LB/SB)	10^5	Approximately full bond
	5-6 (SB/SG)	10^5	Approximately full bond
#7-C	1-2 (S/Bin)	10	Intermediate bond
	2-3 (Bin/B)	10	Intermediate bond
	3-4 (B/LB)	10	Intermediate bond
	4-5 (LB/SB)	10^5	Approximately full bond
	5-6 (SB/SG)	10^5	Approximately full bond

S: Surfacing; Bin: Binder Course; B: Base
LB: Lower Base; SB: Sub-base; SG: Subgrade

Further analysis on normal and shear stress distributions at the interfaces under the contact patch of structure #7-A, #7-B and #7-C was carried out using BISAR and the results are presented in Figures 7.5 , 7.6 and 7.7 respectively. These figures demonstrate that the interface shear reaction modulus does not significantly affect the normal stress at the surfacing/binder course (S/Bin) and binder course/base (Bin/B) interfaces. The figures also demonstrate that the interface shear stresses at S/Bin and Bin/B interfaces increase as the shear reaction modulus increases.

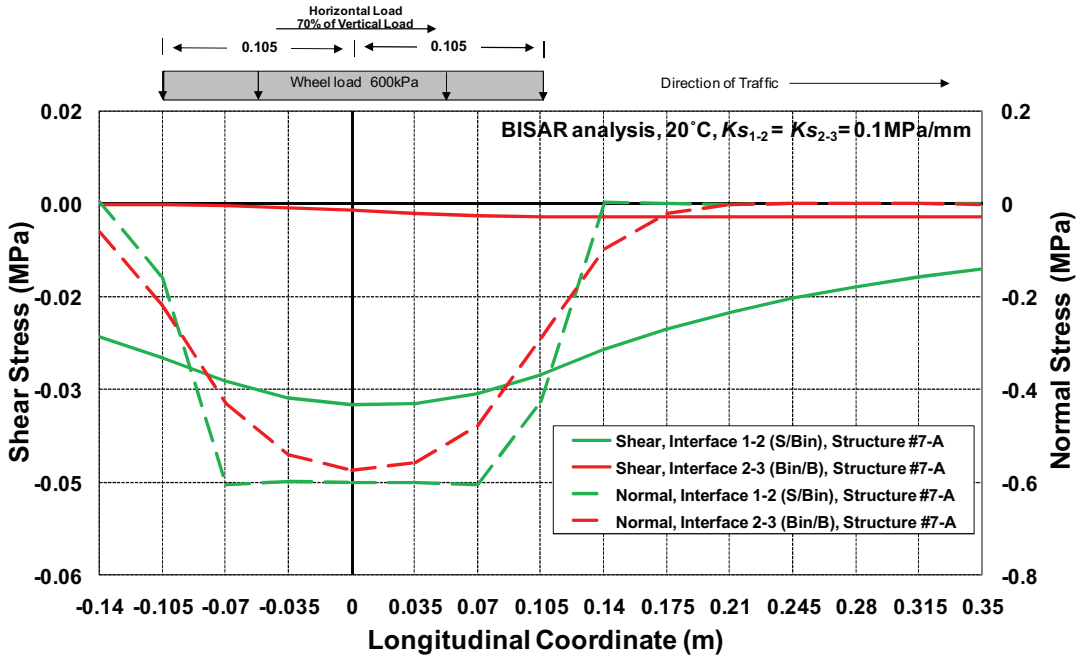

Figure 7.5 – Normal and shear stress distributions under the contact patch of structure #7-A

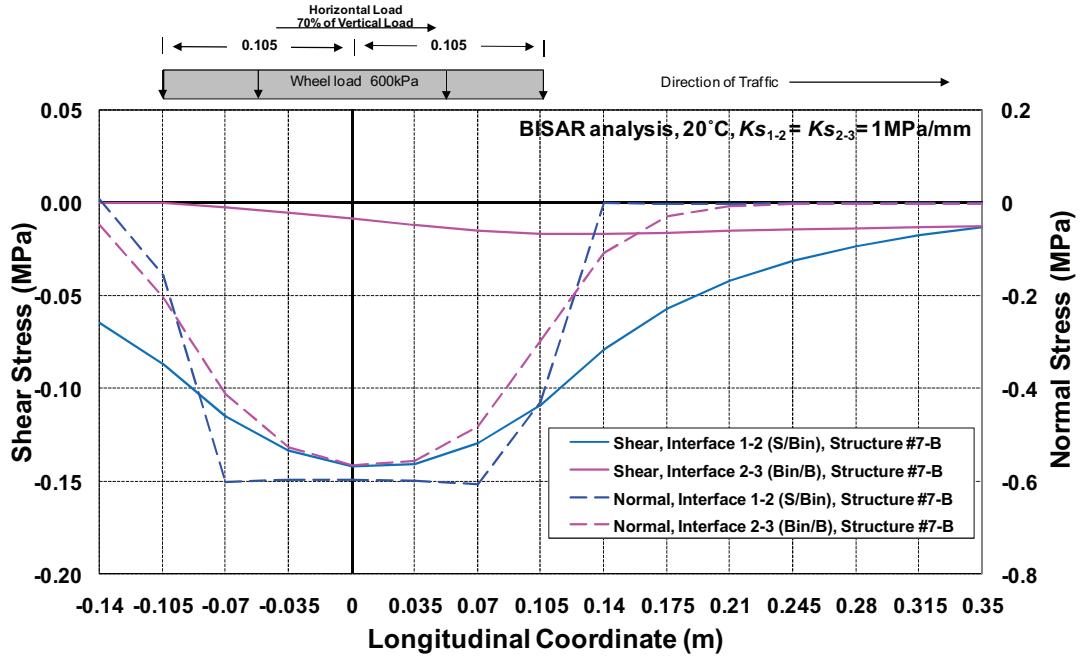

Figure 7.6 – Normal and shear Stress distributions under the contact patch of structure #7-B

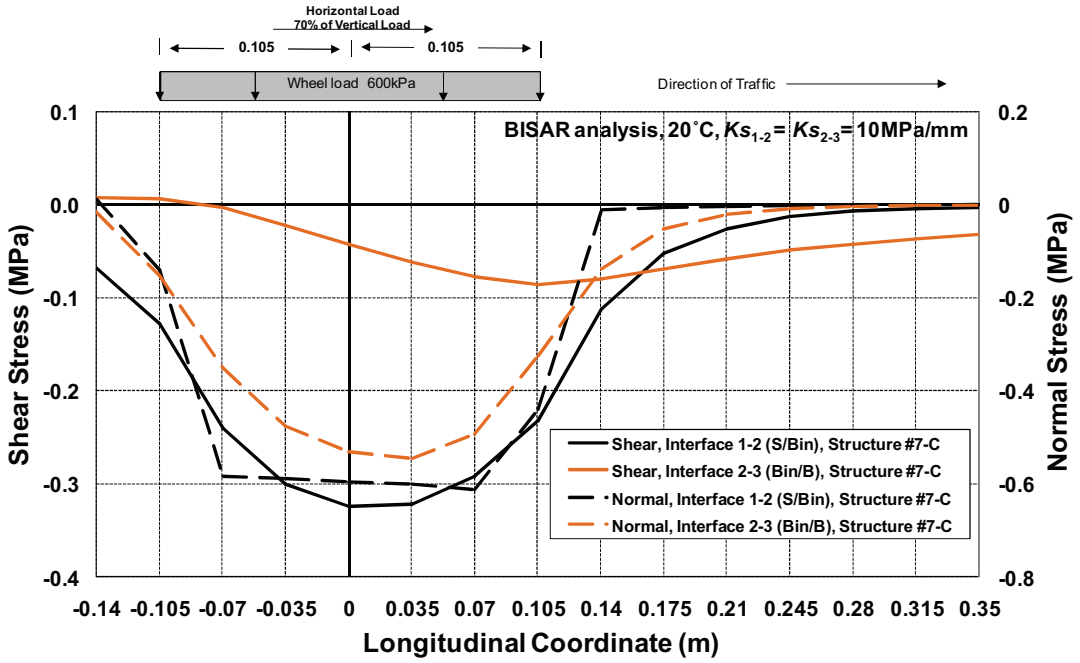

Figure 7.7 – Normal and shear stress distributions under the contact patch of structure #7-C

Assuming an average vehicle speed of 50km/hour and the vehicle is skidding, the displacement rate at the surface of the pavement would be as high as the vehicle speed. However, the displacement rate at the interface would be different to that of at the surface of the pavement. To determine the displacement rate at the interface, it is necessary to plot the relative horisontal displacement at the interface against time. In order to do this, the centre of the wheel load was placed at certain points (longitudinal coordinates of -0.35 to 0.14m) and the relative horizontal displacements at the interfaces at a longitudinal coordinate of 0m were calculated using BISAR. To determine the time, the wheel load was simulated to move from longitudinal coordinate of -0.35 to 0.14m at a speed of 50km/hour (vehicle speed) and the time that corresponds to the movement was recorded. The results are presented in Figure 7.8, where the relative horisontal displacement at the interface is plotted against time and the displacement rate is determined from the rate of increase (gradient) of the relative horizontal displacement at the interface.

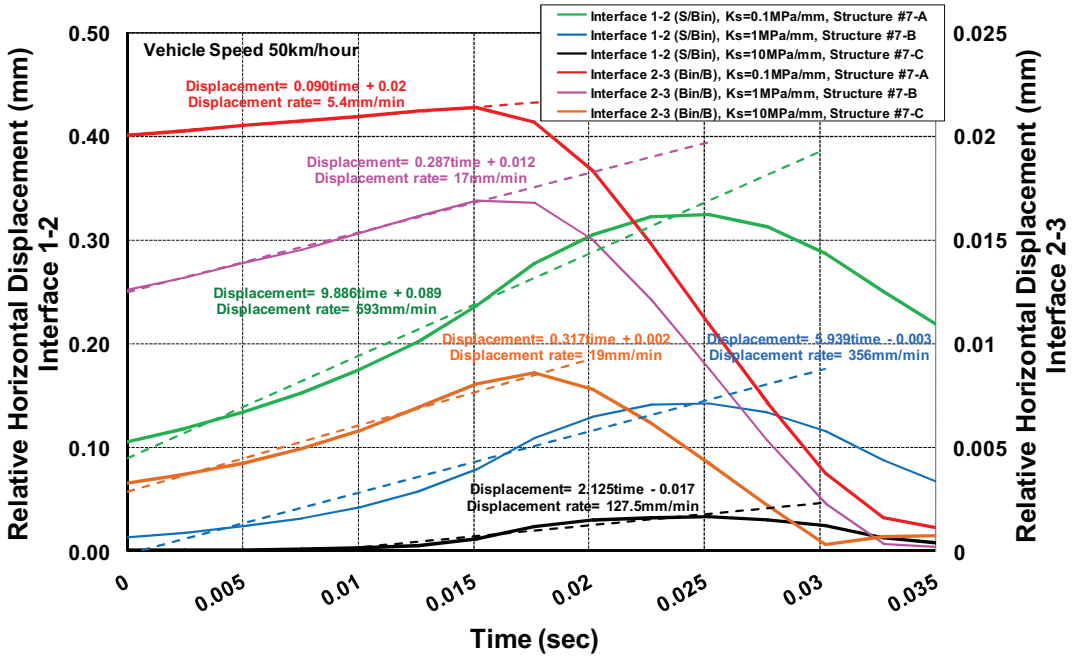

Figure 7.8 – Displacement rate at the interface

Figure 7.8 shows that the relative horizontal displacement at the surfacing/binder course (S/Bin) and binder course/base (Bin/B) interfaces increases as the shear reaction modulus decreases. The figure also shows that, as the shear reaction modulus decreases, the displacement rate at the surfacing/binder course (S/Bin) interface increases and that at the binder course/base (Bin/B) interface decreases. The following displacement rates (associated with a vehicle speed of 50km/hour) were used in the subsequent analysis:

- Structure #7-A

  Displacement rate at S/Bin interface: 593mm/min

  Displacement rate at Bin/B interface: 5.4mm/min

- Structure #7-B

  Displacement rate at S/Bin interface: 356mm/min

  Displacement rate at Bin/B interface: 17mm/min

- Structure #7-C

  Displacement rate at S/Bin interface: 127.5mm/min

  Displacement rate at Bin/B interface: 19mm/min

7.3.2 Effect of Normal Stress

Figures 7.5 , 7.6 and 7.7 demonstrate that significant normal stresses appear at the interfaces, hence it is necessary to consider the effect of normal stress on bond. Figures 7.9 and 7.10 show the shear strength (normalised against the shear strength with no normal stress) and the shear reaction modulus (normalised against the shear reaction modulus with no normal stress) respectively, plotted against the ratio of normal to shear stress (stress ratio) from Canestrari *et al.* [2005]. It can be seen from Figures 7.9 and 7.10 that, as the stress ratio is increased, the shear strength and shear reaction modulus increase with rates of increase (gradient) between approximately 1 and 2.7 and between approximately 3.2 and 6.9 respectively. It was considered that the effect of normal stress on shear strength and shear reaction modulus of a rough interface would be more significant than that of a flat interface; hence the gradient of the rough interface would be higher than that of the flat interface. In the subsequent analysis, intermediate gradient values of 1.85 and 5 have been used for the shear strength and shear reaction modulus respectively, resulting in the following relationships:

$$\tau/\tau_{0n} = (1.85\sigma/\tau) + 1 \qquad \text{(Equation 7.1)}$$

$$Ks/Ks_{0n} = (5\sigma/\tau) + 1 \qquad \text{(Equation 7.2)}$$

where σ/τ is the ratio of normal to shear stress, τ is the shear stress with normal load (MPa), τ_{0n} is the shear stress without normal load (MPa), Ks is the shear reaction modulus with normal load (MPa/mm) and Ks_{0n} is the shear reaction modulus without normal load (MPa/mm).

The modified Leutner test is typically performed without normal load, whereas the distributions of stresses in the theoretical pavement structures presented in Figures 7.5 , 7.6 and 7.7 demonstrate that significant normal stresses appear at the interface. Therefore, correction has to be made for the lack of any compressive normal stress in the modified Leutner test. The nominal interface shear stresses without normal stress were then predicted from the stresses in Figures 7.5 , 7.6 and

7.7 using equation (7.1) and the results of the calculation are presented in Figure 7.11.

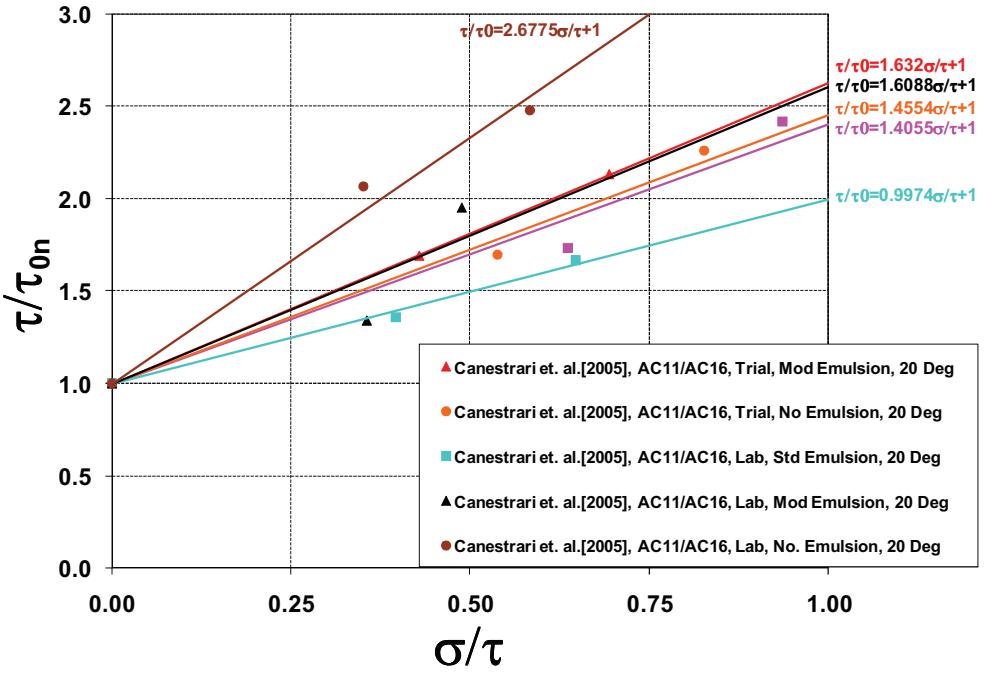

Figure 7.9 – Effect of normal stress on shear stress ratio

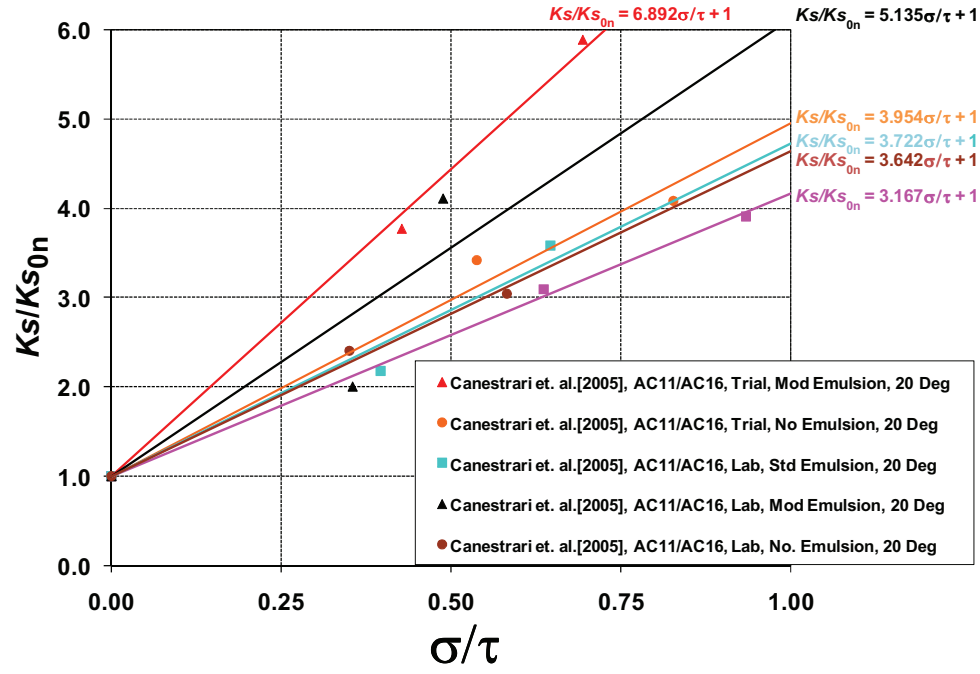

Figure 7.10 – Effect of normal stress on shear reaction modulus ratio

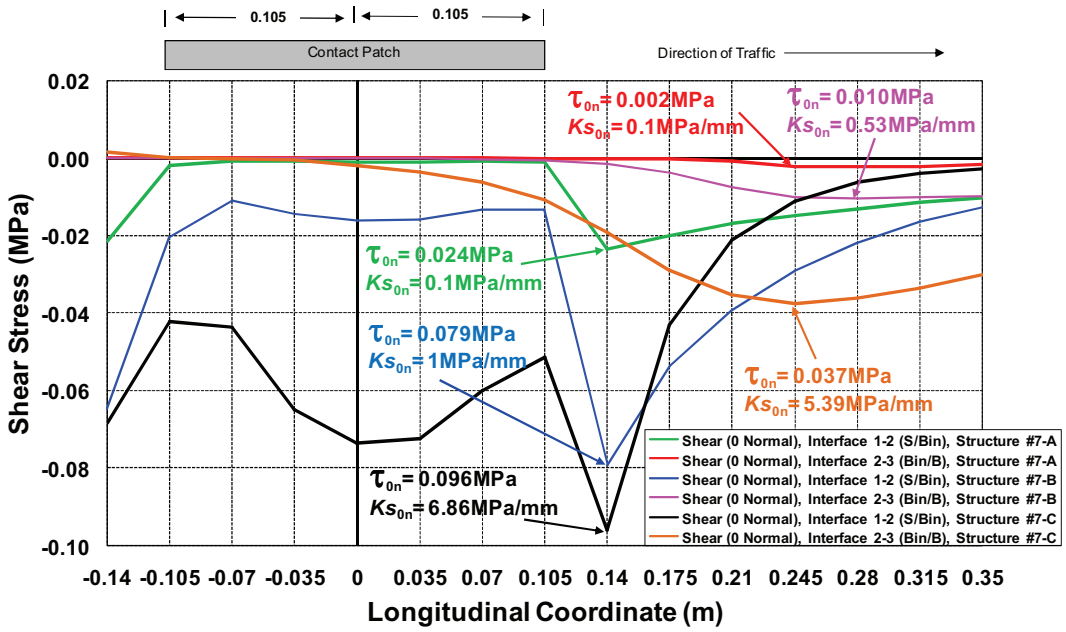

Figure 7.11 – Nominal interface shear stresses without normal load

Figure 7.11 shows that the critical values of nominal shear stress without normal stress at the S/Bin and Bin/B interfaces for structures #7-A, #7-B and #7-C are 0.024 and 0.002 MPa; 0.079 and 0.01 MPa; and 0.096 and 0.037MPa respectively. It is interesting to note that the critical value of nominal interface shear stress without normal stress is located in front of the contact patch. This was thought to be logical because Figures 7.5 , 7.6 and 7.7 show that the shear stress in front of the contact patch is still relatively high whilst the normal stress at the corresponding location is relatively low.

Nominal interface shear reaction moduli without normal stress at the corresponding location of critical shear stresses without normal stress were predicted from the stresses and shear reaction moduli in Figures 7.5 , 7.6 and 7.7 using equation (7.2), resulting in shear reaction moduli without normal stress at the S/Bin and Bin/B interfaces for structures #7-A, #7-B and #7-C of 0.1 and 0.1 MPa/mm; 1 and 0.53 MPa/mm; and 6.86 and 5.39 MPa/mm respectively (see Figure 7.11). The following values of shear stress without normal load and shear reaction modulus without normal stress were used in the subsequent analysis:

- Structure #7-A

  Shear strength at S/Bin interface: 0.024MPa

  Shear reaction modulus at S/Bin interface: 0.1MPa/mm

  Shear strength at Bin/B interface: 0.002MPa

  Shear reaction modulus at Bin/B interface: 0.1MPa/mm

- Structure #7-B

  Shear strength at S/Bin interface: 0.079MPa

  Shear reaction modulus at S/Bin interface: 1MPa/mm

  Shear strength at Bin/B interface: 0.01MPa

  Shear reaction modulus at Bin/B interface: 0.53MPa/mm

- Structure #7-C

  Shear strength at S/Bin interface: 0.096MPa

  Shear reaction modulus at S/Bin interface: 6.86MPa/mm

  Shear strength at Bin/B interface: 0.037MPa

  Shear reaction modulus at Bin/B interface: 5.39MPa/mm

7.3.3 Effect of Repeated loading on bond

A pavement structure is subjected to multiple load applications and a single load application is unlikely to cause the interface to fail. In Chapter 4, an investigation on the behaviour of the interface under repeated loading has been performed using the automatic torque bond test on a limited number of specimens and the result has been presented and discussed. Therefore, the result of the repeated automatic torque bond test was used in this analytical analysis. Figure 7.12 shows the shear strengths normalised against the predicted monotonic shear strength from the repeated automatic torque bond test result at 20˚C in Figure 4.23.

The coefficient of correlation in Figure 7.12 suggests that there is no significant difference between the SMA/DBM-TC and SMA/DBM-BC normalised fatigue curves, hence one correlation line could be used for both specimens. From Figure 7.12, the correlation between the number of cycles to failure and the ratio of shear strength is given by the following equation:

$$\tau/\tau_1 = N^{-0.1871} \qquad \text{(Equation 7.3)}$$

where τ is the shear strength (MPa), τ_1 is the monotonic shear strength (MPa) and N is the number of cycles to failure.

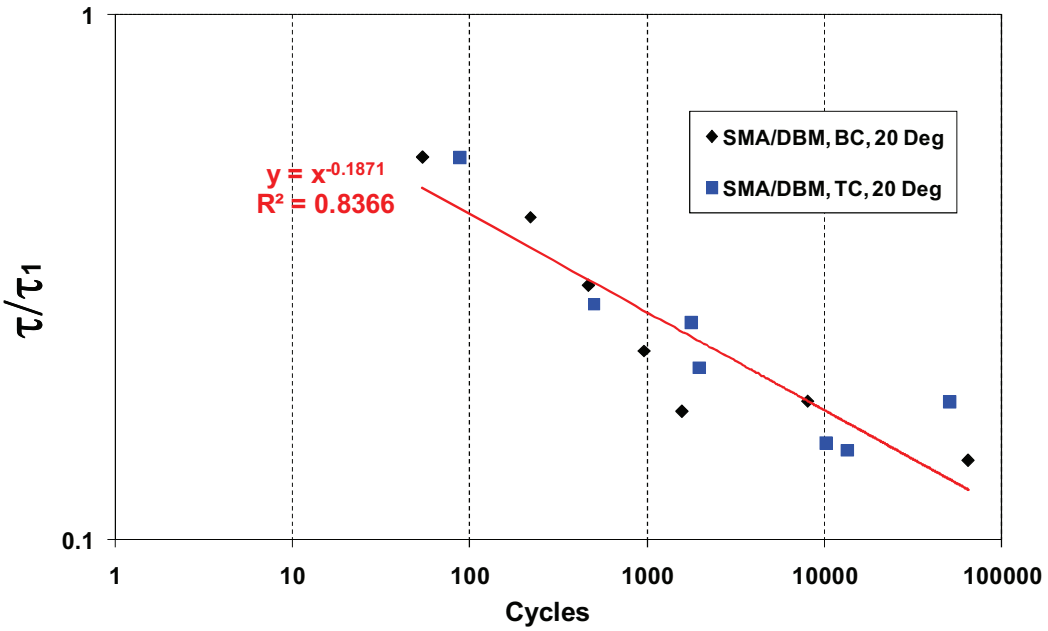

Figure 7.12 – Normalised fatigue curve

Assuming design traffic levels of 80 and 160 million standard axles (msa) and that 10 percent of the traffic is skidding, the design traffic for the first and second interfaces are 8msa and 16msa. Substituting these values and the previously calculated nominal shear stresses without normal load into equation (7.3) suggests that, in order to prevent failure, the monotonic shear strengths under traffic loading conditions at the S/Bin and Bin/B interfaces for structures #7-A, #7-B and #7-C would need to be 0.46 and 0.05 MPa; 1.55 and 0.23 MPa; and 1.88 and 0.83 MPa respectively. The following values of monotonic shear strength together with the corresponding values of shear reaction modulus without normal load from the previous analysis were used in the subsequent analysis:

- Structure #7-A

  Shear strength at S/Bin interface: 0.46MPa

Shear reaction modulus at S/Bin interface: 0.1MPa/mm

Shear strength at Bin/B interface: 0.05MPa

Shear reaction modulus at Bin/B interface: 0.1MPa/mm

- Structure #7-B

  Shear strength at S/Bin interface: 1.55MPa

  Shear reaction modulus at S/Bin interface: 1MPa/mm

  Shear strength at Bin/B interface: 0.23MPa

  Shear reaction modulus at Bin/B interface: 0.53MPa/mm

- Structure #7-C

  Shear strength at S/Bin interface: 1.88MPa

  Shear reaction modulus at S/Bin interface: 6.86MPa/mm

  Shear strength at Bin/B interface: 0.83MPa

  Shear reaction modulus at Bin/B interface: 5.39MPa/mm

7.3.4 Effect of Displacement Rate

The modified Leutner test is typically performed at a constant displacement rate of 50mm/min, which is different to the displacement rates at the interfaces of the theoretical pavement structure associated with a vehicle speed of 50km/hour presented in Figure 7.8. Therefore, the shear stress and shear reaction modulus should be corrected to accommodate the effect of displacement rate. Choi *et. al.* [2005], using the modified Leutner test, performed an investigation on the effects of displacement rate on shear strength and shear reaction modulus shown in Figure 7.13 and Figure 7.14 respectively, resulting in the the following equations:

$$\tau = 0.510\text{Ln}(x) - 0.264 \qquad \text{(Equation 7.4)}$$

$$Ks = 0.332\text{Ln}(x) - 0.151 \qquad \text{(Equation 7.5)}$$

where τ denotes the shear strength at the interface (MPa), *Ks* is the interface shear reaction modulus (MPa/mm) and x is the displacement rate (mm/min).

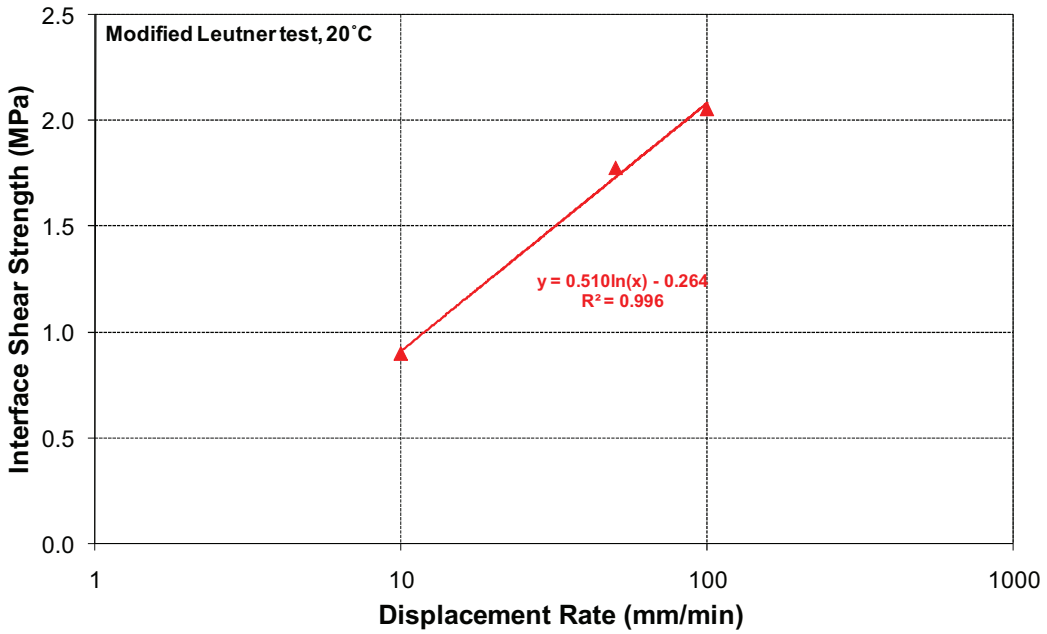

Figure 7.13 – Effect of displacement rate on interface shear strength (From Choi *et al.*, 2005)

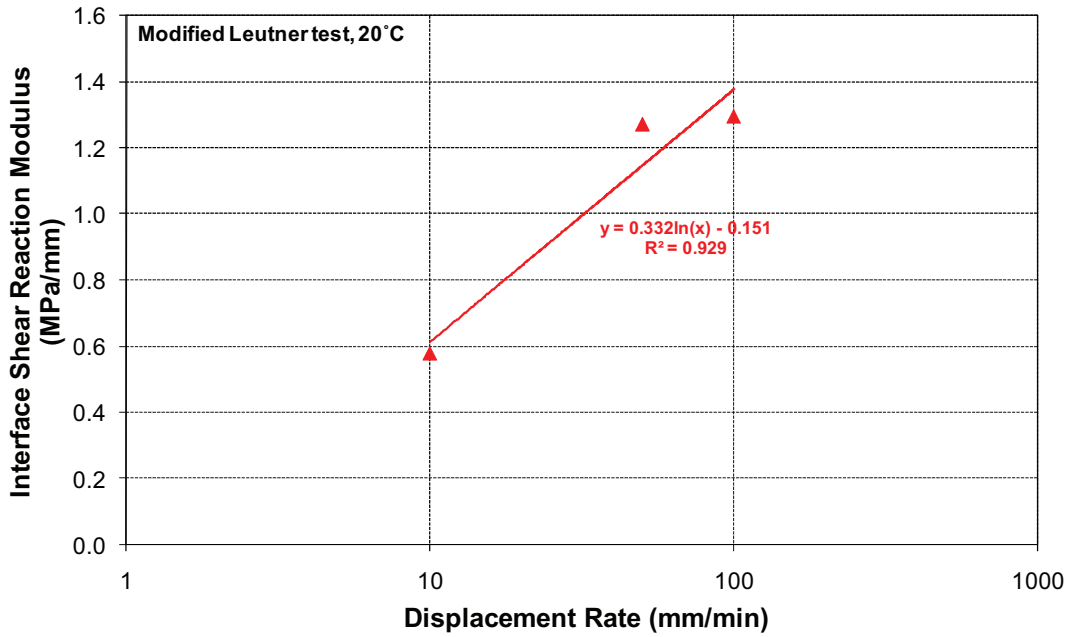

Figure 7.14 – Effect of displacement rate on interface shear reaction modulus (From Choi *et al.*, 2005)

The typical modified Leutner test displacement rate of 50mm/min and the displacement rates of the theoretical pavement structures presented in Figure 7.8 together with equation (7.4) can be used to calculate that the shear strength at the S/Bin and Bin/B interfaces for structure #7-A, #7-B and #7-C would be 1.73 and 0.34; 1.58 and 0.68 and 1.28 and 0.71 times as high as the shear strength of the modified Leutner test at a typical displacement rate of 50mm/min. Similar calculation was carried out using equation (7.5) to calculate that the shear reaction modulus at the S/Bin and Bin/B interfaces for structure #7-A, #7-B and #7-C would be 1.72 and 0.36; 1.57 and 0.69; and 1.27 and 0.72 times as high as the shear reaction modulus of the modified Leutner test at a typical displacement rate of 50mm/min. Therefore, the previously calculated values of interface shear strength and interface reaction modulus would change to the following:

- Structure #7-A
  - Shear strength at S/Bin interface: 0.27MPa
  - Shear reaction modulus S/Bin interface: 0.06MPa/mm
  - Shear strength at Bin/B interface: 0.13MPa
  - Shear reaction modulus at Bin/B interface: 0.28MPa/mm
- Structure #7-B
  - Shear strength S/Bin interface: 0.98MPa
  - Shear reaction modulus S/Bin interface: 0.64MPa/mm
  - Shear strength at Bin/B interface: 0.34MPa
  - Shear reaction modulus at Bin/B interface: 0.77MPa/mm
- Structure #7-C
  - Shear strength S/Bin interface: 1.47MPa
  - Shear reaction modulus S/Bin interface: 5.4MPa/mm
  - Shear strength at Bin/B interface: 1.17MPa
  - Shear reaction modulus at Bin/B interface: 7.48MPa/mm

7.3.5 Effect of Interface Shear Reaction Modulus

The results of the modified Leutner test on field cores presented in Chapter 6 showed that the interface shear reaction modulus ranges between 0.56 and 0.82

MPa/mm, therefore the interface shear strength has to be adjusted according to this typical value of interface shear reaction modulus. Figure 7.15 shows the interface shear reaction modulus from the previous analysis plotted against the corresponding shear strength. The figure suggests that for the tipical interface shear reaction modulus obtained from the bond database of between 0.56 and 0.82 MPa/mm; the required shear strength at the surfacing/binder course (S/Bin) and binder course/base (Bin/B) interfaces would range between 0.71 and 0.83 MPa and between 0.23 and 0.3 MPa respectively.

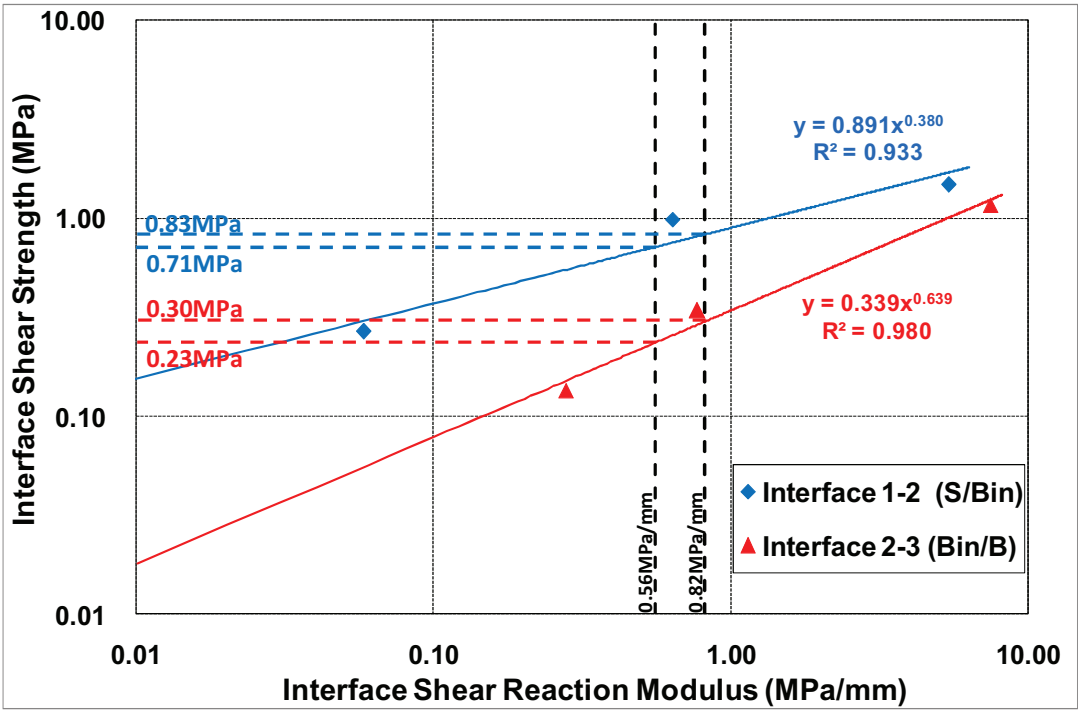

Figure 7.15 – Interface shear reaction modulus plotted against the corresponding interface shear strength

Because several assumptions as well as simplifications were used, the results from the analysis would be different if different assumptions were used. It was assumed in the analysis that 10% of the traffic is skidding. This proportion of skidding traffic might be higher for some locations of roads, for example some intersections where a high proportion of vehicles would brake or decelerate. If the proportion of skidding traffic was assumed to be 50%, the required interface shear strengths at the surfacing/binder course (S/Bin) and binder course/base (Bin/B)

interfaces would change to between 0.97 and 1.1MPa and between 0.32 and 0.4MPa respectively.

In the analysis, the vehicle speed was assumed to be 50km/hour; reducing the vehicle speed to 20km/hr with the wheel sliding would change the required shear strengths at the surfacing/binder course (S/Bin) and binder course/base (Bin/B) interfaces to approximately 0.81-0.94MPa and 0.41-0.5MPa respectively.

7.4 Discussion

From the database of interface shear strengths measured using the modified Leutner test; it is highly possible to achieve modified Leutner shear strengths of 1MPa and 0.5MPa for the surfacing/binder course and binder course/base interfaces respectively. Therefore, these values could be used as a basis for recommending the specification limits of shear bond strength for UK roads.

An analysis to predict the required modified Leutner shear strengths has been performed. From the results of the analysis, the proposed minimum limits of 1MPa for the surfacing/binder course interface and 0.5MPa for the binder course/base interface seem to be reasonable to prevent bond failures within the design life. However, because field verification was not performed to validate the results of the analysis, further investigation and long term field study are required to confirm the results.

As mentioned earlier in the introduction of this Chapter, specification limits for shear bond strength have been proposed as national standards in Germany and Switzerland [Codjia, 1994; Partl and Raab, 1999; Stöckert, 2001; VSS, 2008]. These are shown in Table 7.5 together with equipment, specimen size and loading condition used in the testing. Note that although the Leutner, the LPDS and the modified Leutner tests are very similar, the gaps at the shearing plane are different (see section Section 3.2 of Chapter 3).

It can be seen that applying the lower values of 0.85MPa and 0.57MPa to the average shear strengths from different sites in Figure 7.1 and Figure 7.2, 3 sites (Sites #4, #26 and #28) would fail to meet the surfacing/binder course requirement and all sites would meet the binder course/base requirement. Applying these values to the histograms for the entire set of S/Bin and Bin/B specimens in Figures 7.3 and 7.4 would exclude approximately 12% of the surfacing/binder course interface (S/Bin) specimens and approximately 7% of the binder course/base interface (Bin/B) specimens.

Table 7.5. Proposed limits in Germany and Switzerland

Source	Equipment	Specimen size	Displacement rate	Shear Strength (MPa)	
				S/Bin	Bin/B
Codjia [1994] Germany	Leutner[1]	150mm diameter	50mm/min	0.85	0.57
Partl & Raab [1999] Switzerland	LPDS[2] Leutner[1]	150mm diameter	50mm/min	1.3	
Stöckert [2001] Germany	Leutner[1]	150mm diameter	50mm/min	1.41	1.13
SN 640430B [VSS, 2008] Switzerland	LPDS[2] Leutner[1]	150mm diameter	50mm/min	0.85	0.68

[1] without gap at the shear plane
[2] with 2mm gap at the shear plane

Applying the upper values of 1.41MPa and 1.13MPa would exclude approximately 50% of the surfacing/binder course interface (S/Bin) specimens and approximately 40% of the binder course/base interface (Bin/B) specimens. Using these limits, 11 sites (Sites #4, #13, #14, #16, #17, #18, #22, #23, #26, #27 and #28) would not meet the specification for the surfacing/binder course interface and 6 sites (Sites #1, #2, #4, #5, #19 and #22) would not meet the specification for the binder course/base interface.

Compared to the limits in Table 7.5, the minimum limit of 1MPa for the surfacing/binder course interface proposed in this research study lies in the middle region. Whilst the minimum limit of 0.5MPa for the binder course/base interface lies in the lowest region. In general, Table 7.5 shows that the specification limits proposed in this research study are quite comparable.

7.5 Conclusion

The following key points can be derived from the study:

- Because it is highly possible to achieve modified Leutner shear strengths of 1MPa and 0.5MPa for the surfacing/binder course and binder course/base interfaces respectively, it is recommended that the shear strength of the interface measured using the modified Leutner Shear test should be not less than 1MPa for surfacing/binder course interface and not less than 0.5MPa for binder course/base interface.
- The specification limits proposed in this research study show a reasonably good agreement with results obtained from the analytical analysis and appear to be quite comparable with other limits in Germany and Switzerland.

Chapter 8 CONCLUSIONS AND RECOMMENDATIONS FOR FUTURE RESEARCH

8.1 Conclusions

The research presented in this thesis has been concerned with the assessment of bond between asphalt layers. The conclusions presented in this chapter were drawn from the work undertaken.

8.1.1 Modification to the Leutner Test

- The shear strength measured using the standard Leutner test depends on surface layer thickness where the thickness of the surfacing is less than approximately 25mm.
- Observations from failed specimens containing thin surfacings revealed that a significant amount of bulging had taken place in the top half of the specimen.
- A modification to the Leutner test that involves attaching a 30mm thick, 150mm diameter grooved metal plate to the thin surfacing significantly reduces the effect of surfacing thickness on measured shear strength.
- The measured shear strength increases as the temperature is decreased and the loading rate is increased

8.1.2 Torque Test Investigation

- At a constant torque rate of 600Nm/min, the nominal interface shear strength measured using the automatic torque bond test is higher than that measured using the manual torque bond test.

- The nominal lateral shear is very small and not significant compared to that of the nominal interface shear strength.
- Considering the variability of results, the force needed to induce the torsional load, the possibility to control the loading rate accurately and the ability to distinguish the effect of different interface treatments; it is recommended that the manual torque bond test is performed at an intermediate temperature (i.e. 20ºC) and a constant rotation rate of 600Nm/min.
- There is a reasonably good correlation between the average shear strength measured from the modified Leutner test at a constant displacement rate of 50mm/min and the average nominal shear strength measured from the automatic and manual torque bond tests performed at a constant loading rate of 600Nm/min.

8.1.3 Trafficking Investigation

- Results from the PRD mould-based simulated trafficking showed that the bond strengths for the SMA/14EME, TS1/14EME and SMA/20DBM combinations increased after 100,000 cycles by approximately 130%, 80% and 30% respectively whereas the TS1/20DBM and 14EME/20EME combinations showed no improvement.
- It was found that initially un-bonded specimens showed some bond development with trafficking.
- Results from the more realistic French Wheel Tracker-based simulated trafficking showed that all of the surfacing/binder course material combinations show a greater improvement in bond strength with trafficking compared to the PRD results. For the SMA/14EME and SMA/20DBM material combinations, this improvement in bond strength corresponded to increases of approximately 380% and 200% after 100,000 passes.

8.1.4 Development of bond database on Modified Leutner test

- From the Leutner testing on laboratory manufactured specimens, it was found that the shear strengths range from 1.12MPa to 2.68MPa, the

displacements determined at the shear strength range from 1.05mm to 2.40mm and the shear reaction modulus ranges from 0.48MPa/mm to 1.90MPa/mm.

- Ageing the laboratory manufactured specimens in the oven at 85°C for 120 hours increases the shear strength by 16 to 41%.
- Relative effect of moisture damage on interface shear reaction modulus of different material combinations could be assessed by moisture conditioning specimens using the LINK water sensitivity test protocol for 5 cycles.
- From the Leutner testing on field specimens, it was found that the average shear strengths range from 0.9MPa to 1.67MPa, the average displacements determined at the shear strength range from 1.87mm to 3.180mm and the average shear reaction modulus range from 0.56MPa/mm to 0.82MPa/mm.

8.1.5 Specification Limits

- It is recommended that the shear strength of the interface measured using the modified Leutner Shear test should be not less than 1MPa for surfacing/binder course interface and not less than 0.5MPa for binder course/base interface.

8.2 Recommendation for future research

- Observations from failed specimens containing thin surfacings revealed that a significant amount of bulging had taken place in the top half of the specimen. The bulging is thought to be due to a number of factors including bending stresses in the specimen due to the fact that the shear force is applied a short distance away from the interface resulting in tensile stresses and strains in the top half of the specimen perpendicular to the plane of the interface, compression in the surfacing material resulting in lateral expansion due to Poisson's ratio effects and local buckling of the surfacing material. Some of these factors except the local buckling of the surfacing material were verified with Finite Element (FE) models. Therefore, it is necessary to

investigate the local buckling of the surfacing material related to the appearance of bulging.

- The automatic torque test demonstrates the suitability for investigating the interface behaviour under repeated loading. Strengthening the testing frame is recommended to enable tests at higher loads and frequencies.
- The trafficking investigation has indicated that the binder grade used in the lower layer may affect the development of bond with trafficking and additional testing is required to confirm this.
- The effect of repeated loading has been considered in predicting the required bond strength at the interface. However, the effect of rest periods has not been considered during the repeated loading investigation.

References

Al Hakim B (1997) An improved backcalculation method to predict flexible pavement layers moduli and bonding condition between wearing course and base course. PhD thesis, Liverpool John Moores University, Liverpool, UK

Al Hakim B, Al Nageim H, Pountney D, and Lesley L (1997) The development of an improved pavement back-calculation. Proceedings of the 1st Conference on Rehabilitation and Development of Civil Engineering Infrastructure Systems, Lebanon, paper No. 72

Al Hakim B, Armitage R and Thom NH (1998) Pavement assessment including bonding condition: case studies. Proceedings of 5th International Conference on Bearing Capacity of Roads and Airfields, Trondheim, Norway, Vol. 1, pp.439-448

Ansys Inc. (1999) ANSYS - manuals, theory, elements, procedures. Revision 5.5, Pennsylvania, USA

Armitage RJ, Kruntcheva MR and Willett MR (2000) Trials of the portable seismic pavement analyser (PSPA). Report for Highways Agency, Pavement Engineering Group, Scott Wilson Pavement Engineering Ltd., Nottingham, UK

Babtie Engineering Laboratories (2000) Bond coat torque test. Report Submitted to the Highways Agency, Babtie Engineering Laboratories, Ipswich, UK

Bernhard R (2005) Tire/pavement noise. Presentation material of the Symposium on quiet asphalt pavement technology, The Asphalt Pavement Alliance and Purdue University, Indiana, USA, November

Bognacki CJ, Frisvold A and Bennert T (2007) Investigation of asphalt pavement slippage failures on runway 4R-22L, Newark International Airport. The 2007 Proceeding of the FAA Worldwide Airport Technology Transfer Conference, Atantic City, New Jersey, USA

British Board of Agreement (2000) Guidelines Document for the Assessment and Certification of Thin Surfacing Systems for Highways. Working Draft SG3/98/173, British Board of Agreement, Watford, UK

British Board of Agreement (2004) Guidelines Document for the Assessment and Certification of Thin Surfacing Systems for Highways. SG3/05/234, British Board of Agreement, Watford, UK

British Standards Institution (2003a) Bitumen road emulsions (anionic and cationic). BS434 –1&2, British Standards Institution, London, UK

British Standards Institution (2003b) Bituminous mixtures – Test Methods for hot mix asphalt. Part 22: Wheel tracking. BS EN 12697-22, British Standards Institution, London, UK

British Standards Institution (2003c) Bituminous mixtures - Test methods for hot mix asphalt. Part 23: Determination of the indirect tensile strength of bituminous specimens. BS EN 12697-23, British Standards Institution, London, UK

British Standards Institution (2003d) Bituminous mixtures - Test methods for hot mix asphalt. Part 33: Specimen prepared by roller compactor. BS EN 12697-33, British Standards Institution, London, UK

British Standards Institution (2003e) Concrete pavements. Part 2: Test method for the determination of the bond between two layers. BS EN 13863-2, British Standards Institution, London, UK

British Standards Institution (2003f) Bituminous mixtures - Test methods for hot mix asphalt. Part 36: Determination of the thickness of a bituminous pavement. BS EN 12697-36, British Standards Institution, London, UK

British Standards Institution (2004a) Bituminous mixtures - Test methods for hot mix asphalt. Part 26: Stiffness. BS EN 12697-26, British Standards Institution, London, UK

British Standards Institution (2004b) Bituminous mixtures - Test methods for hot mix asphalt. Part 35: Laboratory mixing. BS EN 12697-35, British Standards Institution, London, UK

British Standards Institution (2005a) Specification for coated macadam for roads and other paved areas. BS4987-1&2, British Standards Institution, London, UK

British Standards Institution (2005b) Sampling and examination of bituminous mixtures for roads and other paved areas. Part 104: Methods of test for the determination of density and compaction. BS598-104, British Standards Institution, London, UK

British Standards Institution (2006a) Bituminous mixtures. Material specification. Part 4: Hot Rolled Asphalt. BS EN 13108-4, British Standards Institution, London, UK

British Standards Institute (2006b) Bituminous mixtures. Material specification. Part 5: Stone Mastic Asphalt. BS EN 13108-5, British Standards Institution, London, UK

British Standards Institution (2007) Asphalt for roads and other paved areas – Specification for transport, laying and compaction and type testing protocols. BS594987, British Standards Institution, London, UK

Brown SF and Brunton JM (1984) The influence of bonding between bituminous layers. The Journal of the Institution of Highways and Transportation, UK, Vol. 31 (5), pp.16-17

Brown LR and Darnell TR (1987) Blistering of asphalt overlays caused by micro-organisms Journal of the Association of Asphalt Paving Technologists, Vol. 56, pp.361-380

Brühwiler E and Wittmann FH (1990) The wedge splitting test, a new method of performing stable fracture mechanics test. Engineering Fracture Mechanics, 35(1/2/3), pp.117– 125

Burmister DM (1945) The general theory of stresses and displacements in layered systems. Journal of Applied Physics, The American Institute of Physics, Melville, USA, Vol. 16, pp.89-94, pp.126-127, pp.296-302

Camanho PP and Davila CG (2002) Mixed-mode decohesion finite elements for the simulation of delamination in composite materials. Technical Memorandum, *NASA/TM-2002–211737*, National Aeronautics and Space Administration, Virginia, USA, pp.1–37

Canestrari F and Santagata E (2005) Temperature effects on the shear behavior of tack coat emulsion used in flexible pavements. The International Journal of Pavement Engineering, Vol. 6, No. 1, pp.39-46

Canestrari F, Ferroti G, Partl MN and Santagata E (2005) Advanced testing and characterization of interlayer shear resistance. TRB 84th Annual Meeting CD-ROM, Washington DC, USA

Carr AG (2001) The behaviour of layered pavement structures: the dynamic shear box. Project Report, The University of Nottingham, Nottingham, UK

Charmot S, Romero P and Dunning M (2005) Forensic analysis of slippage cracking. TRB 84th Annual Meeting CD-ROM, Washington DC, USA

Choi YK (2005) Development of the saturation ageing tensile stiffness test (SATS) for high modulus base materials. PhD Thesis, School of Civil Engineering, The University of Nottingham, UK

Choi YK, Sutanto MH, Collop AC and Airey GD (2005) Bond between asphalt layers. Project Report to the UK Highways Agency, Scott Wilson Pavement Engineering Ltd., Nottingham, UK

Codjia H (1994) Erarbeitung eines bewertungshintergrundes für das prüfverfahren ‘schichtenverbund nach leutner’ und bestimmung der präzision. Veröffentlichungen des Instituts für Straßen-und Eisenbahnwesen der Universität Karlsruhe (TH), Karlsruhe, Germany

Collop AC and Thom NH (2002) The importance of bond between pavement layers. Final Summary Report, School of Civil Engineering, University of Nottingham, Nottingham, UK

Collop AC, Thom NH and Sangiorgi C (2003) Assessment of bond condition using the leutner shear test. Proceeding of the Institution of Civil Engineers, Transport, UK, Vol. 156, Issue TR4, pp.211-217

Cooper Technology (2009) CRT-RC2S/V European Standard roller compactors – steel roller. Technical Specification, Cooper Technology, UK

Crisp E (2004) Development of a shear cohesion test for bitumen emulsion. MEng Dissertation Report, School of Civil Engineering, University of Nottingham, Nottingham, UK

Crispino M, Festa B, Giannattasio P and Nicolosi V (1997) Evaluation of the interaction between the asphalt concrete layers by a new dynamic test. Proceeding of the 8th International Conference on Asphalt Pavements, Seattle, USA, pp.741-754

Cui WC, Wisnom MR and Jones M (1992) A comparison of failure criteria to predict delamination of unidirectional glass/epoxy specimens waisted through the thickness. Composites, Vol. 23, No. 3, pp.158-66

De Beer M, Kannemeyer L and Fisher C (1999) Towards improved mechanistic design of thin asphalt layer surfacings based on actual tyre/pavement contact stress -in-motion (SIM) data in South Africa. Proceeding of the 7th Conference on Asphalt Pavements for Southern Africa, Victory Falls, Zimbabwe, pp.5.4ff

de Bondt AH (1999) Anti-reflective cracking design of (reinforced) asphaltic overlays. PhD Thesis, Delft University of Technology, Delft, Netherlands

Department for Transport (2006) Road traffic statistics for Great Britain 2005. Transport statistics bulletin, Statistics Report SB (06) 28, Deparment for Transport, London, UK

Diakhaté M, Phelipot A, Millien A and Petit C (2006) Shear fatigue behaviour of tack coats in pavements. Road Materials and Pavement Design, Vol.7, No.2/2006, pp.201-222

Diakhaté M, Petit C, Millien A, Phelipot-Mardelé A, Pouteau B and Goacolou H (2007) Comparison of direct shear and torque tests for determining viscoelastic shear behavior of tack coats. Proceeding of The International Conference on Advanced Characterization of Pavement and Soil Engineering Materials, Athens, Greece, pp.281-290

Diakhaté M (2007) Fatigue et comportement des couches d'accrochage dans les structures de chaussée. Thèse de Doctorat, Laboratoire Mécanique et Modélisation des Matériaux et Structures du Génie Civil (3MsGC), Faculte des Sciences et Techniques, Universite De Limoges, France, Octobre

DIN (1999) Asphalt prüfung – ALP A-Stb Teil 4: Prüfung des Schichtenverbundes nach Leutner. DIN2312, Cologne, Germany

DIN (2003) Asphalt prüfung – ALP A-Stb Teil 9: Haftzugfestigkeit von Dünnen Schichten. DIN2974, Cologne, Germany

Douglas Aircraft Company (1984) DC-9 airplane characteristic for airport planning. Douglas Aircraft Company, California, USA

El Halim A, Rickards I, Haas R and Nabi R (1997) Evaluation of design and construction effects on asphalt pavement performance through a portable in-situ shear test device. Proceeding of the 8th International Conference on Asphalt Pavements, Seattle, USA, pp.1311-1327

Erkens S (2002) Asphalt concrete response (ACRe) – determination, modelling and prediction. PhD Thesis, Delft University of Technology, Delft, Netherlands

Ferrotti G (2007) Theoretical and experimental characterization of interlayer shear resistance in flexible pavements. PhD Thesis, Facoltà di Ingegneria, Istituto di Idraulica e Infrastrutture Viarie, Università Politecnica delle Marche, Italy

FSV (1999) RVS 11.065 Teil 1: Grundlagen / Prüfverfahren / Haftverbund von Asphaltschichten. Österreichische Forschungsgesellschaft Straße-Schiene-Verkehr (FSV), Wien, Österreich

Goodman RE, Taylor RL, Brekke TL (1968) A model for the mechanics of jointed rock. Journal of the Soil Mechanics and Foundations Division, American Society of Civil Engineers, New York, USA, Vol.94, No.3, pp.637-659

Hachiya T and Sato K (1997) Effect of tack coat on bonding characteristics at interface between asphalt concrete layers. Proceeding of the 8th International Conference on Asphalt Pavements, Seattle, USA, pp.349-362

Hakim BA (2002) The importance of good bond between bituminous layers. Proceedings of the 9th International Conference on Asphalt Pavements, Copenhagen, August, paper no. 1:5-3

Hearn EJ (1997) Mechanics of materials 1: an introduction to the mechanics of elastic and plastic deformation of solids and structural materials. Third edition, Butterworth-Heinemann, Oxford, UK

Hibbitt, Karlsson and Sorensen, Inc. (2004) ABAQUS user manual. Version 6.5, Rhode Island, USA

Hironaka MC and Holland TJ (1987) Pressure heaving or asphalt pavement overlay. Journal of the Association of Asphalt Paving Technologists, Vol. 56, pp.380-408

Huntsman (2007) Araldite® 2011 structural adhesives. Technical Data Sheet, Huntsman Advanced Material Gmbh, Basel, Switzerland

Kennedy CK (1978) The development of slip-planes in rolled asphalt surfacings. TRRL report LR 813, Transport and Road Research Laboratory, Crowthorne, UK

Kennedy CK and Lister NW (1980) Experimental studies of slippage. The Performance of Rolled Asphalt Road Surfacings, The Institution of Civil Engineers, London, UK, pp.31-56

Kerschhagl J (2009) Manual handling assessment tables (mat). Guideline, Short risk assessment of manual handling of loads stipulated for testing simplified practices, Federal Ministry of Labour, Social Affairs and Consumer Protection, Central Labour Inspectorate, Vienna, Austria

Khweir K and Fordyce D (2003) Influence of layer bonding on the prediction of pavement life. Proceeding of the Institution of Civil Engineers, Transport, UK, Vol. 156, Issue TR2, pp.73-83

Kruntcheva MR, Collop AC, Thom NH (2000a) The portable seismic pavement analyser: laboratory trials. Project Report PGR 2000-02, The University of Nottingham, Nottingham, UK

Kruntcheva MR, Collop AC and Thom NH (2000b) Theoretical and practical aspects of the importance of bonding in a pavement structure. Project Report PGR 2000-08, The University of Nottingham, Nottingham, UK

Kruntcheva MR, Collop AC and Thom NH (2001) Shear box test: Finite element modeling. Project Report PGR01-05, The University of Nottingham, Nottingham, UK

Kulkarni MB (2004) Effect of tack and prime coats, and baghouse fines on composite asphalt pavements. PhD Dissertation, North Carolina State University, North Carolina, USA

Lepert P, Poilane JP and Villard-Bats M (1992) Evaluation of various field measurement techniques for the assessment of pavement interface condition. Proceedings of the 7th International Conference on Asphalt Pavements, Nottingham, UK, Vol. 3, 224-237

Leutner R (1979) Untersuchung des schichtenverbundes beim bituminosen oberbau. Bitumen, ARBIT, Hamburg, Germany, Heft 3

Linsbauer HN and Tschegg EK (1986) Fracture energy determination of concrete with cube shaped specimens. *Zement und Beton 31*, pp.38–40.

Marshall R, Ryman K and Hickling K (2004) Epiglass® multipurpose epoxy resin. Manual, International Paint Ltd., Southampton, UK

Matsuno S and Nishizawa T (1992) Mechanism of longitudinal surface cracking in asphalt pavement. Proceedings of the 7th International Conference on Asphalt Pavements, Nottingham, UK, Vol. 2, pp.277-291

Met Office (2009) Mean annual temperature in the UK. <URL: http://www.metoffice.com/climate/uk/regional/> [Accessed 12 January 2009]

Minitab Inc. (2007) MINITAB statistical glossary. Version 15, Pennsylvania, USA

Mirò Recasens R, Martinez A and Pérez Jiménez F (2005) Assessing heat-adhesive emulsions for tack coats. Proceeding of the Institution of Civil Engineers, Transport, UK, Vol. 158, Issue TR1, pp.45-51

Mohammad LN, Raqib MA, Wu Z and Huang B (2002) Measurement of interlayer bond strength through direct shear tests. The 3rd International Conference of Bituminous Mixtures and Pavements CD-ROM, Thessaloniki, Greece, 21-22 November

Myers LA and Roque R (2001) Evaluation of top-down cracking in thick asphalt pavements and the implications for pavement design. Perpetual Bituminous Pavements, Transportation Research Circular, No. 503, TRB, Washington DC, USA, pp.79-87

Nishiyama T, Lee DH and Bhatti MA (2005) Investigation of bonding condition in concrete overlay by laboratory testing, finite element modelling and field evaluation. TRB 84th Annual Meeting CD-ROM, Washington DC, USA

Nunn ME, Brown A, Weston D and Nicholls JC (1997) Design of long life flexible pavement for heavy traffic. TRL report 250, TRL Ltd. Crowthorne, UK

Ozer H, Al-Qadi IL and Leng Z (2008) A fracture based friction model for pavement interface characterization. TRB 87th Annual Meeting CD-ROM, Washington DC, USA

Partl MN and Raab C (1999) Shear adhesion between top layers of fresh asphalt pavements in Switzerland. Proceeding of the 7th Conference on Asphalt Pavements for Southern Africa, Victory Falls, Zimbabwe, pp.5.130-5.137

Partl MN, Canestrari F, Ferotti G and Santagata FA (2006) Influence of contact surface roughness on interlayer shear resistance. The 10th International Conference on Asphalt Pavements CD-ROM, Quebec, Canada

Peattie KR (1980) The incidence and investigation of slippage failures. The Performance of Rolled Asphalt Road Surfacings, The Institution of Civil Engineers, London, 3-15

Pell PS (1980) Discussion on slippage of rolled asphalt wearing courses. The Performance of Rolled Asphalt Road Surfacings, The Institution of Civil Engineers, London, UK, pp.64-65

Piber H, Canestrari F, Ferrotti G, Lu X, Millien A, Partl MN, Petit C, Phelipot-Mardelé A and Raab C (2009) RILEM interlaboratory test on interlayer bonding of asphalt pavements. Proceeding of the 7th International RILEM Symposium ATCBM09 on Advanced Testing and Characterization of Bituminous Material, Vol.2, Rhodes, Greece, 27-29 May, pp.1181-1189

Pös JK, Kruntcheva MR, Collop AC and Thom NH (2001) Effects on bond between pavement layers. Project Report, The University of Nottingham, Nottingham, UK

Raab C and Partl MN (1999) Methoden zur beurteilung des schichtenverbunds von asphaltbelägen. Eidgenössisches Departement für Umwelt, Verkehr, Energie und Kommunikation/Bundesamt für Strassen, Forschungsauftrag 12/94, Eidgenössische Materialprüfungs- und Forschungsanstalt, Report Nr442, Zurich, Switzerland

Raab C and Partl MN (2004a) Interlayer shear performance: experience with different pavement structures. Proceeding of the 3rd Eurasphalt & Eurobitume Congress, Vienna, Austria, pp.535-545

Raab C and Partl MN (2004b) Einfluß und wirkung von unterhaltsmaßnahmen auf die in-situ-eigenschaften von asphaltbelägen. Eidgenössisches Departement für Umwelt, Verkehr, Energie und Kommunikation/Bundesamt für Strassen, Forschungsauftrag 1998/084, Eidgenössische Materialprüfungs- und Forschungsanstalt, Report Nr1075, Zurich, Switzerland

Raab C and Partl MN (2004c) Effect of tack coats on interlayer shear bond of pavements. Proceeding of the 8th Conference on Asphalt Pavements for Southern Africa, Sun City, South Africa, pp.847-855

Raab C and Partl M (2005) Determination of the mechanical resistance of thin surfacings on asphalt pavements. Proceeding of the 4th International Conference on Maintenance and Rehabilitations of Pavements and Technological Control, Belfast, Northern Ireland, UK, 18-19th August, paper no. 144

Raab C and Partl MN (2007a) Langzeiterfassung des schichtenverbunds – relation zwischen prüfwert nach einbau und langzeitverhalten. Eidgenössisches Departement für Umwelt, Verkehr, Energie und Kommunikation/Bundesamt für Strassen, Forschungsauftrag 2005/503, Eidgenössische Materialprüfungs- und Forschungsanstalt, Report Nr1195, Zurich, Switzerland

Raab C and Partl MN (2007b) Prüfung von haftklebern. Eidgenössisches Departement für Umwelt, Verkehr, Energie und Kommunikation/Bundesamt für Strassen, Forschungsauftrag 1999/277, Eidgenössische Materialprüfungs- und Forschungsanstalt, Report Nr1196, Zurich, Switzerland

Raab C and Partl MN (2009) Interlayer bonding of binder, base and subbase layers of asphalt pavements: Long-term performance. Journal of Construction and Building Materials, Vol.23, pp. 2926–2931

Read J and Whiteoak D (2003) The Shell bitumen handbook. Shell Bitumen, London, UK

Romain JE (1968) Contraintes, déformations et déflexions dans les systémes quadricouches élastiques. Rapport de Recherche No. 147/JER/1968, Centre de Recherches Routiéres, Bruxelles, Belgium

Roffe JC and Chaignon F (2002) Characterisation tests on bond coats: worldwide study, impact, tests, recommendations. The 3rd International Conference of Bituminous Mixtures and Pavements CD-ROM, Thessaloniki, Greece, 21-22 November

Romanoschi SA and Metcalf JB (2001a) Effect of interface condition and horizontal wheel loads on the life of flexible pavement structures. Transportation Research Record No. 1778, Washington DC, USA, pp.123-131

Romanoschi SA and Metcalf JB (2001b) Characterization of asphalt concrete layer interfaces. Transportation Research Record No. 1778, Washington DC, USA, pp.132-139

Romanoschi SA and Metcalf JB (2002) The characterisation of pavement layer interfaces. Proceedings of the 9th International Conference on Asphalt Pavements, Copenhagen, August, paper no. 1:5-2

Romanoschi SA and Metcalf JB (2003) Errors in pavement layer moduli backcalculation due to improper modeling of layer interface condition. TRB 82nd Annual Meeting CD-ROM, Washington DC, USA

Sanders PJ and Nunn M (2005) The Application of Enrobé à Module Élevé in Flexible Pavements. TRL Report 636, TRL Ltd., Crowthorne, UK

Sangiorigi C, Collop AC and Thom NH (2002) Laboratory assessment of bond condition using the leutner shear tester. The 3rd International Conference of Bituminous Mixtures and Pavements CD-ROM, Thessaloniki, Greece, 21-22 November

Sangiorigi C, Collop AC and Thom NH (2002) A non-destructive impulse hammer for evaluating the bond between asphalt layers in a road pavement. SIIV2002, Parma, Italy, October

Santagata FA, Ferrotti G, Partl MN and Canestrari F (2009) Statistical investigation of two different interlayer shear test methods. Journal of Materials and Structures, Vol.42, pp.705-714

Scholz TV (1995) Durability of bituminous paving mixtures, PhD Thesis, School of Civil Engineering, University of Nottingham, Nottingham, UK

SETRA/DTC (1986) Le décollement des couches de revêtement de chaussées. Note d'information Chaussées - Terrassement n' 25', SETRA, Bagneux, France, November

Shaat AA (1992) Investigation of slippage of bituminous layer in overlaid pavement in Northern Ireland. Consultancy Report Submitted for the DOE in Northern Ireland, Belfast, UK

Shahin M, Kirchner K and Blackmon EW (1987) Analysis of asphalt concrete layers slippage and its effect on pavement performance and rehabilitation design. Proceeding of the 6th International Conference on the Structural Design of Asphalt Pavements, University of Michigan, Ann Arbor, Michigan, USA, pp.958-964

Shell (1998) BISAR user manual. Version 3.0, Bitumen Business Group, Shell International Oil Products B.V., Amsterdam, Netherlands

Sholar GA, Page GC, Musselman JA, Upshaw PB and Moseley HL (2004) Preliminary investigation of a test method to evaluate bond strength of bituminous tack coats. Journal of the Association of Asphalt Paving Technologists, Vol. 73, pp.771-801

Simonin JM and Maisonneuve P (1998) Dynamic investigations in assessing the structural condition of pavements. Fifth International Conference on the Bearing Capacity of Roads and Airfields, Trondheim, Norway, July 6-8, pp.187-196

Stein WJvdM and Sadzik E (2007) Application of the portable pavement seismic analyser (PSPA) for pavement analysis. Proceedings of the 26th Southern African Transport Conference (SATC 2007), Pretoria, South Africa, pp.294-304

Stöckert U (2001) Schichtenverbund – prüfung und bewertungshintergrund, straße und autobahn, 11/2001

Sutanto MH (2004) Analisis kekuatan rekat lapisan perekat (tack coat) sebagai perekat antara lapisan permukaan hot rolled sheet (HRS) dengan lapisan pondasi asphalt treated base (ATB). Master thesis, Institut Teknologi Sepuluh November, Surabaya, Indonesia

Sutanto M, Collop A, Airey G, Elliott R, Choi Y (2006) Laboratory measurement of bond between asphalt layers. International Journal of Pavement Engineering and Asphalt Technology, Liverpool, UK, Vol.7, Issue 1, pp.38-57

Tashman L, Nam K and Papagiannakis T (2006) Evaluation of the influence of tack coat construction factors on the bond strength between pavement layers. Report Prepared for Washington State Department of Transportation, Washington Center for Asphalt Technology, Washington State University, Pullman, Washington, USA

The Highways Agency (1999) HD29/99: Data for pavement assessment. Design Manual for Roads and bridges, Volume 7, Section 3, Part 2, The Highways Agency, London, UK

The Highways Agency (2006) HD26/06: Pavement Design. Design Manual for Roads and bridges, Volume 7, Section 3, Part 3, The Highways Agency, London, UK

The Highways Agency (2008) Series 900: Road Pavements – Bituminous Bound Materials. Manual of Contract Documents For Highway Works (MCHW), Volume 1 Specification for Highway Works (SHW), The Highways Agency, London, UK

Thom NH (2007) Personal communication at the Nottingham Transportation Engineering Centre (NTEC), University of Nottingham, UK, 19 March

Tschegg KE, Kroyer G, Tan DM, Stanzl-Tschegg SE and Litzka J (1995) Investigation of bonding between asphalt layers on road construction. Journal of Transportation Engineering, American Society of Civil Engineers, July/August, pp.309-317

TRRL (1976) Interim report of the working party on the slippage of rolled asphalt wearing courses. TRRL report SR 213UC, Transport and Road Research Laboratory, Crowthorne, UK

TRRL (1979) Final report of the working party on the slippage of rolled asphalt wearing courses. TRRL report SR 493, Transport and Road Research Laboratory, Crowthorne, UK

UNI/TS 11214 (2007) Caratterizzazione prestazionale a taglio delle interfacce. Metodo di prova ASTRA

Uzan J, Livneh M and Eshed Y (1978) Investigation of adhesion properties between asphalt concrete layers. Journal of the Association of Asphalt Paving Technologists, Vol. 47, pp.495-521

Vacin O, Ponniah J and Tighe S (2005) Quantifying the shear strength at the asphalt interface. Proceeding of The 1st Annual Inter-university Symposium on Infrastructure Management (AISIM), University of Waterloo, Waterloo, Canada, August

Vereinigung Schweizerischer Strassenfachleute (VSS) (2000) Bituminöses mischgut, bestimmung des schichtenverbunds (nach Leutner). Schweizer Norm, SN 671961, Vereinigung Schweizerischer Strassenfachleute (VSS), Switzerland

VSS (2008) Walzasphalt - konzeption, ausführung und anforderungen an die eingebauten schichten. Schweizer Norm, SN 640430B, Schweizerischer Verband der Strassen- und Verkehrsfachleute (VSS), Switzerland

Walsh ID and Williams JT (2001) HAPAS certificates for procurement of thin surfacing. Highways and Transportation, Vol.48, No.7-8, pp.12-14

Washington State Department of Transportation (2009) Top-down cracking. <URL:http://training.ce.washington.edu/WSDOT/Modules/09_pavement_evaluation/top_down_cracking.htm> [Accessed 12 January 2009]

Wellner F and Ascher D (2007) Untersuchungen zur wirksamkeit des haftverbundes und dessen auswirkung auf die lebensdauer von asphaltbefestigungen. Schlussbericht, Lehrstuhl Straßenbau, Institut für Stadtbauwesen und Verkehr, Technische Universität Dresden, Dresden, Germany

West RC, Zhang J and Moore J (2005) Evaluation of bond strength between pavement layers. NCAT Report 05-08, National Center for Asphalt Technology, Auburn University, Auburn, Alabama, USA

Whiffin AC and Lister NW (1962) The application of elastic theory to flexible pavements. Proceeding of the 1st International Conference Structural Design of Asphalt Pavements, University of Michigan, Ann Arbor, Michigan, USA, pp.499-552

APPENDIX A.1
MODIFIED LEUTNER TESTING PROTOCOL
(With 5mm gap, from Choi *et al.*[2005])

954 (11/04) Method for Laboratory Determination of Interface Properties using the Modified Leutner Shear Test

Scope

1 This Clause specifies a laboratory test method to assess the bonding between adjacent asphalt pavement layers using cylindrical samples. The test method is suitable for bitumen bound materials and is also appropriate for asphalt surfacing applied to concrete.

Terms and Definitions

2 For the purposes of this Clause the terms and definitions given in BS 6100 shall apply, together with the following:

(i) Peak Shear Stress of the Interface

The maximum value of shear stress, determined as the maximum force divided by the initial cross sectional area, of a specimen when tested as described in this Clause.

(ii) Displacement at Peak Shear Stress

The displacement at the maximum value of shear stress, of a specimen when tested as described in this Clause.

(iii) Shear Stiffness Modulus

The shear stress divided by the corresponding displacement, determined from the linear part of a shear stress versus displacement graph, of a specimen when tested as described in this Clause.

Principle of Test

3 Cylindrical test specimens of nominal 150mm diameter shall be subjected to direct shear loading at 20°C using the modified Leutner shear test. The maximum shear stress (in MPa) at the interface between layers shall be determined.

Test Apparatus

4 The following test apparatus shall be used:

(i) Shear test apparatus, as shown in Figure 9/12, composed of a base body (A) on which are fixed the sample support (B) and the lower shear ring (C). The upper shear ring (D) is attached to the upper body (E), which is movable along the guiding bars (F). The gap between shear rings (C and D) is 5mm.

(ii) A loading frame capable of achieving a constant vertical displacement rate of 50.0 ± 2mm per minute and a maximum load of at least 50kN.

(iii) A data logging system to record load and displacement during the test.

Sample Preparation

5 Test specimens shall be cores of 150 ± 2mm diameter; the minimum thickness of the layers above and below the interface to be tested shall be 30mm and 60mm respectively. Specimens shall be cored from an in-service pavement or from a slab manufactured using a laboratory roller compactor in accordance with pr EN 12697-33.

Procedure

6 The diameter and thickness of the specimen shall be determined to the nearest mm.

7 The specimen shall be placed into a suitable temperature controlled conditioning environment at 20 ± 0.5°C for a minimum of 5 hours.

8 The appropriate shear rings, to form a loose fit around the specimen (for example, 151mm diameter shear rings for a 150mm diameter specimen) shall be selected and attached to the Leutner test frame.

9 The specimen shall be placed into the test apparatus and the interface aligned, (Figure 9/12 (G)), between the upper and lower shear rings (Figure 9/12 (C and D)).

10 Tighten the sample support using a suitable spanner.

11 The test apparatus shall be placed into the loading frame and adjusted until the upper shear ring (Figure 9/12 (C)) nearly touches the specimen.

12 Start the data logging system (to record load and displacement) and commence shear loading. The loading rate shall be 50.0 ± 2mm per minute.

13 Stop the shear loading when the test frame reaches its limit of 7mm displacement. The length of time between removal of the specimen from the temperature controlled conditioning environment and completion of testing shall not exceed 15 minutes.

14 After the test has been completed, the apparatus shall be dismantled and the specimen removed.

15 Record the load (F) to the nearest 0.1kN and the displacement (δ) to the nearest 0.1mm.

16 Both sections of the specimen shall be observed (especially the interface) for any visual cracks and unusual appearance (ie. crushed aggregates on edges). Record any comments as necessary.

Calculation and Expression of Results

17 Calculate the shear stress as follows:

$$\tau = \frac{F}{\pi r^2}$$

Where τ = shear stress in (MPa)
F = load (in kN)
r = initial radius of specimen (in mm)

18 Produce a shear stress versus shear displacement graph (an example is shown in Figure 9/13) using the recorded data.

19 Determine the following parameters from the graph:

(i) τ_{max} = peak shear stress of the interface, MPa, expressed to the nearest 0.01

(ii) δ_{max} = displacement at peak shear stress, mm, expressed to the nearest 0.1

(iii) k_{max} = maximum shear stiffness modulus, MPa/mm, expressed to the nearest 0.01

(iv) k = shear stiffness modulus, MPa/mm, expressed to the nearest 0.01

Test Report

20 The test report shall contain not less than the following information:

a) A reference to this test method and test conditions
b) Material descriptions for both layers.
c) Type and amount of tack (bond) coat (if known).
d) For each specimen tested, report:
   - specimen diameter, expressed to the nearest mm
   - layer thicknesses, expressed to the nearest mm
   - maximum load (F), expressed to the nearest 0.1kN
   - displacement at peak shear stress(δ_{max}), expressed to the nearest 0.1mm
   - peak shear stress (τ_{max}), expressed to the nearest 0.01MPa
   - maximum shear stiffness modulus (k_{max}), expressed to the nearest 0.01MPa/mm
   - any cracks or other damage.
e) The test temperature, expressed to the nearest 0.5°C

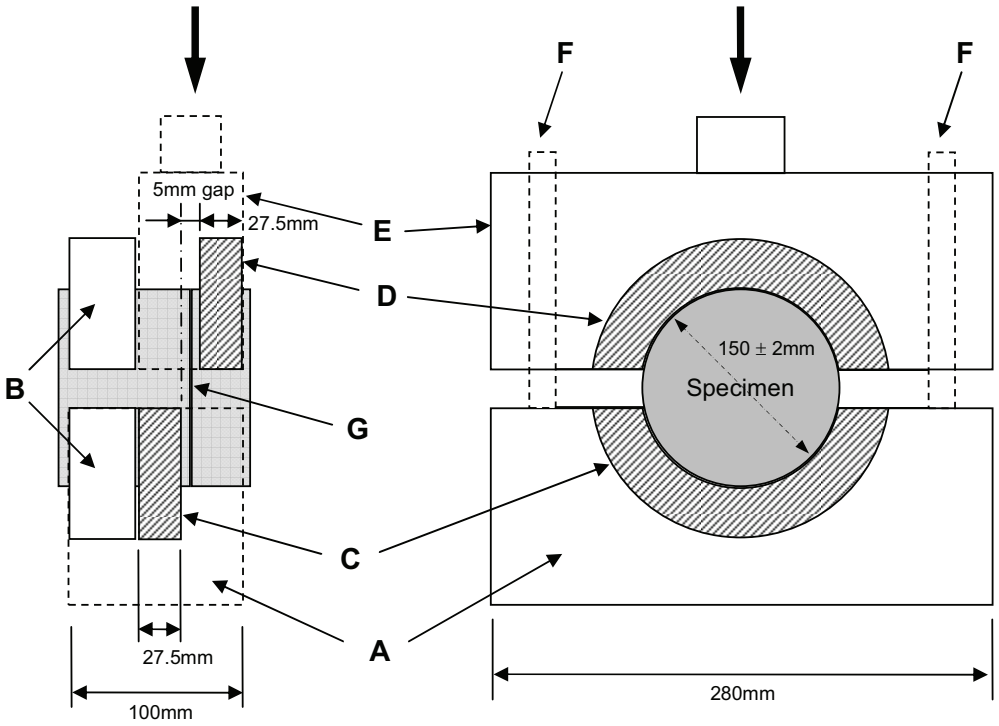

A – base body
B – sample support
C – lower shear ring
D – upper shear ring
E – upper body
F – guiding bar
G – specimen interface

Figure 9/12: (11/04) **Schematic diagram of the modified Leutner shear test apparatus**

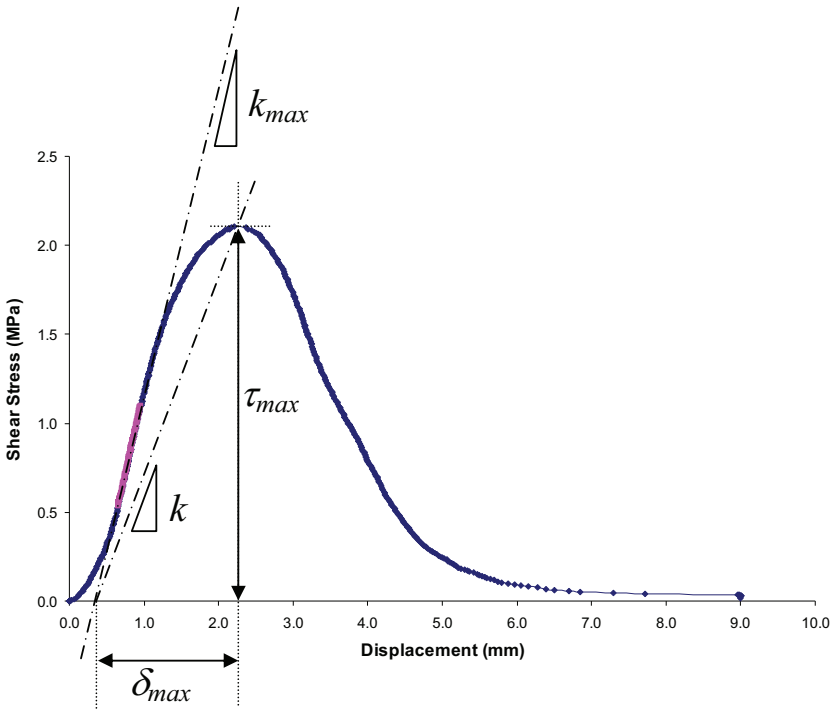

Figure 9/13: (11/04) **Example of shear stress vs displacement data plot**

NG954 (11/04) **Method for Laboratory Determination of Interface Properties using the Modified Leutner Shear Test**

1 The test method is intended to assess the bonding between adjacent asphalt pavement layers using cylindrical samples. It is also appropriate for asphalt surfacing applied to concrete.

2 Clause 954 incorporates by dated or undated reference, provisions from other publications. These normative references are cited at the appropriate places in the text, and the publications are listed in Appendix F. For dated references, subsequent amendments to or revisions of any of these publications apply to this Clause only when incorporated in it by amendment or revision. For undated references the latest edition of the publication referred to applies (including amendments).

3 The Leutner shear test was developed in Germany in the late 1970s as a simple means of undertaking a direct shear test on a bond between two asphalt layers. The test is performed on 150mm diameter cores comprising at least two layers (with a bond between them) taken either from a pavement or produced in the laboratory. The principle of the test is to apply a shear displacement rate across the interface under investigation and monitor the resulting shear force. No normal force is applied to the specimen. The standard loading rate is 50 mm/min and the test is typically carried out at 20°C. It should be noted that a 5mm gap is introduced in this modified version of the shear test, as shown in Figure 9/12, in order to give a certain level of tolerance for interface alignment to the shear plane.

4 With reference to sub-Clause 954.4, the shear test apparatus supplied by the apparatus manufacturer STRASSENTEST GmbH, D-63755 Alzenau, Germany, HR8 8049 (Tel: +49 (0) 60 23 / 50 56-0) has been found to be suitable. Various sizes of standard shearing insets are also available from the same manufacturer, necessary in order to incorporate some variation in specimen diameter. It should be noted that these standard shearing insets require modification to introduce a 5mm gap over the shear plane (see sub-Clause NG954.3 above); this modification is easily available from a local workshop.

5 It is recommended to use a servo-hydraulic universal testing machine with an incorporated data logging system. However, other loading frames (such as the Marshall apparatus) can also be used, providing they fulfil the requirements of sub-Clause 954.4 (ii).

6 The data logging system described in sub-Clause 954.4(iii) shall to be capable of collecting around 40 data points per second.

7 The recommended diameter of the cored specimens is 150 ± 2mm. It is recommended to have at least 5 sets of various insets from 145mm ~ 155mm in diameter.

8 The thickness of the layer below the interface to be tested shall be long enough for a secure grip to be maintained on the specimen during the test (Figure 9/12 B). 60mm is recommended as the minimum thickness. It is recommended that the upper layer shall be at least 30mm thickness, to ensure proper contact with the upper shearing inset (Figure 9/12 D).

9 It is recommended to select shearing insets to form a loose fit around the specimen. For example, if the exact specimen diameter is 150.1mm, 151mm insets will be more suitable than 150mm diameter insets, among the available sets of insets.

10 The sample support shown in Figure 9/12 B needs to be tightened using a hand spanner to give a firm grip. However, care is necessary to avoid over tightening and consequent damage to the specimen.

11 It is necessary to carefully inspect both sections of the sheared specimen. Crushed coarse aggregate on the specimen edge with higher determined bond strengths could indicate misalignment of the specimen interface in the shear plane.

APPENDIX A.2
NEW MODIFIED LEUTNER TESTING PROTOCOL
(Covering specimens containing thin surfacings)

954 (11/07) Method for Laboratory Determination of Interface Properties using the Modified Leutner Shear Test

Scope

1 This Clause specifies a laboratory test method to assess the bonding between adjacent asphalt pavement layers using cylindrical samples. It is also appropriate for asphalt applied to concrete.

Terms and Definitions

2 For the purposes of this Clause the terms and definitions given in BS 6100 shall apply, together with the following:

(i) Peak Shear Stress

The maximum value of shear stress, determined as the maximum force divided by the initial cross sectional area of a specimen when tested as described in this Clause.

(ii) Displacement at Peak Shear Stress

The displacement at the maximum value of shear stress of a specimen when tested as described in this Clause.

(iii) Shear Stiffness Modulus

The peak shear stress divided by the displacement at the peak shear stress of a specimen when tested as described in this Clause.

Principle of Test

3 Cylindrical test specimens of nominal 150mm diameter shall be subjected to direct shear loading at 20°C using the modified Leutner shear test. The maximum shear stress (in MPa) at the interface between layers shall be determined.

Test Apparatus and Materials

4 The following test apparatus and Materials shall be used:

(i) Shear test apparatus, as shown in Figure 9/12, composed of a base body (A) on which are fixed the sample support (B) and the lower shear ring (D). The upper shear ring (C) is attached to the upper body (E), which is movable along the guiding bars (F). The gap between shear rings (C and D) is 5mm.

(ii) A loading frame capable of achieving a constant vertical displacement rate of 50.0 ± 2mm per minute and a maximum load of at least 50kN.

(iii) A data logging system to record load and displacement during the test.

(iv) A metal extension, as shown in Figure 9/13.

(v) A stiff adhesive, such as epoxy resin, with sufficient strength to avoid failure within the adhesive or at the adhesive/asphalt material interface.

Sample Preparation

5 Test specimens shall be cores of 150 ± 2mm diameter; the minimum thickness of the layers above and below the interface to be tested shall be 15mm and 60mm respectively. Specimens shall be cored from an in-service pavement or from a slab manufactured using a laboratory roller compactor in accordance with BS EN 12697-35 and BS EN 12697-33. If the thickness of the layer above the interface is between 15 and 30mm, a metal extension shall be glued on top of the layer above the interface.

Procedure

6 The diameter and thickness of the specimen shall be determined to the nearest mm.

7 The specimen shall be placed into a suitable temperature controlled conditioning environment at 20 ± 0.5°C for a minimum of 5 hours.

8 The appropriate shear rings, to form a loose fit around the specimen (for example, 151mm diameter shear rings for a 150mm diameter specimen), shall be selected and attached to the Leutner test frame.

9 The specimen shall be placed into the test apparatus and the interface aligned, (Figure 9/12 (G)), between the upper and lower shear rings (Figure 9/12 (C and D)). If a metal extension is used, the specimen shall be placed into the test apparatus so that the direction of the grooves is perpendicular to the direction of the applied shear load.

10 Tighten the sample support using a suitable spanner.

11 The test apparatus shall be placed into the loading frame and adjusted until the upper shear ring (Figure 9/12 (C)) nearly touches the specimen.

12 Start the data logging system (to record load and displacement) and commence shear loading. The loading rate shall be 50.0 ± 2mm per minute.

13 Record the load (F) to the nearest 0.1kN and the displacement (δ) to the nearest 0.1mm.

14 Stop the shear loading when the test frame reaches its limit of 7mm displacement. The length of time between removal of the specimen from the temperature controlled conditioning environment and completion of testing shall not exceed 15 minutes.

15 After the test has been completed, the apparatus shall be dismantled and the specimen removed.

16 Both sections of the specimen shall be observed (especially the interface) for any visual cracks and unusual appearance (ie. crushed aggregates on edges). Record any comments as necessary.

Calculation and Expression of Results

17 Calculate the shear stress as follows:

$$\tau = \frac{F}{\pi r^2}$$

Where τ = shear stress in (MPa)
F = load (in kN)
r = initial radius of specimen (in mm)

18 Produce a shear stress versus shear displacement graph (an example is shown in Figure 9/14) using the recorded data.

19 Determine the following parameters from the graph:

(i) τ_{max} = peak shear stress, MPa, expressed to the nearest 0.1

(ii) δ_{max} = displacement at peak shear stress, mm, expressed to the nearest 0.1

(iii) k = shear stiffness modulus = τ_{max}/δ_{max}, MPa/mm, expressed to the nearest 0.1

Test Report

20 The test report shall contain not less than the following information:

a) A reference to this test method and test conditions.
b) Material descriptions for both layers.
c) Type and amount of tack (bond) coat (if known).
d) For each specimen tested, report:
   - specimen diameter, expressed to the nearest mm
   - layer thicknesses, expressed to the nearest mm
   - maximum load (F), expressed to the nearest 0.1kN
   - peak shear stress (τ_{max}), expressed to the nearest 0.1MPa
   - displacement at peak shear stress(δ_{max}), expressed to the nearest 0.1mm
   - shear stiffness modulus (k), expressed to the nearest 0.1MPa/mm
   - any cracks or other damage.
e) The test temperature, expressed to the nearest 0.5°C
f) The use (or otherwise) of a metal extension.

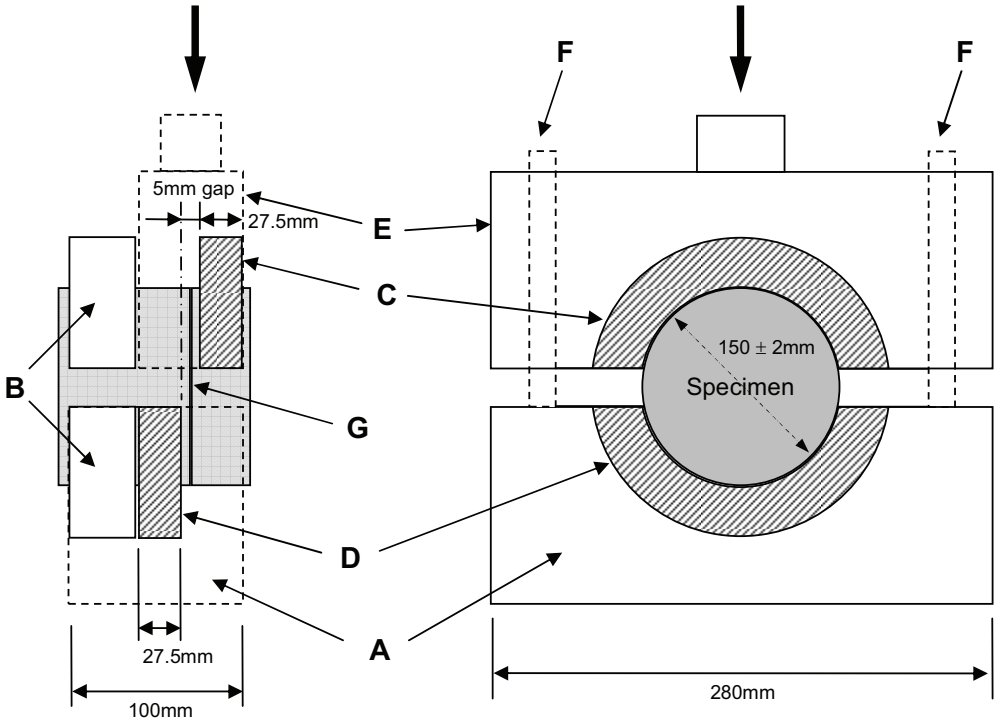

A – base body
B – sample support
C – upper shear ring
D – lower shear ring
E – upper body
F – guiding bar
G – specimen interface

Figure 9/12: (11/07) **Schematic diagram of the modified Leutner shear test apparatus**

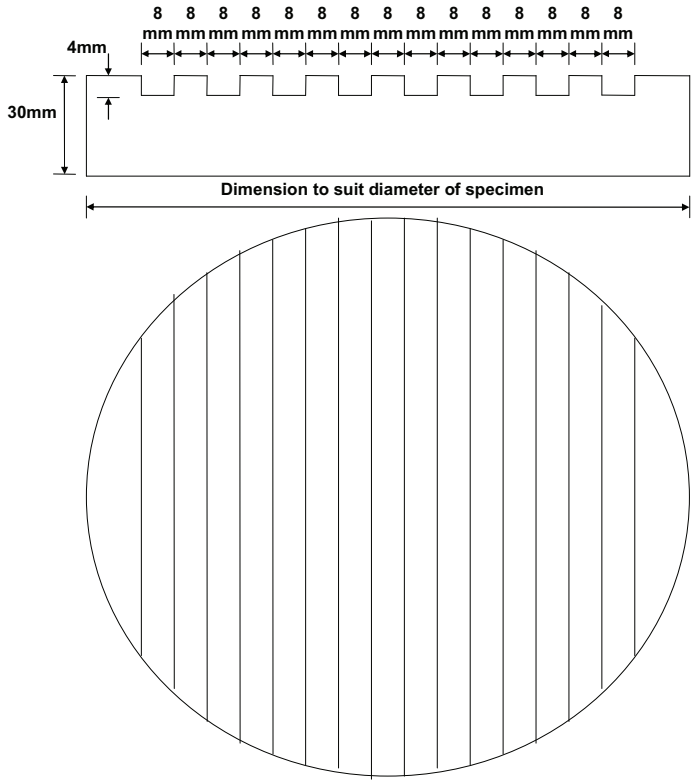

Figure 9/13: (11/07) **Schematic drawing of the metal extension**

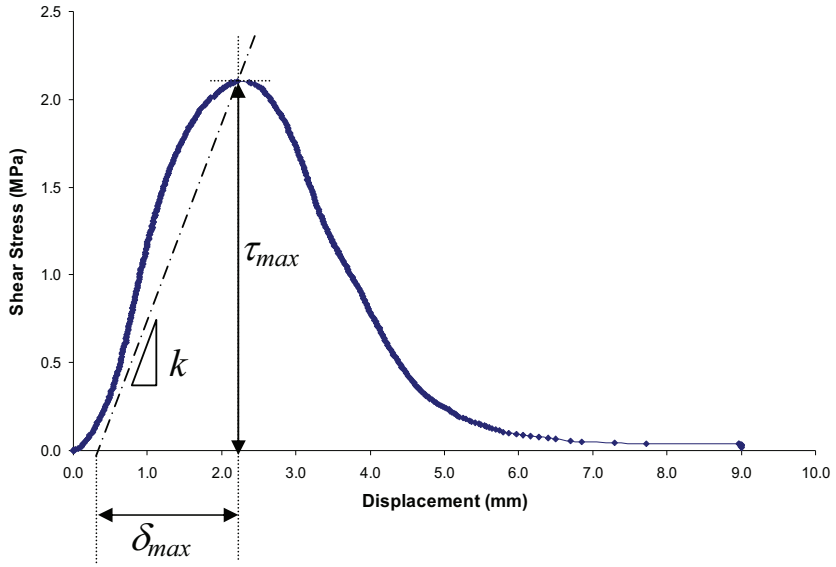

Figure 9/14: (11/07) **Example of shear stress vs displacement data plot**

NG954 (11/07) **Method for Laboratory Determination of Interface Properties using the Modified Leutner Shear Test**

1 The test method is intended to assess the bonding between adjacent asphalt pavement layers using cylindrical samples. It is also appropriate for asphalt applied to concrete.

2 Clause 954 incorporates by dated or undated reference, provisions from other publications. These normative references are cited at the appropriate places in the text, and the publications are listed in Appendix F. For dated references, subsequent amendments to or revisions of any of these publications apply to this Clause only when incorporated in it by amendment or revision. For undated references the latest edition of the publication referred to applies (including amendments).

3 The Leutner shear test was developed in Germany in the late 1970s as a simple means of undertaking a direct shear test on a bond between two pavement layers. The test is performed on 150mm diameter cores comprising at least two layers (with a bond between them) taken either from a pavement or produced in the laboratory. The principle of the test is to apply a shear displacement rate across the interface under investigation and monitor the resulting shear force. No normal force is applied to the specimen. The standard loading rate is 50 mm/min and the test is typically carried out at 20°C. It should be noted that a 5mm gap is introduced in this modified version of the shear test, as shown in Figure 9/12, in order to give a certain level of tolerance for interface alignment to the shear plane.

4 With reference to sub-Clause 954.4, the shear test apparatus supplied by the apparatus manufacturer STRASSENTEST GmbH, D-63755 Alzenau, Germany, HR8 8049 (Tel: +49 (0) 60 23 / 50 56-0) has been found to be suitable. Various sizes of standard shearing rings are also available from the same manufacturer, necessary in order to incorporate some variation in specimen diameter. It should be noted that these standard shearing rings require modification to introduce a 5mm gap over the shear plane (see sub-Clause NG954.3 above); this modification is easily available from a local workshop.

5 It is recommended to use a servo-hydraulic universal testing machine with an incorporated data logging system. However, other loading frames (such as the Marshall apparatus) can also be used, providing they fulfil the requirements of sub-Clause 954.4 (ii).

6 The data logging system described in sub-Clause 954.4(iii) shall to be capable of collecting around 40 data points per second.

7 The recommended material for the metal extension is aluminium.

8 The recommended diameter of the cored specimens is 150 ± 2mm. It is recommended to have a range of shearing rings and metal extensions to cover the range of specimen diameters.

9 The thickness of the layer below the interface to be tested shall be sufficient to ensure a secure grip is maintained on the specimen during the test (Figure 9/12 B). 60mm is recommended as the minimum thickness.

10 The thickness of the layer above the interface shall be sufficient to ensure a proper contact with the upper shearing ring (Figure 9/12 C). The minimum recommended thickness of the layer above the interface is 15mm. If the thickness of the layer above the interface is between 15 and 30mm, a metal extension shall be glued on the top of the layer above the interface.

11 It is recommended that the shearing rings are selected to form a loose fit around the specimen. For example, if the specimen diameter is 150.1mm, 151mm shearing rings shall be selected.

12 It is recommended that the metal extension selected shall have a diameter slightly larger than the diameter of the specimen (the difference shall not be more than 2mm). When a metal extension is used, it is recommended that the shearing rings are selected to form a loose fit around the metal extension. For example, if the metal extension diameter is 151mm, 152mm shear rings shall be selected.

13 The sample support shown in Figure 9/12 B needs to be tightened using a hand spanner to give a firm grip. However, care is necessary to avoid over tightening and consequent damage to the specimen.

14 It is necessary to carefully inspect both sections of the sheared specimen. Crushed coarse aggregate on the specimen edge could indicate misalignment of the specimen interface in the shear plane.

APPENDIX A.3
MANUAL TORQUE TESTING PROTOCOL
(Guidelines Document SG3/98/173 [British British Board of Agreement, 2000])

British Board of Agrément
PO Box 195
Bucknalls Lane
Garston
Watford
Herts
WD25 9BA

Tel: 01923 665300
Fax: 01923 665301
e-mail: mail@bba.star.co.uk
http://www.bbacerts.co.uk

SG3/98/173

GUIDELINES DOCUMENT

FOR THE ASSESSMENT AND CERTIFICATION OF

THIN SURFACING SYSTEMS

FOR HIGHWAYS

Appendix A.3

TORQUE BOND TEST
(Draft for development)

1 Scope

The following protocol describes methods for determining the Bond Strength between a thin surfacing system and its substrate, which may be bituminous or cementitious, by measuring the peak shearing torque, at a known temperature.

Two methods of test are described for tests carried out on site and on cores taken from site and tested in the laboratory.

The test shall only be carried out on thin surfacing systems which have been installed for a period of between 28 and 56 days.

The protocol describes a test procedure that has been developed specifically for the assessment of thin surfacing systems under HAPAS Certification procedures. The method is currently at the draft for development stage and should not be used for specifying purposes.

2 Definitions

τ : inter-layer bond strength in -P (kPa),
M : peak value of applied shearing torque in Newton metres (N m),
D : diameter of core in millimetres (mm)

3 Apparatus

3.1 Equipment

3.1.1 *Core cutting apparatus*: suitable for cutting 100mm (or 150mm)[(1)] diameter cores in bituminous and cementitious materials;

3.1.2 *Torque meter*: fitted with a fiducial reading gauge. The device shall be calibrated over a range of 0-350 N m with a scale readable to at least 10 N m. The device shall be fitted with a socket-fitting allowing steel plates to be fitted and removed.

3.1.3 *Metal Plate*: of mild steel having a diameter of (95±5) mm or (145±5) mm, and a thickness of (14±2) mm. The plate shall incorporate a fitting enabling it to be coupled to the torque meter[(2)].

3.1.4 *Thermometer*: readable to 0.1°C and accurate to 0.5°C.

3.1.5 *Steel Rule*

3.1.6 *Callipers:* for measurement of core diameters;

3.1.7 Mould or other means of confining Laboratory test samples for testing.

3.1.8 *Watch or Timer*: readable and accurate to 1 second.

3.1.9 *Mould*: for confining laboratory test specimens, (e.g. 150 mm^3 concrete cube mould).

3.1.10 *Spirit Level*: for checking laboratory test specimens;

3.1.11 *Oven or refrigerated incubator (optional)*

Note:
1 Subject to review.
2 Fittings of 12.7 mm and 19.05 mm have been found to be suitable.

3.2 Materials

3.2.1 *Adhesive*: (a stiff adhesive, such as rapid setting epoxy resin, with sufficient strength to avoid failure within the adhesive or at the adhesive/thin surfacing interface).

3.2.2 *Mounting material (for laboratory tests)*: e.g. rapid hardening mortar, concrete or grout.

4 Test methods

4.1 Site test method

4.1.1 Core the location to be tested using a 100mm (or 150mm) diameter core barrel to aminimum depth of 20mm below the thin surfacing layer to be tested. Six such cores shall be cut along a 100m length of the installationat nominally even spacing along a diagonal line across the lane width.

4.1.2 Ensure that all debris is removed from the rebate formed by the core barrel. Clean and dry the surface to be tested.

4.1.3 Use the bonding agent to secure the metal plate to the surface of the core, taking care to ensure that the plate is parallel to the surface.

4.1.4 When the bonding agent has developed sufficient strength, (i.e. failure should not occur within the adhesive), fit the torque meter to the metal plate, using adapters and extension rods as appropriate.

4.1.5 Apply torque to the core at a steady rate so that failure occurs in (60±30) seconds. Care must be taken to ensure that the torque is applied parallel to the core surface (within ±10o). Torque is applied to the plate until failure of the bond occurs. Observe and record the time to failure to within ±2 seconds.

4.1.6 Record the value of torque at failure, M, in Newton metres. Measure and record the bond interface temperature immediately after failure.

4.1.7 Examine the core and substrate and record the condition of the bond interface (e.g. smooth, planer, rough or irregular). Record the substrate type (e.g. bituminous or cementitious surface). Where known record details of the substrate condition prior to surfacing, (i.e. planed, untreated or regulated).

4.1.8 Measure and record the core diameter at two locations approximately 90° apart using callipers and record the mean value, D, to an accuracy of 1 mm.

4.1.9 Measure and record the depth of the surfacing to the substrate interface to an accuracy of 1mm.

4.1.10 Calculate the bond strength in accordance with section 5.

4.2 Laboratory test method

4.2.1 Cut a 100mm (or 150mm) diameter core to a minimum depth of 80mm below the bottom of the surface layer. Extract the core taking care not to damage the surface layer of the core or the bond interface with the substrate. Six such cores shall be taken along a 100m length of the installation at nominally even spacing along a diagonal line across the lane width.

4.2.2 Trim the core to a length suitable for mounting if appropriate.

4.2.3 Place the core in the mould, using mortar or grout as a bedding layer if appropriate, so that the upper layer and the bond interface to be tested is (20±10) mm above the rim of the mould. Fill the mould with the mortar/grout and trim flush with the mould rim, ensuring that the core is perpendicular to, and the upper surface parallel with, the mould surface. Check using the spirit level.

4.2.4 Fix the metal plate to the core using the adhesive and allow to set.

4.2.5 Unless otherwise specified[1], condition the mounted cores by storing at a temperature of (20±2)°C for a minimum of 4 hours and for not more than 16 hours before testing. Record the times and temperatures employed.

4.2.6 Unless otherwise specified, test the core at a temperature of (20±2)°C: where other temperatures are used the test shall be completed within 5 minutes of removal from the conditioning environment.

4.2.7 Fix or clamp the mould containing the mounted core to a suitably rigid surface. Carry out the test as described in 4.1.5.

4.2.8 Examine the core and record all the relevant information as described in 4.1.6 to 4.1.9.

5 Calculation of Bond Strength and expression of results

Calculate the bond strength for each specimen using the following formula:

$$\tau = \frac{12M \times 10^6}{\pi D^3}$$

Calculate the arithmetic mean of the inter-layer bond strength, τ, for the six specimens

6 Test report

6.1 The test report shall include the following information:

i) Name of organisation carrying out the test
ii) Method of test used
iii) Description of materials (system and substrate)
iv) Date of test
v) Peak torque at failure (N m)
vi) Inter-layer bond strength (kPa), (individual and mean values)
vii) Time to failure (seconds)
viii) Diameter of core (mm)
ix) Depth of Bond interface (mm)
x) Temperature of the Bond interface at test (°C)
xi) Conditioning details (duration and temperature)
xii) Site or Laboratory test
xiii) Identification of Site or Scheme
xiv) Core location
xv) Age of the installation / specimen at the time of test
xvi) Nature of the Bond interface

7 Precision

The precision for this test method has not been determined.

Note:

1 Temperatures outside this range may be specified, e.g. in order to compare data obtained from site tests carried out at temperatures other than (20±2)°C. In this case additional laboratory apparatus (i.e. ovens or refrigerated incubators) may be required. Conditioning of specimens in a soaked condition may also be undertaken. Details of the conditioning used prior to testing shall be recorded.

APPENDIX A.4
MANUAL TORQUE TESTING PROTOCOL
(Guidelines Document SG3/05/234 [British British Board of Agreement, 2004])

British Board of Agrément
PO Box 195
Bucknalls Lane
Garston
Watford
Herts
WD25 9BA

Tel: 01923 665300
Fax: 01923 665301
e-mail: mail@bba.star.co.uk
http://www.bbacerts.co.uk

SG3/05/234

GUIDELINES DOCUMENT

FOR THE ASSESSMENT AND CERTIFICATION OF

THIN SURFACING SYSTEMS

FOR HIGHWAYS

July 2004

Note: This document may be revised from time to time to take account of improvements and amendments to test and assessment methods and material innovations. Readers are advised to contact the British Board of Agrément hotline to check the latest edition.

Telephone: 01923 665400 Fax: 01923 665301
e-mail: mail@bba.star.co.uk

Appendix A.3

TORQUE BOND TEST
(Draft for development)

1 Scope

The following protocol describes methods for determining the Bond Strength between a thin surfacing system and its substrate, which may be bituminous or cementitious, by measuring the peak shearing torque, at a known temperature.

Two methods of test are described for tests carried out on site and on cores taken from site and tested in the laboratory.

The test shall only be carried out on thin surfacing systems which have been installed for a period of between 28 and 56 days(1).

The protocol describes a test procedure that has been developed specifically for the assessment of thin surfacing systems under HAPAS Certification procedures. The method is currently at the draft for development stage and should not be used for specifying purposes.

2 Definitions

τ : inter-layer bond strength in kiloPascals (kPa),
M : peak value of applied shearing torque in Newton metres (N m),
D : diameter of core in millimetres (mm)

3 Apparatus

3.1 Equipment

3.1.1 *Core cutting apparatus*: suitable for cutting 100mm(1) diameter cores in bituminous and cementitious materials;

3.1.2 *Torque meter*: fitted with a fiducial reading gauge. The device shall be calibrated over a range of 0-350 N m with a scale readable to at least 10 N m. The device shall be fitted with a socket-fitting allowing steel plates to be fitted and removed.

3.1.3 *Metal Plate*: of mild steel having a diameter of (95±5), and a thickness of (14±2) mm. The plate shall incorporate a fitting enabling it to be coupled to the torque meter.(2)

3.1.4 *Thermometer*: readable to 0.1°C and accurate to 0.5°C.

3.1.5 *Steel Rule*

3.1.6 *Callipers:* for measurement of core diameters;

3.1.7 Mould or other means of confining laboratory test samples for testing.

3.1.8 *Watch or Timer*: readable and accurate to 1 second.

3.1.9 *Mould*: for confining laboratory test specimens, (e.g. 150 mm concrete cube mould).

3.1.10 *Spirit Level*: for checking laboratory test specimens;

3.1.11 *Oven or refrigerated incubator (optional)*

Note:
1 **Cores may be cut prior to the 28 days post-installation period and stored at 5 ± 2°C prior to testing.**
2 **Fittings of 12.7 mm and 19.05 mm have been found to be suitable.**

3.2 Materials

3.2.1 *Adhesive*: (a stiff adhesive, such as rapid setting epoxy resin, with sufficient strength to avoid failure within the adhesive or at the adhesive/thin surfacing interface).

3.2.2 *Mounting material (for laboratory tests)*: e.g. rapid hardening mortar, concrete or grout.

4 Test methods

4.1 Site test method

4.1.1 Core the location to be tested using a 100 mm (±5mm) diameter core barrel to a depth of 20 mm below the thin surfacing layer to be tested. The method for sampling shall be to cut six cores at nominally even spacing along a diagonal line across the lane width. Cores shall be taken from a 100m length of the installation or the total installation where this is less than 100m.

4.1.2 Ensure that all debris is removed from the rebate formed by the core barrel. Clean and dry the surface to be tested.

4.1.3 Use the bonding agent to secure the metal plate to the surface of the core, taking care to ensure that the plate is parallel to the surface.

4.1.4 When the bonding agent has developed sufficient strength, (i.e. failure should not occur within the adhesive), fit the torque meter to the metal plate, using adapters and extension rods as appropriate.

4.1.5 Apply torque to the core at a steady rate so that the torque wrench sweeps an angle of 90° within (30±15) s. Care must be taken to ensure that the torque is applied parallel to the core surface (within ± 10°). Torque is applied to the plate until failure of the bond occurs or a torque of 300 N m is exceeded.

4.1.6 Record the value of torque at failure, M, in Newton metres. Measure and record the bond interface temperature immediately after failure.

4.1.7 Examine the core and substrate and record the condition of the bond interface (e.g. smooth, planer, rough or irregular). Record the substrate type (e.g. bituminous or cementitious surface). Where known record details of the substrate condition prior to surfacing, (i.e. planed, untreated or regulated).

4.1.8 Measure and record the core diameter at two locations approximately 90° apart using callipers and record the mean value, D, to an accuracy of 1 mm.

4.1.9 Measure and record the depth of the surfacing to the substrate interface to an accuracy of 1mm.

4.1.10 Calculate the bond strength in accordance with section 5.

4.2 Laboratory test method

4.2.1 Cut a 100mm (or 150mm) diameter core to a minimum depth of 80mm below the bottom of the surface layer. Extract the core taking care not to damage the surface layer of the core or the bond interface with the substrate. Six such cores shall be taken along a 100m length of the installation at nominally even spacing along a diagonal line across the lane width.

4.2.2 Trim the core to a length suitable for mounting if appropriate.

4.2.3 Place the core in the mould, using mortar or grout as a bedding layer if appropriate, so that the upper layer and the bond interface to be tested is (20±10) mm above the rim of the mould. Fill the mould with the mortar/grout and trim flush with the mould rim, ensuring that the core is perpendicular to, and the upper surface parallel with, the mould surface. Check using the spirit level.

4.2.4 Fix the metal plate to the core using the adhesive and allow to set.

4.2.5 Unless otherwise specified[(1)], condition the mounted cores by storing at a temperature of (20±2)^{o}C for a minimum of 4 hours and for not more than 16 hours before testing. Record the times and temperatures employed.

4.2.6 Unless otherwise specified, test the core at a temperature of (20±2)°C: where other temperatures are used the test shall be completed within 5 minutes of removal from the conditioning environment.

4.2.7 Fix or clamp the mould containing the mounted core to a suitably rigid surface. Carry out the test as described in 4.1.5.

4.2.8 Examine the core and record all the relevant information as described in 4.1.6 to 4.1.9.

5 Calculation of Bond Strength and expression of results

Calculate the bond strength for each specimen using the following formula:

$$\tau = \frac{12M \times 10^6}{\pi D^3}$$

Calculate the arithmetic mean of the inter-layer bond strength, τ, for the six specimens

6 Test report

6.1 The test report shall include the following information:

i) Name of organisation carrying out the test
ii) Method of test used
iii) Description of materials (system and substrate)
iv) Date of test
v) Peak torque at failure (N m)
vi) Inter-layer bond strength (kPa), (individual and mean values)
vii) Time to failure (seconds)
viii) Diameter of core (mm)
ix) Depth of Bond interface (mm)
x) Temperature of the Bond interface at test (^{o}C)
xi) Conditioning details (duration and temperature)
xii) Site or Laboratory test
xiii) Identification of Site or Scheme
xiv) Core location
xv) Age of the installation / specimen at the time of test
xvi) Nature of the Bond interface
xvii) Mode of Failure

7 Precision

The precision for this test method has not been determined.

Note:

1 Temperatures outside this range may be specified, e.g. in order to compare data obtained from site tests carried out at temperatures other than (20±2)^{o}C. In this case additional laboratory apparatus (i.e. ovens or refrigerated incubators) may be required. Conditioning of specimens in a soaked condition may also be undertaken. Details of the conditioning used prior to testing shall be recorded.

APPENDIX B
BOXPLOT ANALYSIS

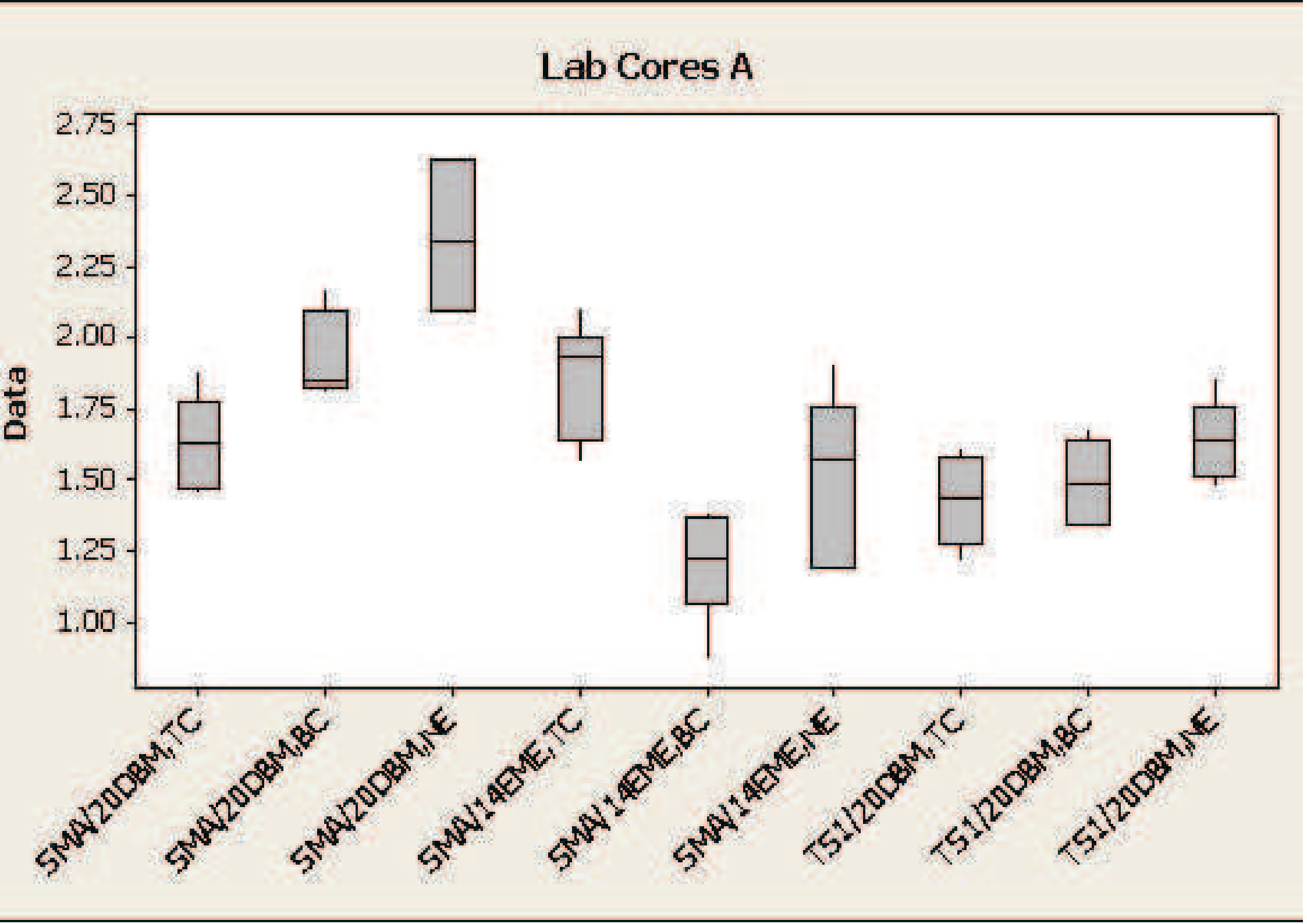
Lab Cores A
Data
2.75
2.50
2.25
2.00
1.75
1.50
1.25
1.00
SMAJ20CBM,TC
SMAJ20CBM,BC
SMAJ20CBM,NE
SMAJ14EME,TC
SMAJ14EME,BC
SMAJ14EME,NE
TS1J20CBM,TC
TS1J20CBM,BC
TS1J20CBM,NE

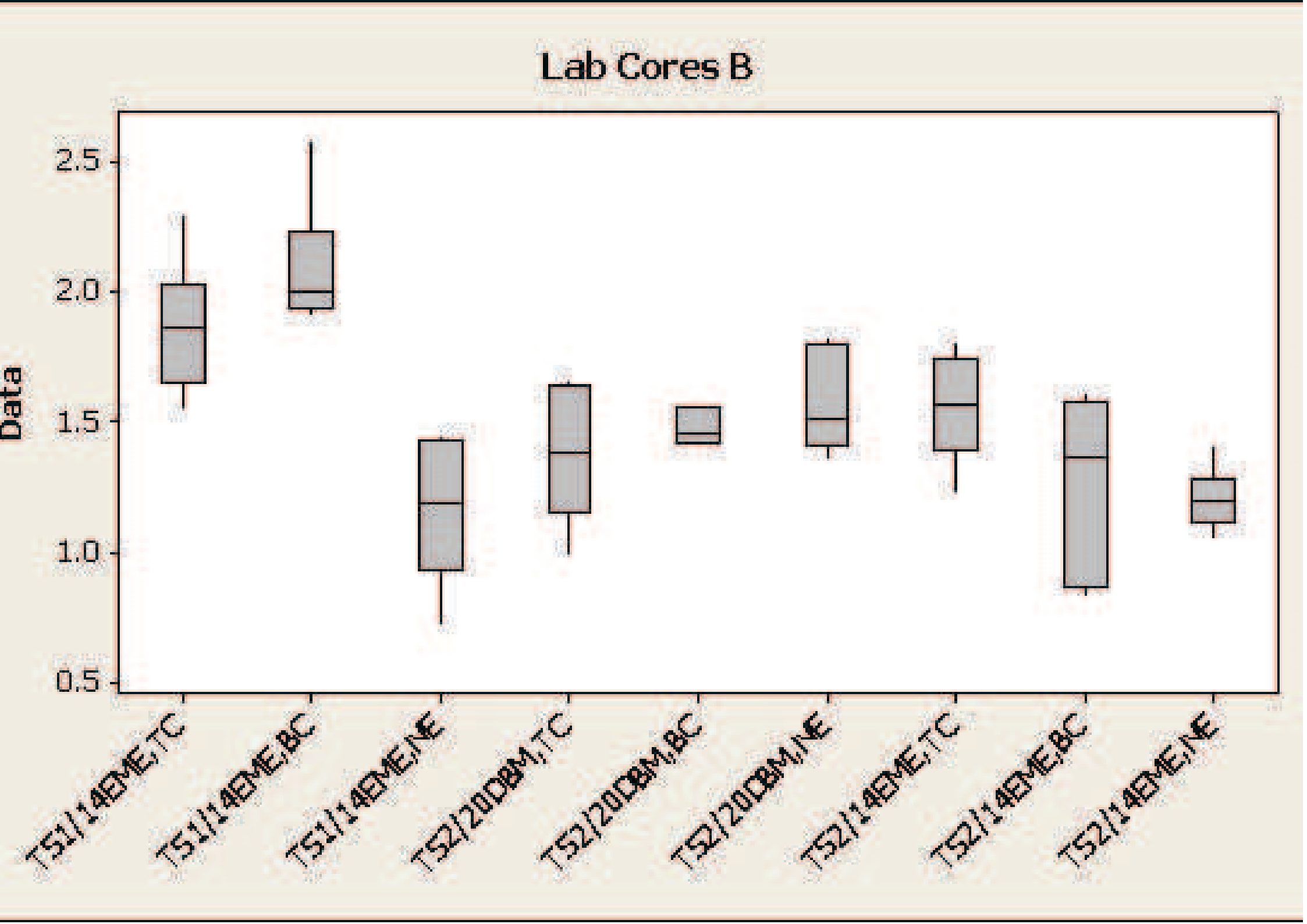
Lab Cores B
Data
2.5
2.0
1.5
1.0
0.5
TS1/14EME,TC
TS1/14EME,BC
TS1/14EME,NE
TS2/20DBM,TC
TS2/20DBM,BC
TS2/20DBM,NE
TS2/14EME,TC
TS2/14EME,BC
TS2/14EME,NE

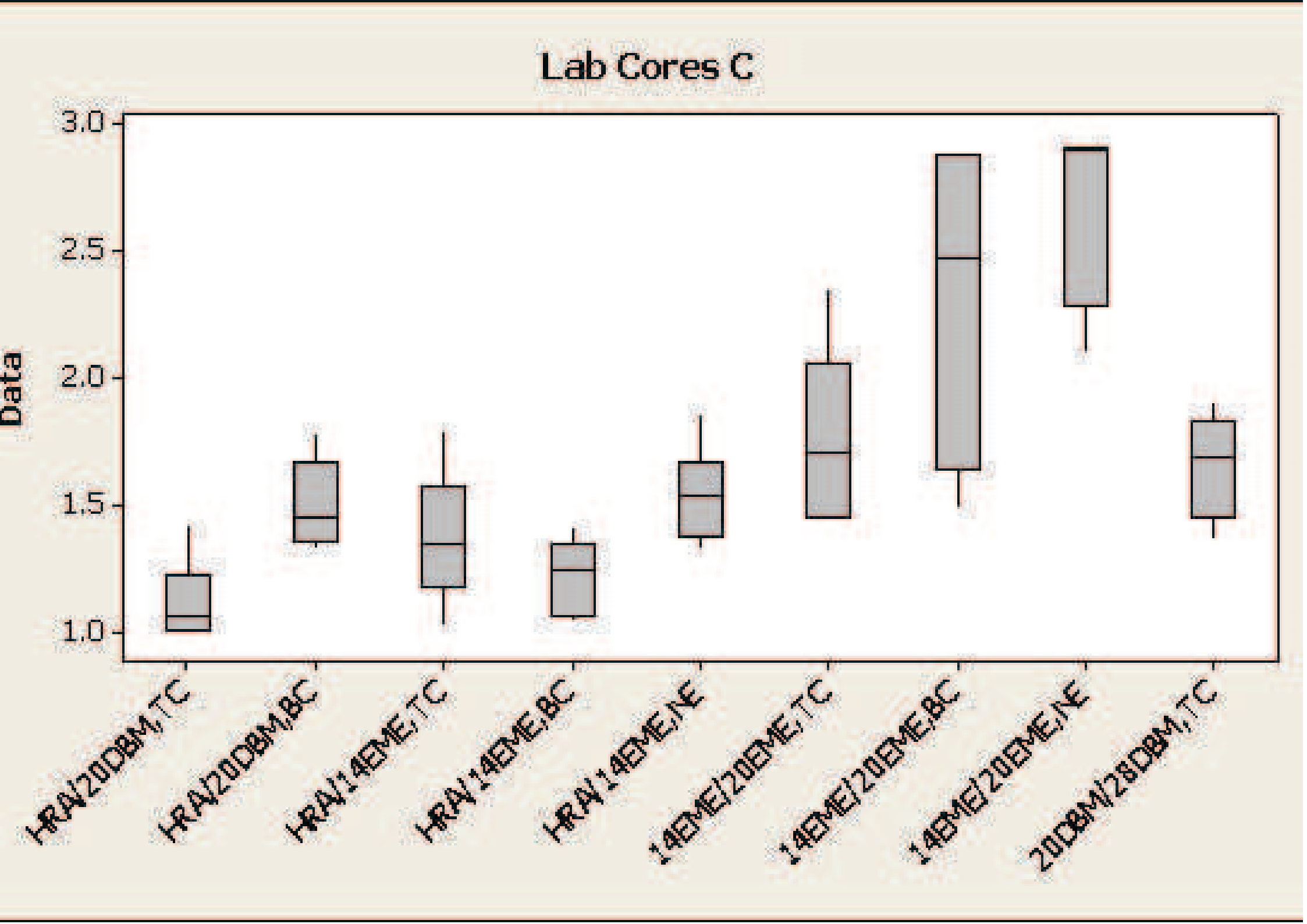
Lab Cores C
Data
3.0
2.5
2.0
1.5
1.0
HRA\20DBM,TC
HRA\20DBM,BC
HRA\14EME,TC
HRA\14EME,BC
HRA\14EME,NE
\14EME\20EME,TC
\14EME\20EME,BC
\14EME\20EME,NE
20DBM\28DBM,TC

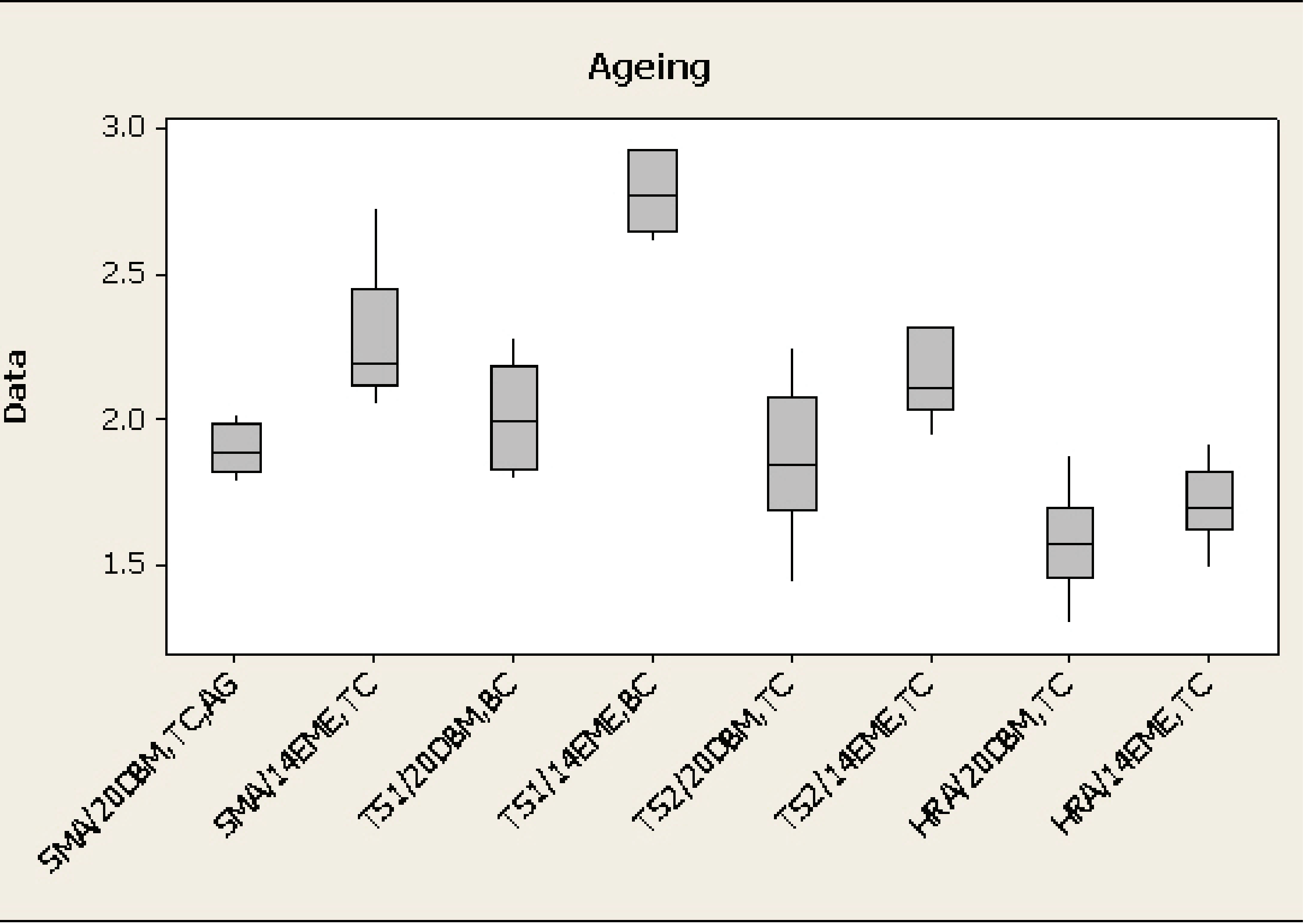
Ageing
Data
3.0
2.5
2.0
1.5
SMA/20DBM,TC,AG
SMA/14EME,TC
T51/20DBM,BC
T51/14EME,BC
T52/20DBM,TC
T52/14EME,TC
HRA/20DBM,TC
HRA/14EME,TC

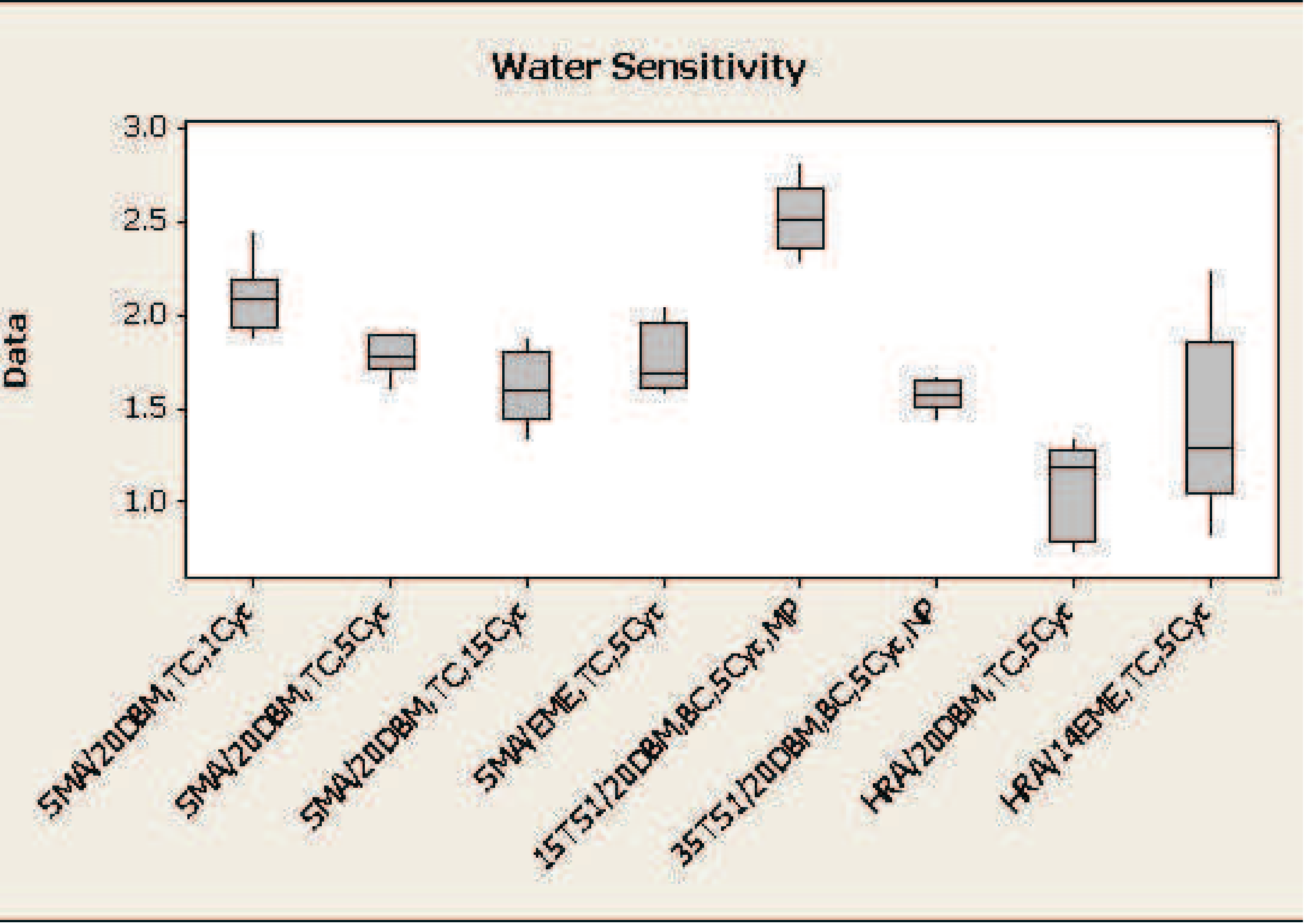
Water Sensitivity
Data
3.0
2.5
2.0
1.5
1.0
SMA/20DBM;TC;1Cyc
SMA/20DBM;TC;5Cyc
SMA/20DBM;TC;15Cyc
SMA/EME;TC;5Cyc
15TS1/20DBM/BC;5Cyc;MP
35TS1/20DBM/BC;5Cyc;MP
HRA/20DBM;TC;5Cyc
HRA/14EME;TC;5Cyc